Green Energy and Technology

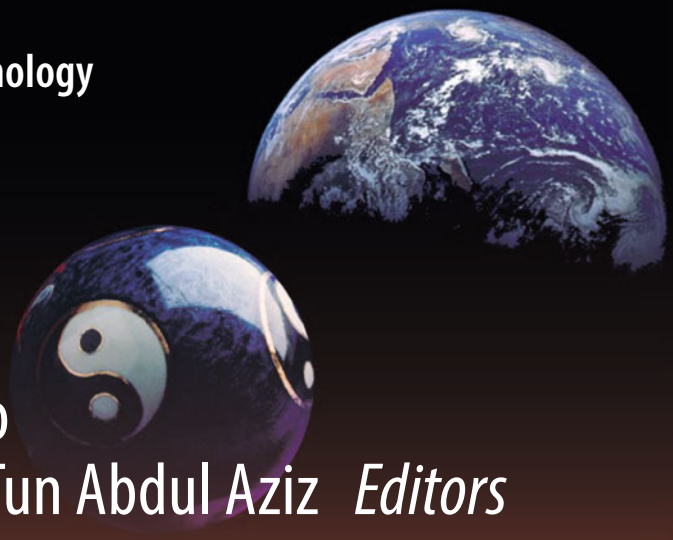

Dominic C. Y. Foo
Mustafa Kamal Tun Abdul Aziz *Editors*

Green Technologies for the Oil Palm Industry

Springer

Green Energy and Technology

More information about this series at http://www.springer.com/series/8059

Dominic C. Y. Foo
Mustafa Kamal Tun Abdul Aziz
Editors

Green Technologies for the Oil Palm Industry

Springer

Editors
Dominic C. Y. Foo
Department of Chemical
and Environmental Engineering
University of Nottingham
Malaysia Campus
Semenyih, Selangor, Malaysia

Mustafa Kamal Tun Abdul Aziz
Department of Chemical
and Environmental Engineering
University of Nottingham
Malaysia Campus
Semenyih, Selangor, Malaysia

ISSN 1865-3529 ISSN 1865-3537 (electronic)
Green Energy and Technology
ISBN 978-981-13-2235-8 ISBN 978-981-13-2236-5 (eBook)
https://doi.org/10.1007/978-981-13-2236-5

Library of Congress Control Number: 2018952624

This Springer imprint is published by the registered company Springer Nature Singapore Pte Ltd.
The registered company address is: 152 Beach Road, #21-01/04 Gateway East, Singapore 189721, Singapore

Dominic C. Y. Foo would like to dedicate this book to his wife Cecilia, his kids Irene, Jessica and the new born baby Helena.

Mustafa Kamal Tun Abdul Aziz would like to dedicate this book to his late father, Tun (Dr.) Abdul Aziz Abdul Majid and mother, Toh Puan Raja Teh Zaitun Kamarulzaman, as well as to Noor Azian, Abdul Muhaimin and Abdul Aziz.

Foreword

The Malaysian oil palm industry has faced various challenges since its first commercial planting in Malaysia in 1917. Over the last 100 years, the industry has faced health, nutrition and environmental issues. We have always been at the forefront in responding to these numerous challenges. Malasia is often seen as the leading innovator in managing the requirements of sustainability, conservation and economic development in a balanced manner, in line with the 3Ps (People, Planet, Profit) and the UN's Sustainable Development Goals (SDGs).

However, more and rigorous sustainability demands are being made on agro-based industries globally. This is particularly true for the energy sector, which has been targeted for the accelerated effects of climate change coupled with the release of more greenhouse gas (GHG) emissions, despite adaptations of renewable energy mandate. This has led to the emergence of green technologies which aim provide more environment-friendly and sustainable forms of renewable energy.

The Malaysian oil palm sector is fortunate to be gifted with a multitude of green technologies. For example, methane gas captured at palm oil mills that can reduce up to 40% of palm oil's GHG emissions and utilising oil palm biomass such as empty fruit bunches, fronds, shells, and trunks to produce renewable energy, second-generation biofuels and bio-based chemicals, are providing key drivers for oil palm cultivators.

This book focuses on the innovative utilisation of green technologies in palm oil milling processes, and how these innovations enhance the values found in the palm oil supply chain. While such innovations are technically viable, the real challenge would be their adoption in the commercial environment.

Finally, we would like to congratulate the editors for initiating this project and making this publication a reality. We hope that the book would be a useful reference to the oil palm industry that is looking to explore and adopt new green technology innovations in their pursuit of higher sustainability commitments.

Petaling Jaya, Malaysia

Datuk Dr. Kalyana Sundram
Chief Executive Officer
Malaysian Palm Oil Council (MPOC)

Preface

The palm oil industry is an important commodity sector in Malaysia. Oil palm tree originated in West Africa and was planted in Peninsular Malaysia as earlier as 1917. Significant growth in the plantation area was observed in the 70s, following the collapse of the global price of rubber (which was the main agricultural output of Malaysia back then).

The Malaysia Palm Oil Board (MPOB) reported that in the year 2017, Malaysia had 5.81 million hectares of oil palm planted area and produced approximately 20 million MT of crude palm oil (CPO). Total exports of oil palm products (palm oil, palm kernel oil, palm kernel cake) were reported at 23.97 million MT, contributing to the total export revenue increasing to RM 77.85 billion (approximately USD 19.5 billion). The three main export markets for Malaysian palm oil are India (2.03 million MT, 12.2% of total palm oil exports), the European Union (1.99 million MT, 12.0%) and China (1.92 million MT, 11.6%). On the other hand, the EU was the major export market for palm kernel oil (0.25 million MT, 25.9%), followed by China (0.17 million MT, 17.6%) and Turkey (0.08 million MT, 8.3%). For palm kernel cake (PKC), the major export markets in 2017 were New Zealand (0.65 million MT, 29.4% of total PKC export) and the EU (0.48 million MT, 21.9%).

Even though the trading records have seen a healthy growth in the long run, the palm oil industry does suffer some recurring issues, such as low oil extraction rate (MPOB reported the 2017 national oil extraction rate as 19.7%), labour-intensive and some controversial issues on sustainability, e.g. deforestation. It is also worth noting that the availability of cheap foreign labour has suppressed the initiative for innovation in the palm oil industry.

This book is meant to address some of the above issues. It comprises eight chapters outlining the state-of-the-art advances in palm oil milling processes from renowned experts and researchers. These chapters may be read independently of each other without a particular sequence. Synopses of all chapters are given as follows.

Synopses of Chapters in Part I—New Technologies for Palm Oil Mills

This part consists of four chapters on new technologies developed for the palm oil milling processes. Chapter "Flowsheet Synthesis and Optimisation of Palm Oil Milling Processes with Maximum Oil Recovery" by Foong and co-workers describes an optimisation model that can be used for synthesising a palm oil milling process flow sheet that maximises oil recovery. In Chapter "Alternative Solvent Design for Oil Extraction from Palm Pressed Fibre via Computer Aided Molecular Design", computer-aided molecular design (CAMD) tool was used to design alternative solvent for oil extraction from palm-pressed fibre. Chapter "Green Extraction Process for Oil Recovery Using Bio-Ethanol" by Abdul Aziz and co-workers discusses process development for green extraction processes for waste oil recovery. Chapter "Palm Oil Mill Effluent (POME) Treatment—Current Technologies, Biogas Capture and Challenges" by Chan and Chong outlines the state-of-the-art techniques for POME treatment, as well as the latest technologies developed for biogas capture, which is commonly carried out in Malaysian palm oil mill.

Synopses of Chapters in Part II—Palm Biomass and Biomass Supply Chain

This part consists of four chapters that focus on palm biomass and its supply chain problems. Chapter "Numerical Methods to Estimate Biomass Calorific Values via Biomass Characteristics Index" by Tang et al. describes the development of a new index that may be used to estimate calorific values for various biomass. Foo's Chapter "A Simple Mathematical Model for Palm Biomass Supply Chain" describes a linear programming model that can be used to determine optimum allocation of biomass. The next chapter, How's "An Overview of Palm Biomass Supply Chain Modelling", describes the state-of-the-art techniques for detailed modelling and optimisation of a palm biomass supply chain. Finally, Chapter "Cooperative Game Theory Analysis for Implementing Green Technologies in Palm Oil Milling Processes", by Andiappan et al., introduces the eco-industrial park concept for the oil palm industrial players.

Together, these eight chapters present some newly developed green technologies in the palm oil industry. It is our hope that the readers will be inspired by the idea and innovation discussed in these chapters, which might then help to add value to the palm oil industry and its value chain.

Semenyih, Malaysia

Dominic C. Y. Foo
Mustafa Kamal Tun Abdul Aziz

Acknowledgements

First and foremost, we wish to thank the authors who contributed their invaluable expertise in the form of chapters covering various green technologies in palm oil processing. The value of this book is based primarily on their inputs. We are also grateful to the staff of Springer Nature, who provided invaluable assistance throughout the long process of publication.

Both editors would like to acknowledge the Ministry of Higher Education, Malaysia, for providing Long Term Research Grant Scheme (LRGS; UPM/700-1/3/LRGS—Enhancing Productivity and Sustainability of Palm Oil Milling Industry) that funded some of the research activities between the years 2013–2018.

Finally, we would like to thank our family members for their support throughout our professional careers. In particular, Dominic Foo would like to thank his wife Cecilia Cheah for the tremendous support, especially in taking care of their kids—Irene, Jessica and Helena. Mustafa Kamal would like to acknowledge his research officers Noor Baini Binti Nabila Mohamad and Mohd Rizuan Bin Mansor for their dedicated research work and Universiti Teknologi Sdn Bhd (UTSB) for managing the LRGS fund.

Dominic C. Y. Foo
Mustafa Kamal Tun Abdul Aziz

Contents

Part I
New Technologies for Palm Oil Mills

Flowsheet Synthesis and Optimisation of Palm Oil Milling Processes with Maximum Oil Recovery

Steve Z. Y. Foong, Viknesh Andiappan, Dominic C. Y. Foo and Denny K. S. Ng

Abstract Crude palm oil (CPO) is produced in palm oil mills (POMs) using fresh fruit bunches (FFBs), harvested from oil palm plantations. FFB passes through multiple unit operations in the milling process, each consists of different technologies. Palm oil millers have tried to improve the milling technologies collectively and individually to enhance the extraction efficiency, meeting the process and product requirements. However, oil lost in the milling process remains the major issue in POM and leads to heavy loss of profit. In order to address such issue, oil recovery technologies were introduced and implemented in the current POM. Nevertheless, such technologies come with additional capital investment and operating costs that may outweigh the profit generated. Therefore, in this work, a systematic approach is presented to synthesise the palm oil milling processes with oil recovery technologies which is technically and economically feasible.

Keywords Palm oil mill · Process synthesis · Process optimisation
Oil recovery technologies

S. Z. Y. Foong · D. C. Y. Foo · D. K. S. Ng (✉)
Department of Chemical and Environmental Engineering/Centre of Sustainable Palm Oil Research (CESPOR), The University of Nottingham Malaysia Campus, Broga Road, 43500 Semenyih, Malaysia
e-mail: Denny.Ng@nottingham.edu.my

S. Z. Y. Foong
e-mail: Stevefoong92@gmail.com

D. C. Y. Foo
e-mail: Dominic.Foo@nottingham.edu.my

V. Andiappan
School of Engineering and Physical Sciences, Heriot-Watt University Malaysia, Wilayah Persekutuan Putrajaya, 62200 Putrajaya, Malaysia
e-mail: V.murugappan@hw.ac.uk

D. C. Y. Foo and M. K. Tun Abdul Aziz (eds.), *Green Technologies for the Oil Palm Industry*, Green Energy and Technology, https://doi.org/10.1007/978-981-13-2236-5_1

Nomenclature

Abbreviation	Description
AOT	Annual Operational Time
CPO	Crude Palm Oil
CPKO	Crude Palm Kernel Oil
DC	Decanter Cake
DOE	Department of Environment
EFB	Empty Fruit Bunch
FFB	Fresh Fruit Bunch
L	Oil Loss
LPS	Low Pressure Steam
MILP	Mixed-Integer Linear Programming
MINLP	Mixed-Integer Nonlinear Programming
MPOB	Malaysian Palm Oil Board
MPS	Medium Pressure Steam
MT	Metric Tonne
PEFB	Pressed Empty Fruit Bunch
PK	Palm Kernel
PKS	Palm Kernel Shell
POM	Palm Oil Mill
POME	Palm Oil Mill Effluent
PPF	Palm Pressed Fibre
PSE	Process Systems Engineering
R	Oil Recovery
X	Mass Conversion

Sets	Description
e	Index for electricity
i	Index for feedstocks
j	Index for technologies at level j
j'	Index for technologies at level j'
p	Index for intermediate products
p'	Index for final products
u	Index for utility

Variables	Description
B_j	Binary variable denoting the existence of technology j
$B_{j'}$	Binary variable denoting the existence of technology j'
CRF	Capital recovery factor
$CAPEX$	Total capital cost
E_e^{Con}	Total electricity consumption
E_e^{Demand}	Total electricity demand
EP	Economic performance
F_{LPS}^{Con}	Total flowrate of low pressure steam

F_{MPS}^{Con}	Total flowrate of medium pressure steam
F_{u}^{Con}	Total flowrate of utilities
F_{water}^{Con}	Total flowrate of utility water
F_{u}^{Demand}	Total utility demand
F_{j}^{Design}	Design capacity of technology j
$F_{j'}^{\text{Design}}$	Design capacity of technology j'
F_{ij}	Flowrate of feedstock i to technology j
$F_{j'p'}$	Flowrate of final product p' from technology j'
F_{jp}	Flowrate of intermediate product p from technology j
F_{p}	Flowrate of intermediate products p
$F_{p'}$	Flowrate of final products p'
$F_{pj'}$	Flowrate of intermediate products p to technology j'
F_{PL}	Total flowrate of pressed liquid
F_{SFB}	Total flowrate of sterilised fruit bunch
GP	Total gross profit
O_{i}	Oil content of feedstock i
O_{p}	Oil content of intermediate product p
$O_{p'}$	Oil content of final product p'
$OPEX$	Total operating cost
OP_{p}	Oil percentage of intermediate product p
$OP_{p'}$	Oil percentage of final product p'
z_{j}	Number of units of technology j selected
$z_{j'}$	Number of units of technology j' selected

Parameters	**Description**
C_{e}	Cost of electricity e
C_{i}	Cost of feedstock i
C_{u}	Cost of utility u
$\mathrm{C}_{p'}$	Cost of final product p'
CC_{j}	Capital cost for technology j
$\mathrm{CC}_{j'}$	Capital cost for technology j'
F_{i}	Flowrate of feedstock i
L_{ijp}	Percentage oil loss technology j
$\mathrm{L}_{pj'p'}$	Percentage oil loss technology j'
OC_{j}	Operating cost for technology j
$\mathrm{OC}_{j'}$	Operating cost for technology j'
OP_{i}	Oil percentage of feedstock i
r	Discount rate
R_{ijp}	Percentage oil recovery technology j
$\mathrm{R}_{pj'p'}$	Percentage oil recovery technology j'
$\mathrm{t}_{k}^{\max}$	Operational lifespan
U_{ujp}	Utility specification of intermediate product p for technology j
$\mathrm{U}_{uj'p'}$	Utility specification of final product p' for technology j'
X_{ijp}	Component mass conversion of feedstock i
$\mathrm{X}_{pj'p'}$	Component mass conversion of intermediate product p

Y_{ej}	Electricity consumption rate per unit of technology j
$Y_{ej'}$	Electricity consumption rate per unit of technology j'
$Y_{ej'p'}$	Electricity consumption rate of technology j' per unit of final product p' produced
Y_{ejp}	Electricity consumption rate of technology j per unit of intermediate product p produced

1 Introduction

Over the past few decades, palm oil industry has expanded dramatically as one of the major oils and fats providers for global needs. In year 2016, palm oil contributes up to 30% of oils and fats production globally [39]. As reported by American Soybean Association [60], palm oil accounts for 68.9 million metric tonnes (MT) out of 203 million MT of vegetable oils consumed worldwide (contributed to 34%). Note that more than 20 million MT of crude palm oil (CPO) are produced annually in Malaysia [34], making Malaysia the second largest producer and exporter of palm oil products after Indonesia. As the second largest producer and exporter of CPO, Malaysia plays an important role in fulfilling the growing global need for oils and fats sustainability.

In the palm oil industry, fresh fruit bunch (FFB) is first harvested in oil palm plantation and sent to palm oil mill (POM) to produce CPO. On the other hand, the generated palm kernel (PK) is sent to kernel crushing plant for production of crude palm kernel oil (CPKO). During the milling process, by-products, such as palm pressed fibre (PPF), palm kernel shell (PKS), emptyfruit bunch (EFB), decanter cake (DC) and palm oil mill effluent (POME) are generated. Both CPO and CPKO will be further refined into various products (e.g. edible oil, stearine, lubricant, etc.) in refinery. A major issue found in the POM is the low oil recovery (or high oil lost) during milling process. To address this issue, various technologies such as tilted steriliser, double screw press, vacuum clarifier, etc. have been developed. However, such technologies come with additional capital investment and operating costs. Therefore, a study to trade-off between increments in oil yield with costs is necessary. Besides, the total oil balance of the entire milling process based on the input of oil in FFB and output of oil from the milling process has yet to be studied. Hence, there is a need to develop a systematic approach for flowsheet synthesis and optimisation of palm oil milling process with maximum oil recovery.

In the following sections, systematic approaches for flowsheet synthesis are first reviewed. In Sect. 2, a problem statement for this work is presented, followed by the development in palm oil milling processes in Sect. 3. A detailed formulation for material balance, utility balance and economic analysis is given in Sect. 4. Next, a typical palm oil milling process in Malaysia is synthesised and optimised based on the proposed framework in Sect. 5. Lastly, a conclusion of this work is drawn and given at the end of this chapter.

1.1 Systematic Approach for Flowsheet Synthesis

Various process synthesis tools have been established to design chemical processes in the industry [23, 58]. Nishida et al. [43] defined process design as the *selection of a particular interconnection of processing systems which meet certain constraints out of a large number of alternatives*. A flowsheet is the optimal interconnection of processing systems as well as the optimal type and design of the units within a process system [17]. *Process Systems Engineering* (PSE) is a field in which systematic computer-based approaches are developed to synthesise a flowsheet [53]. Various approaches have been developed to provide a methodological framework in designing chemical processes [57].

Conventionally, flowsheet synthesis is carried out in a hierarchical approach which is divided into three distinct levels, namely synthesis optimisation, design optimisation and operational optimisation, to be solved in sequence [15]. The hierarchical approach is well recognised in the field of process synthesis [12, 11]. The onion model is proposed as a hierarchical decision-making tool for process synthesis [30, 56]. Following that, hierarchical approach has been used in various studies for the synthesis of wastewater treatment [16], thermal [37], biorefinery [42, 52] and chlor-alkali production systems [55], etc. On the other hand, mathematical programming approaches were developed for flowsheet synthesis by screening a wide range of possible flowsheet alternatives under any possible circumstance. As shown in the literature, many mathematical optimisation approaches for flowsheet synthesis have been presented. For instance, Grossmann and Santibanez [19] presented a mixed-integer linear programming (MILP) model for flowsheet synthesis. Biegler et al. [4] developed an alternative MILP model for flowsheet synthesis with consideration of mass and energy balances, equipment sizing and costing, economic evaluation, process simulation and optimisation. Besides, various mathematical optimisation models have been developed to synthesise water network [27], trigeneration [32, 62], biorefinery [28, 41], hydrocarbon biorefineries [61], industrial symbiosis [40], biomass trigeneration [2, 3], biogas systems [46], etc.

Most papers discussed earlier focused on integrated biorefinery, resources network or energy systems in which water and energy (i.e. heat and electricity) consumptions are used as the major parameter in the optimisation models. However, it is noted that limited of these works discussed on the synthesis of POM flowsheet. Recently, Foong et al. [14] presented a systematic approach to synthesise palm oil milling process. CPO serves as the main product and income generator in a POM. With respect to that, it is essential to trace the oil content across the flowsheet synthesised which has not been done in the previous research works. The optimal technology selection for FFB processing with consideration of oil content, energy consumptions, process capacity and their respective economic interests shall be performed. With respect to this, it is essential to develop a systematic approach to synthesise and optimise a milling process with maximum oil recovery. To illustrate the proposed approach, a typical palm oil milling process case study in Malaysia is solved.

2 Problem Statement

Due to the variety in established technologies available in market, the synthesis of an optimal POM configuration is highly complicated. A simplified generic graphical representation of model is shown in Fig. 1. The synthesis problem addressed is stated as follows. The feedstock i with given flowrate of F_i (in this case, FFB is the only feedstock) can be converted to intermediate product $p \in P$ (e.g. sterilised fruit bunch, F_{SFB}, pressed liquid, F_{PL}, etc.) through technology $j \in J$. Intermediate product p can then be further converted to final product $p' \in P'$ (e.g. CPO and PK) via technology $j' \in J'$. By-products (e.g. PKS, PPF, DC, etc.) are represented as a form of intermediate product p or final product p' in the model. The oil content of feedstock i, intermediate product p and final product p' are defined as O_i, O_p and $O_{p'}$ respectively. Note that every technology $j \in J$ and $j' \in J'$ may have more than one inlet and outlet stream, allowing every stream to merge or split, depending on constraints set on the model. Besides, intermediate product p can also be taken as final product p' if it could be sold directly. The mass conversion (X), oil loss (L) and oil recovery (R) of technology j from feedstock i and technology j' from intermediate product p are specified as X_{ijp}, $X_{pj'p'}$, L_{ijp}, $L_{pj'p'}$ R_{ijp} and $R_{pj'p'}$ respectively. Meanwhile, utility consumption F_u^{Con} (e.g. low pressure steam, F_{LPS}^{Con}, medium pressure steam, F_{MPS}^{Con} and utility water, F_{water}^{Con}) and electricity consumption E_e^{Con} for the entire mill are specified as U_{ujp}, Y_{ejp} for technology j and $U_{uj'p'}$, $Y_{ej'p'}$ for technology j'.

In this work, the objective is to develop a systematic approach, generating an optimal and robust POM configuration with maximum economic performance (*EP*). The oil loss and oil recovery in every technologies $j \in J$ and $j' \in J'$ will be traced accordingly. Usually, the available equipment in the market have a fixed design capacity of technology j (F_j^{Design}) and j' ($F_{j'}^{Design}$); therefore, the proposed approach will determine the number of units required for technologies j and j' selected, represented by z_j and $z_{j'}$ respectively. The total capital cost, *CAPEX* and total operating cost, *OPEX* can be calculated based on the costs of selected technologies j and j' (CC_j, $CC_{j'}$, OC_j and $OC_{j'}$). The following section provides a better insight on the process in which the development of palm oil milling technologies will be discussed in detail.

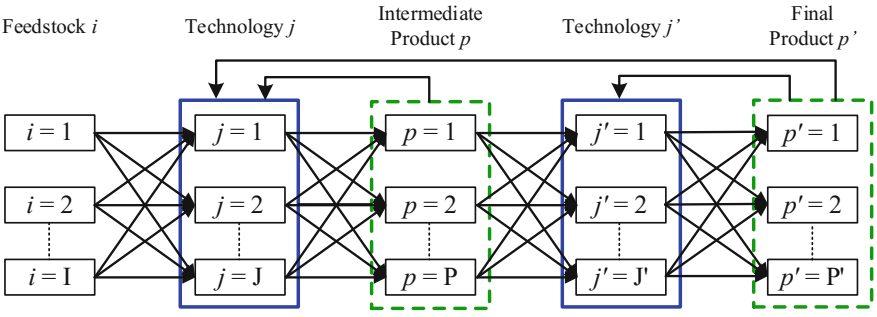

Fig. 1 Generic representation of superstructure for scenarios [14]

3 Development in Palm Oil Milling Processes

Figure 2 shows a typical process flow diagram of palm oil milling process. As shown, the process can be generally divided into several unit operations. Firstly, FFB is sterilised to ease the separation of fruitlets and EFB. Most of the POMs in Malaysia are using horizontal cylindrical vessels with three bar steams for sterilisation process [49]. Since the last decade, continuous steriliser [26] and tilting steriliser [31] were introduced to improve milling efficiency by lowering labour and maintenance cost. However, the capital cost of the new type of steriliser is higher comparing to the conventional horizontal steriliser. Depending on the type of sterilisation technology and availability of steam, several sterilisation patterns from single- to triple-peak steam cycles are practised [13]. By using different patterns of sterilisation process, the oil yield will be improved. Upon sterilisation, the fruitlets and EFB are threshed via rotating or fixed drum equipped with rotary beater bars [9]. Meanwhile, POME and EFB are generated in sterilisation and threshing process respectively.

The separated fruitlets, which consist of palm nuts and mesocarp fibres, are then sent to the digestion process. Under the high-pressure condition in a steam-jacket drum, fruitlets will be digested in which oil is released through the rupture of oil-

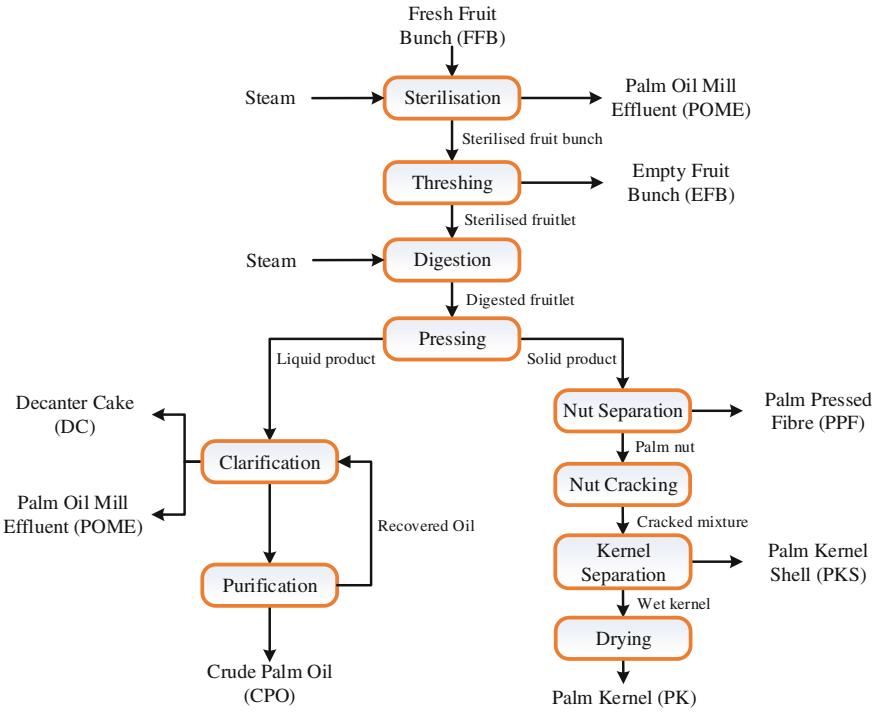

Fig. 2 Typical palm oil mill processing unit operations [14]

bearing cells [49]. Next, the digested fruitlets go through a pressing system to squeeze out the oil from mesocarp fibres in the fruitlets. Mechanical screw press is commonly used in the pressing process. Double screw press with twin screws rotating in opposite directions was introduced to increase the pressing efficiency [47]. Due to its larger capacity and shorter processing time, double screw press is favourable in the milling industry [22]. During the pressing process, solid and liquid products are generated. The solid product consists of a mixture of mesocarp fibres and palm nuts. Meanwhile, a mixture of water (45–55%), palm oil (35–45%) and fibrous materials are also produced [8].

For the solid products, the fibres and palm nuts can be separated via inclined rotary separator [45], or depericarper which based on air floatation concept [20]. Maycock [38] introduced ripple mill cracker where the palm nuts were cracked and air cyclone is used to remove the dust particles of the cracked mixture [24]. The cracked mixture from the palm nuts, which consist of PK and PKS is separated via clay bath or hydrocyclone based on the difference in specific gravity [21]. Meanwhile, a new cracking process known as Rolek nut cracker [50], followed by a multiple-staged winnowing system [51] with higher efficiency were introduced.

To improve the removal efficiency of the entrained impurities (water and fibrous materials) from the oil, hot water is added in clarification tank [49]. Jorgensen and Singh [25] proposed to combine a two-phase decanter with a rotate drum drier to reduce the amount of water needed. Recently, three-phase decanter is introduced to replace clarification tank and sludge centrifuge [1]. In this process, the entrained solid particles are removed as DC while water is removed as POME. The oil is then further purified into CPO through centrifugal and drying operations. In order to minimise deterioration in oil quality, the purified CPO must be stored between 32 and 40 °C [6].

Based on above discussion, it is noted that there are many alternative technologies that can be used to improve the overall efficiency of POM. Note also that throughout the milling process, various by-products are generated with oil being trapped and remains unrecovered. For example, 10.6 g/L of oil and grease were trapped in POME [5]. Meanwhile, EFB and PPF contains approximate 3–4% [18] and 1.8–3.96% [59] (wet basis) of residual oil respectively. According to [7], an estimation of 10% oil lost across multiple unit operations in the milling process. Therefore, oil loss is a critical issue in POM as it causes a significant impact on the economic performance of POMs. To overcome this issue, various research and development works were conducted to recover the oil from by-products. For instance, EFB screw press and three-phase decanter were introduced to recover oil from EFB and improve the overall oil extraction efficiency. However, most technology providers only focused on individual equipment or process. The oil balance for the entire milling processes is not being assessed. Hence, this is the subject of this work. It is important to synthesis and optimise the entire milling process simultaneously to maximise oil recovery in POM, thus achieving a greater economic performance. Material and energy flows of the entire process as well as expected productivity of the developed POM flowsheet can be determined. Based on the proposed approach, aspects such as process synthesis (e.g. system configuration and technology selection) and design optimisation (e.g. capacity, number of units) within the milling process can also be identified.

The following section clarifies the developed model, the parameters and the variables involved in a more descriptive manner. The equations formulating the optimisation model are clearly presented and defined methodically to deliver a smooth learning of the constructed model.

4 Mathematical Model Formulation

As mentioned earlier, a systematic optimisation approach to synthesise a palm oil milling process is developed in this work. Figure 1 shows the generic superstructure of a palm oil milling process. The following subsections present a detailed formulation for the proposed model. Note that italic mathematical notations represent variables in the mathematical model while non-italic notations are fixed parameters.

4.1 Material Balance

Equation (1) shows the component balance for feedstock i where F_i represents the flowrate of feedstock i which may be sent to potential technology j with flowrate of F_{ij}

$$\mathrm{F}_i = \sum_{j=1}^{\mathrm{J}} B_j F_{ij} \quad \forall i \tag{1}$$

$$B_j \in \{0, 1\} \quad \forall j, \tag{2}$$

where B_j is a binary variable denoting the existence of technology j (Eq. 2). Multiple technology j options are given for selection, but, in order to reduce the maintenance and operation costs, only one type of technology j will be selected. Hence, additional constraint Eq. (3) is introduced.

$$\sum_{j=1}^{\mathrm{J}} B_j = 1 \tag{3}$$

The oil content of feedstock i (O_i) is calculated using Eq. (4)

$$O_i = \mathrm{F}_i \mathrm{OP}_i \quad \forall i \tag{4}$$

where OP_i is the oil percentage of feedstock i.

In technology j, feedstock i is converted to intermediate product p with conversion X_{ijp}. The total production rate for intermediate product p (F_p) for all technologies j is given in Eq. (5).

$$F_p = \sum_{i=1}^{\mathrm{I}} \sum_{j=1}^{\mathrm{J}} B_j F_{ij} \mathrm{X}_{ijp} \quad \forall p \tag{5}$$

Next, intermediate product p can be distributed to secondary technology j' for further processing to produce final product p'. The component balance for intermediate product p is shown in Eq. (6) where F_p represents the flowrate of intermediate product p which may be sent to secondary technology j' with flowrate of $F_{pj'}$

$$F_p = \sum_{j'=1}^{\mathrm{J}'} B_{j'} F_{pj'} \quad \forall p \tag{6}$$

$$B_{j'} \in \{0, 1\} \quad \forall j' \tag{7}$$

where $B_{j'}$ is a binary variable denoting the existence of technology j' (Eq. 7) and additional constraint Eq. (8) is introduced to avoid multiple technology j' selected.

$$\sum_{j'=1}^{\mathrm{J}'} B_{j'} = 1 \tag{8}$$

Technology j' then converts the intermediate product p ($F_{pj'}$) to final product p' with conversion $\mathrm{X}_{pj'p'}$. The total production rate for final product p' ($F_{p'}$) for technologies j' is given in Eq. (9).

$$F_{p'} = \sum_{p=1}^{\mathrm{P}} \sum_{j'=1}^{\mathrm{J}'} B_{j'} F_{pj'} \mathrm{X}_{pj'p'} \quad \forall p' \tag{9}$$

Equations (10) and (11) show the oil content of intermediate product p (O_p) and final product $p'\left(O_{p'}\right)$ respectively

$$O_p = O_i - \sum_{i=1}^{\mathrm{I}} \sum_{j=1}^{\mathrm{J}} B_j F_{ij} \mathrm{L}_{ijp} + \sum_{i=1}^{\mathrm{I}} \sum_{j=1}^{\mathrm{J}} B_j F_{ij} \mathrm{R}_{ijp} \quad \forall i,\ p \tag{10}$$

$$O_{p'} = O_p - \sum_{p=1}^{\mathrm{P}} \sum_{j'=1}^{\mathrm{J}'} B_{j'} F_{pj'} \mathrm{L}_{pj'p'} + \sum_{p=1}^{\mathrm{P}} \sum_{j'=1}^{\mathrm{J}'} B_{j'} F_{pj'} \mathrm{R}_{pj'p'} \quad \forall p,\ p' \tag{11}$$

where L_{ijp} and $\mathrm{L}_{pj'p'}$ represent these percentage oil loss while R_{ijp} and $\mathrm{R}_{pj'p'}$ represents the oil recovery across technologies j and j'. The oil percentage of intermediate product p (OP_p) and final product $p'\left(O\,P_{p'}\right)$ could then be calculated using Eqs. (12) and (13).

$$O\,P_p = \frac{O_p}{F_p} \times 100\% \quad \forall p \tag{12}$$

$$OP_{p'} = \frac{O_{p'}}{F_{p'}} \times 100\% \quad \forall p' \tag{13}$$

Despite that only two stages of conversion by technologies j and j' were shown in Fig. 1, the formulation can be expanded in a repetitive manner for any number of conversion stages to match the case study requirement.

4.2 Utility Balance

Utilities u (e.g. steam, electricity and water) are required for material conversion in technologies j and j'. Depending on the technology selected, amount and quality of utilities u consumed, varies accordingly. Total utility u consumption, F_u^{Con} and electricity e consumption, E_e^{Con} can be calculated with Eqs. (14) and (15).

$$F_u^{\mathrm{Con}} = \sum_{i=1}^{\mathrm{I}} \sum_{j=1}^{\mathrm{J}} B_j F_{ij} \mathrm{U}_{ujp} + \sum_{p=1}^{\mathrm{P}} \sum_{j'=1}^{\mathrm{J}'} B_{j'} F_{pj'} \mathrm{U}_{uj'p'} \quad \forall p' \tag{14}$$

$$E_e^{\mathrm{Con}} = \sum_{j=1}^{\mathrm{J}} \sum_{p=1}^{\mathrm{P}} B_j F_{ij} \mathrm{Y}_{ejp} + \sum_{j'=1}^{\mathrm{J}'} \sum_{p'=1}^{\mathrm{P}'} B_j F_{pj'} \mathrm{Y}_{ej'p'} + \sum_{j=1}^{\mathrm{J}} z_j \mathrm{Y}_{ej} + \sum_{j'=1}^{\mathrm{J}'} z_{j'} \mathrm{Y}_{ej'} \forall p' \tag{15}$$

where F_{ij} and $F_{pj'}$ are the flowrate of feed i and intermediate product p into technology j and j', U_{ujp} and $\mathrm{U}_{uj'p'}$ are the utility requirement per unit flowrate, Y_{ejp} and $\mathrm{Y}_{ej'p'}$ are the specified electricity consumption per product formation, Y_{ej} and $\mathrm{Y}_{ej'}$ are the electricity consumption per unit operation while z_j and $z_{j'}$ are the number of equipment unit needed for technologies j and j' respectively. As shown in Eqs. (16) and (17), the equipment units needed, z_j and $z_{j'}$ are determined based on the operating capacity

$$z_j \times \mathrm{F}_j^{\mathrm{Design}} \geq \sum_{p=1}^{\mathrm{P}} B_j F_{jp} \quad \forall j \tag{16}$$

$$z_{j'} \times \mathrm{F}_{j'}^{\mathrm{Design}} \geq \sum_{p'=1}^{\mathrm{P}'} B_{j'} F_{j'p'} \quad \forall j' \tag{17}$$

where $\mathrm{F}_j^{\mathrm{Design}}$ and $\mathrm{F}_{j'}^{\mathrm{Design}}$ represent the design capacities available to be purchased for technologies j and j' respectively. Both z_j and $z_{j'}$ are positive integers to reflect the number of units of technologies j and j' with given design capacity obtained in the literature. However, the design capacities used can be revised according to current market availability to provide a produce an up-to-date result.

In this work, it is assumed that due to inevitable losses in transmission and distribution of utility such as electricity and steam, an additional 20% of utility u consumption, F_u^{Con} and electricity e consumption E_e^{Con} were required, given in Eqs. (18) and (19)

$$F_u^{\text{Demand}} = 1.2\, F_u^{\text{Con}} \quad \forall u \tag{18}$$

$$E_e^{\text{Demand}} = 1.2\, E_e^{\text{Con}} \tag{19}$$

where F_u^{Demand} and E_e^{Demand} are the total utility demand and electrical demand of the milling process synthesised.

4.3 Economic Analysis

The economic feasibility (over a specified operation) of the milling process developed is evaluated via Eq. (20)

$$EP = GP - CRF \times CAPEX \tag{20}$$

where GP, CRF and $CAPEX$ represents the gross profit, capital recovery factor and total capital costs of the process developed respectively. Note that EP shall always be positive and a greater value indicates a greater interest in investing on the system developed. In the event where EP is a negative value, it means the cost is higher than the revenue and it is an infeasible design. GP can be calculated using Eq. (21)

$$\begin{aligned} GP = {} & \text{AOT} \\ & \times \left(\sum_{p'=1}^{\text{P}'} F_{p'} \text{C}_{p'} - \sum_{i=1}^{\text{I}} F_i \text{C}_i - \sum_{u=1}^{\text{U}} F_u{}^{\text{Demand}} \text{C}_u - \sum_{e=1}^{\text{E}} E_e{}^{\text{Demand}} \text{C}_e \right) \\ & - OPEX \quad \forall p', \forall i, \forall u \end{aligned} \tag{21}$$

where AOT is the annual operational time, $OPEX$ is the total operating costs, $\text{C}_{p'}$ is the selling price of final product p', C_i is the cost of feedstock (FFB), while C_u and C_e is the cost of utility and electricity purchased. The CRF is used to annualise capital costs by converting its present value into a stream of equal annual payments over a specified operation lifespan, $t_k^{\max}$ and discount rate, r. CRF is determined via Eq. (22).

$$CRF = \frac{\text{r}\,(1+\text{r})^{t_k^{\max}}}{(1+\text{r})^{t_k^{\max}} - 1} \quad k \in j, j' \tag{22}$$

$CAPEX$ and $OPEX$ are calculated based on the selected technologies j and j' as well as their equipment unit z_j and $z_{j'}$ required as shown in Eqs. (23) and (24)

$$CAPEX = \sum_{j=1}^{J} z_j \mathrm{CC}_j + \sum_{j'=1}^{J'} z_{j'} \mathrm{CC}_{j'} \tag{23}$$

$$OPEX = \sum_{j=1}^{J} z_j \mathrm{OC}_j + \sum_{j'=1}^{J'} z_{j'} \mathrm{OC}_{j'} \tag{24}$$

where OC_j and $\mathrm{OC}_{j'}$ are operating costs while CC_j and $\mathrm{CC}_{j'}$ are capital costs for technologies j and j' respectively.

To illustrate this proposed optimisation approach, a case study is presented based on information from literature and Malaysian palm oil industry. The developed MINLP model is solved via LINGO v14, with Global Solver [29], with an Intel® Core™ i5 (2 × 3.20 GHz) with 8 GB DDR3 RAM desktop unit.

5 Case Study

As discussed previously, FFBs obtained from plantation are converted into products CPO and PK in a POM. In the process, utilities such as water, steam and electricity are consumed. By-products such as PKS, EFB, POME, etc. are also being generated (as shown in Fig. 3). In Malaysia, a typical POM processes 60 t/h of FFBs for 12 h every day. In this case study, a potential owner in Malaysia is interested to optimise its POM to increase economic performance, *EP* with maximum oil recovery. As mentioned previously, the milling process consists of several unit operations and variety of technology available in the market for each operation. Thus, it is important to screen every alternative configuration to synthesise an optimal milling process. Table 1 shows the given economic parameters considered in this work.

According to MPOB [36], the oil content of FFB feedstock, OP_i is given in a range between 22 and 25%. For conservative measure, the FFB oil content is assumed as 22% in this work. Besides, the price of CPO generated fluctuates throughout the year, depending on the international economic conditions [33]. As a result, the price of FFB feedstock, other products and by-products changes with the price of CPO. In this case study, it is assumed that the average prices of CPO maintain at 548 USD/t. Table 2 shows the average pricing of the raw material, products and utilities used in this study.

Table 1 Economic parameters for case study

Annual operational time, AOT	4350 h/year
Operation lifespan, t_k^{max}	15 years
Discount rate, r	5%
Capital recovery factor, *CRF*	0.0963
Currency conversion rate	1 USD (4 MYR)

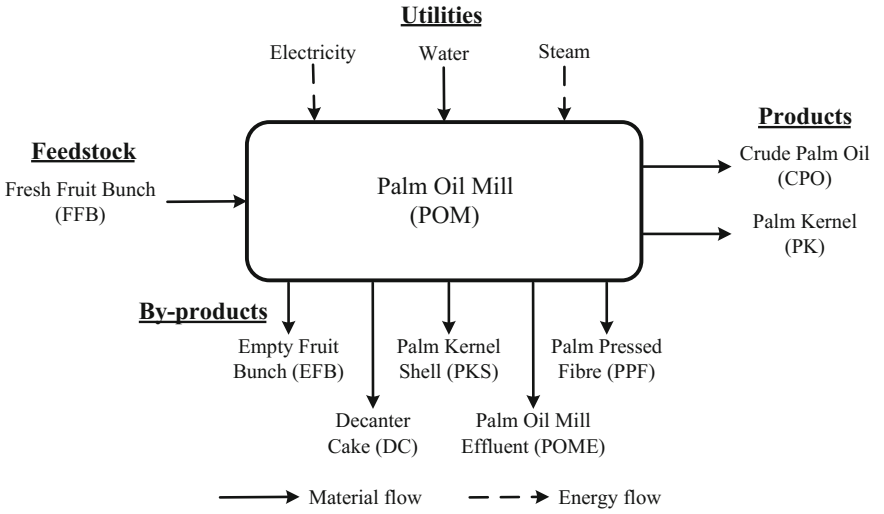

Fig. 3 Material and energy flow in palm oil mill [14]

Table 2 Cost of raw material, product and utilities

Materials/Utilities	Price
Raw material	
Fresh fruit bunch, FFB (USD/t)	121
Products	
Crude palm oil, CPO (USD/t)	548
Palm kernel, PK (USD/t)	389
By-Products	
Pressed empty fruit bunch, PEFB (USD/t)	8
Palm kernel shell, PKS (USD/t)	45
Palm pressed fibre, PPF(USD/t)	23
Decanter cake, DC (USD/t)	43
Utilities	
Utility water (USD/m^3)	0.55
Electricity (USD/kWh)	0.084
Medium pressure steam, MPS (USD/t)	17
Low pressure steam, LPS (USD/t)	12

All products and by-products are assumed to be sold at the POM. Hence, transportation cost and supply chain issue will not be considered in this work. A superstructure that incorporate all available technologies of a palm oil milling process is developed to include all possible technologies and configurations is showed in Fig. 4. A single box presented in the superstructure for technologies j and j' may consist of more than one equipment unit z_j and $z_{j'}$ required due to constant design capacity, F_j^{Design} and $F_{j'}^{Design}$ for each technology (as described in Eqs. 16 and 17).

Mathematical model based on Eqs. (1)–(24) was applied to synthesise and optimise a palm oil milling process for quantitative analysis. A list of technologies considered with design capacity, material conversion, utility requirement, oil loss, oil recovery, capital and operating cost in this case study is delivered in the Appendix.

To demonstrate the proposed work, a study with a milling process with maximum *EP* and oil recovery is synthesised to be compared with a conventional milling process practiced in the industry.

In this study, optimisation objective is set to maximise economic performance, *EP* subject to the mass and energy constraints. It is assumed the mill will have an operation lifespan, t_k^{max} of 15 years. The average material prices and utility costs are given in Table 2. The model is optimised based on optimisation objective as listed in Eq. (25), subject to the constraints given in Eqs. (1)–(24). The optimisation problem consists of 297 continuous variables with 52 nonlinear variables, 48 integer variables and 285 constraints. Negligible computational time (16 s) is required to achieve the global solution for the model developed (Fig. 5).

$$\text{Maximise } EP \tag{25}$$

The optimised economic parameters for the case study is summarised in Table 3, with the optimised POM configurations shown in Fig. 6. For comparison purpose, a conventional milling process is shown in Fig. 6, and its economic parameters are also given in Table 3. The *EP* values of 4.29 and 2.91 Million USD/y for optimal and conventional configurations are determined. It is clearly show that the synthesised flowsheet with oil recovery technologies is the better choice to invest on. It is found that additional 1.24 Million USD (=8.04–6.80 Million USD) of capital investment, *CAPEX* is required for the optimal configuration. Likewise, much higher gross profit, *GP* value (5.42 Million USD/y) was reported for the optimal design as compared to the conventional design (3.56 Million USD/y). Table 4 shows the net output of the POM and its utility consumptions. As shown, 12.4 t/h of CPO is produced in the optimal configuration. Meanwhile, in the conventional configuration, only 11.9 t/h of CPO is produced by the same amount of FFB feedstock (60 t/h). This is due to the increment in oil recovery by 3.90% (=9.62–5.72%), resulting in higher CPO yield for the optimal configuration. Note that the percentage of oil recovery represents the total oil content recovered in by-products (e.g. POME, PPF, EFB, etc.) from the oil content of FFB feedstock. Besides, a reduction in 4.1 m^3/h (21.9 − 17.8 m^3/h) of utility water is required, and 2.9 t/h (=44.6 − 41.7 t/h) of POME is generated in the optimal configuration. This means that the design is more environmental friendly than the conventional design. Furthermore, the total unit of equipment required is reduced by 2 units in the optimal configuration (shown in Tables 5 and 6). However, this configuration also requires higher operating costs, *OPEX* and consumes more electricity (Tables 3 and 4) due to the difference in technologies selected.

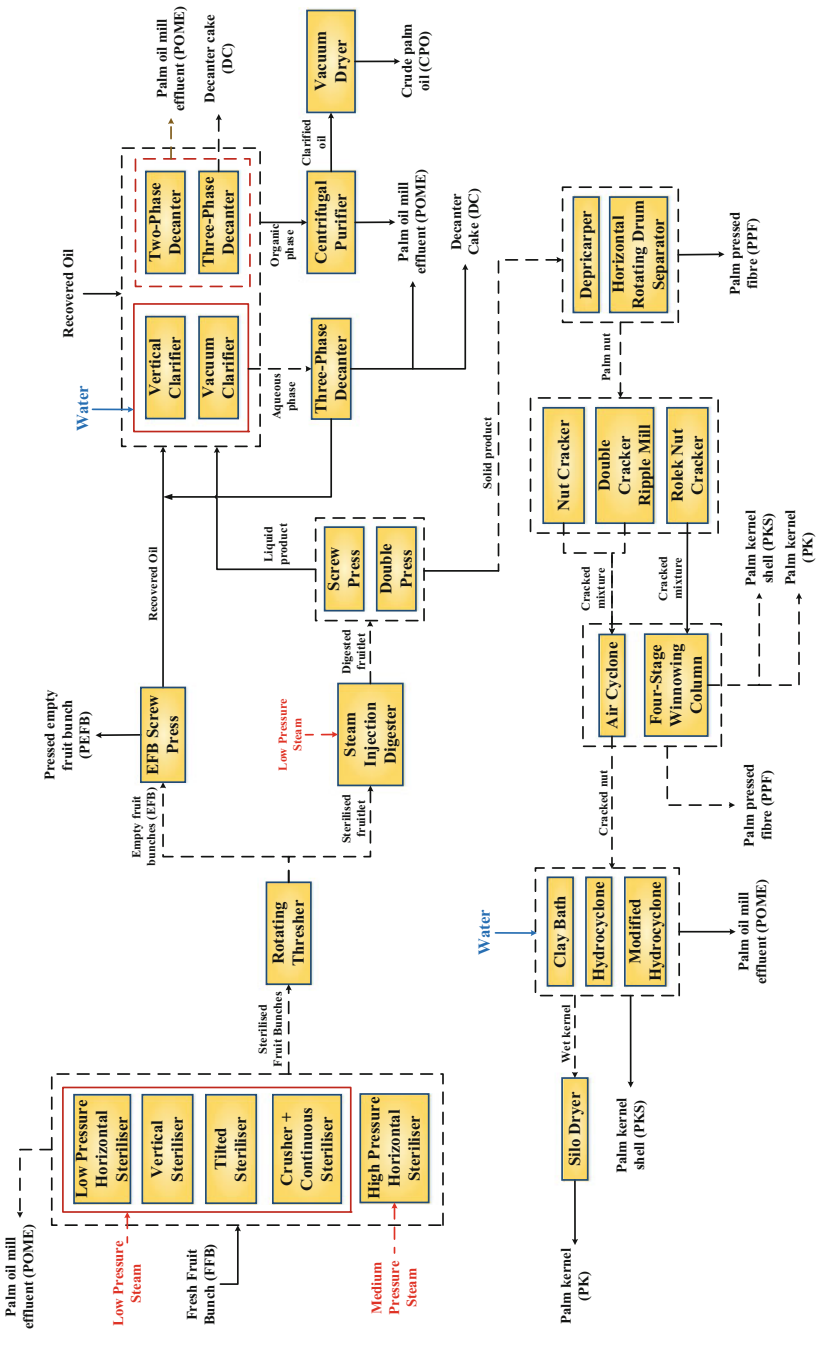

Fig. 4 Superstructure for palm oil milling processes [14]

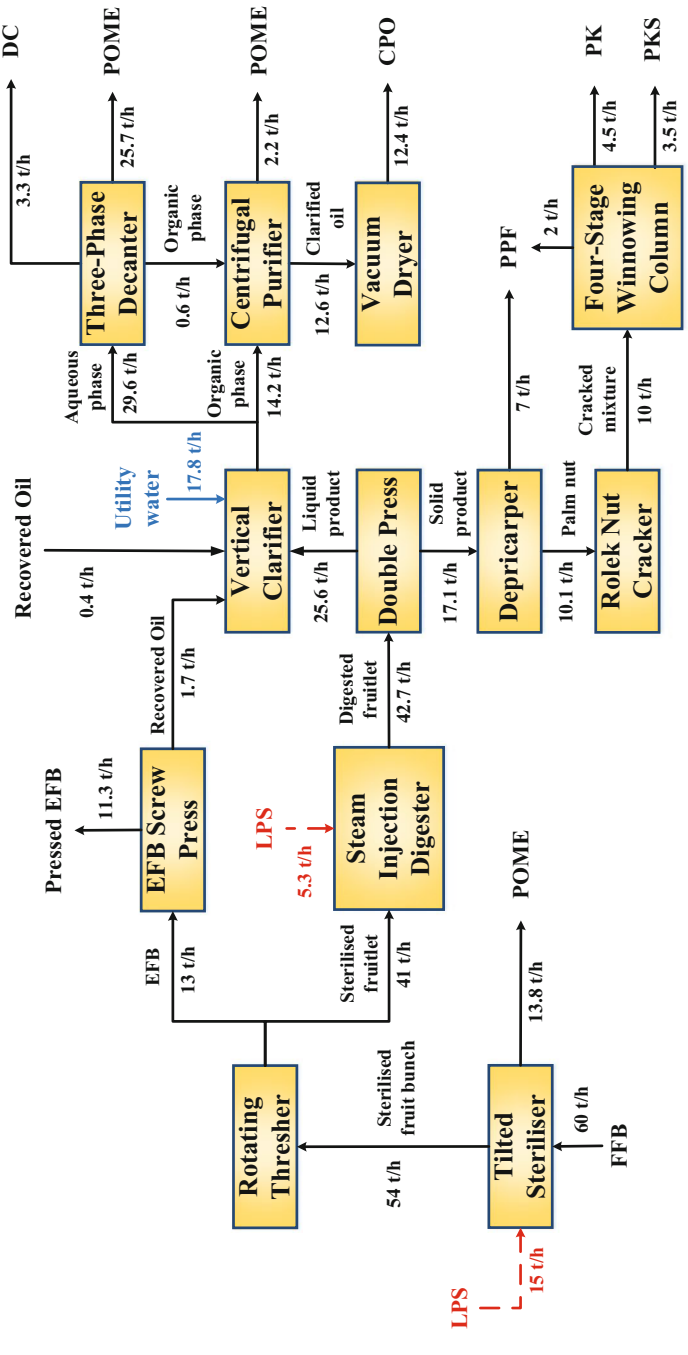

Fig. 5 Optimum palm oil mill configuration [14]

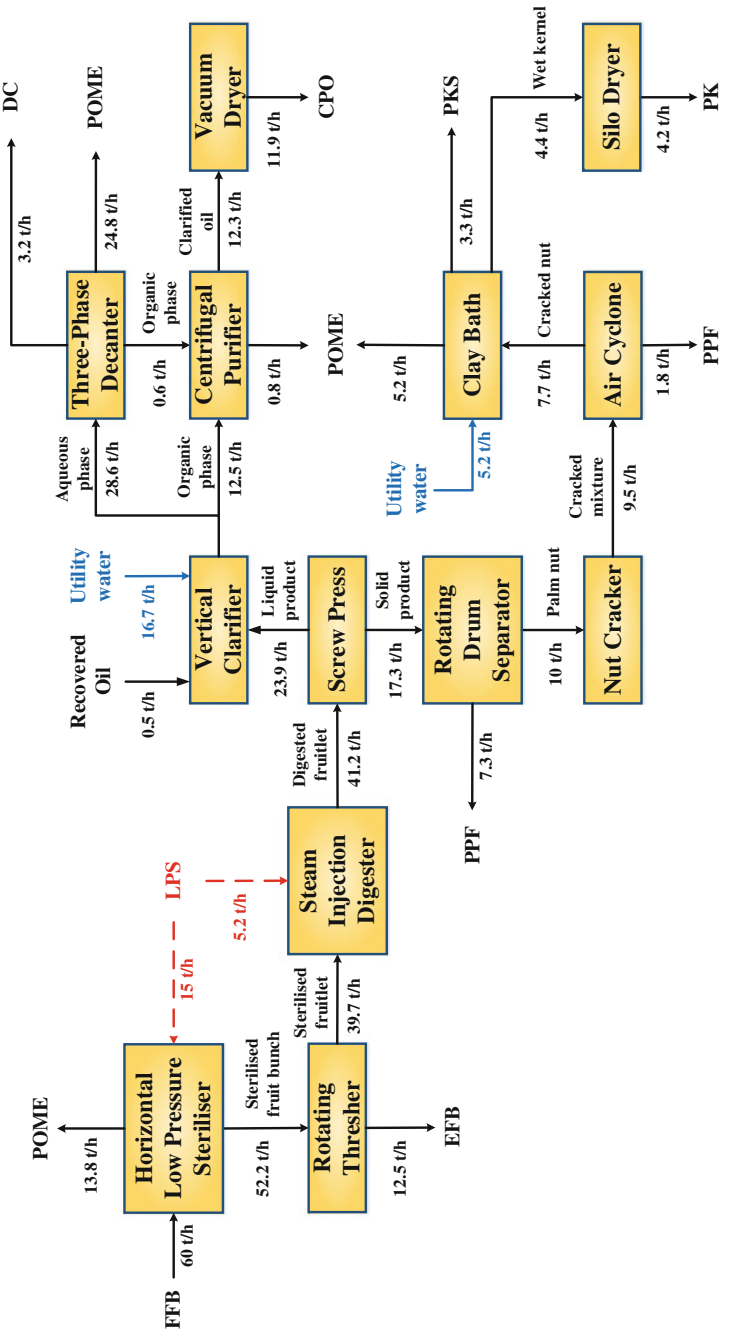

Fig. 6 Conventional palm oil mill configuration [14]

Table 3 Economic analysis for case study

Economic analysis	Optimal configuration	Conventional configuration
Capital cost, *CAPEX* (Million USD)	8.04	6.80
Operating cost, *OPEX* (Million USD/y)	1.13	1.03
Gross Profit, *GP* (Million USD/y)	5.42	3.56
Economic Performance, *EP* (Million USD/y)	4.29	2.91

Table 4 Products, by-products and utilities for case study

Materials	Flowrates	
	Optimal configuration	Conventional configuration
Products		
Crude palm oil, CPO (t/h)	12.4	11.9
Palm kernel, PK (t/h)	4.5	4.2
By-products		
Palm oil mill effluent, POME(t/h)	41.7	44.6
Palm kernel shell, PKS (t/h)	3.5	3.4
Decanter cake, DC (t/h)	3.3	3.2
Palm pressed fibre, PPF(t/h)	9.1	9.0
Empty fruit bunch, PEFB (t/h)	N/A	12.5
Pressed empty fruit bunch, PEFB (t/h)	11.3	N/A
Utilities consumption		
Utility water (m^3/h)	17.8	21.9
Low pressure steam, LPS (t/h)	20.3	20.2
Electricity, E (kWh)	940	840
Others		
Total oil lost (t/h)	0.78	1.30
Total oil recovered (t/h)	0.76	1.27
Percentage of oil recovery(%)	9.62	5.72

Table 5 Selected technologies and required units for optimal configuration

Technology selected	Design capacity	Optimum configuration (unit)
Tilted steriliser	20 t fresh fruit bunch	3
Rotating drum	40 t sterilised fruit bunch	2
Steam injection digester	20 t sterilised fruitlet	3
EFB screw press	10 t empty fruit bunch	2
Double screw press	25 t digested fruitlet	2
Depericarper	10 t pressed cake	2
Rolek nut cracker	10 t palm fruit nut	2
Four-stage winnowing column	15 t cracked mixture	1
Vertical clarifier	7 t pressed liquid	3
Vertical vacuum dryer	10 t organic phase	2
Three-phase decanter	20 t aqueous phase	2
Total unit		24

Table 6 Selected technologies and required units for conventional configuration

Technology selected	Design capacity	Conventional configuration (unit)
Horizontal low pressure steriliser	20 t fresh fruit bunch	3
Rotating drum	40 t sterilised fruit bunch	2
Steam injection digester	20 t sterilised fruitlet	3
Screw press	20 t digested fruitlet	2
Rotating drum separator	10 t pressed cake	2
Nut cracker	8 t palm fruit nut	2
Air Cyclone	8 t cracked mixture	2
Clay bath	5 t cracked nut	2
Silo dryer	15 t cracked mixture	1
Vertical clarifier	7 t pressed liquid	3
Centrifuge Purifier + Vacuum Dryer	10 t organic phase	2
Three-phase decanter	20 t aqueous phase	2
Total unit		26

6 Conclusion

In this work, a systematic approach for synthesis and optimisation of palm oil milling process with maximum oil recovery is presented. A systematic approach is adapted to simplify the overall formulation without losing the insights of interest for the effective design, synthesis and integration of the process. Various technologies currently available in the market were taken into consideration in developing the case study. The optimisation objective is to maximise *EP* generated based on a fixed amount of fruit available (60 t/h of FFBs). Technology selection and network design are performed simultaneously in a systematic manner with the material and energy flows for the process presented. It is shown that the optimal milling process developed generates higher *EP* as compared to the conventional process practiced in the industry. To top that up, the increment in oil recovery and environmental friendlier design further attracts the interest of potential owners to invest on the configuration developed. It is worth mentioning that the proposed approach can be easily revised and re-formulated to handle the possible uncertainties that may arise from the advancement of technologies, market price, etc. Future works may consider the variation in FFB feedstock supply throughout the year.

7 Further Reading

A detailed study with multiperiod consideration and sensitivity analysis on palm oil milling processes can be found in the original paper [14].

Acknowledgements The financial support from the Ministry of Higher Education, Malaysia through LRGS Grant (LRGS UPM Vot 5526100 and LRGS/2013/UKM-UNMC/PT/05) is gratefully acknowledged. Industrial data provided by Havy's Oil Mill is also accredited in building a realistic case study in this work.

Appendix

Capital cost and conversion data

Sterilisation technologies	Capital cost (USD) and Capacity	Materials and utilities	Amount required	Conversion of intermediate product	Oil loss (%)	Oil Rec.	References
Horizontal low-pressure steriliser	1,000,000/unit	Operating cost	200,000/unit	–	3.0%	–	*[49]
		Electricity	30 kWh/unit	–			
	20 t FFB/unit	LPS	0.25 t/t FFB	0.15 t steam lost			
		FFB	1 t	0.87 t sterilised fruit bunch			
				0.23 t POME			
Horizontal high-pressure steriliser	800,000/unit	Operating cost	160,000/unit	–	2.0%		[44]
		Electricity	17 kWh/unit	–			
	10 t FFB/unit	MPS	0.2 t/t FFB	0.11 t steam lost			
		FFB	1 t	0.90 t sterilised fruit bunch			
				0.19 t POME			
Vertical steriliser	1,000,000/unit	Operating cost	120,000/unit	–	4.0%		[49]
		Electricity	40 kWh/unit	–			
	20 t FFB/unit	LPS	0.305 t/t FFB	0.205 t steam lost			
		FFB	1 t	0.87 t sterilised fruit bunch			
				0.23 t POME			
Tilted steriliser	1,200,000/unit	Operating cost	180,000/unit	–	2.5%		[31]
		Electricity	75.4 kWh/unit	–			
	20 t FFB/unit	LPS	0.25 t/t FFB	0.14 t steam lost			
		FFB	1 t	0.90 t sterilised fruit bunch			
				0.23 t POME			
Crusher + Continuous Steriliser	1,050,000/unit	Operating cost	157,500/unit	–	3.0%		[26]
		Electricity	90 kWh/unit	–			
	20 t FFB/unit	LPS	0.36 t/t FFB	0.18 t steam lost			
		FFB	1 t	0.88 t sterilised fruit bunch			
				0.30 t POME			

(continued)

(continued)

Threshing technology	Capital cost (USD) and Capacity	Materials and utilities	Amount required	Conversion of intermediate product	Oil loss (%)	Oil Rec.	Reference
Rotating drum	225,000/unit	Operating cost	33,750/unit	–	4.0%	–	*[9]
	40 t sterilised fruit bunch/unit	Electricity	28 kWh/unit	–			
		Sterilised fruit bunch	1 t	0.76 t sterilised fruitlet			
				0.24 t empty fruit bunch			
Oil recovery technology	Capital cost (USD) and Capacity	Materials and utilities	Amount required	Conversion of intermediate product	Oil loss (%)	Oil Rec.	Reference
EFB screw press	120,000/unit	Operating cost	20,000/unit	–	–	60%	*[35]
	10 t empty fruit bunch/unit	Electricity	15 kWh/unit	–			
		Empty fruit bunch	1 t	0.1317 t recovered oil			
				0.8683 t pressed EFB			
Digestion technology	Capital cost (USD) and capacity	Materials and utilities	Amount required	Conversion of intermediate product	Oil loss	Oil Rec.	Reference
Steam injection digester	150,000/unit	Operating cost	15,000/unit	–	–	–	*[49]
	20 t sterilised fruitlet/unit	Electricity	18 kWh/unit	–			
		LPS	0.13 t/t FFB	0.09 t steam lost			
		Sterilised fruitlet	1 t	1.04 t digested fruitlet			
Pressing technologies	Capital cost (USD) and capacity	Materials and utilities	Amount required	Conversion of intermediate product	Oil loss(%)	Oil Rec.	Reference
Screw press	100,000/unit	Operating cost	20,000/unit	–	5.0%	–	*[48]
	20 t digested fruitlet/unit	Electricity	25 kWh/unit	–			
		Digested fruitlet	1 t	0.58 t pressed liquid			
				0.42 t pressed cake			
Double pressing	180,000/unit	Operating cost	36,000/unit	–	3.0%	–	[22, 47]
	25 t digested fruitlet/unit	Electricity	40 kWh/unit	–			
		Digested fruitlet	1 t	0.60 t pressed liquid			
				0.40 t pressed cake			

(continued)

(continued)

Nut separation technologies	Capital cost (USD) and capacity	Materials and utilities	Amount required	Conversion of intermediate product	Oil loss	Oil Rec.	References
Depericarper	250,000/unit	Operating cost	25,000/unit	–	–	–	[20]
	10 t pressed cake/unit	Electricity	68.6 kWh/unit	–			
		Press cake	1 t	0.59 t palm fruit nut			
				0.41 t PPF			
Rotating drum separator	200,000/unit	Operating cost	30,000/unit	–	–		*[45]
	10 t pressed cake/unit	Electricity	55.2 kWh/unit	–			
		Press cake	1 t	0.58 t palm fruit nut			
				0.42 t PPF			
Nut cracking technologies	Capital cost (USD) and capacity	Materials and utilities	Amount required	Conversion of intermediate product	Oil loss	Oil Rec.	References
Nut cracker	130,000/unit	Operating cost	26,000/unit	–	–	–	*[21]
	8 t palm fruit nut/unit	Electricity	26.4 kWh/unit	–			
		Palm fruit nut	1 t	0.95 t cracked mixture			
				0.05 t uncracked nut			
Double cracker ripple mill	175,000/unit	Operating cost	34,000/unit	–	–	–	[38]
	8 t palm fruit nut/unit	Electricity	35.3 kWh/unit	–			
		Palm fruit nut	1 t	0.98 t cracked mixture			
				0.02 t uncracked nut			
Rolek nut cracker	180,000/unit	Operating cost	36,000/unit	–	–	–	[50]
	10 t palm fruit nut/unit	Electricity	31.1 kWh/unit	–			
		Palm fruit nut	1 t	0.99 t cracked mixture			
				0.01 t uncracked nut			
Kernel separation technologies	Capital cost (USD) and capacity	Materials and utilities	Amount required	Conversion of intermediate product	Oil loss	Oil Rec.	References
Air Cyclone	70,000/unit	Operating cost	10,000/unit	–	–	–	*[24]
	8 t cracked mixture/unit	Electricity	18.6 kWh/unit	–			
		Cracked mixture	1 t	0.81 t cracked nut			
				0.19 t PPF			

(continued)

(continued)

Kernel separation technologies	Capital cost (USD) and capacity	Materials and utilities	Amount required	Conversion of intermediate product	Oil loss	Oil Rec.	References
Four-stage winnowing column	250,000/unit	Operating cost	13,000/unit	–	–	–	[52]
	15 t cracked mixture/unit	Electricity	29.2 kWh/unit	–			
		Cracked mixture	1 t	0.19 t palm pressed fibre			
				0.357 t PKS			
				0.453 PK			
Clay bath	35,000/unit	Operating cost	3500/unit	–	–	–	[24]
	5 t/unit	Electricity	40.2 kW/unit	–			
		Water	1.8 t/t cracked nut	1.8 t POME			
				0.571 t wet kernel			
		Cracked mixture	1 t	0.429 t PKS			
Hydrocyclone	40,000/unit	Operating cost	4000/unit	–	–	–	[21]
	5 t cracked mixture/unit	Electricity	37.5 kWh/unit	–			
		Water	1.7 t/t cracked nut	1.7 t POME			
				0.571 t wet kernel			
		Cracked mixture	1 t	0.429 t PKS			
Modified Hydrocyclone	50,000/unit	Operating cost	5000/unit	–	–	–	*
	5 t cracked mixture/unit	Electricity	30.5 kWh/unit	–			
		Water	1.5 t/t cracked nut	1.5 t POME			
				0.571 t wet kernel			
		Cracked mixture	1 t	0.429 t PKS			
Kernel drying technology	Capital cost (USD) and capacity	Materials and utilities	Amount required	Conversion of intermediate product	Oil loss	Oil Rec.	Reference
Silo dryer	50,000/unit	Operating cost	5000/unit	–	–	–	*
	5 t wet kernel/unit	Electricity	37.1 kW/unit	–			
		Wet kernel	1 t	0.95 t PK			
Clarification technologies	Capital cost (USD) and capacity	Materials and utilities	Amount required	Conversion of intermediate product	Oil loss (%)	Oil Rec.	References
Two-phase decanter	230,000/unit	Operating cost	28,000/unit	–	4.0%	–	[25, 54]
	20 t pressed liquid/unit	Electricity	45 kWh/unit	–			
		Pressed liquid	1 t	0.61 t organic phase			
				0.39 t POME			

(continued)

(continued)

Clarification technologies	Capital cost (USD) and capacity	Materials and utilities	Amount required	Conversion of intermediate product	Oil loss (%)	Oil Rec.	References
Three-phase decanter	300,000/unit	Operating cost	35,000/unit	–	3.0%	–	[1]
	20 t pressed liquid/unit	Electricity	50 kWh/unit	–			
		Pressed liquid	1 t	0.58 t organic phase			
				0.33 t POME			
				0.09 t decanter cake			
Vertical clarifier	150,000/unit	Operating cost	15,000/unit	–	5.0%	–	[10]
	7 t pressed liquid/unit	Electricity	32 kWh/unit	–			
		Water	0.696 t/t pressed liquid	0.54 t organic phase			
				1.156 t aqueous phase			
		Pressed liquid	1 t				
Vacuum clarifier	265,000/unit	Operating cost	27,500/unit	–	3.5%	–	*
	7 t pressed liquid/unit	Electricity	43 kWh/unit	–			
		Water	0.696 t/t pressed liquid	0.52 t organic phase			
		Pressed liquid	1 t	1.176 t aqueous phase			
Purifying technologies	Capital cost (USD) and capacity	Materials and utilities	Amount required	Conversion of intermediate product	Oil loss	Oil Rec.	Reference
Centrifuge purifier + Vacuum dryer	390,000/unit	Operating cost	55,000/unit	–	–	–	*
	10 t organic phase/unit	Electricity	35 kWh/unit	–			
		Organic phase	1 t	0.928 t crude oil			
				0.034 t POME			
Three-phase decanter	300,000/unit	Operating cost	35,000/unit	–	–	70%	*
	20 t aqueous phase/unit	Electricity	50 kWh/unit	–			
		Aqueous phase	1 t	0.02 t recovered oil			
				0.867 t POME			
				0.113 t decanter cake			

Note

1. Capital and operating costs for each technology are estimated based on current supplier availability
2. Only maintenance costs were included in the operating cost calculation. Labour costs were not being considered in the model
3. The authors declare no competing financial interest

*Industrial information obtained from Havy's Oil Mill

References

1. Alfa Laval (2015) PANX decanters for crude palm oil: high-performance three-phase decanters. http://www.alfalaval.com/products/separation/centrifugal-separators/decanters/PANX/. Accessed 3 Apr 2017
2. Andiappan V, Ng DKS, Bandyopadhyay S (2014) Synthesis of biomass-based trigeneration systems with uncertainties. Ind Eng Chem Res 53:18016–18028. https://doi.org/10.1021/ie502852v
3. Andiappan V, Tan RR, Aviso KB, Ng DKS (2015) Synthesis and optimisation of biomass-based tri-generation systems with reliability aspects. Energy 89:803–818. https://doi.org/10.1016/J.ENERGY.2015.05.138
4. Biegler LT, Grossmann IE, Westerberg AW (1997) Systematic methods for chemical process design. Prentice Hall, Old Tappan, NJ
5. Chaisri R, Boonsawang P, Prasertsan P, Chaiprapat S (2007) Effect of organic loading rate on methane and volatile fatty acids productions from anaerobic treatment of palm oil mill effluent in UASB and UFAF Reactors. J Sci Educ Technol 29:311–323
6. Chong CL (2000) Storage, handling and transportation of palm oil and palm oil products. In: Advances in oil palm research, vol 2. Malaysian Palm Oil Board, Kajang, pp 806–844. https://doi.org/20056703955
7. Cock J, Donough CR, Oberthür T, Indrasuara K, Rahmadsyah Gatot AR, Dolong T (2014) Increasing palm oil yields by measuring oil recovery efficiency from the fields to the mills. In: International Oil Palm Conference (IOPC)
8. Department of Environment (DOE), Ministry of Science, Technology and the Environment (1999) The extraction process for crude palm oil and sources of pollution. In: Industrial process and the environment-crude palm oil industry, pp 11–21
9. Department of Industrial Works (1997) Environmental management guideline for the palm oil industry. Environ Advis Assist Ind
10. Dexter ZD, Joseph CG, Zahrim AY (2016) A review on palm oil mill biogas plant wastewater treatment using coagulation-ozonation. In: International conference on chemical engineering and bioprocess engineering. IOP Publishing, pp 1–5. https://doi.org/10.1088/1755-1315/36/1/012029
11. Douglas JM (1985) A hierarchical decision procedure for process synthesis. AIChE J 31:353–362. https://doi.org/10.1002/aic.690310302
12. Douglas JM (1988) Conceptual design of chemical processes. McGraw-Hill, New York. https://doi.org/10.1002/jctb.280460308
13. EnergyWise (2013) Selection of sterilizer technology for energy efficient operation of palm oil mills—EnergyWise. Sustain. Palm Oil. http://rank.com.my/energywise/?p=310#sthash.9s0KT99m.dpbs. Accessed 17 July 2017
14. Foong SZY, Lam YL, Andiappan V, Foo DCY, Ng DKS (2018) A systematic approach for the synthesis and optimization of palm oil milling processes. Ind Eng Chem Res. acs.iecr.7b04788. https://doi.org/10.1021/acs.iecr.7b04788
15. Frangopoulos CA, von Spakovsky MR, Sciubba E (2002) A brief review of methods for the design and synthesis optimization of energy systems. Int J Thermodyn 5:151–160. https://doi.org/10.5541/IJOT.1034000097
16. Freitas ISF, Costa CAV, Boaventura RAR (2000) Conceptual design of industrial wastewater treatment processes: primary treatment. Comput Chem Eng 24:1725–1730. https://doi.org/10.1016/S0098-1354(00)00450-6
17. Gandikota MS, Davis JF (1990) An expert system framework for the preliminary design of process flowsheets. In: Knowledge based computer systems. Springer, Heidelberg, pp 88–104. https://doi.org/10.1007/BFb0018371

18. Gomez JC, Mokhtar MN, Sulaiman A, Baharuddin AS, Busu Z (2015) Recovery of residual crude palm oil from the empty fruit bunch spikelets using environmentally friendly processes. Sep Sci Technol 50:1677–1683. https://doi.org/10.1080/01496395.2014.994781
19. Grossmann IE, Santibanez J (1980) Applications of mixed-integer linear programming in process synthesis. Comput Chem Eng 4:205–214. https://doi.org/10.1016/0098-1354(80)85001-0
20. HUATAI Cereals and Oils Machinery (2014) Palm Kernel Recovery Station. http://www.palmoilmachine.com/Palm_Kernel_Recovery_Station_62.html. Accessed 11 Apr 2017
21. Hartley CWS (1988) The oil palm (Elaeis guineensis Jacq.), 3rd edn. Longman Scientific & Technical, Harlow, Essex, England
22. Harun MY, Che Yunus MA, Morad NA, Ismail MHS (2015) An industry survey of the screw press system in palm oil mills: operational data and malfunction issues. Eng Fail Anal 54:146–149. https://doi.org/10.1016/j.engfailanal.2015.04.003
23. Hendry JE, Rudd DF, Seader JD (1973) Synthesis in the design of chemical processes. AIChE J 19:1–15. https://doi.org/10.1002/aic.690190103
24. Iezany MR (2013) Enhancing the efficiency process for separation of dry shell and palm Kernel. Fac Chem Nat Resour Eng Univ. Malaysia Pahang
25. Jorgensen HK, Singh G (1980) An introduction of the decanter—drier system in the clarification station for crude oil and sludge treatment. Semin Malaysian Dep Environ
26. Kandiah S, Basiron Y, Suki A, Taha RM, Tan YH (2006) Continuous sterilization: the new paradigm for modernizing palm oil milling. J Oil Palm Res 144–152
27. Karuppiah R, Grossmann IE (2006) Global optimization for the synthesis of integrated water systems in chemical processes. Comput Chem Eng 30:650–673. https://doi.org/10.1016/j.compchemeng.2005.11.005
28. Kasivisvanathan H, Ng RTL, Tay DHS, Ng DKS (2012) Fuzzy optimisation for retrofitting a palm oil mill into a sustainable palm oil-based integrated biorefinery. Chem Eng J 200–202:694–709. https://doi.org/10.1016/j.cej.2012.05.113
29. LINDO Systems Inc. (2016) LINGO the modeling language and optimizer
30. Linnhoff B, Townsend DW, Boland D, Hewitt GF, Thomas BEA, Guy AR, Marsland RH (1982) User guide on process integration for the efficient use of energy, 1st edn. Institution of Chemical Engineers, Rugby, UK
31. Loh TK (2010) Tilting sterilizer. palm oil. Eng Bull 94:29–42
32. Lozano MA, Carvalho M, Serra LM (2011) Allocation of economic costs in trigeneration systems at variable load conditions. Energy Build 43:2869–2881. https://doi.org/10.1016/j.enbuild.2011.07.002
33. Malaysian Palm Oil Board (MPOB) (2018) Prices of palm products; Monthly. Econ Ind Dev Div. http://bepi.mpob.gov.my/index.php/en/statistics/price/monthly.html. Accessed 21 Feb 2018
34. Malaysian Palm Oil Board (MPOB) (2017) Production of crude palm oil 2017. http://bepi.mpob.gov.my/index.php/en/statistics/production/177-production-2017/792-production-of-crude-oil-palm-2017.html. Accessed 10 Feb 2018
35. Malaysian Palm Oil Board (MPOB) (2015) Production of strand fibre from Empty Fruit Bunch (EFB). http://www.hurfar.com.my/pdf/projects4.pdf. Accessed 10 Apr 2017
36. Malaysian Palm Oil Board (MPOB) (2011) About palm oil. http://www.palmoilworld.org/about_palmoil.html. Accessed 26 Aug 2017
37. Manninen J, Zhu XX (2001) Level-by-level flowsheet synthesis methodology for thermal system design. AIChE J 47:142–159. https://doi.org/10.1002/aic.690470114
38. Maycock JH (1990) Innovations in palm oil mill processing and refining. Palm Oil Research Institute of Malaysia
39. Mielke T (2017) Global supply, demand and price outlook for vegetable oils as well as for palm oil. ISTA Mielke GmbH, OIL WORLD, Hambg

40. Ng RTL, Ng DKS, Tan RR, El-Halwagi MM (2014) Disjunctive fuzzy optimisation for planning and synthesis of bioenergy-based industrial symbiosis system. J Environ Chem Eng 2:652–664. https://doi.org/10.1016/j.jece.2013.11.003
41. Ng RTL, Tay DHS, Ng DKS (2012) Simultaneous process synthesis, heat and power integration in a sustainable integrated biorefinery. Energy Fuels 26:7316–7330. https://doi.org/10.1021/ef301283c
42. Ng D, Pham V, El-Halwagi M, Jiménez-Gutiérrez A, Spriggs H (2009) A hierarchical approach to the synthesis and analysis of integrated biorefineries. In: Design for energy and the environment. CRC Press, pp 425–432. https://doi.org/10.1201/9781439809136-c38
43. Nishida N, Stephanopoulos G, Westerberg AW (1981) A review of process synthesis. AIChE J 27:321–351. https://doi.org/10.1002/aic.690270302
44. Noerhidajat Yunus R, Zurina ZA, Syafiie S, Ramanaidu V, Rashid U (2016) Effect of high pressurized sterilization on oil palm fruit digestion operation. Int Food Res J 23:129–134
45. Obincowelds Construction Company Ltd. (2015) Palm nut fibre separator. http://obincoweldconst.blogspot.my/2015/05/palm-fruit-fibre-separator.html. Accessed 11 Apr 2017
46. Othman MN, Lim JS, Theo WL, Hashim H, Ho WS (2017) Optimisation and targeting of supply-demand of biogas system through Gas System Cascade Analysis (GASCA) framework. J Clean Prod 146:101–115. https://doi.org/10.1016/j.jclepro.2016.06.057
47. Palm Oil Mill Consultants and Training (2017) Press station operations. http://palmoilmill.co.nz/index.php/processing-knowledge/10-press-station-operations. Accessed 10 Apr 2017
48. Palm Oil Research Institute of Malaysia (PORIM) (1985) Oil extraction. In: Palm oil factory process handbook, Part 1: general description of the palm oil milling process. Shah Alam, pp 39–55. https://doi.org/665.355.2
49. Poku K (2002) Small-scale palm oil processing in Africa, FAO Agricultural Services Bulletin. Food and Agriculture Organization of the United Nations
50. Rohaya MH, Nasrin AB, Choo YM, Ma A, Ravi N (2006) A commercial scale implementation of Rolek™ palm nut cracker: techno-economic viability study for production of shell-free Kernel. J Oil Palm Res 18:153–167
51. Rohaya MH, Ridzuan R, Che Rahmat CM, Choo YM, Nasrin AB, Nu'man AH (2016) Dry separation of palm Kernel and palm shell using a novel five-stage winnowing column system. Technologies 4:1–15. https://doi.org/10.3390/technologies4020013
52. Rudd DF, Powers GJ, Siirola JJ (1973) Process synthesis. Prentice-Hall. https://doi.org/10.1002/aic.690270302
53. Sargent R (2005) Process systems engineering: a retrospective view with questions for the future. Comput Chem Eng 29:1237–1241. https://doi.org/10.1016/j.compchemeng.2005.02.008
54. Singh G, Manoharan S, Kanapathy K (1982) Commercial scale bunch mulching of oil palms (Malaysia). In: Proceedings of the international conference on oil palm agriculture. Eighties, Kuala Lumpur, pp 367–377
55. Smith R (2016) Conceptual chemical process design for sustainability. In: Sustainability in the design, synthesis and analysis of chemical engineering processes. Elsevier, New York, pp 67–85. https://doi.org/10.1016/B978-0-12-802032-6.00003-7
56. Smith R (1995) Chemical process design. McGraw-Hill
57. Stephanopoulos G, Reklaitis GV (2011) Process systems engineering: from solvay to modern bio- and nanotechnology. Chem Eng Sci 66:4272–4306. https://doi.org/10.1016/j.ces.2011.05.049
58. Subramaniam V (2013) Residual oil recovery system: crude palm oil recovery from pressed mesocarp fibre in the palm oil mill. In: International exhibition and conference on water technologies, environmental technologies, and renewable energy. Mumbai, India
59. Sánchez ÓJ, Cardona CA (2012) Conceptual design of cost-effective and environmentally-friendly configurations for fuel ethanol production from sugarcane by knowledge-based process synthesis. Bioresour Technol 104:305–314. https://doi.org/10.1016/j.biortech.2011.08.125

60. The American Soybean Association (ASA) (2016) International: world vegetable oil consumption. http://soystats.com/international-world-vegetable-oil-consumption/. Accessed 29 Mar 2017
61. Wang B, Gebreslassie BH, You F (2013) Sustainable design and synthesis of hydrocarbon biorefinery via gasification pathway: integrated life cycle assessment and technoeconomic analysis with multiobjective superstructure optimization. Comput Chem Eng 52:55–76. https://doi.org/10.1016/j.compchemeng.2012.12.008
62. Yoshida S, Ito K, Yokoyama R (2007) Sensitivity analysis in structure optimization of energy supply systems for a hospital. Energy Convers Manag 48:2836–2843. https://doi.org/10.1016/J.ENCONMAN.2007.06.045

Alternative Solvent Design for Oil Extraction from Palm Pressed Fibre via Computer-Aided Molecular Design

Jecksin Ooi, Michael Angelo B. Promentilla, Raymond R. Tan, Denny K. S. Ng and Nishanth G. Chemmangattuvalappil

Abstract *Palm pressed fibre* (PPF) is a by-product from palm oil milling process. There are approximately 5–7% of residual oils retained in PPF after the oil extraction process. Hexane is commonly used as solvent for extraction of the residual oil due to its low cost and high oil solubility. However, the high boiling point of hexane leads to degradation of carotenes during oil recovery. Besides, hexane is highly flammable and causes air pollution through fugitive emissions. Thus, there is interest in identifying alternative solvents to extract residual oil from PPF. In this chapter, a new approach that combines *Computer-Aided Molecular Design* (CAMD) and *Analytic Hierarchy Process* (AHP) is presented. The proposed approach can determine the alternative solvents that exert favourable attributes for oil extraction. Both physical and environmental properties are chosen as design criteria to generate solvents with improved performance and environmental characteristics. Nonetheless, it is difficult to evaluate the relative importance of each property since properties that belong to different categories cannot be compared on a common scale. This issue needs to be addressed seriously as different relative weights will identify different solvents. The main attraction of this AHP–CAMD approach is that the relative importance weight of those identified properties can be systematically defined. AHP structures the CAMD problem in a hierarchical manner that allows physical and environmental properties to be compared under the same analysis. Through this approach, the identified alternative solvents have comparable or better performance as compared to hexane.

J. Ooi · D. K. S. Ng · N. G. Chemmangattuvalappil (✉)
Department of Chemical and Environmental Engineering, Centre of Sustainable Palm Oil Research (CESPOR), The University of Nottingham Malaysia Campus, Broga Road, 43500 Semenyih, Selangor, Malaysia
e-mail: Nishanth.C@nottingham.edu.my

M. A. B. Promentilla · R. R. Tan
Centre for Engineering and Sustainable Development Research, De La Salle University, 2401 Taft Avenue, 0922 Manila, Philippines

D. C. Y. Foo and M. K. Tun Abdul Aziz (eds.), *Green Technologies for the Oil Palm Industry*, Green Energy and Technology, https://doi.org/10.1007/978-981-13-2236-5_2

Keywords Computer-aided molecular design (CAMD) · Oil recovery
Palm pressed fibre (PPF) · Solvent design · Multi-objective optimisation
Analytic hierarchy process (AHP)

1 Introduction

Oil palm products are the most widely used vegetable oil in the world. United States Department of Agriculture (USDA) latest monthly report stated that 66.87 million metric tonnes of palm oil have been produced worldwide for the first ten months in 2017 [44]. The world's production of oil palm products is expected to reach 84 million tonnes due to increasing demand from the industries by the year 2020 [23]. For this reason, production of oil palm products has grown over the past decade in Southeast Asia especially in Malaysia and Indonesia. Both countries have been recognised as the main palm oil producers and exporters which contribute to more than 85% of the world's oil palm production [12].

Palm pressed fibre (PPF) is a by-product produced from palm oil milling process. When fresh fruit bunches (FFB) is processed for crude palm oil (CPO) production, it will constitute large amounts of residues, where approximately 15% of PPF is produced per mass fraction of FFB [20]. PPF is normally burnt as a fuel in biomass boiler to generate heat and power to sustain the palm oil milling operation. According to [7], there is nearly 5–7% of residual oil entrapped within the PPF after extraction of CPO. The residual oil is enriched with 4500–8500 ppm of sterols, 2400–3500 ppm of vitamin E and 4000–6000 ppm of carotenes [7]. The concentration of these micronutrients is significantly higher than that found in CPO, which only contains 326–527 ppm of sterols, 600–1000 ppm of Vitamin E and 500–700 ppm of carotenes [15]. For this reason, residual oil has greater potential for producing high-value food products compared to CPO.

Due to the aforementioned benefits, various extraction techniques are studied by researchers worldwide to determine techniques that result in higher palm oil yield. For examples, Neoh et al. [30] compared the extraction yield of diacylglycerol (DAG) and lauric acid with different hexane extraction methods such as cold extraction, reflux extraction and Soxhlet techniques. As shown in the previous results [30], cold extraction is the most preferred technique as cold extraction extracts more DAG and triglycerides (TAG) compared to the other two extraction techniques. On the other hand, another experiment work has been conducted by Lau et al. [27] to investigate the potential use of supercritical carbon dioxide (SC–CO_2) extraction to recover residual oil from PPF. The results show that SC–CO_2 extraction technique has the ability in producing two types of residual fibre oils enriched with carotene and vitamin E, respectively. Moreover, Chua et al. [8] employed the use of central composite design (CCD) to study the effect of operational condition of ultrasound-assisted extraction (UAE) on the yield of oil extraction from PPF. Nevertheless, among those available technologies, solvent extraction is extensively applied for oil extraction for economic reasons [26]. Hexane is the solvent of choice for extracting residual oil because of

its low cost, easy oil recovery and high solubility of oil [11]. Besides, hexane has low polarity which enables it to effectively extract non-polar carotenes.

However, hexane suffers from several drawbacks. For example, fugitive emissions of hexane vapour in the plant contribute to the formation of photochemical smog. Its high boiling point results in high degradation rate of carotenes during oil recovery process. In addition, strict regulation is enforced by European Directives and Registration, Evaluation, Authorisation and Restriction of Chemicals (REACH) on the use of hexane as solvent due to its toxicity [46]. Being highly flammable, hexane does not only impose extra safety concerns but also higher operating cost as extra layers of protection must be installed in the plant. Due to these limitations of hexane, there is a growing interest in searching for alternate solvents that have all the ideal properties such as having favourable physical attributes and being safe to both consumer and environment.

However, according to Johnson and Lusas [22], an ideal solvent probably does not exist; a better substitute can be identified. There are numerous desirable properties that dictate whether a solvent is suitable for oil extraction process. To identify a 'better' solvent, several features need to be considered, which include low boiling point, good diffusivity, selectivity towards triglycerides, non-toxic, low flammability, solvent stability, etc. In the current industry practice, in order to determine the 'better' solvents, it involves experimental studies and trial-and-error approach that are time-consuming and costly. For this reason, a systematic methodology that can identify promising solvents with the least amount of time and effort should be used. *Computer-Aided Molecular Design* (CAMD) technique is one of the promising methodologies that can be used to identify the solvents that match the predefined target properties (both physical and chemical properties). CAMD techniques have demonstrated its capability in designing molecules for different applications such as refrigerant design, solvent design and polymer design [2]. Thus, CAMD techniques can be adapted to determine alternate solvents instead of using conventional approaches that need large amount of information and knowledge.

This chapter focuses on identifying alternate solvents with performance comparable to or better than hexane via CAMD techniques. As mentioned previously, several attributes should be considered when selecting a solvent for oil extraction. Therefore, to identify an alternate solvent that simultaneously excels in performance and being environmental friendly, both physicochemical and environmental properties are considered as design criteria. To optimise these target properties simultaneously, CAMD problem is formulated as a multi-objective optimisation problem. Weighted sum method is commonly used to solve multi-objective CAMD problem. However, the main limitation in weighted sum method is the subjectivity involved in assigning the weighting factors to each target property. It is rather difficult to evaluate the relative importance weighting of each target property that belonged to different categories as they cannot be compared on a common scale. In addition, the definition of 'better' solvent depends on the defined objectives [22]. Hence, it is important to solve this issue as different weighting factors of each objective will lead to the identification of different alternative solvents. To address this issue, *Analytic Hierarchy*

Process (AHP) is integrated into CAMD framework to generate solvents that possess favourable attributes for oil extraction.

1.1 Computer-Aided Molecular Design (CAMD)

Chemical product design is a procedure by which customer needs are identified and translated into commercial products [28]. According to Cisternas and Gálvez [9], a chemical product is described as a system formed by various chemical substances that are designed and manufactured for one or more purposes. Bottom–up approach is the conventional technique used in determining new chemical products. This approach is normally done based on design heuristics, experimental studies and expert judgements [32]. These traditional approaches are very costly, time-consuming and inefficient, since they are primarily based on trial-and-error approaches [45]. On the other hand, top–down approaches start with identifying the needs to fulfil, followed by finding the molecules that exhibit properties that can meet the needs. This is also known as reverse engineering approaches, which can be done by various CAMD techniques.

CAMD techniques are important tools for chemical product design as they are able to predict, estimate and design molecules with a set of predefined target properties [16]. CAMD is able to design molecules with certain chemical structures based on a given set of target properties and molecular building blocks [13]. Over the recent decades, CAMD techniques have been applied to design different chemical products. Odele and Macchietto [32] have demonstrated CAMD techniques through the design of solvents for liquid extraction and gas absorption process. A CAMD framework which uses structure–property correlation in estimating the target properties of polymer repeat unit has been developed by Camarda and Maranas [5] to solve the optimal polymer design problem. Hostrup et al. [17] proposed a hybrid methodology which integrates CAMD approach and molecular modelling techniques to design extractive agent for distillation process and solvent for wastewater treatment. Other than these works, a continuous-molecular targeting approach for computer-aided molecular design [CoMT–CAMD] is presented by Bardow et al. [3] to solve an integrated solvent and process design problem. The proposed approach is demonstrated through the design of solvent and process for carbon dioxide capture where perturbed chain polar statistical associating fluid theory (PCP-SAFT) equation of state is used as a thermodynamic model. Struebing et al. [39] combined quantum mechanical computations of the reaction rate constant of solvents into CAMD framework to identify high-performance solvents with improved reaction rates. The approach has been illustrated through a case study called Menschutkin reaction, and the results obtained were validated by the kinetic experiments. Polymer molecules that are likely to be effective carriers in drug delivery can be generated using CAMD approach proposed by Pavurala and Achenie [34]. The designed polymer molecules are ranked based on desirability curves, which were developed using water absorption and glass transition temperature properties. Recently, the application of CAMD

techniques in the design of ionic liquids has also been reported. Karunanithi and Mehrkesh [24] developed a computer-aided ionic liquid design (CAILD) approach to generate ionic liquids through genetic algorithm (GA) and decomposition-based solution approach. Chong et al. [6] further extended CAMD approach using proper structural constraints to design optimal ionic liquids for CO_2 capture. The MINLP model formulated in his work has the ability to identify optimal ionic liquid which has the highest CO_2 solubility. Gebreslassie and Diwekar [14] have also introduced a novel CAMD methodology to design optimal solvents for extracting acetic acid from process waste streams based on EACO algorithm. Besides, a novel two-stage optimisation approach was presented by Ng et al. [31] to design optimal bio-based fuels that meet customer requirements from palm-based biomass and identify optimal biomass conversion routes in an integrated biorefinery. Furthermore, Ten et al. [41] presented a novel methodology by incorporating both safety and healthy aspects into CAMD framework to design solvents that are safe and does not bring health-related risks to the consumers for gas sweetening application. In this work, the safety and health indicators are measured based on the molecular properties that have effect on both aspects. Khor et al. [25] have demonstrated CAMD technique to identify alternate solvents for the oil extraction from PPF. In their work, safety and health properties have been optimised simultaneously together with physical properties to design solvents which are safe for food industry. From the above-mentioned reviews, it can be concluded that CAMD techniques have great potential in searching for new or alternate solvents for various applications.

2 Proposed AHP–CAMD Framework for Alternate Solvent Designs in Residual Oil Extraction

In this work, AHP is integrated into CAMD framework to design alternate solvents for residual oil extraction from PPF. The designed solvents should possess desirable physical attributes for extracting residual oil from PPF while having minimal impact on the environment. Through this AHP–CAMD approach, the relative importance between each target property can be systematically defined. As such, the designed solvents will be able to achieve good functionalities while having favourable environmental characteristics. The proposed AHP–CAMD framework for the design of alternative solvents for residual oil extraction from PPF is summarised in the following steps:

2.1 Determination of Design Objective and Target Properties

The procedure starts with the determination of molecular design objective by identifying the chemical product needs. To replace hexane, the designed solvents should pos-

sess comparable/better physical and environmental properties. The designed solvents should have a low boiling point (T_b) to minimise the degradation rate of carotenes. Besides, low viscosity (μ) and surface tension (σ) of solvent are desired to ensure good percolation and surface wetting, which will lead to higher rates of oil extraction [4]. Moreover, the difference of Hildebrand solubility parameter (δ) between solvent and carotene (R_{carotene}) should be kept small to ensure that both carotene and triglycerides (TAGs) have high solubility in the designed solvent. The assumption made is that both carotene and TAGs will be soluble in the solvent when R_{carotene} value is small as δ values of carotene and TAGs are relatively close. On the contrary, the unwanted free fatty acid (FFA) which primarily comprises linoleic acid (LA), palmitic acid (PA) and oleic acid (OA) should have low solubility in the solvent.

To ensure that the designed solvent is environment-friendly while having desirable product functionalities, a few important environmental properties are identified. First, the designed solvents should have low terrestrial and aquatic toxicity potential, which can be represented by high oral rat LD_{50} acute toxicity and fathead minnow LC_{50} toxicity, respectively. The designed solvent should also possess low tendency in forming photochemical smog, which can be characterised by low photochemical oxidation potential (PCO). In addition, the designed solvent should have minimum soil sorption coefficient ($\log K_{\text{oc}}$) and bioconcentration factor (BCF) to prevent the accumulation of the escaping solvent in one place as well as in the aquatic organism.

The above-mentioned desirable product needs can be quantified by measurable properties, which are clearly shown in Table 1. Thus, these nine physicochemical and environmental properties are selected as the objective functions to be optimised to design solvents which simultaneously excel in performance and being environmental friendly.

2.2 *Identification of Property Prediction Models*

The following step includes the identification of property prediction models for the predetermined target properties shown in Table 1. Group contribution method (GCM) equations are used to estimate the properties such as F_p, T_b, σ, μ, δ, M_w, LC_{50}, LD_{50}, PCO, $\log K_{\text{ow}}$ and BCF, whereas empirical correlation is used to calculate $\log K_{\text{oc}}$. Both GCM equations and empirical correlations are shown in Table 2.

Next, upper and lower limits of property constraint are identified to ensure that the generated solvents are suitable for oil extraction process. F_p is chosen as property constraint as it is important to ascertain process safety features during solvent design. Since the higher the F_p value, the lower the fire and explosion potential, only lower limit is introduced to F_p. In addition, upper and lower limits are added to target properties such as T_b, R_{carotene}, $\log K_{\text{ow}}$ and BCF to make sure that the designed solvents will have similar or improved performance than hexane. Table 3 shows the upper and lower limits of properties for solvent design.

Table 1 The desirable product needs with their translated quantitative properties

Desirable product needs		Quantitative properties
Physical attributes	Reduce the degradation rates of carotene	Low boiling point (T_b)
	Ensure good diffusivity	Low viscosity (μ) and surface tension (σ)
	Ensure both carotene and triglycerides (TAGs) have high solubility in designed solvents	Small difference of Hildebrand solubility parameter (δ) between solvent and carotene (R_{carotene})
Environmental aspects	Low aquatic toxicity	High fathead minnow LC_{50}
	Low terrestrial toxicity	High oral rat LD_{50}
	Reduce the formation of photochemical smog	Low photochemical oxidation potential (PCO)
	Minimise the accumulation of solvent in one place	Low soil sorption coefficient ($\log K_{\text{oc}}$)
	Minimise concentration of solvent in aquatic organism	Low bioconcentration factor (BCF)

2.3 Analytic Hierarchy Process (AHP) Stage

Multiple target properties are chosen for the solvent design in oil extraction since the alternative solvent is expected to achieve favourable physical and environmental attributes. As these target properties belong to different categories (e.g. physical and environmental aspects), it is important to have a common platform to compare their relative importance with respect to the overall features of an ideal product. Thus, AHP is integrated into CAMD framework to calculate the weightage of each target property through a pairwise comparison technique.

2.3.1 Development of Hierarchical Structure

The first step of AHP begins with treating the solvent design problem as a decision problem where it is structured in a hierarchical manner. In a typical decision hierarchy model, the overall objective is at the topmost level, followed by criteria and/or sub-criteria in the intermediate levels, and finally the decision alternatives at the bottom. The latter layer exists explicitly in when AHP is used with a finite set of predefined alternatives. However, it is only implicit when AHP is used in conjunction with mathematical programming, where the latter is used to generate the alternatives. The three-level hierarchy model for solvent design to extract residual oil from PPF is shown in Fig. 1.

Table 2 GCM equations and empirical correlation for chosen target properties

Property,p	Equations/correlations	Universal constants	References
T_b (K)	$\exp\left[\frac{T_b}{T_{b0}}\right] = \sum_i N_i T_{b1i}$	$T_{b0} = 244.5165$ K	[19]
F_p (K)	$F_p - F_{p0} = \sum_i N_i F_{p1i}$	$F_{p0} = 170.7058$ K	[19]
δ (MPA$^{1/2}$)	$\delta - \delta_0 = \sum_i N_i \delta_{1i}$	$\delta_0 = 21.6654$ MPA$^{1/2}$	[19]
σ (mN/m)	$\sigma = \sum_i N_i \sigma_{1i}$	–	[10]
μ (cP)	$\ln \mu = \sum_i N_i \mu_{1i}$	–	[10]
M_w (g/mol)	$M_w = \sum_i N_i M_{w1i}$	–	–
LD_{50} (mg/kg)	$-\log LD_{50} - A_{LD50} - B_{LD50} M_w = \sum_i N_i LD_{501i}$	$A_{LD50} = 1.9372$ $B_{LD50} = 0.0016$	[18]
LC_{50}	$-\log LC_{50}(FM) + FM_0 = \sum_i N_i LC_{501i}$	$FM_0 = 2.1949$	[18]
PCO	$-\log PCO = \sum_i N_i PCO_{1i}$	–	[18]
$\log K_{oc}$	$\log K_{oc} = 1.03 \log K_{ow} - 0.61$	–	[37]
$\log K_{ow}$	$\log K_{ow} - K_{ow0} = \sum_i N_i K_{ow1i}$	$K_{ow0} = 0.4876$	[19]
BCF	$\log BCF = \sum_i N_i BCF_{1i}$	–	[18]

Table 3 Upper and lower limits of properties for solvent design

Property	Lower limit	Upper limit
F_p (K)	242	–
T_b (°C)	40	80
$R_{carotene}$ (unit)	–	3.4
$\log K_{oc}$	–	4.5
log BCF	–	3.3

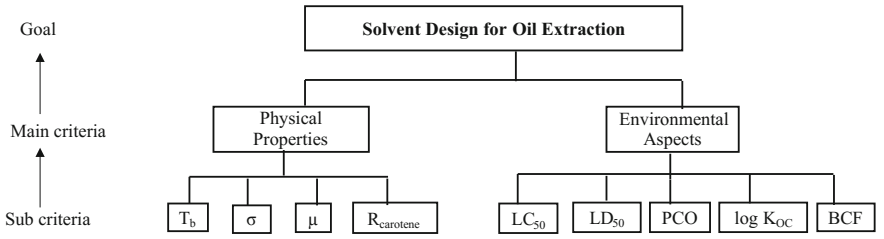

Fig. 1 AHP decision hierarchy model for alternate solvent design used in oil extraction

2.3.2 Construction of Pairwise Comparison Matrix

Following that, pairwise comparison is performed to evaluate the relative importance of criterion of a particular level with respect to a specific criterion in the next higher level. For instance, criteria are compared pairwise with respect to the overall objective of the decision problem. The comparison between two criteria is made by asking the question: 'How much more important is criterion A compared to criterion B with respect to a satisfaction of the overall goal?' The relative importance between two criteria can be deduced in reference to literature review or based on expert's judgement.

Since the evaluation of relative importance depends on one's judgement, it is inevitable that there will still be some degree of subjectivity involved in the process. However, it appears that it is more reliable to obtain the weighting factor of each property by carrying out pairwise comparison, rather than obtaining them directly by subjective estimation. The use of pairwise comparison has been used for a long time by psychologists, such as Thurstone [42] and Yokoyama [47]. They argue that it is simpler and more accurate to express one's opinion on only two properties, than simultaneously on all of them [21]. AHP thus provides a systematic framework by which such pairwise judgements can be consolidated into a set of consistent weight factors. The methodology is based on pairwise comparison matrices of size $(n \times n)$ which is constructed as shown in Eq. (1):

$$A = \begin{pmatrix} a_{11} & a_{12} & \cdots & a_{1n} \\ a_{21} & a_{22} & \cdots & a_{2n} \\ \vdots & \vdots & \ddots & \vdots \\ a_{n1} & a_{n2} & \cdots & a_{nn} \end{pmatrix}, \quad \text{For } i,\ j = 1, 2, \ldots, n \tag{1}$$

where A is the positive reciprocal pairwise comparison matrix, $a_{ij} = \frac{w_i}{w_j}$, $a_{ji} = \frac{1}{a_{ij}}$ and $a_{ij} > 0$. The ratio $\frac{w_i}{w_j}$ indicates the intensity of importance of element in the ith row over the element in the jth column with respect to the specific element in the upper level. The total number of comparisons to be done can be identified with Eq. (2):

Table 4 Conventional AHP numerical scale for subjective judgements by Saaty [36]

Intensity of importance	Linguistic equivalent for comparison of criteria
1	Equally important
3	Moderately more important
5	Strongly more important
7	Very strongly more important
9	Extremely more important

$$\text{No. of comparisons} = \left(\frac{n(n-1)}{2}\right) \tag{2}$$

where n is the matrix size.

The standard 9-point scale [36] is used to transform the verbal or subjective judgements into numerical quantities representing the values of a_{ij}. Table 4 shows the meaning of the comparison scale used in the weighting of two elements. Intermediate values (2, 4, 6 and 8) can be used to represent judgements that lie between those listed in the scale.

2.3.3 Calculation of Eigenvector from Pairwise Comparison Matrix

The principal eigenvector, w of the matrix A, is used to represent the relative importance weighting factor of each criterion which is given by Eq. (3):

$$Aw = \lambda_{\max} w \tag{3}$$

where $\lambda_{\max}$ is the principal eigenvalue that can calculate the consistency of the pairwise comparative judgment matrix. The larger the difference between the $\lambda_{\max}$ and the order of matrix, the more inconsistent the matrix is.

w can be solved via power method using a spreadsheet by the following steps:

i. Raise the pairwise comparison matrix to the power of two.
ii. Calculate and normalise the sums of row to compute the eigenvector.
iii. Iterate the process until the value of eigenvector remains unchanged from the previous calculation.

2.3.4 Consistency Verification

The consistency of pairwise comparison can be determined by consistency ratio (CR), which is expressed by Eq. (4).

$$\text{CR} = \frac{\text{CI}}{\text{RI}} \tag{4}$$

where CI is the consistency index and RI is the random index.

CI can then be calculated using Eq. (5):

$$\mathrm{CI} = \frac{\lambda_{\max} - n}{n - 1} \tag{5}$$

where $\lambda_{\max}$ represents the principal eigenvalue and n represents matrix size.

RI is the consistency index of a randomly generated reciprocal matrix from the 9-point scale and its value depends on n. Table 5 shows the random index table for AHP [36]. The inconsistency is considered satisfactory if CR is<10%. However, if CR >10%, the judgement elicitation has to be performed again.

Steps shown in Sects. 2.3.1–2.3.4 are repeated for all the hierarchy level stated in Sect. 2.3.1. After obtaining the relative importance weighting factor (principal eigenvector w) of each criterion and sub-criterion, the weighting factor of each sub-criterion is multiplied by the weighting factor of its main criterion to obtain its final weighting factor in the overall system.

2.4 Computation of Weights from Decision-Maker's Value Judgement

This section presents the relative importance weights calculated after performing steps Sects. 2.3.1–2.3.4. In this work, all the judgements are elicited based on literature sources. First, physical and environmental aspects are compared pairwise by asking the questions: 'which aspect is more important and how much more important is it to satisfy the requirement in designing a solvent for oil extraction?' For this work, more priority is given to the physical aspect compared to the environmental aspect to ensure that the designed solvent will possess better performance and being environmental friendly. Besides, some constraints are introduced to the environmental properties to assure that the designed solvent follows the environmental regulations. Thus, physical properties as a group are assumed to be strongly more important than environmental properties as a group. Since the pairwise comparison matrix is only in the order of two, the judgement will always be consistent as the value of $\lambda_{\max}$ is equal to n. Table 6 reports the assessment of relative importance of main criteria with respect to the design goal.

Next, the comparison between physical sub-properties is made by asking the questions: 'which is more important and how much more important is it with respect to a satisfaction of the physical properties of solvent?' Since the main goal of this work is to minimise the degradation rate of carotene by lowering the T_b of solvent, T_b is strongly more important than R_{carotene}. μ and σ are slightly more important than R_{carotene} as it is more important to ensure that the solvent is able to diffuse into the matrix of PPF to extract the residual oil. High surface tension can impede the penetration of designed solvent into the matrix of PPF, whereas less viscous solvent is preferred as part of the extraction process is governed by capillary flow [22]. The

Table 5 Random index for AHP

Size of matrix (n)	1	2	3	4	5	6	7	8	9	10
Random index (RI)	0	0	0.52	0.89	1.11	1.25	1.35	1.4	1.45	1.49

Table 6 Pairwise comparison matrix of main properties with respect to goal

	Physical properties	Environmental properties	Priority vector
Physical properties	1	5	0.8333
Environmental properties	1/5	1	0.1667
$\lambda_{max} = 2$, CI = 0.0, CR = 0.0			

Table 7 Pairwise comparison matrix of sub-physical properties

	T_b	$R_{carotene}$	σ	μ	Priority vector
T_b	1	5	3	3	0.5320
$R_{carotene}$	1/5	1	1/2	1/2	0.0971
σ	1/3	2	1	1	0.1854
μ	1/3	2	1	1	0.1854
$\lambda_{max} = 4.004$; CI = 0.0013; CR = 0.0016					

diffusion of residual oil from the matrix of PPF into the designed solvent can be modelled using Eq. (6) [43]. Equation (6) clearly dictates that viscosity of solvent will affect the diffusion of residual oil.

$$D_{AB} = \frac{117.3 \times 10^{-18} (\varphi M_B)^{0.5} \, \mathrm{T}}{\mu v_A^{0.6}} \tag{6}$$

where D_{AB} is the diffusivity of oil in solvent B, M_B is the molecular weight of solvent, T is the temperature, μ is the solution viscosity, v_A is the molar volume of oil and φ is the association factor for solvent. The intensity of importance allocated to each pairwise comparison is reported in Table 7. The inconsistency of the pairwise comparison is considered satisfactory as the calculated CR is only 0.16% which is less than 10%.

Lastly, similar question is also asked when comparing the environmental sub-properties in pairwise manner. An assumption made is that the environmental impact caused by residual oil extraction from PPF using solvent is comparable to that from plant or oilseed as the process of extracting oil from plant or oilseed is alike. Moncada et al. [29] have performed an environmental assessment on the extraction of essential oil from Rosemary and Oregano. The report clearly shows that solvent extraction using hexane has contributed severe impacts on aquatic toxicity and photochemical oxidation potential. By comparing solvent extraction using hexane with supercritical fluid and water distillation technology, solvent extraction using hexane is less favourable in terms of environmental aspects. Similar result trends are observed for potential environmental impact (PEI) per kilogramme of essential oil extracted from both Oregano and Rosemary using hexane. Based on the result obtained for Rosemary oil, the PEIs per kilogramme of rosemary oil extracted for terrestrial toxicity, aquatic

Table 8 Pairwise comparison matrix of sub-environmental properties

	LC_{50}	LD_{50}	PCO	log K_{oc}	BCF	Priority vector
LC_{50}	1	1/3	1/6	3	3	0.1869
LD_{50}	3	1	1/5	3	3	0.0951
PCO	6	5	1	7	7	0.5943
log K_{oc}	1/3	1/3	1/7	1	1	0.0618
BCF	1/3	1/3	1/7	1	1	0.0618
$\lambda max = 5.15$; CI = 0.037; CR = 0.034						

Table 9 Final weighting factors of target properties in the overall system

Target property	Final weighting factor
T_b	0.4433
$R_{carotene}$	0.0810
σ	0.1545
μ	0.1545
LC_{50}	0.0311
LD_{50}	0.0159
PCO	0.0991
BCF	0.0103
log K_{oc}	0.0103

toxicity and photochemical oxidation potential are approximately 0.005, 0.03 and 0.07, respectively [29]. Therefore, to design a solvent which will have less tendency to form photochemical smog, it is assumed that photochemical oxidation potential is very strongly more important than terrestrial toxicity, whereas aquatic toxicity is slightly more important than terrestrial toxicity. Also, it is important to ensure that the designed solvent will be less likely to accumulate in one place as degradation products with low biodegradability may persist in the environment. Since log K_{oc} is a measure of the tendency of solvent to accumulate in one place whereas BCF is a measure of tendency of solvent to accumulate in aquatic organism, both log K_{oc} and BCF are assumed to be equally important while designing the molecules. Upper bounds have been introduced to both log K_{oc} and BCF to ensure that the designed solvent is not bio-accumulative. Table 8 shows the intensity of importance allocated to each environmental property. CR of 3.4% shows that the inconsistency in decision judgement is acceptable.

After obtaining the relative weighting factor of main criteria and sub-criteria, the final weighting factors of each sub-property in the overall system is calculated by multiplying their weighting factor with the weighting factor of its main property. The final weighting factors of target properties computed in this work are reported in Table 9.

2.5 Molecular Design Stage

Next, suitable molecular building blocks are selected based on the molecular structures of the commonly used solvents for oil extraction. The chosen molecular groups for solvent design for oil extraction include CH_3, CH_2, CH, C, OH, COOH, CH_3CO, CHO, CH_3O, NH_2, $CH_2=CH$, CH_2O and CH–O. The structural constraints shown in Eqs. (7) and (9) are applied to ensure that a structurally feasible molecule can be formed without having any free bonds. To generate a molecule, the summation for the number of occurrences for all selected groups must be greater than zero. This rule is explained mathematically by Eq. (7):

$$\sum_{i=1}^{G_T} N_i > 0 \tag{7}$$

where N_i is the number of occurrences of group i, while G_T is the total number of groups selected to generate the molecules. In addition, to ensure that a molecule has no free attachment, the octet rule of structural feasibility, which is dictated in Eq. (8), is applied:

$$\sum_{i=1}^{G_T} N_i(2 - v_i) = 2g \tag{8}$$

where v_i is the valence of group i and g is 1, 0, −1 or −2 for acyclic, monocyclic, bicyclic and tricyclic compounds, respectively. In this work, only simple-structured acyclic compounds are considered. Hence, Eq. (8) can be further reduced to Eq. (9) for acyclic compounds.

$$\sum_{i=1}^{G_T} N_i(2 - v_i) = 2 \tag{9}$$

2.6 Optimisation Model

Based on the identified design objective, CAMD problem is formulated as multi-objective optimisation problem where target physicochemical and environmental properties are to be optimised simultaneously together with the property and structural constraints. This multi-objective optimisation model is solved using weighted sum method which ensures that a Pareto-optimal solution is generated. This method allows multiple objectives to be converted into an aggregated scalar objective function by first allocating each objective function with a weighting factor, and then summing up all the contributors to obtain the overall objective function. However, all the target properties are represented by various measurement units and scales. Hence,

Table 10 Property and property operator

Property, p	Property operator, Ω_p
T_b	$\exp(T_b/T_{b0})$
σ	σ
M_w	M_w
μ	$\ln \mu$
δ	$\delta - \delta_0$
F_p	$F_p - F_{p0}$
LC_{50}	$-\log LC_{50}(FM) + FM_0$
LD_{50}	$-\log LD_{50} - A_{LD50} - B_{LD50} M_w$
PCO	$-\log PCO$
BCF	$\log BCF$
$\log K_{oc}$	$\log K_{ow} - K_{ow0}$

it is important to carry out a normalisation step to bring them to the same magnitude. Before performing normalisation step, the identified target property models are first transformed into their property operators as shown in Table 10. The property operators are depicted by the linear combinations of the number of occurrence for molecular group of type-*i* and its corresponding contribution.

After determining the property operators, property operators are normalised using Eqs. (10) and (11). Equation (10) is applied to normalise target property that needs to be maximised, whereas Eq. (11) is used to normalise target property that needs to be minimised. The normalised target property is then referred as normalised target property operator, λ_{pm}.

$$\lambda_p = \frac{\Omega_p - \Omega_{p\min}}{\Omega_{p\max} - \Omega_{p\min}} \tag{10}$$

$$\lambda_p = \frac{\Omega_{p\max} - \Omega_p}{\Omega_{p\max} - \Omega_{p\min}} \tag{11}$$

where $\Omega_{p\min}$ and $\Omega_{p\max}$ are the minimum and maximum value of target property operator.

λ_{pm} will now have values range from 0 to 1. The consistent set of weighting factor computed from AHP approach (as shown in Table 9) together with λ_{pm} can then be used to represent the overall objective function, which is shown in Eq. (12):

$$\begin{aligned} F_{\text{weighted sum}} = {} & 0.4433\lambda_{T_b} + 0.1545\lambda_\sigma + 0.1545\lambda_\mu + 0.081\lambda_{R_{\text{carotene}}} + 0.0311\lambda_{LC_{50}} \\ & + 0.0159\lambda_{LD_{50}} + 0.0991\lambda_{PCO} + 0.0103\lambda_{\log_{K_{oc}}} + 0.0103\lambda_{BCF} \end{aligned} \tag{12}$$

where $F_{\text{weighted sum}}$ is the overall objective function.

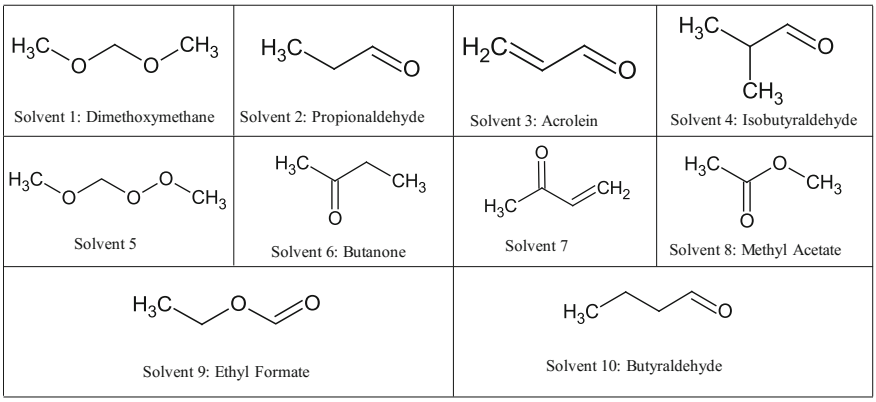

Fig. 2 Molecular structure of the best ten solvents [33]

The design objective of this work is to maximise $F_{\text{weighted sum}}$. The solution with the highest $F_{\text{weighted sum}}$ value will be the most optimal molecule. After identifying a solution from the optimisation model, integer cut is performed to obtain a ranked list of optimal and near-optimal molecules.

3 Proposed AHP–CAMD Framework Solution

Ten solvents with the highest $F_{\text{weighted sum}}$ values are generated. The molecular structures of these ten molecules are displayed in Fig. 2.

Tables 11 and 12 depict the properties of the generated solvents. From the results, solvent 1 has the highest $F_{\text{weighted sum}}$ values which make it ranked the first among all the generated solvents. Nonetheless, there will be uncertainties in prediction models and values of target properties. For this reason, the generated ranking for each designed solvent is not absolute. The ranking of the designed solvents solely represents the identification of promising potential candidates from a huge search space. Solvent at a higher ranking means that it has a greater possibility to be useful for a specific application. After obtaining a ranked list of molecules, the potential solutions need to be further examined and verified through experiments.

The properties of the designed solvents are then analysed and compared with that of hexane. The properties of hexane are shown in Table 13. The generated results reveal that the top four solvents (solvent 1–4) have lower T_b than that of hexane. Furthermore, R_{carotene} of solvent 1 is significantly smaller than that of hexane. The result is promising as it indicates that higher mutual miscibility is found between carotenes and solvent 1 compared to that of hexane. According to Reichardt and Welton [35], the larger the differences in δ values between two solvents, the weaker their mutual miscibility. Besides, it has been observed that all generated solvents have lower log K_{oc} and BCF values than that of hexane. The generated solvent will

Table 11 The generated solvent with their respective properties

Solvent	$F_{\text{weighted sum}}$	T_b (°C)	σ (mN/m)	μ (cp)	Solubility ($\text{mPA}^{1/2}$)	R_{carotene} (unit)	R_{TAG} (unit)	R_{LA} (unit)	R_{PA} (unit)	R_{OA} (unit)
1	0.89	48.49	20.18	0.31	18.11	0.31	0.91	2.01	2.01	1.91
2	0.67	42.30	23.23	0.41	20.37	2.57	3.17	4.27	4.27	4.17
3	0.64	40.36	24.34	0.34	19.95	2.15	2.75	3.85	3.85	3.75
4	0.46	61.69	22.86	0.44	19.54	1.74	2.34	3.44	3.44	3.34
5	0.42	74.51	21.95	0.46	18.24	0.44	1.04	2.14	2.14	2.04
6	0.40	71.34	23.98	0.37	19.25	1.45	2.05	3.15	3.15	3.05
7	0.37	69.62	25.09	0.31	18.82	1.02	1.62	2.72	2.72	2.62
8	0.26	77.57	25.10	0.42	19.81	2.01	2.61	3.71	3.71	3.61
9	0.20	68.95	25.00	0.61	20.50	2.70	3.30	4.40	4.40	4.30
10	0.18	78.60	23.85	0.51	20.22	2.42	3.02	4.12	4.12	4.02

Table 12 The generated solvent with their respective properties (continued)

Solvent	M_w (g/mol)	F_p (°C)	−log LC_{50}	LD_{50} (mg/kg)	PCO	log k_{oc}	BCF
1	76.10	−7.00	−2.95	711.06	0.45	−0.28	3.99
2	58.08	−6.85	−1.21	831.00	1.04	−0.16	2.54
3	56.06	−8.01	−0.56	558.31	2.77	−0.40	2.60
4	72.11	−1.74	−1.16	899.72	1.04	0.10	3.83
5	92.09	14.40	−3.45	682.47	0.66	−0.88	2.51
6	72.11	1.76	−1.73	749.04	0.49	0.26	26.66
7	70.09	0.60	−1.08	506.77	1.30	0.02	27.33
8	74.08	10.46	−2.63	719.56	0.51	−0.81	8.29
9	74.08	14.54	−1.71	840.56	1.53	−0.76	1.60
10	72.11	4.67	−0.92	930.69	0.93	0.29	3.16

have low soil sorption since log K_{oc} values are less than 1.5 [1]. On the other hand, since the BCF values of all generated solvents are less than 250, they are less likely to cause bioaccumulation in aquatic organism [1]. Moreover, it can be concluded that the generated solvents are less likely to cause aquatic toxicity as the $-\log LC_{50}$ values are lower than that of hexane. In terms of safety aspects, the generated solvents will be less flammable than hexane by referring to their F_p values. Thus, the generated solvents are having better characteristic in safety aspects compared to that of hexane. The generated solutions are then further compared with the existing literature. It is figured out that solvent 8 (methyl acetate) has been shown to be suitable solvent for extracting oil from oilseeds [40]. The result is further supported by a recent study, which revealed that methyl acetate is effective in extracting tocopherols from edible oil [38]. Hence, it can be concluded that the solvent generated using this proposed methodology is on a par with those solvents used in experimental studies.

4 Conclusion

This chapter develops a novel AHP–CAMD approach to identify alternate solvents to replace hexane as solvent used in residual oil extraction from PPF. During the decision-making stage, the environmental properties of the solvent are considered together with its physicochemical properties. In order to optimise these target properties, CAMD problem is formulated as multi-objective optimisation model, which is then solved by weighted sum method. The AHP–CAMD approach allows the comparison between physicochemical and environmental properties to be made under the same analysis. Besides, the process of evaluating the relative importance between each property can be done more systematically and consistently using pairwise comparisons. Thus, consistent relative weighting factors, which reflect the preference of decision-maker, can be allocated to each target property. The results show that the

Table 13 Properties of hexane

Property	Property value
Tb (°C)	68.7
σ (mN/m)	17.91
μ (cp)	0.297
R_{carotene} (unit)	2.9
R_{TAG} (unit)	2.3
R_{LA} (unit)	1.2
R_{PA}(unit)	1.2
R_{OA} (unit)	1.3
F_p (°C)	−30.9
$-\log \text{LC}_{50}$	4.54
LD_{50} (mg/kg)	28000
PCO	0.4306
$\log k_{\text{oc}}$	3.62
BCF	51.357

designed solvents exhibit good functionalities and favourable environmental characteristics. Future work can be conducted by further extend the CAMD framework to include the evaluation of environmental impact potential of an oil extraction process. This is because the performance and environmental hazard of a chemical process is likely to be affected by the characteristic of chemical solvent. A methodology that allows the identification of a molecule with desirable functionalities that simultaneously improve the environmental characteristics of a unit process should be developed.

Acknowledgements The financial support from the Ministry of Higher Education, Malaysia through the LRGS Grant (LRGS/2013/UKM-UNMC/PT/05) is gratefully acknowledged.

References

1. Allen DT, Shonnard DR (2002) Green engineering: environmentally conscious design of chemical processes. Prentice Hall PTR, Upper Saddle River, NJ
2. Austin ND, Sahinidis NV, Trahan DW (2016) Computer-aided molecular design: an introduction and review of tools, applications, and solution techniques. Chem Eng Res Des 116:2–26. https://doi.org/10.1016/j.cherd.2016.10.014
3. Bardow A, Steur K, Gross J (2010) Continuous-molecular targeting for integrated solvent and process design. Ind Eng Chem Res 49:2834–2840. https://doi.org/10.1021/ie901281w
4. Bockisch M (ed) (1998) Chapter 5—the extraction of vegetable oils. In: Fats and oils handbook. AOCS press, pp 345–445. https://doi.org/10.1016/B978-0-9818936-0-0.50010-X
5. Camarda KV, Maranas CD (1999) Optimization in polymer design using connectivity indices. Ind Eng Chem Res 38:1884–1892. https://doi.org/10.1021/ie980682n

6. Chong FK, Foo DCY, Eljack FT, Atilhan M, Chemmangattuvalappil NG (2015) Ionic liquid design for enhanced carbon dioxide capture by computer-aided molecular design approach. Clean Technol Environ Policy 17:1301–1312. https://doi.org/10.1007/s10098-015-0938-5
7. Choo Y-M, Yap S-C, Ooi C-K, Ma A-N, Goh S-H, Ong AS-H (1996) Recovered oil from palm-pressed fiber: a good source of natural carotenoids, vitamin E, and sterols. J Am Oil Chem Soc 73:599–602. https://doi.org/10.1007/BF02518114
8. Chua SC, Tan CP, Mirhosseini H, Lai OM, Long K, Baharin BS (2009) Optimization of ultrasound extraction condition of phospholipids from palm-pressed fiber. J Food Eng 92:403–409. https://doi.org/10.1016/j.jfoodeng.2008.12.013
9. Cisternas LA, Gálvez ED (2006) Principles for chemical products design. In: Marquardt W, Pantelides C (eds) 16th European symposium on computer aided process engineering and 9th international symposium on process systems engineering. Elsevier, pp 1107–1112. http://dx.doi.org/10.1016/S1570-7946(06)80194-X
10. Conte E, Martinho A, Matos HA, Gani R (2008) Combined group-contribution and atom connectivity index-based methods for estimation of surface tension and viscosity. Ind Eng Chem Res 47:7940–7954. https://doi.org/10.1021/ie071572w
11. de Oliveira RC, de Barros STD, Gimenes ML (2013) The extraction of passion fruit oil with green solvents. J Food Eng 117:458–463. https://doi.org/10.1016/j.jfoodeng.2012.12.004
12. Euler M, Krishna V, Schwarze S, Siregar H, Qaim M (2017) Oil palm adoption, household welfare, and nutrition among smallholder farmers in Indonesia. World Dev 93:219–235. https://doi.org/10.1016/j.worlddev.2016.12.019
13. Gani R (2004) Chemical product design: challenges and opportunities. Comput Chem Eng 28:2441–2457. https://doi.org/10.1016/j.compchemeng.2004.08.010
14. Gebreslassie BH, Diwekar UM (2015) Efficient ant colony optimization for computer aided molecular design: Case study solvent selection problem. Comput Chem Eng 78:1–9. https://doi.org/10.1016/j.compchemeng.2015.04.004
15. Goh SH, Choo YM, Ong SH (1985) Minor constituents of palm oil. J Am Oil Chem Soc 62:237–240. https://doi.org/10.1007/BF02541384
16. Harper PM, Gani R (2000) A multi-step and multi-level approach for computer aided molecular design. Comput Chem Eng 24:677–683. https://doi.org/10.1016/S0098-1354(00)00410-5
17. Hostrup M, Harper PM, Gani R (1999) Design of environmentally benign processes: integration of solvent design and separation process synthesis. Comput Chem Eng 23:1395–1414. https://doi.org/10.1016/S0098-1354(99)00300-2
18. Hukkerikar AS, Kalakul S, Sarup B, Young DM, Sin G, Gani R (2012) Estimation of environment-related properties of chemicals for design of sustainable processes: development of group-contribution + (GC+) property models and uncertainty analysis. J Chem Inf Model 52:2823–2839. https://doi.org/10.1021/ci300350r
19. Hukkerikar AS, Sarup B, Ten Kate A, Abildskov J, Sin G, Gani R (2012) Group-contribution + (GC+) based estimation of properties of pure components: Improved property estimation and uncertainty analysis. Fluid Phase Equilib 321:25–43. https://doi.org/10.1016/j.fluid.2012.02.010
20. Husain Z, Zainac Z, Abdullah Z (2002) Briquetting of palm fibre and shell from the processing of palm nuts to palm oil. Biomass Bioenerg 22:505–509. https://doi.org/10.1016/S0961-9534(02)00022-3
21. Ishizaka A, Labib A (2011) Review of the main developments in the analytic hierarchy process. Expert Syst Appl 38:14336–14345. https://doi.org/10.1016/j.eswa.2011.04.143
22. Johnson LA, Lusas EW (1983) Comparison of alternative solvents for oils extraction. J Am Oil Chem Soc 60:229–242. https://doi.org/10.1007/BF02543490
23. Johnson and Johnson (2017) Responsible palm oil sourcing criteria (RPOSC) [WWW Document]. URL https://www.jnj.com/about-jnj/company-statements/responsible-palm-oil-sourcing-criteria. Accessed 25 Oct 17
24. Karunanithi AT, Mehrkesh A (2013) Computer-aided design of tailor-made ionic liquids. AIChE J 59:4627–4640. https://doi.org/10.1002/aic.14228

25. Khor SY, Liam KY, Loh WX, Tan CY, Ng LY, Hassim MH, Ng DKS, Chemmangattuvalappil NG (2017) Computer aided molecular design for alternative sustainable solvent to extract oil from palm pressed fibre. Process Saf Environ Prot 106:211–223. https://doi.org/10.1016/j.psep.2017.01.006
26. Kumar SPJ, Prasad SR, Banerjee R, Agarwal DK, Kulkarni KS, Ramesh KV (2017) Green solvents and technologies for oil extraction from oilseeds. Chem Cent J 11:9. https://doi.org/10.1186/s13065-017-0238-8
27. Lau H Lik Nang, Choo YM, Ma AN, Chuah CH (2008) Selective extraction of palm carotene and vitamin E from fresh palm-pressed mesocarp fiber (Elaeis guineensis) using supercritical CO2. J Food Eng 84:289–296. https://doi.org/10.1016/j.jfoodeng.2007.05.018
28. Moggridge GD, Cussler EL (2000) An introduction to chemical product design. Chem Eng Res Des 78:5–11. https://doi.org/10.1205/026387600527022
29. Moncada J, Tamayo JA, Cardona CA (2016) Techno-economic and environmental assessment of essential oil extraction from Oregano (Origanum vulgare) and Rosemary (Rosmarinus officinalis) in Colombia. J Clean Prod 112:172–181. http://dx.doi.org/10.1016/j.jclepro.2015.09.067
30. Neoh BK, Thang YM, Zain MZM, Junaidi A (2011) Palm pressed fibre oil: a new opportunity for premium hardstock? Int Food Res J 18:769–773
31. Ng LY, Andiappan V, Chemmangattuvalappil NG, Ng DKS (2015) Novel methodology for the synthesis of optimal biochemicals in integrated biorefineries via inverse design techniques. Ind Eng Chem Res 54:5722–5735. https://doi.org/10.1021/acs.iecr.5b00217
32. Odele O, Macchietto S (1993) Computer aided molecular design: a novel method for optimal solvent selection. Fluid Phase Equilib 82:47–54. https://doi.org/10.1016/0378-3812(93)87127-M
33. Ooi J, Promentilla MAB, Tan RR, Ng DKS, Chemmangattuvalappil NG (2017) A systematic methodology for multi-objective molecular design via analytic hierarchy process. Process Saf Environ Prot 111:663–677. https://doi.org/10.1016/j.psep.2017.08.039
34. Pavurala N, Achenie LEK (2014) Identifying polymer structures for oral drug delivery—a molecular design approach. Comput Chem Eng 71:734–744. https://doi.org/10.1016/j.compchemeng.2014.07.015
35. Reichardt C, Welton T (2011) Solvents and solvent effects in organic chemistry, 4th ed. Wiley
36. Satty TL (1980) The analytical hierarchy process: planning, priority setting, resource allocation. RWS Publ, Pittsbg
37. Seth R, Mackay D, Muncke J (1999) Estimating the organic carbon partition coefficient and its variability for hydrophobic chemicals. Environ Sci Technol 33:2390–2394. https://doi.org/10.1021/es980893j
38. Sicaire A-G, Vian M, Fine F, Joffre F, Carré P, Tostain S, Chemat F (2015) Alternative bio-based solvents for extraction of fat and oils: solubility prediction, global yield, extraction kinetics, chemical composition and cost of manufacturing. Int J Mol Sci 16:8430–8453. https://doi.org/10.3390/ijms16048430
39. Struebing H, Ganase Z, Karamertzanis PG, Siougkrou E, Haycock P, Piccione PM, Armstrong A, Galindo A, Adjiman CS (2013) Computer-aided molecular design of solvents for accelerated reaction kinetics. Nat Chem 5:952–957
40. Su EZ, Xu WQ, Gao KL, Zheng Y, Wei DZ (2007) Lipase-catalyzed in situ reactive extraction of oilseeds with short-chained alkyl acetates for fatty acid esters production. J Mol Catal B Enzym 48:28–32. https://doi.org/10.1016/j.molcatb.2007.06.003
41. Ten JY, Hassim MH, Chemmangattuvalappil N, Ng DKS (2016) A novel chemical product design framework with the integration of safety and health aspects. J Loss Prev Process Ind 40:67–80. https://doi.org/10.1016/j.jlp.2015.11.027
42. Thurstone LL (1927) A law of comparative judgment. Psychol Rev 34:273–286. https://doi.org/10.1037/h0070288
43. Tzia C, Liadakis G (2003) Extraction optimization in food engineering, food science and technology. CRC Press

44. United States Department of Agriculture (2017) Oilseeds: world markets and trade [WWW Document]. URL https://www.fas.usda.gov/psdonline/circulars/oilseeds.pdf. Accessed 25 Oct 17
45. Venkatasubramanian V, Chan K, Caruthers JM (1994) An international journal of computer applications in chemical engineeringcomputer-aided molecular design using genetic algorithms. Comput Chem Eng 18:833–844. https://doi.org/10.1016/0098-1354(93)E0023-3
46. Yara-Varon E, Fabiano-Tixier AS, Balcells M, Canela-Garayoa R, Bily A, Chemat F (2016) Is it possible to substitute hexane with green solvents for extraction of carotenoids? A theoretical versus experimental solubility study. RSC Adv 6:27750–27759. https://doi.org/10.1039/C6RA03016E
47. Yokoyama M (1921) The nature of the affective judgment in the method of paired comparisons. Am J Psychol 32:357–369. https://doi.org/10.2307/1414000

Green Extraction Process for Oil Recovery Using Bioethanol

Mustafa Kamal Abdul Aziz, Takayuki Okayama, Ryota Kose, Noor Azian Morad, Noor Baini Nabila Muhamad, Mohd Rizuan Bin Mansor and Freddie Panau

Abstract In this chapter, a novel green extraction process known as *solvent extraction–crystallisation–evaporation* (SECE) is introduced. The SECE is meant to be a sustainable approach for oil recovery from palm oil milling and refining processes. It utilises bioethanol as the extraction solvent instead of hexane. SECE is demonstrated for the extraction of residual oil from spent bleaching clay (SBC, i.e. waste from the palm oil refining processes), as well as from various waste products in the milling process, e.g. mesocarp fibres, decanter cake, etc.

Keywords Spent bleaching clay · Residual oil · Process intensification
Palm wax · Extraction · Crystallisation · Pilot plant

M. K. Abdul Aziz (✉)
Department of Chemical and Environmental Engineering, University of Nottingham Malaysia, Broga Road, 43500 Semenyih, Selangor, Malaysia
e-mail: clear.utm@gmail.com

T. Okayama · R. Kose
Division of Natural Resources and Ecomaterials, Institute of Agriculture, Tokyo University of Agriculture and Technology, Tokyo 183-8509, Japan
e-mail: okayama@cc.tuat.ac.jp

R. Kose
e-mail: kose@cc.tuat.ac.jp

N. A. Morad · N. B. N. Muhamad · M. R. B. Mansor
Center of Lipids Engineering and Applied Research (CLEAR), Malaysia-Japan International Institute of Technology (MJIIT), Universiti Teknologi Malaysia, 54100 Kuala Lumpur, Malaysia
e-mail: azian.morad@gmail.com

N. B. N. Muhamad
e-mail: baininabila@gmail.com

F. Panau
Faculty of Engineering and Science, Curtin University Sarawak Malaysia, CDT 250, 98009 Miri, Sarawak, Malaysia

D. C. Y. Foo and M. K. Tun Abdul Aziz (eds.), *Green Technologies for the Oil Palm Industry*, Green Energy and Technology, https://doi.org/10.1007/978-981-13-2236-5_3

1 Introduction

In the palm oil refining process, bleaching clay is used to remove colour, phospholipids, oxidised products, metals and residual gums from the oil [1]. The spent bleaching clay (SBC), containing 30–40% oil, is generally disposed of without proper treatment. The disposal of SBC in landfills may cause fire and pollution hazards due to the substantial oil content in the clay. This disposal constituted a significant economic waste and an environmental burden [2]. For the year 2017, the annual production of crude palm oil (CPO) has reached nearly 20 million tonne, valued at RM 77.8 billions (approximately USD 19 billions) [3]. Based on that, approximately 0.8% of bleaching clays which is 160,000 tonne are used in palm oil refining. Hence, the potential residual oils that can be recovered from SBC yearly are estimated to be approximately 48,000 MT (based on 30% of oil absorbed in SBC). Recovery of residual oil from SBC offers an additional annual revenue of RM 144 million (assuming RM 3000/MT) to the palm oil processing industry. Several processes have been developed to recover residual oil from the SBC, such as solvent extraction [4, 2], supercritical carbon dioxide extraction [5] or a combination of both techniques [1]. The extraction of the oil using organic solvent specially hexane is commonly reported [2] since it is cheap and can be vaporised easily, despite the fact that it can be hazardous to human health and environment. The use of hexane has become the common issues in the environmental debate. Therefore, an alternative green solvent is required to replace the use of hexane.

This chapter presents a green extraction process, known as *solvent extraction–crystallisation–evaporation* (SECE), which is a pilot scale-up equipment that can be used to recover residual oil using a green solvent, i.e. bioethanol. The entire process is operated in mild vacuum condition. The overall process is shown in Fig. 1. The process is first described for the recovery of residual oil from spent bleaching clay (SBC), and next on the various waste products in the milling process, e.g. mesocarp fibres, decanter cake, etc.

2 Materials and Methodology

2.1 SBC and Solvent Preparation

SBC used in this study was obtained from Malaysian local palm oil refinery operated by Sime Darby Jomalina Sdn. Bhd., Selangor, Malaysia. Bioethanol of 99.8% purity was used for the extraction process. The ratio of solid to solvent (wt/v) was set to 1:10. The SBC was packed in a stainless steel mesh cylinder with 26 μm aperture size. Each packed mesh contains 500 g of SBC samples.

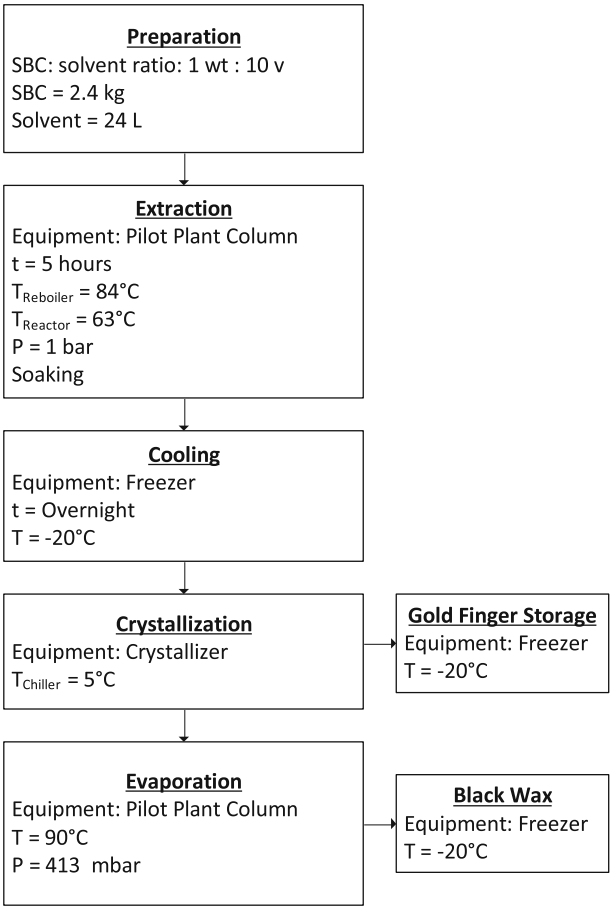

Fig. 1 Process flowchart of SECE process for residual oil recovery (T = temperature; t = time; P = pressure)

2.2 Pilot Plant Solvent Extaction

The extraction process was performed in Centre of Lipid Engineering and Applied Research, Universiti Teknologi Malaysia (CLEAR UTM). The pilot-scale round-bottomed mineral oil jacketed vessel is connected to a condenser (see Fig. 2).

The extracting medium, i.e. bioethanol (20 L), was poured into the 50-L round-bottom vessel. The packed clay (2 kg) samples were soaked in the solvent, and the vessel opening was tightly closed (see Fig. 3).

The extraction was charged with solvent. Then, the experiments were performed at two different pressure conditions, i.e. 0.9 atm (91.325 kPa) and 1.0 atm (101.325 kPa), with boiler temperature set to 90 °C. Note that temperature beyond 90 °C is to be

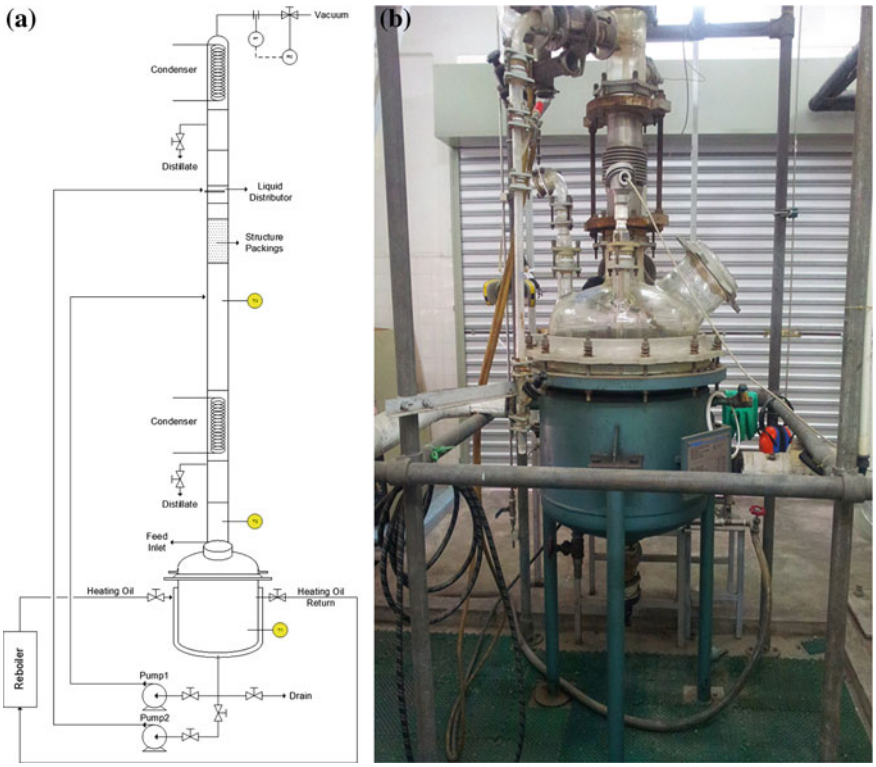

Fig. 2 Pilot-scale SECE: **a** schematic diagram; **b** experimental rig

avoided, in order to avoid temperature-related reactions in the oil, e.g. oxidation. The vacuum condition will reduce the oil density, which will enhance oil recovery (see discussion in Sect. 3). The process was carried out for 5 h duration. For both extraction processes, reflux solvent is being recycled to the extraction vessel. Upon completion, the SBC was removed from the extraction vessel and taken out from the stainless steel mesh cylinder. The experiments were carried out in triplicates.

To obtain the initial oil content in the SBC, 100 g of samples were soaked in 1 L of bioethanol in a 2-L round-bottom flask. The extraction was carried out with continuous stirring for 5 h at 90 rpm. The extractant was filtered by suction to separate the extracts from the SBC powder. The solvent was then removed by means of a rotary evaporator. The experiments were carried out in triplicates. The oil obtained (W_{lse}) is used as a benchmark for deoiling efficiency calculation (see the following section).

Fig. 3 The mesh containers containing palm wastes are immersed in bioethanol

2.3 Fractional Crystallisation and Evaporation

For the incubation process, the extractant was stored at −25 °C in a deep freezer for 12 h to grow the crystal of wax. The mixture was then loaded to a chilled water-jacketed crystallizer (see Fig. 2a). The vessel internal consists of five layers of stainless steel mesh screen (Fig. 2b). The water-jacketed crystallizer vessel was maintained at 5 °C. The high-density oil wax which is light gold in colour is known as *gold finger* (GF, Fig. 4); in this study, it was allowed to settle on the screen by gravity force. The percentage yield was calculated with Eq. (1):

$$\text{GF (wt\%)} = \frac{W_{\text{GF}}}{W_{\text{SBC}}} \times 100\% \tag{1}$$

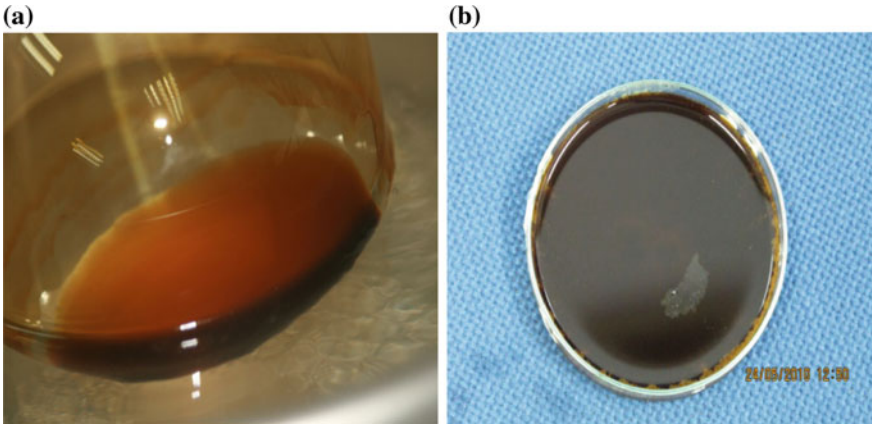

Fig. 4 **a** Fresh palm wax or gold finger (GF) **b** degraded and polymerised palm wax due to time lags and air exposure or black wax (BW)

where W_{GF} and W_{SBC} are the weights of the separated solid and the weight of the SBC used for the extraction process, respectively.

To recover the remaining oils in the filtrate from the crystallizer vessel, the solvent was then separated using rotary vacuum evaporation at 60 °C bath temperature and 175 mbar pressure. The percentage yield of extracted oil known as *black wax* (BW, Fig. 4) in this study was determined using Eq. (2):

$$\text{BW (wt\%)} = \frac{W_{BW}}{W_{SBC}} \times 100\% \tag{2}$$

where W_{BW} is the weight of the residual oil recovered from the evaporator.

The percentage of deoiling efficiency was determined using Eq. (3):

$$\text{Deoiling efficiency (\%)} = \frac{W_{pse}}{W_{lse}} \times 100\% \tag{3}$$

where W_{pse} and W_{lse} are the weights of the total oil extracted using pilot plant scale extraction and the weight of the total oil extracted using lab-scale extraction, respectively.

2.4 Analysis of the Characteristic of the Extracted Oils

The characteristics of SBC residual oil, such as FFA, carotene content, saponification value and kinematic viscosity, were determined via AOCS Ca 5a-40, AOCS Cd 3.2 and ASTM D445 methods, respectively. All the above measurements were performed by SGS Laboratory Services (M) Sdn Bhd.

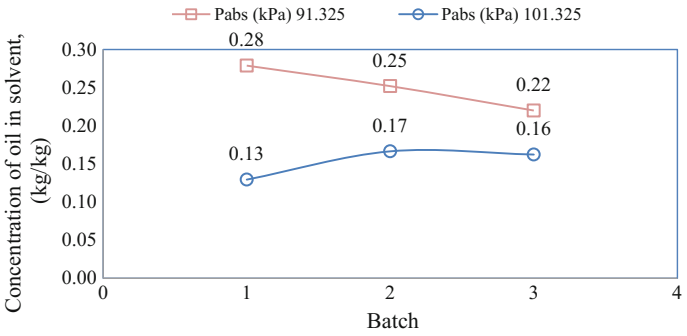

Fig. 5 Effect of extraction pressure on the yield of SBC residual oil

3 Results and Discussion

To develop a green extraction and sustainable approach for recovery of oil, bioethanol was used as a solvent. Different from industrial solvent, which is petroleum-based ethanol, bioethanol is the fermentation product of glucose from renewable biomass (edible starch and non-edible cellulose, etc.), thus, bioethanol is 'safe', clean, 'green' and sustainable.

The concept of this pilot-scale extraction with reflux at 0.9 atm corresponds to a typical percolations process used in the extraction of plant matrix such as Soxhlet extraction. In extraction under reflux, the plant material is immersed in a solvent in a round-bottomed flask, which is connected to a condenser. The solvent is heated until it reaches its boiling point. As the vapour is condensed, the solvent is recycled back into the flask. In this experiment, vacuum pressure was exerted to achieve the reflux. However, the reflux does not occur at atmospheric condition; therefore, the extraction process corresponds to soaking in hot ethanol below its boiling point.

3.1 Effects of Pressure on Extraction Efficiency

Figure 5 shows the concentration of oil extracted at two different operating pressures, i.e. 0.9 and 1.0 atm. Pressure is observed to markedly influence the amount of oil extracted from the SBC. The oil extracted varies between 22.0 and 27.89% (average value of 25.03% ± 2.02) and 12.94–16.65% (average value of 15.27% ± 1.56) for the operating pressure of 0.9 and 1.0 atm, respectively. The deoiling efficiencies calculated using Eq. (3) were determined as 59.4% (0.9 atm) and 36.2% (1.0 atm), respectively.

This shows that extraction performed under slight vacuum gives a higher efficiency. This is due to the fact that vacuum condition lowers the density of bioethanol surrounding the SBC particles, which creates more turbulence between bioethanol

and the oil molecules. At lower pressure, the turbulent bioethanol creates more bubbles around the SBC bed, thus raising the contact between the solid matrix and the solvent, which enhanced the solubility of the oil in the solvent.

The comparison of the different conditions of the extraction is shown in Fig. 5. Extraction under vacuum condition corresponds to percolation effect. This reduces the solvent density at lower pressure to create more percolation bubbles by refluxing the solvent during the extraction process. This condition gives higher efficiency as compared to the static soaking condition with refluxing at atmospheric extraction when percolation bubbles are lesser.

However, the overall extraction efficiency is still low. This is attributed to the confinement of the sample within the stainless steel mesh, which restricts the mass transfer of oil into the solvent. This can be improved by packing the SBC samples into smaller stainless steel mesh container of 50 g each for better mass transfer and interaction between samples and solvent. Further improvement can be made through better mixing by having higher reflux through reduced pressure to higher vacuum. Incorporating mechanical agitator in the system can facilitate mass transfer process during extraction.

The percentage yields of residual oils recovered in this study were comparable to that reported by other workers [5] equivalent to 40% of residual oil yields over dried SBC dry weight.

3.2 Yield of Gold Finger (GF) and Black Wax (BW)

It can be observed from Fig. 6 that the GF yield ranges between 9.0 and 24.6% and the BW yield ranges between 3.29 and 6.5%. GF yield is directly proportional to the percentage of total oil yield. On the other hand, BW yield is not influenced by the percentage of total oil yield and is constant at 4.78% $\pm$ 0.84, as shown in Fig. 6. The relationship between percentage of total oil yield and gold finger is also illustrated with linear regression (see Fig. 6).

3.3 Characterisation of Residual Oils Extracted

The results in Table 1 show that the free fatty acid (FFA) of GF recovered by SECE crystallisation is much lower than that of BW, which was recovered by means of rotary evaporation. The increased final FFA value of 25.9% is attributable to the hydrolysis of some of the triglycerides during the heating in evaporation [6]. In addition, the FFA content of GF, i.e. 1.23%, is also lower than the FFA content of crude palm oil (CPO) which is typically in the range of 3–5%. FFA is of low molecular weight and concentrated in the liquid phase. Furthermore, the dark colour of BW dictates that the coloured matter (i.e. carotenoid and chlorophyll pigments) that was removed by the SBC in the refining process is concentrated in BW instead of concentrated in GF.

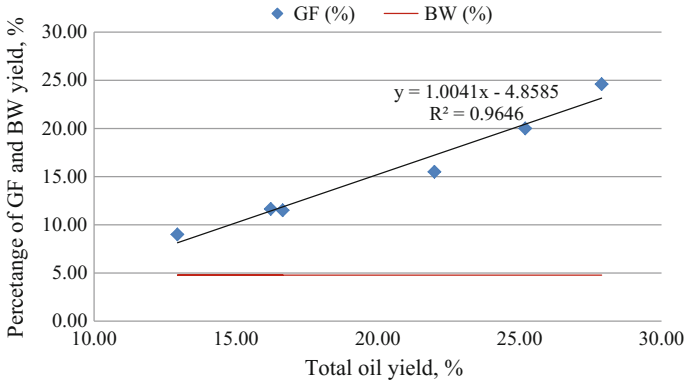

Fig. 6 The relationship of GF and BW yield to the percentage of total oil yield

Table 1 Characteristic of extracted residual oils of SBC

Characteristic	GF	BW	CPO
FFA (%)	1.23	25.19	3 to 5
Saponification value (mg KOH/g)	198	202.3	194 to 205
Kinematic viscosity at 30 °C (mm^2/s)	66.07	77.89	45.34 at 40 °C
Carotene (ppm)	3.3	103.1	474 to 689

This was further verified by the measurement of carotene content. BW reported to have 103.1 ppm carotene content which was higher than the carotene content of GF which was only 3.3 ppm (see Table 1).

4 Potential Uses of GF and BW as Green Chemicals

The residual palm oils and its derivative components are mainly used as packaging, adhesive, cosmetics and pharmaceuticals products. In this research, the application in gas resistance packaging was studied and briefly reviewed here.

Table 1 shows that GF has the lowest FFA content and chemically stable from hydrolysis reaction. In addition, its low Saponification value denotes that it is mainly pure saturated oil and much more stable. However, it has the lowest carotene content and hence quite bland in colour with low in red colouration. These properties make it similar to the Refined Bleached Palm Oil (RBDPO), which is suitable for pharmaceutical applications as face masks and low efficacy cosmetics. Its food used is limited by its residual solvent (bioethanol) content.

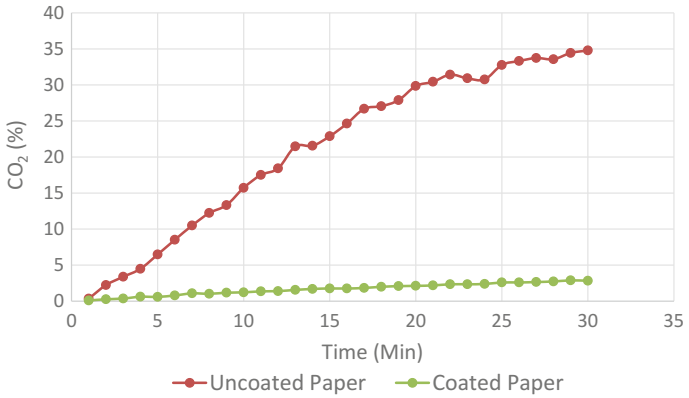

Fig. 7 CO_2 gas penetration measured for unwaxed and waxed layered coated papers

On the other hand, black wax (BW) has higher FFA content prone to hydrolysis and thus chemically unstable. It is darker than GF because it has reacted unsaturated triglycerides and carotene contents during the heating process in evaporation. Hence, BW is suitable to be used as a wax coating for papers and packaging as it is gas resistance. Figure 7 shows the results of an experiment for carbon dioxide (CO_2) gas penetration of packaging paper (made by empty fruit bunches) that is laminated with a layer of BW (up to 20 wt% of BW-to-paper ratio). It is observed that gas penetration of CO_2 into the packaging paper is reduced by 90%.

From the experiment, the mass transfer coefficients of CO_2 of the unwaxed EFB paper and waxed EFB paper are calculated as 2.713×10^{-5} and 1.874×10^{-7} m^2/min, respectively. It is obvious that the biodegradable palm wax acts as a good gas resistance packaging material.

5 SECE for Oil Recovery in Palm Oil Milling Process

In a typical palm oil mill, residual oils are found in various palm waste products. These include mesocarp fibres, decanter cake, etc., as shown in Fig. 8. The residual oils of these palm waste products contain high palm wax content which caused fouling in downstream processes in the mill (e.g. agitator blades, heat exchange parts and coats storage tanks). Hence, it is important to have an integrated pilot-scale unit that is low cost, modular and portable, which can be placed in any location of a mill to remedy the problem rapidly before it creates downstream perturbation to the whole production system.

Figure 9 shows an integrated unit that is based on the same SECE process discussed earlier. The integrated pilot plant is smaller by 50 percent as compared to the SECE unit discussed in Sect. 2. Hence, a pre-mixed 2% weight of 20 g pure palm wax

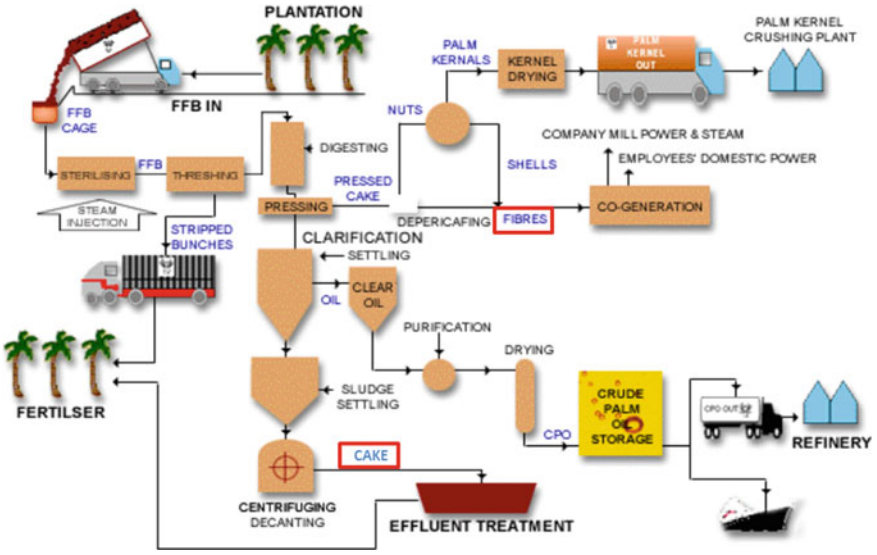

Fig. 8 High concentration of palm waxes is found in various parts of the mill, e.g. mesocarp fibres and decanter cake

in 1000 l of ethanol was prepared to simulate the solvent extraction ratio of 10:1 with dry extract. The volume of the solution was limited to 50% vapour space at high vacuum, in order to flash the ethanol, which can help to super cool the vessel to below the crystallisation temperature of residual oil of below 10 °C. In the initial run, the lowest rotating speed of 1 revolutions per hour (r.p.h.) was set to allow crystals growth with no interference from centrifugal speeds. Time limit of crystals growth was set to 24 h, the same as in the independent SECE units in Sect. 2. In the crystal harvesting stage, the lower temperature and airtight design of the vacuum filtration unit yielded more gold crystals in the vacuum filtration unit. The innovative features of this integrated unit include the following:

i. The hybrid cooling–heating arrangement enabling both heating and cooling of the same vessel at different times by a single thermal fluid.
ii. A small rotating speed of the vessel starting at 1 revolution per hour.
iii. A high vacuum condensate recovery system to recover solvent.
iv. A new micro-freeze drying unit into the vacuum pump filter to capture minute crystals in the exhaust and to transfer crystals online to other solids' recovery system.

However, a lower yield of 12.4% was obtained for the integrated SECE unit, as compared to 25.03% as reported for the SECE unit in Sect. 2. This is mainly due to the higher (−4.3 °C) chilling temperature which produced only 5 °C temperature in this crystalliser. The higher vacuum and the slowest rotational speed did not influence the crystals yield. Note that the product quality is the same as that shown in Table 1.

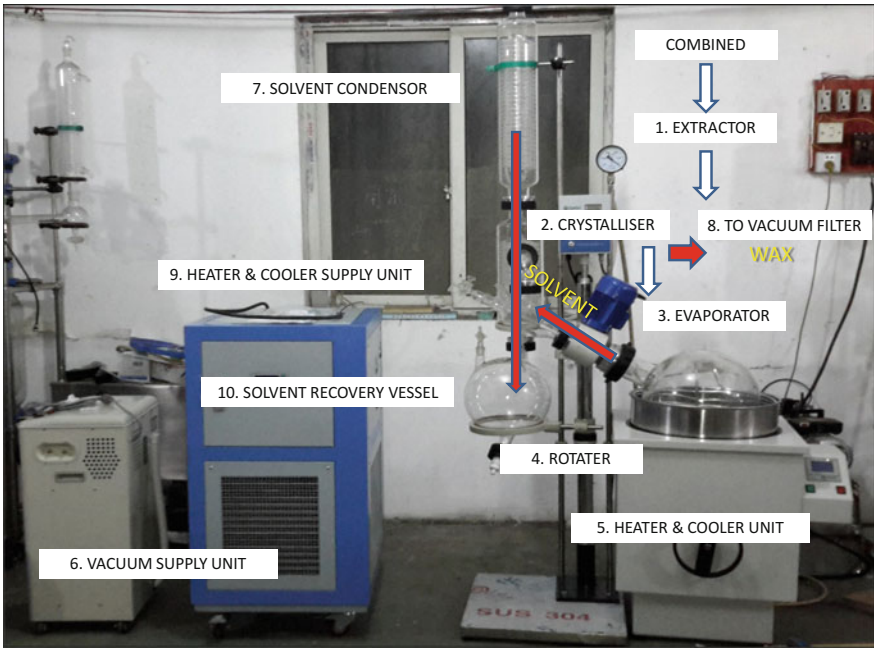

Fig. 9 The integrated SECE unit consists of the following sections: 1. extractor to recover palm oil residues; 2. crystalliser to remove wax from the solvent; 3. evaporator for solvent removal from the wax; 4. rotating device; 5. combined heating and cooling unit; 6. vacuum with secondary cold trap to capture vapour; 7. electrical heater and cooling with dual purpose thermal fluids; 8. extracted wax crystals are sent to an offline separate cold vacuum nanofilter (see Fig. 4); 9. solvent condenser; 10. solvent recovery vessel under vacuum

Table 2 Weights of wax crystallised in each cycle

Cycle	Wax initial (g)	Cycle yield (g)	Wax remained (g)
First cycle GF wax	40	2.66	37.34
Second cycle GF wax	40	1.27	38.73
Third cycle nanofiltered GF wax	40	1.01	38.99
Total yield	40	4.94	35.06

An unexpected benefit of the integrated SECE unit is the fractional crystallisation mode to control size of the crystals formed. In a further experiment of crystallisation and vacuum filtration, nanocrystals were captured by the nanofilter of 0.05 microns size. To fractionate nanopalm wax, a two-step procedure was used. The first batch of large palm wax crystals is first filtered. The second filtrate batch contained nanopalm wax captured on 0.05 microns nanofilter. It is brown-gold colour, stable and is a very thin filtrate upon the filter (see Fig. 10). The yield is 2% versus 13% of a single-state process (Table 2).

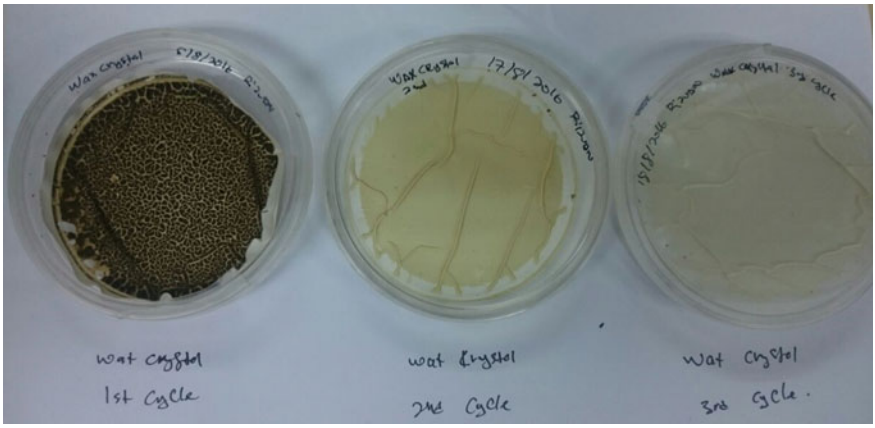

Fig. 10 The three-step fractionation crystallisation experiment using the liquid residue of the filter of the single-batch crystallisation experiment furthered yielded a better looking palm wax with its distinctive gold colour. In the second cycle sample, there was a better palm wax and consequently in the third cycle ultrafine nanosized palm wax was recovered

6 Conclusion

The extraction of residual oils from spent bleaching clay (SBC) has been demonstrated using the newly developed known as *solvent extraction–crystallisation–evaporation* (SECE) process, utilising bioethanol as the extraction solvent. It was observed that the percentage of oil yields was affected by the pressure. At 0.9 atm, the oil yield was 25.03% ± 2.02 and at 1 atm the oil yield was 15.27% ± 1.56. The characteristic of GF and BW shows suitability for food and non-food application, respectively. Similar setup was demonstrated for the oil recovery from palm oil mill waste products, with an integrated unit. This design achieved a portable and modular construction and performance. Unfortunately, it could not overcome the key limitation of lower crystallisation temperature of (−20 °C) and obtained lower product yield of about 13%. Additionally, it has a fractional crystallisation capability to capture by the nanofilter crystals of 0.05 microns size.

Acknowledgements Authors would like to acknowledge Ministry of Agriculture and Agro-Based Industries (MOA) for the Technofund Grant (Project No-tf0310c113) to finance this research study. Individuals who have contributed to this work are also gratefully acknowledged.

References

1. Loh SK, Choo YM, Ma AN (2006) A study of residual oils recovered from spent bleaching earth: their characteristics and applications. Am J Appl Sci 3(10):2063–2067

2. Nursulihatimarsyila AW, Cheah KY, Chuah TG, Siew WL, Choong TSY (2010) Deoiling and regeneration efficiencies of spent bleaching clay. Am J Appl Sci 7(3):434–437
3. New Straits Times (NST) (2018) Malaysia targets RM80b palm oil exports in 2018. www.nst.com.my. Accessed June 2018
4. Alhamed YAS, Al-Zahrani AA (1999) Techno-economical evaluation of oil recovery and regeneration of spent bleaching clay. J King Saud Univ Eng Sci 11(2):115–126
5. King JW, List GR, Johnson JH (1992) Supercritical carbon dioxide extraction of spent bleaching clays. J Supercrit Fluids 5(1):38–41
6. Lee CG, Seng CE, Liew KY (2000) Solvent efficiency for oil extraction from spent bleaching clay. J Am Oil Chem Soc 77(11):1219–1223

Palm Oil Mill Effluent (POME) Treatment—Current Technologies, Biogas Capture and Challenges

Yi Jing Chan and Mei Fong Chong

Abstract With the growing volume of palm oil production, *palm oil mill effluent* (POME) is an inevitable by-product that causes serious environmental hazards if discharged directly to the environment. This is mainly due to its high concentrations of chemical oxygen demand (COD) and biochemical oxygen demand (BOD). Note however that, with its high organic content, POME is a great source for biogas production. Therefore, POME pollution abatement coupled with biogas capture and utilisation are vital in order to promote sustainable development goal for the palm oil industry. Conventionally, POME is treated by employing open ponding system without capturing biogas released from the anaerobic process. This treatment system is inefficient, requires large footprint, long hydraulic retention time (HRT) and is unable to consistently comply with the proposed stringent BOD regulatory limit of 20 mg/L to be imposed by Department of Environment (DOE). Hence, the current POME treatment trend is gearing towards biogas capture technology and integrated POME treatment system with the ultimate aim of achieving zero discharge concept in the palm oil mill. This can be achieved by integrating several bioprocesses, with the aim to transform POME into value-added products. This chapter will discuss the current POME treatment and biogas capture technologies, as well as to identify issues and challenges faced by the palm oil miller which deters the development of biogas plants in the mill. Development of biogas from POME will no doubt contribute substantially in Malaysia's renewable energy sector in the near future.

Keywords POME · Biogas · Anaerobic digestion · Integrated system

Y. J. Chan (✉) · M. F. Chong
Department of Chemical and Environmental Engineering, Centre of Sustainable Palm Oil Research (CESPOR), University of Nottingham Malaysia Campus, Semenyih, Selangor, Malaysia
e-mail: Yi-Jing.Chan@nottingham.edu.my

D. C. Y. Foo and M. K. Tun Abdul Aziz (eds.), *Green Technologies for the Oil Palm Industry*, Green Energy and Technology, https://doi.org/10.1007/978-981-13-2236-5_4

1 Introduction

The palm oil industry in Malaysia has grown by leaps and bounds over the last five decades. Annual palm oil production has increased steadily from 0.09 million tonne in 1960 to 8.3 million tonne in 1998, and notched up to a record of 19.9 million tonne in 2017 [1]. Concurrent to this high production, a large quantity of industrial wastewater, commonly referred to as *palm oil mill effluent* (POME) has been generated. Generally, for every 100 MT of fresh fruit bunches (FFB) being processed, a total of 22 MT of crude palm oil (CPO) and 67 MT of POME will be generated in the mill [2]. In other words, the quantity of POME is actual threefold of that of CPO, which is the main product of the mill. This problem has become more apparent as the number of palm oil mills in Malaysia continues to grow rapidly from 334 mills in 1999 to 454 mills in 2017 [1, 3]. POME is a combination of wastewater streams generated from three main processing steps in the mill, i.e. sludge separation from CPO clarification (0.4 t/t FFB), condensate from fruits sterilisation (0.2 t/t FFB) and effluent from wet separation of kernel and shell (0.07 t/t FFB) [2].

Raw POME is a brownish colloidal suspension comprising 95–96% water, 0.6–0.7% oil and grease, as well as 4–5% solids, as shown in Fig. 1 [4]. It is hot, acidic and contains high organic matters as indicated by its high Biochemical Oxygen Demand (BOD) (Table 1), which is 100 times as polluting as domestic sewage. When the untreated POME is discharged directly to the river, natural decomposition will take place, in which dissolved oxygen in the river water will be depleted rapidly. This will cause the destruction of aquatic life and natural ecosystem. Although the highly polluting POME is non-toxic, it has an unpleasant odour and thereby creating a nuisance to the neighbourhood of the mills.

Based on the extent of pollution, the palm oil milling industry is identified as the largest pollution contributor to the rivers in Malaysia [5]. In realising the pollution menace caused by the palm oil industry, the government had imposed parameter

Fig. 1 Raw POME

Table 1 Characteristics of POME and Department of Environment (DOE) standards for its discharge [23, 52]

General parameters[a]	Mean	Range	DOE standard
pH	4.2	3.4–5.2	5–9.0
Temperature	85	80–90	45
Biochemical oxygen demand (BOD_3)	25,000	10,000–44,000	100[b]
Chemical oxygen demand (COD)	50,000	16,000–100,000	–
Total solids (TS)	40,500	11,500–79,000	–
Total suspended solids (SS)	18,000	5000–54,000	400
Total volatile solids (TVS)	34,000	9000–72,000	–
Oil and grease	6000	4000–8000	50
Ammoniacal nitrogen	35	4–80	150[c]
Total nitrogen (TN)	750	80–1400	200[c]

Note
[a]all parameter in mg/L except pH and temperature (°C)
[b]sample incubated for 3 days at 30 °C
[c]value on filtered sample

limits for the discharge of POME through the enactment of Environmental Quality Acts (EQA) in 1978 as shown in Table 1.

To progress towards a greener environment, the Malaysian Department of Environment (DOE) has imposed more stringent regulations where the BOD discharge limit is reduced from 100 to 20 mg/L in environmentally sensitive areas of Sabah and Sarawak [6, 7]. However, the new regulation with 20 mg/L BOD is yet to be gazetted effectively, especially within the Peninsular of Malaysia, due to the lack of technology with limited land available for ponding treatment system. Hence, an efficient and feasible technology for POME treatment is an urgent need in order to achieve the stringent standard requirement on effluent discharge.

2 POME Treatment Technologies

The enforcement of laws promulgated under the EQA has led to the development of several technologies for POME treatment. In general, POME could be treated by physical, chemical or biological processes. These technologies are briefly described next.

Table 2 Advantages and disadvantages between various POME treatment methods [19, 38, 53]

Treatment types	Advantages	Disadvantages
Membrane	• Produce consistent and good water quality regardless of the influent variations • Require smaller space • Can disinfect treated water	• Short membrane life, membrane fouling, expensive compared to conventional treatment
Evaporation	• Solid concentrate from process can be utilised as feed material for fertiliser manufacturing	• High energy consumption
Coagulation-flocculation	• Improve the separation of particulate species • Can treat POME within short period of time without involving a vast area of land	• High chemical costs • The residual aluminium and • Iron concentrations from the coagulants may inhibit biological treatment process in wastewater and reduce microorganism respiration rate
Anaerobic	• Low energy requirements (no aeration) • Produce methane gas as a valuable end product • Generated sludge from process • Could be used as biofertiliser	• Long retention time • Low start-up period (2–4 months) • Large area required for conventional digesters • Potential odour problems
Aerobic	• Shorter retention time • Produce higher effluent quality than anaerobic process	• High energy requirement (aeration) • High sludge production

2.1 Physico-Chemical Treatments

Some examples of physical and chemical approaches are simple skimming devices [8, 9]; land disposal [10]; use as animal fodder [10, 11]; chemical coagulation, flocculation and flotation [12]; electroflotation [13]; membrane technology [14, 15]; evaporation [16]; and adsorption [17]. However, very few have implemented such systems at full-scale operation because of their unsatisfactory performance, high capital investment, high operating and maintenance cost as shown in Table 2. Moreover, most of these approaches can only be adopted as pre-treatment or tertiary treatment steps for POME as they are still required to couple with other treatment system in order to meet the discharge limit.

2.2 Biological Treatment

Biological treatment includes anaerobic and aerobic processes. They are more promising and sustainable technology for POME treatment. With its high organic content, POME is a good source of nutrients for microorganisms and therefore, production of methane generated from anaerobic digestion is highly potential. With appropriate analysis and environmental control, almost all wastewaters containing biodegradable constituents with a BOD/COD ratio of 0.5 (or greater) can be treated easily by biological means [18]. As shown in Table 1, BOD: COD ratio of raw POME is approximately 0.5, implicating that POME is suitable to be treated by biological processes. The principal processes used for the biological treatment of wastewater can be classified with respect to their metabolic function as aerobic, anaerobic, and combined anaerobic–aerobic processes.

2.2.1 Conventional Anaerobic Treatment Methods

In general, aerobic systems are suitable for the treatment of low-strength wastewaters (biodegradable COD concentrations less than 1000 mg/L) while anaerobic systems are suitable for the treatment of high strength wastewaters (biodegradable COD concentrations over 4000 mg/L) [19]. Therefore, the very high level of organic matters in POME requires the adoption of anaerobic digestion as the primary treatment process. More than 50% of palm oil mills in Malaysia have adopted ponding system, involving anaerobic digestion for the treatment of POME (Fig. 2). This is mainly due to their low capital costs, simplicity and ease of handling [20]. Normally, the anaerobic digestion is operated at low rate, with organic loading rate (OLR) of 0.2–0.35 kg BOD/m^3.day [21]. Open digesting tanks are used for POME treatment when limited land area is available for ponding system. It has been reported that open ponding system is capable in reducing the concentration of pollutants such as COD (100–1725 mg/L), BOD (100–610 mg/L) and ammoniacal nitrogen (100–200 mg/L) [22, 23]. However, these conventional methods have several drawbacks, such as long hydraulic retention time (HRT; 45–65 days), large areas of lands, and consistent desludging of the settled POME. More importantly, the treated effluent fails to meet the discharge standard consistently [24]. Besides, the potential for biogas utilisation is often being overlooked by the palm oil industry. The produced biogas from anaerobic digestion process emits directly to the atmosphere, posing a detrimental greenhouse effect on the environment [24, 25].

2.2.2 Aerobic Treatment

Aerobic biological processes are commonly used in the treatment of organic wastewaters for achieving high degree of treatment efficiency. The aerobic treatment of POME was investigated by using: fungus Trichoderma viride in the fermentation of

Fig. 2 Typical anaerobic pond of a palm oil mill

POME [26]; a tropical marine yeast (Yarrowia lipolytica) NCIM 3589 in the degradation of POME in a lagoon [27]; trickling filter [28]; rotating biological contactors [29]; and activated sludge process with a diffused aeration system [30]. Nevertheless, the aerobic treatment system is not commonly used in treating wastewater of high organic load, especially raw POME. The high organic level makes aerobic treatment on its own difficult to achieve the desired efficiency in both technical and economical points of view. Moreover, the BOD: N: P ratio of raw POME is reported as 100:3:0.8 (may be calculated based on data in Table 1), is slightly nutrient deficient for aerobic treatment; the latter requires a minimum nutrient ratio of 100:5:1 [18].

2.2.3 Conventional Anaerobic–Aerobic Treatment

Consequently, prior to aerobic treatment, anaerobic treatment may be used to reduce the organic strength of POME. Vijayaraghavan et al. [30] proved that the aerobic treatment of the anaerobically digested POME resulted in higher BOD and COD removal efficiencies than the aerobic treatment of diluted raw POME. It is due to the presence of partially degraded organics in the anaerobically digested POME, making them more amenable to aerobic digestion. There are many examples in which anaerobic processes provide partial stabilisation before further treatment with aerobic processes due to the relatively high organic strength of many industrial wastewaters (14,500–65,700 mg/L) [31, 32]. Published researches also reported that series reactors of anaerobic–aerobic processes are feasible for treating municipal, sewage and high organic strength wastewater resulting in lower energy requirements and less sludge production [33, 34].

In the case of POME treatment, some of the palm oil mills in Malaysia have adopted open tank digesters and extended aeration systems where POME is treated in an anaerobic digestion process followed by extended aeration in a pond (Fig. 3). Normally, the open tank digesters are operated at low rate, with OLR of 0.8–1.0 kg BOD/m^3.day. If properly operated and maintained, this treatment system is capable of removing COD by 81% [35] and is able to meet the discharge limit [21]. However, one

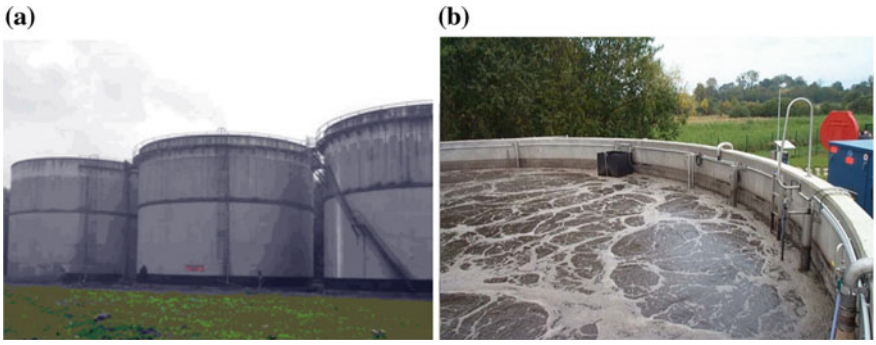

Fig. 3 **a** Anaerobic tank digesters; **b** extended aeration system

of the major problems of this system is that it occupies a vast area of land and requires a relatively long HRT of 20 days for the anaerobic process and 20 days for aerobic process. Besides, there is no system that captures the produced methane gas. Although this practice appears to be at minimal cost, the constraint lies on the availability of sufficient land for building the ponds and the length of the HRT taken to treat the POME. Continuous hikes in land and labour costs, as well as external pressures from global environmentalists are forcing palm oil millers to reconsider alternatives. Hence, treating POME within a short period of time at reduced space utility by using high-rate anaerobic and aerobic bioreactor with biogas trapping facilities may offer a viable alternative to replace these conventional anaerobic–aerobic systems.

2.3 Greener Technology for POME Treatment—Biogas Capture System

Biogas production process exploits the natural ability of microorganisms to degrade organic wastes in the absence of oxygen, i.e. anaerobic digestion. Biogas typically composes of 50–75% methane (CH_4), 25–45% carbon dioxide (CO_2), trace amounts of H_2S and other gases. POME with high organic contents may be considered as a renewable energy source. It is projected that the total power output is approximately 480 MW, if biogas produced from all palm oil mills in Malaysia (a total of 445 mills) could be captured and used [2]. Note that this estimation is based on gas engine conversion efficiency of 40% and biogas power plant operation hours of 7000 h per year [2]. Therefore, palm oil millers have shown great interest in recent years to implement greener and more sustainable technologies in their mills such as biogas capture technology, as well as moving towards zero waste approach [23].

In the current practise, biogas from POME in Malaysian mills is captured and utilised for the following purposes, which include steam generation, combined heat and power (CHP) for simultaneous production of steam and electricity, electric-

Table 3 Comparison between covered lagoon systems and continuously stirred tank reactor [3, 36, 54]

Technology	Covered lagoon systems	Continuously stirred tank reactor/digester tank
Waste types	Thin liquid	Liquid and solid
HRT (days)	20–90	20–40
COD removal efficiency (%)	70–85	80–90
Operation complexity	Low	Medium
Total capital cost[a] including burner (million USD)	1.96	2.24
Payback period	3.6	4.3
Energy yield	Medium	Good
CH_4 produced/COD_{in} (kg/kg)	0.03–0.16	0.07–0.23

[a]type of biogas utilisation: co-firing

ity generation for grid connection and downstream business activities [36]. The implementation of biogas capture is considered as one of the activities in Economic Transformation Programme (ETP) under the Palm Oil National Key Economic Area (NKEA) in Malaysia. It aims to increase the gross national income (GNI) by year 2020 [23].

There are two commonly used biogas capture technologies, i.e. covered lagoon and continuous stirred tank reactors (CSTR). According to Loh et al. [36], approximately 50 palm oil mills in Malaysia have employed tank-type technologies to capture the produced biogas, while 36 mills use covered lagoon systems. Table 3 shows the comparison between covered lagoon systems and CSTR systems. Their basic principles are briefly described next.

2.3.1 Covered Lagoon

A cost-effective way to capture biogas from the conventional open anaerobic ponds is to retrofit the existing ponding/lagoon system through the installations of floating plastic membranes on the open ponds. As it is more economical and easier to operate as compared to other anaerobic digester technologies, most palm oil mills in Malaysia installed sealed cover over existing anaerobic POME ponds to create an anaerobic digester system, as shown in Fig. 4 [3]. The sealed cover material is usually made of linear low-density polyethylene liners (LLDPE), or synthetic high-density polyethylene (HDPE) geo-membrane that are resistant to bad weather, biological degradation and UV radiation. This covered lagoon design typically handles a solids content of less than 2% and commonly operates in the mesophilic temperature range [37].

However, despite its simplicity, anaerobic lagoon exhibits several drawbacks. In general, it has poor bacteria-to-substrate contact, with a low loading rate. Besides,

Fig. 4 Covered lagoon

covered lagoon requires a long hydraulic retention time and has a large footprint. The production rate of a covered anaerobic pond was reported to be 0.03–0.16 kg CH_4/kg COD treated [3]. The low methane production is mainly due to the lower efficiency of anaerobic pond system and the lack of operational control.

2.3.2 Continuous Stirred Tank Reactors (CSTRs)

Continuous stirred tank reactors (CSTRs) are typically concrete cylinders with a low height-to-diameter ratio. CSTR is equivalent to a closed-tank digester with mechanical agitator which provides more area of contact with the biomass and thus improving biogas production [38]. In operating the CSTR, feeding of POME should be continuous for maximum efficiency. It can be operated at mesophilic or thermophilic conditions. CSTR typically can handle a higher solids content of 3–10% than covered lagoon. Based on the economic analysis of biogas capture and utilisation in a 60 MT/h palm oil mill as shown in Table 3, the investment cost of CSTR is slightly higher than that of covered lagoon system—[39]. This estimation is based on the biogas system where the captured biogas is co-fired in the biomass boiler.

It was also reported that the CSTRs have better performance as compared to the covered lagoon, in terms of the amount of methane gas produced per kg of COD treated in the system. The closed anaerobic digester tank was capable of producing 0.07–0.23 kg CH_4/kg COD treated [3]. The CSTR technology employs readily available microorganisms in the POME. Despite higher capital cost, CSTR has a higher rate of historical success and higher methane production (as compared to the covered lagoon). However, the major drawbacks of the CSTR include less efficient biogas production at high feeding rates and less biomass retention.

2.3.3 High-Rate Advanced Anaerobic Bioreactors

In recent years, new technologies have been developed to alleviate the problems faced by the conventional treatment systems. Improved high-rate anaerobic bioreactors with higher treatment efficiency and lower site area have been adopted in the treatment of POME. These include anaerobic filter and anaerobic fluidised bed reactor [40]; two-stage upflow anaerobic sludge blanket (UASB) reactor [41]; membrane anaerobic system [42]; modified anaerobic baffled bioreactor [43]; thermophilic upflow anaerobic filter [44]; expanded granular sludge bed (EGSB) [15] and anaerobic hybrid reactor (upflow anaerobic sludge blanket fixed film (UASFF) bioreactor) [4]. A comparison of various advanced anaerobic bioreactors available in Malaysia is tabulated in Table 4.

These high-rate bioreactors are more effective in biodegradation, with shorter retention times, higher methane yield (without compromising the OLR). It has been reported that these high-rate anaerobic bioreactors were able to achieve higher than 78% COD removal efficiency, and biogas product with at least 50% of methane at higher OLR (ranging between 1.6 and 40.0 kg COD/m^3.day under mesophilic condition) [19].

Note however that, POME treatment using anaerobic high-rate bioreactor alone is insufficient to satisfy the new discharge standard. Thus, aerobic bioreactor is required to polish the effluent. The mill owners are reluctant to adopt these advanced bioreactors as most of them are designed and performances were only evaluated at laboratory scale. Their results may differ for a full-scale plant, due to the fact that actual working conditions are not as easily controlled or predicted.

On top of that, several technical problems have been reported in the operation of these anaerobic bioreactors. In particular, anaerobic filters and UASFF are susceptible to the clogging problem within the packing [44–47]. Attributable to high TSS concentration (Table 1) in POME, OLRs in these reactors should be reduced to ensure high treatment efficiency. In addition, UASB and EGSB reactors are frequently confronted with the foaming and scum formation problems especially at high OLRs, which are mainly caused by high concentration of oil and grease (O&G) in POME (Table 1) [15].

Thus far, almost all reported advanced technologies are standalone without proper integration for sustainable resource management and recovery [36]. Most of them are unable to degrade the organic matter to meet the effluent BOD discharge limit of 20 mg/L imposed by DOE. Therefore, it is essential to integrate the advanced anaerobic bioreactors with sustainable polishing technologies in order to move towards zero discharge POME treatment system.

2.3.4 Integrated Zero Discharge POME Treatment System

The zero discharge concept in the POME treatment system theoretically means all the incoming effluent is completely treated, no waste is being discharged. The ultimate target is to recover usable materials such as oil, sludge and water from the POME.

Table 4 Comparison of various advanced anaerobic bioreactors available in Malaysia [38, 39, 49]

Treatment method	Tank material	OLR (kg COD/m^3.day)	Capital cost (USD million)	Power output (MW)	HRT (days)	Anaerobic COD removal efficiency (%)	Anaerobic TSS removal efficiency (%)	Volume of biogas generated (m^3/MT POME)
AnaEG	Carbon steel	1.6	2.43[a]	1.4	9	93.7	37.9	28
IAAB	Reinforced concrete (RC)	8–13	3.55[a]	2.4	5–7	82–93	75–92	16–35
UASB	–	10.6	–	–	4	98.4	–	–
Anaerobic fluidised bed reactor	–	40	–	–	0.25	78	–	–
UASFF	–	11.58	–	–	3	97	–	–

[a]estimation is based on a typical 60 MT/h palm oil mill with on-grid electricity generation

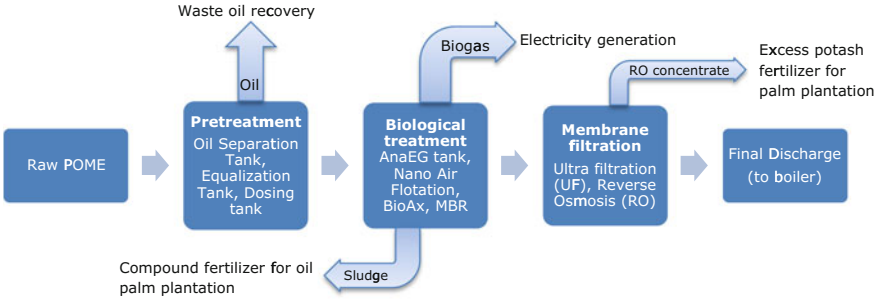

Fig. 5 AnaEG system for POME treatment [39]

Doing this leads to minimum waste generation and to convert the treated anaerobic and aerobic sludges to fertiliser without discharging into the environment [7, 39]. To date, there were only several studies being reported on the integrated zero discharge treatment, one at pre-commercialised plant [48], two at pilot studies and the other engineered at laboratory scale [39, 49].

(a) **Anaerobic expanded granular sludge bed (AnaEG™) technology**

A zero discharge integrated POME treatment technology which consists of *advanced anaerobic expanded granular sludge bed* (AnaEG) and *biotechnological aerobic process* (BioAX) was developed at Kilang Kelapa Sawit (KKS) Labu, Malaysia, Sime Darby [7, 39]. As shown in Fig. 5, the AnaEG system consists of three major units, i.e. pre-treatment, biological treatment and membrane separation. The pretreatment unit is meant for the recovery of waste oil from POME. Biological treatment, on the other hand, is to produce biogas from POME and to generate final discharge with BOD lower than 20 mg/L. Membrane separation is meant to purify wastewater for reuse or recycling. The treated sludge from the AnaEG system is recovered as biofertiliser and it shows good fertiliser values than raw POME, due to the fact that organic fertiliser derived from treated sludge contains a higher percentage of nitrogen, phosphorus and potassium (NPK) [39]. Besides, the BOD of the treated effluent after BioAX stage was always less than 20 mg/L, with 80% consistency [7]. High-quality biogas is also reported with CH_4 content ranging between 65 and 70% [39]. The reported HRT for AnaEG system is 9 days, which is significantly shorter than the conventional treatment system. The volume of biogas generated is 28 m^3/MT POME, which is comparable to those reported values for CSTR and covered lagoon.

Overall, AnaEG system displays great potential in achieving zero discharge for the palm oil industry, in view of its capabilities in producing biofertiliser from treated POME and recycled water for boiler use. However, based on the economic analysis of the biogas system for a typical 60 MT/h FFB palm oil mill, the total capital cost of this system (see Table 4) [39] is slightly higher than those of CSTR and covered lagoon. Therefore, the economic aspects of this technique need to be further addressed for commercial uptake. Besides, the high oil and solids content in the POME should

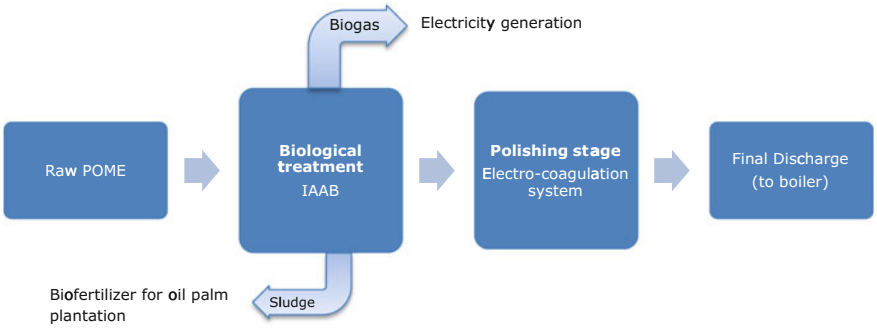

Fig. 6 An IAAB system for the treatment for POME

be reduced before entering this system; this requirement makes it to possess more pre-treatment facilities.

(b) **Integrated anaerobic–aerobic bioreactors (IAAB)**

This IAAB system consists of a novel bioreactor based on the integration of anaerobic, aerobic and sedimentation processes (Fig. 6). The basic configuration of the bioreactor is depicted in Fig. 7. It was first developed at lab scale with a reactor volume of 60 L in 2009 (see Fig. 8), followed by a 1.8 m^3 pilot scale IAAB in 2012 and a 3000 m^3 pre-commercialised scale IAAB at Havys Oil Mill in 2015 (see Fig. 9) [48, 55]. As shown, the IAAB is a single reactor configuration with compartmentalisation. The rectangular tank is divided into three compartments, in which anaerobic, aerobic and sedimentation are to be carried out sequentially. The final discharge from the settling compartment was reported to meet the discharge standard of BOD 20 mg/L consistently [19]. To achieve zero liquid discharge, the treated water is further polished for recycling and reuse in the palm oil mill. The main advantages of IAAB include higher organic removal efficiency (up to 99.9%), higher biogas yield (up to 35 m^3/MT POME), much shorter retention time, i.e. 5–7 days (instead of 60 days with the current ponding system), and most importantly, reduced land footprint by 80%. Besides, the IAAB system is self-sustained in term of power consumption, for the OLR operating range of 8–13 kg COD/L/day. The relatively high performance of the IAAB was found to be attributed to several factors, which includes adequate retention of Mixed Liquor Volatile Suspended Solids (MLVSS) concentrations (population of microorganism in both anaerobic and aerobic compartments), development of good settling activated sludge and high recirculation ratio adopted in the anaerobic compartment leading to good hydraulic contact between the substrate and the sludge.

As compared to AnaEG, IAAB is simpler in terms of process and operation as it has lesser unit operations (see Fig. 7). Besides, IAAB has smaller land footprint due its lower HRT. Furthermore, no chemical is required for the operation of IAAB, which in turns leads to lower operating cost. In term of COD removal efficiency, AnaEG showed higher efficiency of 94%, as compared to 85% for IAAB (Table 4), however, at a much lower loading rate of 1.6 kg COD/m^3.day as compared to 12.8 kg

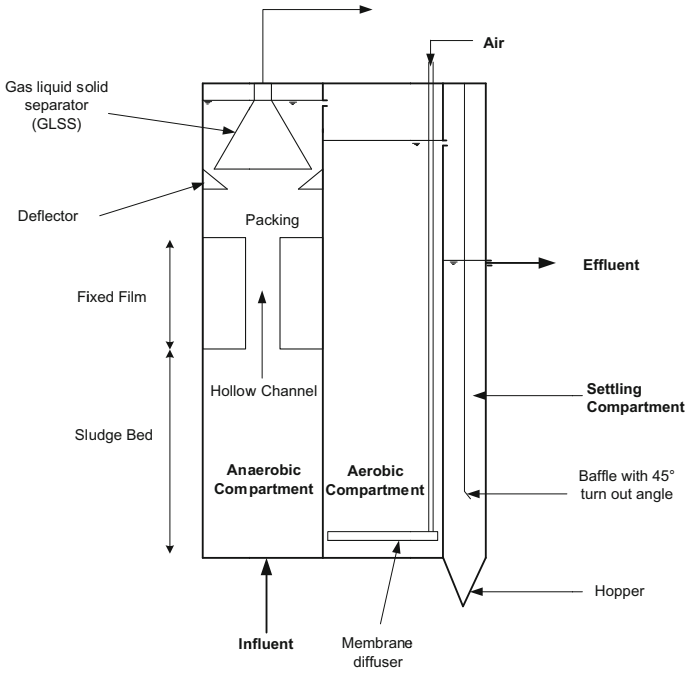

Fig. 7 Basic configuration of IAAB

COD/m^3.day for IAAB. This indicates that IAAB is capable to handle higher loading rates.

3 Current Issues, Challenges and Areas of Improvement

Malaysian government envisages all palm oil mills (estimated to reach 500 by year 2020) to have biogas trapping facilities installed by 2020 [2]. However, up to 2015, merely 17% of those mills had implemented biogas capture system [36]. In fact, Malaysia faced many issues and challenges in moving towards nationwide biogas capture implementation. Many problems encountered are related to technology, finance, governance and grid connectivity, which are discussed next.

3.1 Technology Challenges

The performance of the various biogas capture technologies is closely associated to the robustness of the technology in withstanding fluctuation of POME volume,

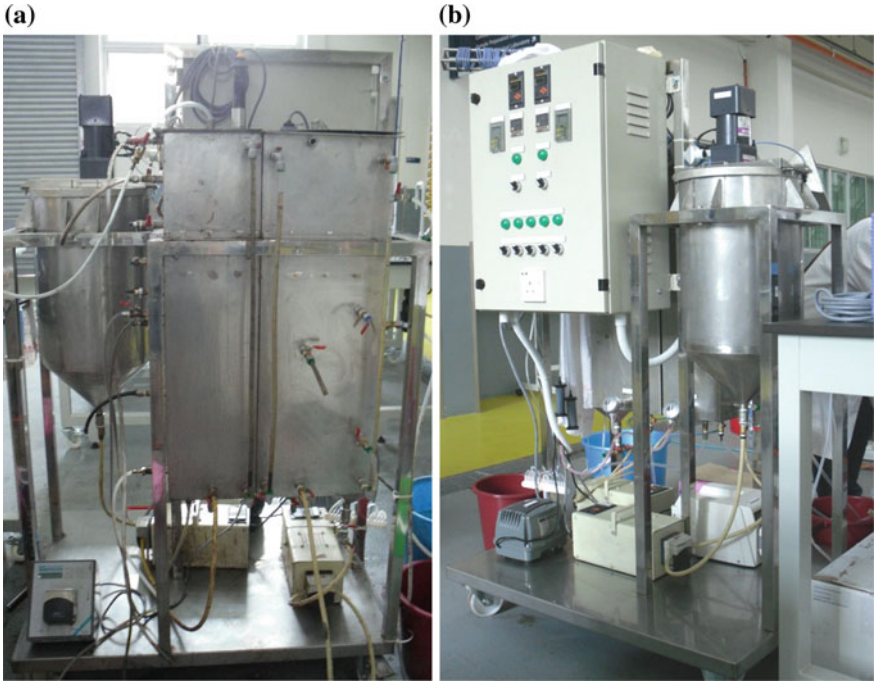

Fig. 8 Actual view of IAAB system **a** laboratory scale front view **b** rear view

OLR and flow characteristics in the digester. Besides, the operating conditions of the digester such as microorganism's quality and populations, solid removals, reaction temperature, HRT and mixing system, etc. are also the key factors that will affect performances of the biogas capture technologies. One of the most critical issues is the seasonal fluctuation of oil palm FFB yield, which affects the volume of POME. Excess biogas would need to be flared off during the high crop season. Conversely, during the low crop season, there is insufficient of POME for the microorganisms and thus, less biogas is generated. As a result, most biogas plants of the existing palm oil mills have an average power output of 1 MW, although they have an installed capacity of 2 MW [2]. Therefore, designing a robust biogas trapping facility that can accommodate the fluctuating characteristics in the volume and quality of POME is important. The aforementioned problem during the low crop season can be potentially solved by co-digesting POME with the empty fruit bunch (EFB) and mesocarp fibre (MF), which are generated along the production of CPO. EFB and MF may serve as a good carbon source to be co-digested with POME for biogas production. Besides, EFB and/or MF can counteract the low carbon and nitrogen content of POME in anaerobic digestion process. Both nutrients are equally important for microorganisms that carry out the digestion process, as carbon is the main food source for growth while nitrogen assists in enzyme production.

Fig. 9 Pre-commercialised scale of IAAB system (courtesy of Havys Oil Mill Sdn. Bhd.)

On the other hand, there are a few areas that are worth consideration in the integrated POME treatment approach. In the first place, the main wastewater source in the milling process should be reduced as it leads to huge production of POME. Second, the unwanted constituent of the biogas, i.e. H_2S should also be reduced during the biogas production process. This is because H_2S causes corrosion in some machineries through the formation of sulfuric acid (when H_2S reacts with water). Therefore, H_2S has to be removed from biogas through scrubber before the biogas is sent to the gas engine for power generation. The reduction of H_2S can be achieved

by employing special pre-treatment technique; the latter involves a series of physical and chemical treatments (oil separation tank, equalisation tank, air flotation and dosing tank), in order to break down the big molecules, i.e. particularly the protein-rich organic matter for easy biodegradation. Through pretreatment, H_2S concentration can be reduced to 200 mg L^{-1} [36]. This is important as the H_2S concentration can go as high as 3000 mg L^{-1}, which result in higher scrubbing cost.

3.2 Safety and Operational Risks

The key challenges to the operators of the biogas plant include operational, potential explosion, corrosion hazards and GHG gas emissions reduction. Therefore, the safety aspect in operating biogas trapping facilities is vital. A Malaysian Standard (MS2581:2014) guidelines on general requirement, installation requirement, specific requirement, safety requirement, competent personnel requirement and maintenance and operation, etc. has been developed [36]. Unsatisfactory performance of the POME treatment plant is often due to the lack of competent personnel or operators. Therefore, the biogas plant operators need to ensure a stable operation while managing the seasonal POME characteristics change. Close monitoring of biogas and power generation systems during operation and maintenance are equally important.

3.3 Knowledge Transfer Between Industry and Academia

The advanced POME treatment technologies such as AnaEg and IAAB system are found to be effective and are able to achieve zero discharge concepts in the POME treatment as well as to maximise the utilisation of biogas generated as a source of renewable energy. However, some of the millers are sceptical. This is mainly due to the lack of companies' commercial data. Collaboration with industry and academia to produce commercial data to show the efficiency of the biogas technology may improve millers' confidence in investing in new technology [2].

3.4 High Investment Cost

One of the key challenges for the palm oil millers to build biogas plant for power generation system in the palm oil mills is its relatively high investment cost (as compared to the conventional ponding system). A survey conducted by Yahaya and Lau [50] reveals that many palm oil mills are not willing to acquire and adopt advanced POME treatment technology. In some cases, the palm oil millers claimed that the utilisation of biogas for power generation required high initial capital cost. The common perception is that this investment is not economically viable, as it does not give

immediate profit and requires a long payback period (about 5 years via feed-in-tariff (FiT) payment) [3].

In reality, the utilisation of biogas for power generation is lack of demand and not so attractive to the palm oil millers. This is because most of the palm oil mills are already self-sufficient in energy, as MF and palm shell (PS) are utilised in the biomass boiler for steam and power generation for the production of CPO [51, 36]. Moreover, the national grid is well structured and the fuel is heavily subsidised. Therefore, anaerobic digestion-based biogas production in Malaysia has far lesser relevance to short energy supply than in its neighbouring countries such as Cambodia. Furthermore, palm oil mills are normally far from one another and isolated from any energy-intensive industrial activities within their vicinities. This in turn makes some of the well-developed biogas utilisation approaches (e.g. rural electrification and decentralised biogas power production) irrelevant, less attractive, and has little success. To overcome this, bottled bio-compressed natural gas (bioCNG) to ease transportation seems a viable approach [36]. In fact, biogas can be compressed the same way natural gas is compressed to CNG after removing its impurities such as CO_2, H_2S, and moisture.

3.5 Government Supports

Many mill owners have reflected that there are no clear-cut biomass and biogas policies and sufficient incentives to convince them in venturing into such projects. Besides, the procedural and approval processes for developing biogas plant in palm oil mill are long, tedious and currently requiring too detailed technical information [36]. This clearly indicates that attractive incentives and supports of the government will be a major factor that attracts the millers to adopt the new technologies. A more concerted governmental effort is required in processing applications, facilitating and coordinating nationwide biogas implementation under the current set up [36].

3.6 Grid Interconnectivity

It is difficult for those biogas plants to be connected to the national grid, especially for palm oil mills which are located in rural areas which are far from the interconnection point. This is due to the fact that the distance between the biogas power generation plant and the location of the interconnection point at the distribution system must be within 10 km to avoid power lost [3]. Longer distance will increase the connection cost and also power lost. To overcome this, those palm oil mills that are located near to each other but far away from the national grid interconnection point could connect their biogas plant together to form a mini-grid system for rural application. This system has high potential to be implemented in the states of Sabah and Sarawak (in Borneo island), where national grid electricity is out of reach in the rural areas [3].

Another challenge is that most of the parties involved in biogas development do not have expertise in grid interconnectivity knowledge. Therefore, regular series of interactive sessions between the parties involved and the relevant authorities are essential. First, this can assist in educating and creating awareness on engineering aspects of grid connection; and second to deal with policy intervention to ensure smooth implementation [36].

4 Conclusions

Treating POME in a sustainable manner by capturing biogas is vital to transform the palm oil industry into a greener industry. Covered lagoon and CSTR are currently the most commonly used biogas capture technologies. Due to the more stringent requirement of BOD 20 mg/L to be imposed by DOE, the existing treatment methods may face difficulty in complying with the discharge limit consistently. Therefore, the current POME treatment trend is gearing towards the reduction of the BOD content of POME (to less than 20 mg/L), reduction of HRT and footprint, while at the same time trapping the produced biogas. The ultimate aim of doing these is to achieve zero discharge concept in the palm oil mill. There are two advanced technologies, AnaEG and IAAB which show great potential in achieving zero effluent discharge due to their high treatment efficiency and methane yield along with the production of biofertiliser and recycled water. Nevertheless, there are barriers that hindered the palm oil millers to adopt these advanced integrated POME treatment system. These are closely related to technology, finance, governance and grid connectivity. With stronger support and more financial assistances from government, it is envisaged that all palm oil mill will be equipped with biogas facilities in the near future. While most researches are working on POME treatment via end-of-pipe processes, it is a good idea to consider a cleaner production. This can be done by reducing the main wastewater source in the milling process, as it is the root cause of abundant POME generation. Besides, practicing knowledge transfer between industry and academia can help to reduce any scepticism of the advanced technology and the realisation of advanced bioreactors into cost-effective full-scale plant.

Acknowledgements The authors would like to gratefully acknowledge the financial supports from Havys Oil Mill Sdn. Bhd. and Eureka Synergy Sdn Bhd for funding the pre-commercialised scale IAAB project.

References

1. MPOB (2018) Malaysian palm oil board. Retrieved 1 July 2018, from Home page: http://bepi.mpob.gov.my/index.php/en/statistics/production/186-production-2018.html
2. Yap CC, Soh KL, Chong MF, Chan YJ, Christina V (2017) Palm oil potential: the problem of methane emissions at Malaysia's palm oil mills can be turned on its head – if the industry buys

into biogas. Chem Eng 910:42–45
3. Chin MJ, Poh PE, Tey BT, Chan ES, Chin KL (2013) Biogas from palm oil mill effluent (POME): Opportunities and challenges from Malaysia's perspective. Renew Sustain Energy Rev 26:717–726
4. Najafpour GD, Zinatizadeh AAL, Mohamed AR, Hasnain Isa M, Nasrollahzadeh H (2006) High-rate anaerobic digestion of palm oil mill effluent in an upflow anaerobic sludge-fixed film bioreactor. Process Biochem 41:370–379
5. Wu TY, Mohammad AW, Jahim JM, Anuar N (2007) Palm oil mill effluent (POME) treatment and bioresources recovery using ultrafiltration membrane: effect of pressure on membrane fouling. Biochem Eng J 35:309–317
6. Bello MM, Abdul Raman AA (2017) Trend and current practices of palm oil mill effluent polishing: application of advanced oxidation processes and their future perspectives. J Environ Manage 198:170–182
7. Tabassum S, Zhang Y, Zhang Z (2015) An integrated method for palm oil mill effluent (POME) treatment for achieving zero liquid discharge—A pilot study. J Clean Prod 95:148–155
8. Ng WJ, Goh AC, Tay JH (1988) Palm oil mill effluent treatment - liquid-solid separation with dissolved air flotation. Biological Wastes 25:257–268
9. Roge W, Velayuthan A (1981) Preliminary trials with Westfalia-3-phase decanters for palm oil separation. In: Pushparajah E, Rajadurai M (eds) Palm oil production technology eighties, Rep. Proc. Int. Conf., Inc. Soc. Plant. Kuala Lumpur, Malaysia, pp 327–334
10. Ma AN, Ong A (1986) Palm oil processing—new development in effluent treatment. Water Sci Technol 18:35–40
11. Sutanto J (1983) Solvent extraction process to achieve zero-effluent and to produce quality animal feed from mill sludge. Planter 59:17–35
12. Ahmad AL, Chong MF, Bhatia S (2008) Population Balance Model (PBM) for flocculation process: simulation and experimental studies of palm oil mill effluent (POME) pretreatment. Chem Eng J 140:86–100
13. Ho CC, Chan CY (1986) The application of lead dioxide-coated titanium anode in the electroflotation of palm oil mill effluent. Water Res 20(12):1523–1527
14. Ahmad AL, Chong MF, Bhatia S (2007) Mathematical modeling of multiple solutes system for reverse osmosis process in palm oil mill effluent (POME) treatment. Chem Eng J 132:183–193
15. Zhang Y, Yan L, Qiao X, Chi L, Niu X, Mei Z, Zhang Z (2008) Integration of biological method and membrane technology in treating palm oil mill effluent. J Environ Sci 20(5):558–564
16. Ma AN (1999) Innovations in management of palm oil mill effluent. The Planter 75:381–389
17. Ahmad AL, Sumathi S, Hameed B (2005) Adsorption of residual oil from palm oil mill effluent using powder and flake chitosan: equilibrium and kinetic studies. Water Res 39(12):2483–2494
18. Metcalf and Eddy (2003) Wastewater engineering treatment and reuse, 4th edn. McGraw Hill, New York
19. Chan YJ, Chong MF, Law CL (2011) A complete palm oil mill effluent (POME) treatment system using a novel integrated anaerobic–aerobic bioreactor (IAAB). Ph.D. thesis, Malaysia University of Nottingham
20. Liew W, Kassim M, Muda K, Loh SK, Affam A (2015) Conventional methods and emerging wastewater polishing technologies for palm oil mill effluent treatment: a review. J Environ Econ Manage 14:222–235
21. Ma AN (1993) Current status of palm oil processing wastes management. Palm Oil Res. Instit. Malaysia (PORIM) 111–136
22. Zahrim AY, Nasimah A, Hilal N (2014) Pollutants analysis during conventional palm oil mill effluent (POME) ponding system and decolourisation of anaerobically treated POME via calcium lactate-polyacrylamide. J Water Process Eng 4:159–165
23. Zainal NH, Jalani NF, And Mamat R, Astimar AA (2017) A review on the development of Palm Oil Mill Effluent (POME) final discharge polishing treatments. J Oil Palm Res 29(4):528–540
24. Chin KK, Lee SW, Mohammad HH (1996) A study of palm oil mill effluent treatment using a pond system. Water Sci Technol 34(11):119–123

25. Rupani PF, Pratap Singh R, Ibrahim MH, Esa N (2010) Review of current palm oil mill effluent (POME) treatment methods: vermicomposting as a sustainable practice. World Appl Sci J 11(1):70–81
26. Abdul K, Mohamed I, Kamil AQA (1989) Biological treatment of palm oil mill effluent using Trichoderma viride. Biol Wastes 27:143–152
27. Oswal N, Sarma PM, Zinjarde SS, Pant A (2002) Palm oil mill effluent treatment by a tropical marine yeast. Biores Technol 85:35–37
28. Zuhairi AA, Omar MAK, Norulaini NNAR, Hakimi MI (2001) Treatment of palm oil mill effluent (POME) using attached-film bioreactor: trickling filter as a case study. J Ind Technol 10(1):41–54
29. Najafpour GD, Yieng HA, Younesi H, Zinatizadeh AAL (2005) Effect of organic loading on performance of rotating biological contactors using palm oil mill effluents. Process Biochem 40:2879–2884
30. Vijayaraghavan K, Ahmad D, Aziz MEBA (2007) Aerobic treatment of palm oil mill effluent. J Environ Manage 82(1):24–31
31. Agdag ON, Sponza DT (2005) Anaerobic/aerobic treatment of municipal landfill leachate in sequential two-stage up-flow anaerobic sludge blanket reactor (UASB)/completely stirred tank reactor (CSTR) systems. Process Biochem 40(2):895–902
32. Aggelis GG, Gavala HN, Lyberatos G (2001) Combined and separate aerobic and anaerobic biotreatment of green olive debittering wastewater. J Agric Eng Res 80(3):283–292
33. Garbossa LHP, Lapa KR, Zaiat M, Foresti E (2005) Development and evaluation of a radial anaerobic/aerobic reactor treating organic matter and nitrogen in sewage. Braz J Chem Eng 22(4):511–519
34. Jenícek P, Dohányos M, Zábranská J (1999) Combined anaerobic treatment of wastewaters and sludges. Water Sci Technol 40(1):85–91
35. Yacob S, Shirai Y, Hassan MA, Wakisaka M, Subash S (2006) Start-up operation of semi-commercial closed anaerobic digester for palm oil mill effluent treatment. Process Biochem 41:962–964
36. Loh SK, Nasrin AB, Mohamad Azri S, Nurul Adela B, Muzzammil N, Daryl Jay T, Stasha Eleanor RA, Lim WS, Choo YM, Kaltschmitt M (2017) First report on Malaysia's experiences and development in biogas capture and utilization from palm oil mill effluent under the economic transformation programme: current and future perspectives. Renew Sustain Energy Rev 74:1257–1274
37. Karthikeyan OP, Heimann K, Muthu SS (2016) Recycling of solid waste for biofuels and bio-chemicals. Springer, Berlin
38. Poh PE, Chong MF (2009) Development of anaerobic digestion methods for palm oil mill effluent (POME) treatment. Bioresour Technol 100:1–9
39. Loh SK, Lai ME, Muzzammil N, Lim WS, Choo YM, Zhang Z (2013) Zero discharge treatment technology of palm oil mill effluent. J Oil Palm Res 25(3):273–281
40. Borja R, Banks CJ (1995) Comparison of an anaerobic filter and an anaerobic fluidized bed reactor treating palm oil mill effluent. Process Biochem 30:511–521
41. Chaisri R, Boonsawang P, Prasertsan P, Chaiprapat S (2007) Effect of organic loading rate on methane and volatile fatty acids productions from anaerobic treatment of palm oil mill effluent in UASB and UFAF reactors. Songklanakarin J Sci Technol 2:311–323
42. Fakhrul-Razi A, Noor MJMM (1999) Treatment of palm oil mill effluent (POME) with the membrane anaerobic system (MAS). Water Sci Technol 39(10–11):159–163
43. Faisal M, Unno H (2001) Kinetic analysis of palm oil mill wastewater treatment by a modified anaerobic baffled reactor. Biochem Eng J 9:25–31
44. Mustapha S, Ashhuby B, Rashid M, Azni I (2003) Start-up strategy of a thermophilic upflow anaerobic filter for treating palm oil mill effluent. Process Saf Environ Prot 81(4):262–266
45. Borja R, Banks CJ, Sanchez E (1996) Anaerobic treatment of palm oil mill effluent in a two stage up-flow anaerobic sludge blanket (UASB) reactor. J Biotechnol 45:125–135
46. Poh PE, Yong WJ, Chong MF (2010) Palm oil mill effluent (POME) characteristic in high crop season and the applicability of high rate bioreactors for the treatment of POME. Ind Eng Chem Res 49:11732–11740

47. Zinatizadeh AAL, Mohamed AR, Abdullah AZ, Mashitah MD, Hasnain Isa M, Najafpour GD (2006) Process modeling and analysis of palm oil mill effluent treatment in an up-flow anaerobic sludge fixed film bioreactor using response surface methodology (RSM). Water Res 40(17):3193–3208
48. Lim S. (2018) Transforming sustainable oil palm research into reality. University of Nottingham Malaysia Blog, May 16. http://blogs.nottingham.edu.my/campusnews/2018/05/16/transforming-sustainable-oil-palm-research-into-reality/
49. Chan YJ, Chong MF, Law CL (2013) Optimization of palm oil mill effluent treatment in an integrated anaerobic-aerobic bioreactor. Sustain Environ Res 23(3):153–170
50. Yahaya SM, Lau S (2013) Pollution control: how feasible is zero discharge concepts in Malaysia palm oil mills. Am J Eng Res 2(10):239–252
51. Vijaya S, Ma AN, Choo YM, Nik Meriam NS (2008) Life cycle inventory of the production of crude palm oil—a gate to gate case study of 12 palm oil mills. J Oil Palm Res 20:484–494
52. Ahmad AL, Ismail S, Bhatia S (2003) Water recycling from palm oil mill effluent (POME) using membrane technology. Desalination 157(1–3):87–95
53. Lees EJ, Noble B, Hewitt R, Parsons SA (2001) The impact of residual coagulant on the respiration rate and sludge characteristics of an activated microbial biomass. Process Saf Environ Prot 79:283–290
54. Electrigaz Technologies Inc. (2007). Feasibility study anaerobic digester and gas processing facility in the Fraser valley. British Columbia
55. Chan YJ, Chong MF, Law CL (2012) An integrated anaerobic–aerobic bioreactor (IAAB) for the treatment of palm oil mill effluent (POME): start-up and steady state performance. Process Biochem 47:485–495

Part II
Palm Biomass and Biomass Supply Chain

Numerical Methods to Estimate Biomass Calorific Values via Biomass Characteristics Index

Jiang Ping Tang, Hon Loong Lam and Mustafa Kamal Abdul Aziz

Abstract The oil palm industry contributes a huge amount of valuable crude palm oil (CPO) as export commodity for Malaysia. It also produces a large quantity of biomass as plantation waste, which can be utilized as potential fuel sources. In order to shed light on the energy output estimation from the biomass, a comprehensive study on the physical properties of the biomass, i.e., bulk density and moisture content is crucial. A *Biomass Characteristics Index* (BCI) is proposed to represent the relationship between bulk density and moisture content. A numerical framework is developed to determine the BCI. This index is used to estimate the biomass bulk density and moisture content prior to the calorific value calculation. A regression graph is plotted to illustrate the relationship among those values with respect to different appearance or shapes of biomass. The result shows that the biomass of different sizes and shapes has its own specific BCI. The classification of biomass according to its specific BCI can be used to forecast the related bulk density and moisture content. Therefore, it reduces the hassle and time constraint to get those values through the conventional empirical method.

Keywords Physical appearance · Moisture content · Bulk density
Empty fruit bunch · Alternative biomass supply

1 Introduction

Biomass is widely used as an alternate fuel source for power generation. Biomass is transformed to reusable matter from waste especially agricultural residues. Thermal processes such as gasification, pyrolysis, and combustion may be used to convert biomass into specific form (e.g., pellet, bulk, and granule) for energy generation

J. P. Tang · H. L. Lam (✉) · M. K. A. Aziz
Faculty of Engineering, Centre of Excellence for Green Technologies,
The University of Nottingham Malaysia Campus, Jalan
Broga, 43500 Semenyih, Selangor, Malaysia
e-mail: Honloong.lam@nottingham.edu.my

D. C. Y. Foo and M. K. Tun Abdul Aziz (eds.), *Green Technologies for the Oil Palm Industry*, Green Energy and Technology, https://doi.org/10.1007/978-981-13-2236-5_5

purpose via combine heat and power, co-firing, etc. After the development of two decades, biofuel has evolved from the first to the third generation. First generation biofuel is obtained directly from traditional food feedstock such as sugarcane and corn, or direct burning of solid biomass. As less processing technology is involved, the quantity of first generation biofuel is limited and is not a cost-effective solution for the environment. Thus, second-generation biofuel is proposed, with a wide range of feedstocks available through forestry and agricultural residues, energy crops, food waste, industrial and municipal wastes. Due to different conditions of the raw materials in terms of moisture content and size, postprocessing (shredding, densifying, pulverizing and handling) and conversion technologies (gasification, pyrolysis, and combustion) are needed before these raw materials can be used as fuel sources. The advancement of the processing technology has increased the amount of fuel for power generation plant as compared to the first generation biofuel. For example, gasification of biomass converts the maximum available energy content to increase the efficiency of power generation [1]. In addition, the utilization of the abovementioned residues has a positive effect on the environment, considering the amount of waste that goes directly into landfill. The third generation biofuel is known as advanced biofuel [2], which is originated from algae biomass and nonfood feedstock. It is important to note, however, that the third generation biofuel is still facing challenges from technical, economical, and geographical issues. Notwithstanding, the development of biofuel shows little progress in tropical developing countries such as Southeast Asia countries, which is predominantly limited to first-generation biofuel production. Despite the abundance of forest and agriculture residues, there is a lack of mature technologies to further develop new biofuel. Compared to European countries—wherein their natural resources are relatively scarce and face severe weather threats—who have been sprinting to boost biofuel development; biofuel development in Southeast Asian countries on the other hand, remains stagnant at an early stage. The varied and rich profusion of biomass residues that are readily available have yet to be fully utilized for biofuel projects; at present they are directly burnt as fuel without much processing [3].

2 Literature Review

In Malaysia, huge amount of biomass wastes is available from the palm oil mills. Among those residues, the most reusable matters are empty fruit bunch (EFB) and palm kernel shell (PKS) [4]. The factor that determines the usefulness of this biomass is their calorific value. Higher calorific value indicates that it is more efficient as an energy source [5]. Another aspect of the biomass that should be taken into account is their physical characteristics, which consisted of the moisture content and bulk density (Fig. 1). Both of these properties are interrelated and are linked to the structure and physical appearance of biomass. While moisture content is the quantity of water that contains in the biomass material, bulk density is defined as the ratio of biomass mass over its volume. These characteristics affect the operational aspects of a biomass supply chain [6], such as its collection, handling, storage, and logis-

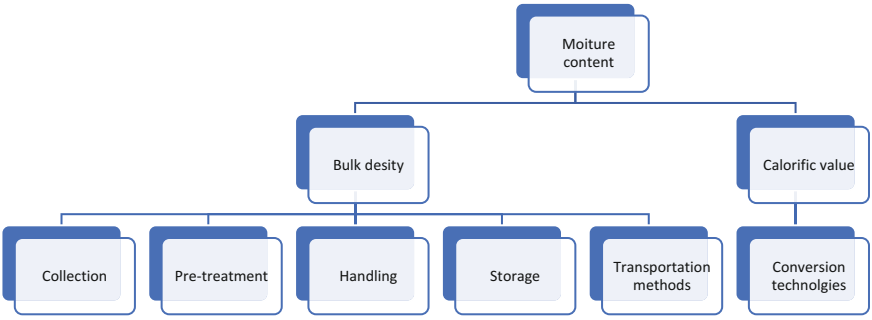

Fig. 1 Biomass characteristics relationships mapping

tics. There are several points needed to be noted. First, raw biomass is associated with high moisture content, low bulk density, and low calorific value. Low bulk density leads to the difficulties in material handling, storage, and transportation [7]. For instance, the biomass of large particle size such as oil palm trunk requires pretreatment of sizing or drying, special handling during collection, suitable storage facility, and careful transportation route selection to the process facility. These increase the total cost incurred for the biomass supply chain. Second, higher moisture content decreases the calorific value of biomass [8], hence different conversion technologies have to be selected for cost saving in the supply chain [9]. Moreover, the low-bulk density and high-moisture content of EFB make it more difficult to be compacted, thus increasing the total volume and increased difficulties in storage and transportation [10]. Besides, bulk density changes with types, size, and shape of the biomass itself. As shown in Figs. 2 and 3, the appearance and shape of raw EFB is completely different from those of shredded bunches. Therefore, bulk density of the dry raw EFB is lower than that of the shredded EFB, as its smaller particle size occupies lesser space with the same weight of mass [11].

Apart from moisture content, air volume also influences the bulk density. Free air space (FAS) is measured for solid organic waste during the composting process. The distribution of air in the waste will affect its performance of composting [12]. FAS represents the ratio of air volume over global volume (air, water, solid). A pycnometer will be used for FAS measurement. At higher bulk density, the air voids will be displaced as the solid becomes more compacts. This shows a linear relationship between FAS and bulk density for manure compost [13]. There are numerous studies that relate air porosity to bulk density [14] and the relationships are established for different biomass types. Therefore, it is possible that biomass have air voids trap inside the material itself, especially for fibrous biomass like EFB. The space in between the particle of biomass material is a perfect spot for air voids.

The analysis of moisture content and bulk density of biomass have been reported in different studies, depending on their application areas (refer to Table 1), either for the pretreatment processes or the final product (pellet for most cases). Note however that the focus of those research work was mainly targeted on the performance of final

Fig. 2 Raw EFB

Fig. 3 Shredded fiber from EFB

product rather than the raw biomass itself. There is no analysis on properties with regards to raw biomass appearance before the pretreatment stage. The appearance of raw biomass has essential information that determines the handling, transportation, and storage issues [15]. This information can be fed into biomass supply chain for the purpose of resource planning and optimization [16]. A well-designed supply chain plays an important role to achieve the efficiency in cost and energy utilization [17].

Table 1 Overview of bulk density and moisture content on biomass

Application area	Measured characteristics	References	Scope of research
Biofuel	Bulk density	Antonio Bizzo et al. [18]	The generation of residual biomass during the production of bioethanol from sugarcane, its characterization and its use in energy production
Bulk density determination	Wet bulk density, dry bulk density	Lam et al. [19]	Bulk density of wet and dry wheat straw and switchgrass particles
CHP plant	Moisture content, calorific value	Chiew et al. [8]	System analysis for effective use of palm oil waste as energy resources
Briquette	Moisture content, bulk density, calorific value	Liu et al. [20]	Study of briquetted biomass co-firing mode in power plants
Classification	Moisture content, bulk density, ash content, particle dimension and size distribution	Shankar Tumuluru et al. [21]	A review on biomass classification and composition, co-firing issues and pretreatment methods
Combustion	Bulk density, moisture content	Elmay et al. [22]	Energy recovery of date palm residues in a domestic pellet boiler
Compaction	Moisture content, bulk density, particle density	Mani et al. [23, 24]	Evaluation of compaction equations applied to wheat straw, barley straw, corn stover, and switchgrass
Compaction	Bulk density, particle size	Chevanan et al. [25]	Bulk density and compaction behavior of knife mill chopped switchgrass, wheat straw, and corn stover
Densification	Moisture content, bulk density, durability, percent fines, calorific value	Tumuluru et al. [26]	A review of biomass densification systems to develop uniform feedstock commodities for bioenergy application
Densification	Moisture content, particle size, bulk density	Kaliyan and Morey [27]	Densification characteristics of corn cobs

(continued)

Table 1 (continued)

Application area	Measured characteristics	References	Scope of research
Fly ash properties	Bulk density	Jaworek et al. [28]	Properties of biomass versus coal fly ashes deposited in electrostatic precipitator
Grinding performance	Moisture content, bulk density, particle density	Mani et al. [23, 24]	Grinding performance and physical properties of wheat and barley straws, corn stover, and switchgrass
Pelletizing	Particle density, bulk density, moisture, crushing resistance, compression resistance	Zamorano et al. [29]	A comparative study of quality properties of pelletized agricultural and forestry lopping residues
Pelletizing	Bulk density	Liu et al. [20]	The properties of pellets from mixing bamboo and rice straw
Pelletizing	Moisture content, bulk density, true density, durability	Theerarattananoon et al. [30]	Physical properties of pellets made from sorghum stalk, corn stover, wheat straw, and big bluestem
Pelletizing	Moisture, bulk density	Samuelsson et al. [31]	Effect of biomaterial characteristics on pelletizing properties and biofuel pellet quality
Pelletizing	Bulk density, particle density, durability, moisture sorption rate and moisture sorption isotherm	Fasina [32]	Physical properties of peanut hull pellets
Physical characterization	Bulk density, particle density	Wu et al. [7]	Physical properties of wood pellets, wood chips, and torrefied pellets
Pyrolysis	Moisture content	Abdullah et al. [33]	Characterization of oil palm empty fruit bunches for fuel application

(continued)

Table 1 (continued)

Application area	Measured characteristics	References	Scope of research
Physical characterization	Bulk density, apparent density, true density and moisture	Cardoso et al. [34]	Physical characterization (density, particle size and shape distributions) of sweet sorghum bagasse, tobacco residue, soy hull, and fiber sorghum bagasse particles
Pelletizing	Compressive force, particle size and moisture content	Mani et al. [35]	Effects of compressive force, particle size and moisture content on mechanical properties of biomass pellets from grasses
Torrefaction	Moisture content, gross calorific value, weight, volatile matter, fixed carbon, bulk density	Patel et al. [36]	Improved fuel characteristics of cotton stalk, prosopis, and sugarcane bagasse through torrefaction
Torrefaction	Moisture content	Sadaka and Negi [37]	Improvements of biomass physical and thermochemical characteristics via torrefaction process
Torrefaction	Moisture content, ash	Sabil et al. [38]	Effects of torrefaction on the physiochemical properties of oil palm EFB, mesocarp fiber and kernel shell

Second, acquisition of bulk density and moisture content are obtained through empirical methods such as the British Standard ("Solid Biofuels—Determination of Bulk Density" [39]. Results from those methods may vary from sample to sample and are limited by handling procedures. There is no standard or reference value for bulk density and moisture content for biomass such as EFB. Most of the relevant researches merely focus on either one of the characteristics (i.e., bulk density or moisture content alone) or component breakdown of biomass. Hence, there is a lack of comprehensive and all-rounded analysis that integrates all physical properties of the biomass.

For example, the work of Chevanan et al. [25] focused on the characterization of bulk density of switchgrass, wheat straw, and corn stover, and also proposed separate

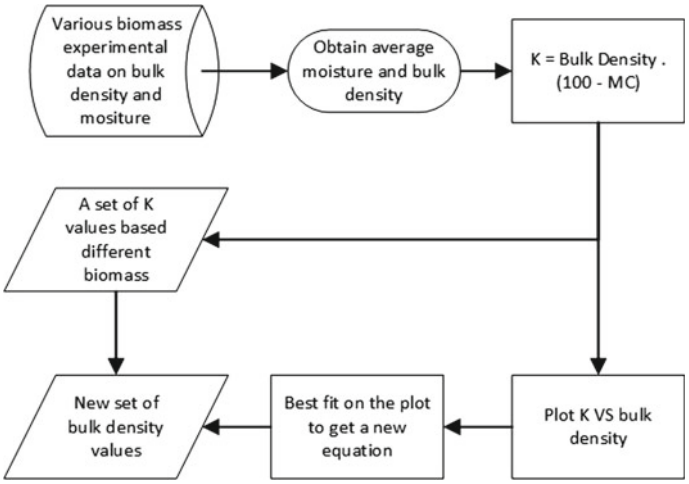

Fig. 4 Flowchart of BCI calculation

relationship model for each respective biomass. However, there is no consolidated model of characterization for various biomass proposed.

In the conventional approach, these properties are obtained through empirical methods on an individual sample basis. There are several drawbacks of such conventional empirical methods: (i) a huge amount of experimental results is needed to construct a biomass properties curve; (ii) the accuracy of analysis result might be affected by the data variations. These create a limitation in properties estimation and further affect the optimum biomass utilization. To address this issue, there is a need to search for a direct representation of the properties.

In this chapter, *Biomass Characteristics Index* (BCI) is proposed to correlate the physical appearance of biomass to its properties—bulk density and moisture content. Numerical method is used to perform BCI calculation. The methodology will be discussed in detail in the following section.

3 Biomass Characteristics Index (BCI)

Numerical method may be used to analyze the physical properties of biomass. It is an efficient method that saves time and fosters a better understanding on the relationships between moisture content and bulk density of different biomass, as compared to the analytical methods. With regression analysis established on the BCI curve, prediction can be made easily. The workflow diagram of BCI is represented in Fig. 4, while the detailed calculation and the BCI curve establishment are presented in the next section.

3.1 Relationships Between Bulk Density and Moisture Content

Raw biomass materials are exposed to the open environment, and its moisture content is inherently high. Wet biomass has a larger volume especially for fibrous biomass like EFB. Larger pore space in the biomass reduces its bulk density. Sims [40] provided an intuitive formula that relates bulk density and moisture content of a biomass (Eq. 1).

$$\text{Bulk Density}\left(\frac{\text{kg}}{\text{m}^3}\right) = \frac{13600}{(100 - \text{MC})} \tag{1}$$

where MC (in %) is the moisture content of biomass in wet basis.

Note however that the constant value of 13,600 is only applicable for wood chips as reported in Sims [40]. Hence, a more generalized equation (Eq. 2) with a constant parameter of k applies to different types of biomass.

$$\text{Bulk Density}\left(\frac{\text{kg}}{\text{m}^3}\right) = \frac{k}{(100 - \text{MC})} \tag{2}$$

Note that the constant k is a reference index for various appearances of biomass and is proposed as BCI.

3.2 BCI Calculation

A systematic numerical approach for BCI consists of the following steps (Fig. 4):

(a) Database construction

To obtain a series of BCI, a complete biomass database is a prerequisite. Various forms of biomass with different bulk densities and moisture contents are needed prior to the establishment of the biomass database; the latter covers most biomass available in the market (of different appearance and shape).

(b) BCI calculation

From the above database, BCI can be calculated from bulk density and moisture content using Eq. 3.

$$\text{BCI} = \text{Bulk Density}\left(\frac{\text{kg}}{\text{m}^3}\right) \times (100 - \text{MC}) \tag{3}$$

(c) Relationships among BCI, bulk density and moisture content

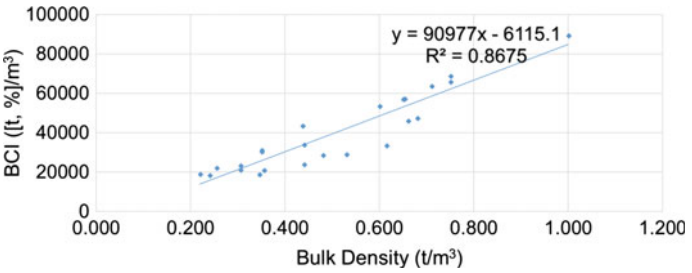

Fig. 5 BCI versus bulk density plot

After a full set of BCI is obtained, a graph is plotted to show the relationships between BCI and bulk density. From the graph, linear regression is best fitted on the plots. A new regression equation is obtained through the fit.

4 Illustrative Example

A simple example is demonstrated for a set of biomass with different appearance and shapes. The database comprises most of the commonly found biomass in the market, with their bulk density and moisture content (Table 2). Average value of bulk density and moisture content are calculated for BCI in Eq. 3. For example, the bulk density and moisture content of EFB are 40% and 0.355 t/m^3, respectively (Table 2). Hence, Eq. 3 determines the BCI value for EFB as 21,300.

A linear relationship is shown by plotting the BCI values versus the average bulk densities in a graph, with linear regression fitted on the plotted data (Fig. 5). The best fit linear regression equation is derived as shown in Eq. 4, with *R*-squared value of 0.8675.

$$y = 90977x - 6115.10 \tag{4}$$

5 Analysis

The validity of the calculated BCI values can be verified through comparison with the actual data. As shown in Table 3, the error differences are relatively small for selected biomass. The highest differences are observed for EFB and FFB, which are 52.07 and 33.79%, respectively. This is due to the nature of these biomass that have a broad range of moisture content [41].

Table 4 shows that the calculated BCI value for EFB of different moisture content varies between 5600 and 46,750. However, for the whole spectrum of biomass material, the average value of moisture content and bulk density are used. The BCI

Table 2 Characteristics of various biomass

Biomass types	Moisture (Min) (%)	Moisture (Max) (%)	Average moisture (%)	Bulk density (t/m^3, Min)	Bulk density (t/m^3, Max)	Average bulk density (t/m^3)	BCI
Air dry wood chips	20.00	25.00	22.50	0.190	0.290	0.240	18,600
Green wood chips	40.00	50.00	45.00	0.280	0.410	0.345	18,975
Kiln dry wood chips	10.00	15.00	12.50	0.190	0.250	0.220	19,250
Empty fruit bunch	15.00	65.00	40.00	0.160	0.550	0.355	21,300
Kiln dry wood chunks	10.00	15.00	12.50	0.200	0.310	0.255	22,313
Air dry wood chunks	20.00	25.00	22.50	0.240	0.370	0.305	23,638
Green wood chunks	40.00	50.00	45.00	0.350	0.530	0.440	24,200
Mesocarp oily fiber	30.00	N/A	30.00	N/A	N/A	0.305	21,350
Kiln dry sawdust	10.00	15.00	12.50	0.240	0.370	0.350	30,625
Fresh fruit bunch	40.00	N/A	40.00	N/A	N/A	0.480	28,800
Green sawdust	40.00	50.00	45.00	0.420	0.640	0.530	29,150
Straw bales	7.00	14.00	10.50	0.200	0.500	0.350	31,325
Green round-wood	40.00	50.00	45.00	0.510	0.720	0.615	33,825
Air dry round-wood	20.00	25.00	22.50	0.350	0.530	0.440	34,100
Ash	0.00	N/A	0.00	N/A	N/A	0.437	43,700
Sterilized fruit	30.00	N/A	30.00	N/A	N/A	0.660	46,200
Fruitlets	30.00	N/A	30.00	N/A	N/A	0.680	47,600
Wood pellets	7.00	14.00	10.50	0.500	0.700	0.600	53,700

(continued)

Table 2 (continued)

Biomass types	Moisture (Min) (%)	Moisture (Max) (%)	Average moisture (%)	Bulk density (t/m^3, Min)	Bulk density (t/m^3, Max)	Average bulk density (t/m^3)	BCI
Press expelled cake	12.00	N/A	12.00	N/A	N/A	0.650	57,200
Palm nuts	12.00	N/A	12.00	N/A	N/A	0.653	57,464
Cracked mixture	12.00	N/A	12.00	N/A	N/A	0.653	57,464
Dry EFB cut fiber	10.00	N/A	10.00	N/A	N/A	0.710	63,900
Shell	12.00	N/A	12.00	N/A	N/A	0.750	66,000
Coal	6.00	10.00	8.00	0.700	0.800	0.750	69,000
Wood briquettes	7.00	14.00	10.50	0.900	1.100	1.000	89,500

Table 3 Comparison of collected and BCI forecast bulk density

Oil palm biomass	Collected data (t/m^3)	Forecast from BCI (t/m^3)	Difference (t/m^3)	Difference (%)
Empty fruit bunch	0.628	0.301	0.327	52.07
Mesocarp oily fiber	0.257	0.302	0.045	17.51
Fresh fruit bunch	0.580	0.384	0.196	33.79
Ash	0.550	0.548	0.002	0.36
Sterilized fruit	0.640	0.575	0.065	10.16
Fruitlets	0.640	0.590	0.050	7.81
Press expelled cake	0.550	0.696	0.146	26.55
Palm nuts	0.653	0.699	0.046	7.04
Cracked mixture	0.535	0.699	0.164	30.65
Shell	0.650	0.793	0.143	22.00

Table 4 Calculated BCI value for EFB

Moisture content (%)	Bulk density (t/m^3)	BCI
65.00	0.160	5600
15.00	0.550	46,750

curve fits linearly and without any serious distortion as the R^2 value is determined as 0.8675 (see Fig. 4).

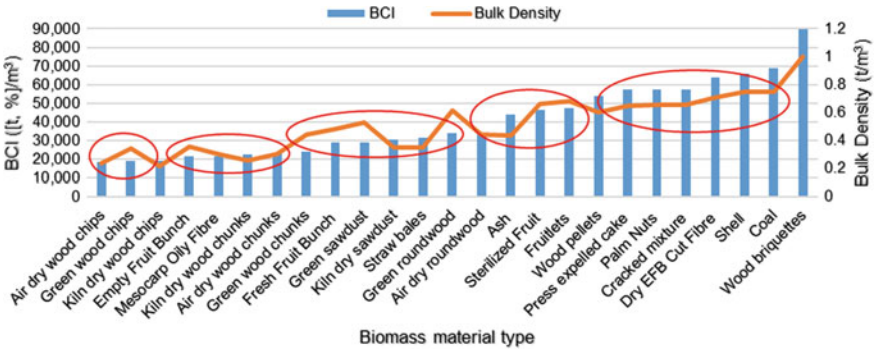

Fig. 6 Clustering of biomass with similar shapes

Table 5 Comparison of calorific value for EFB

Moisture content (%)	Calorific value		
	Experimental [42] (MJ/kg)	Experimental work of the author (with BOM calorimeter) (MJ/kg)	ECN Phyllis 2 [43] (MJ/kg)
5.00	17.17	18.20	15.86
60.00	9.13	6.86	6.68

BCI can be used as a properties forecast tool on multiple biomass materials. Classification of biomass type is useful for industrial application [15]. Figure 6 shows BCI and bulk density values are lined up on a bar chart to reflect its dependency. The clustering in red circle on different biomass, as well as the bulk density values can also be noted from the chart. From Fig. 5, it is noticeable that all chip materials (air dry, green, and kiln dry wood chips) have a similar range of BCI values, i.e., 18,600–19,250. A similar trend is also observed for different types of chunks. This means that biomass with similar shape have relatively similar bulk density and BCI values, and thus the group of biomass can be identified by simply referring to the BCI category. In the other words, BCI can forecast the physical properties of biomass based on a narrow BCI range, even without having to examine the actual sample. From there, bulk density and moisture content are predictable. However, it is important to note that there is a notch for green roundwood bulk density observed from Fig. 6. This indicates the possibility of the existence of other similar biomass material which is not covered in this study, given that BCI is a conceptual framework at current stage.

As discussed earlier, specific BCI value is able to provide the information of bulk density (Fig. 6) and moisture content of the biomass. In addition, calorific value can be determined through the relationships with moisture content. Aziz et al. [42] reported that the relationships between calorific value and moisture content are not necessarily in linear form, especially for EFB. The results are compared with those reported in experimental work (conducted by the author) and also biomass database ("Phyllis2, Database for Biomass and Waste" [43] (see Table 5).

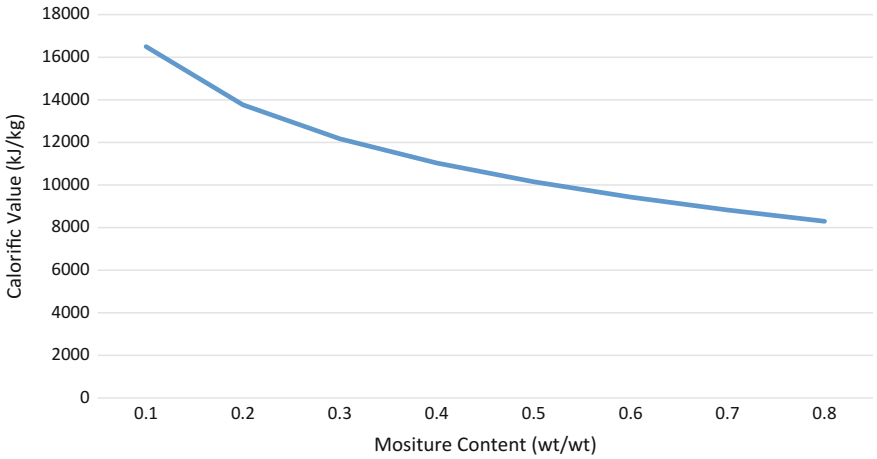

Fig. 7 Calorific values (kJ/kg) versus moisture content (% wt./wt.) for EFB [42]

Table 5 verifies that Fig. 6 is reliable in predicting calorific value of EFB by referring to its moisture content. Therefore, BCI can be enhanced to cover the information of calorific value. Incorporation of calorific value, moisture content and bulk density into BCI value creates a robust tool in biomass supply chain for physical properties estimation.

6 Demonstration of Application Case Study

6.1 BCI Alternative Sourcing

In conventional biomass process design, the value of bulk density and moisture content for a given biomass material are needed in the system efficiency calculation. As discussed earlier, the material of similar appearance and shape will have a specific range of BCI values. For instance, a co-firing plant (Fig. 7) is planning to source green wood chunks as an alternate fuel for kiln dry wood chunks, due to the insufficient supply of the latter. Before purchasing this feedstock, the energy density has to be estimated. By referring to the BCI of green wood chunks (24,200), its bulk density is estimated to be 350 kg/m^3 (using the linear regression equation from Fig. 5) with average moisture content of 45%. Typical calorific value for 45% moisture content of green wood chunks is 10 MJ/kg (refer to Fig. 7). Therefore, the estimated energy density of green wood chunks is calculated as 3500 MJ/m^3 (=350 kg/m^3 × 10 MJ/kg). For the kiln dry wood chunks of 45% moisture content, the calorific value is reported as 9.20 MJ/kg [44]. This means that the green wood chunks are good substitution for kiln dry wood chunks. The estimated energy value enables the management team to make quick decision in the procurement process effectively by considering other

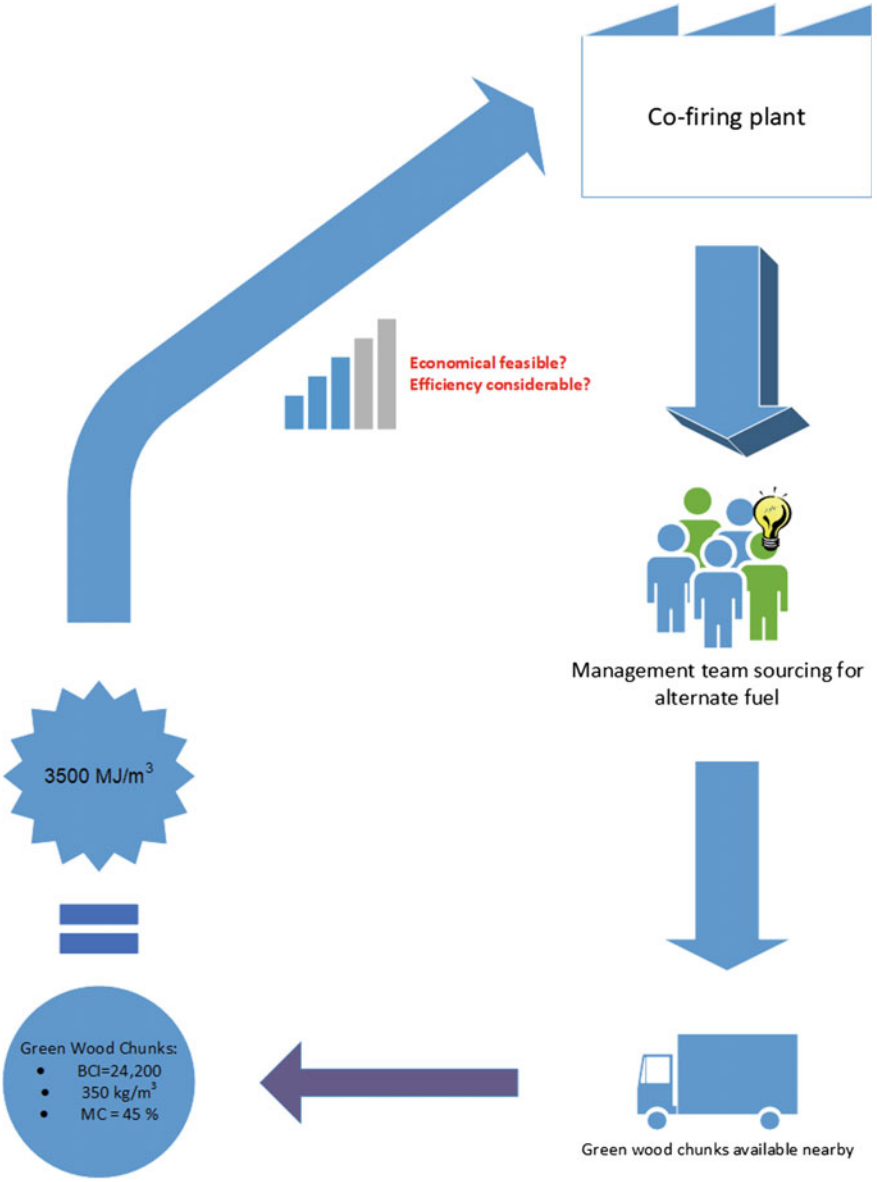

Fig. 8 Flow diagram of alternative sourcing using BCI

factors, e.g., storage cost and combustion efficiency. As shown, this empirical model allows the determination of bulk density and moisture content values without going through the hassle of performing experimental work, which allows the management of the co-firing plant to make instance decision (Fig. 8).

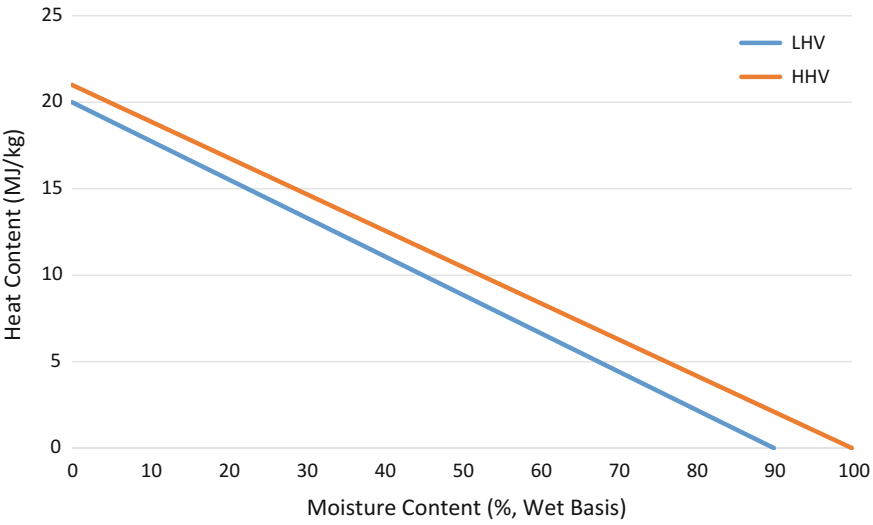

Fig. 9 Typical higher heating value and lower heating value of biomass versus its moisture content [45]

6.2 Biomass Materials Filtering Using BCI

In terms of biomass management planning, bulk density or moisture content of the biomass need to be identified in advance for the ease of transportation or to maximize the output in the power plant. This is because different levels of bulk density or moisture content of biomass requires different types of treatment and cost. For instance, biomass with wet and large volume occupy more space and thus causing higher transportation cost. Also, biomass with high moisture content has a lower calorific value (Fig. 9) and thus decreasing the efficiency of the plant.

By referring to the BCI, the desired value of bulk density or moisture content can be obtained conveniently. For example, when a biomass power generation plant (Fig. 10) experiences low feedstock problem with their existing fuel (straw bales), and the management wishes to source an alternative feedstock as fuel source for replacement, the BCI will be useful. The BCI of straw bales is given as 31,325 in Table 2. The latter also shows that the green sawdust, kiln dry sawdust, air dry roundwood, and green round wood are possible substitute, with BCI value of approximately 30,000. Obviously, kiln dry sawdust is the most suitable replacement as its bulk density (350 kg/m^3) and moisture content (12.50%) are closer to those of straw bales (350 kg/m^3, 10.50%). Alternatively, air dry round wood will be the next suitable substitution (440 kg/m^3, 22.50%) if straw bales are not available. In terms of management, the procurement of the suitable material can be done in an accurate manner without further delays (Fig. 10).

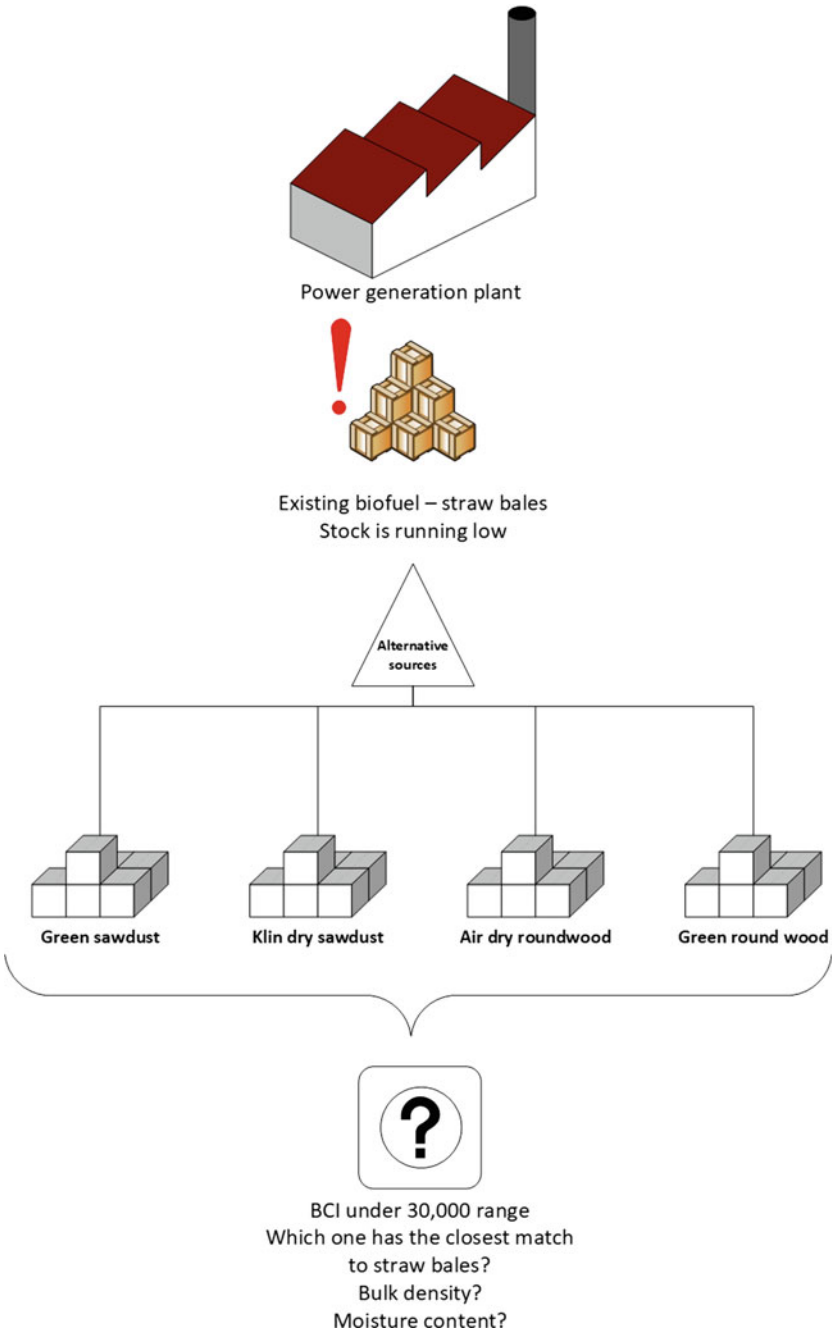

Fig. 10 Biomass material filtering illustration

7 Conclusion

This chapter proposes a numerical framework of BCI in forecasting the physical properties of various biomass. The method is applicable for appearance and shapes of different biomass materials. By referring to the BCI value of the biomass material, the forecast of bulk density and moisture contents can be obtained effectively without running any time-consuming experiments. The values provided by the BCI are useful for industrial application (e.g., design of biomass power plant), as it can be used to predict the calorific value of biomass fuel and the output (e.g., power) from the plant. Thus, it can potentially improve the overall biomass management process design and development. Above all, BCI is an efficient design tool wherein output can be maximized, while waste can be minimized.

Acknowledgements The financial supports from Long Term Research Grant Scheme (UPM/700-1/3/LRGS), University of Nottingham Early Career Research and Knowledge Transfer Award (A2RHL6), and Institute of Advanced Technology of Universiti Putra Malaysia are gratefully acknowledged.

References

1. Fodor Z, Klemeš JJ (2012) Waste as alternative fuel—minimising emissions and effluents by advanced design. Process Saf Environ Protect 90(3):263–284. https://doi.org/10.1016/j.psep.2011.09.004
2. IEA (2012) Future biomass-based transport fuels summary and conclusions from the workshop. Future biomass-based transport fuels summary and conclusions from the IEA bioenergy ExCo67 workshop
3. Goh SC, Lee TK (2010) Will biofuel projects in Southeast Asia become white elephants? Energy Policy 38(8):3847–3848. Elsevier. https://doi.org/10.1016/J.ENPOL.2010.04.009
4. Ng WPQ, Lam HL, Ng FY, Kamal M, Lim JHE (2012) Waste-to-wealth: green potential from palm biomass in Malaysia. J Cleaner Product 34(Supplement C):57–65. https://doi.org/10.1016/j.jclepro.2012.04.004
5. Everard CD, McDonnell KP, Fagan CC (2012) Prediction of biomass gross calorific values using visible and near infrared spectroscopy. Biomass Bioenergy 45(Supplement C):203–211. https://doi.org/10.1016/j.biombioe.2012.06.007
6. Annevelink B, Anttila P, Väätäinen K, Gabrielle B, García-Galindo D, Leduc S, Staritsky I (2017). Modeling biomass logistics. In Modeling and optimization of biomass supply chains. Elsevier, pp 79–103. https://doi.org/10.1016/B978-0-12-812303-4.00004-5
7. Wu MR, Schott DL, Lodewijks G (2011) Physical properties of solid biomass. Biomass Bioenergy 35(5):2093–2105. https://doi.org/10.1016/j.biombioe.2011.02.020
8. Chiew YL, Iwata T, Shimada S (2011) System analysis for effective use of palm oil waste as energy resources. Biomass Bioenergy 35(7):2925–2935. https://doi.org/10.1016/j.biombioe.2011.03.027
9. Elbersen W, Lammens TM, Alakangas EA, Annevelink B, Harmsen P, Elbersen B (2017) Lignocellulosic biomass quality. In Modeling and optimization of biomass supply chains. Elsevier, pp 55–78. https://doi.org/10.1016/B978-0-12-812303-4.00003-3
10. Miccio F, Silvestri N, Barletta D, Poletto M (2011) Characterization of woody biomass flowability. Chem Eng Trans 24

11. Basu P (2013) Biomass characteristics. In Biomass gasification, pyrolysis and torrefaction. Elsevier, pp 47–86. https://doi.org/10.1016/B978-0-12-396488-5.00003-4
12. Druilhe C, Benoist J-C, Bodin D, Tremier A (2013) Development and validation of a device for the measurement of free air space and air permeability in solid waste. Biosyst Eng 115(4):415–422. https://doi.org/10.1016/j.biosystemseng.2013.05.006
13. Agnew JM, Leonard JJ, Feddes J, Feng Y (2003). A modified air pycnometer for compost air volume and density determination. Can Biosyst Eng/Le Genie Des Biosyst Au Canada 45
14. Ruggieri L, Gea T, Artola A, Sánchez A (2009) Air filled porosity measurements by air pycnometry in the composting process: a review and a correlation analysis. Bioresour Technol 100(10):2655–2666. https://doi.org/10.1016/j.biortech.2008.12.049
15. Lam HL, Ng WPQ, Ng RTL, Huay Ng E, Aziz MKA, Ng DKS (2013). Green strategy for sustainable waste-to-energy supply chain. Energy 57(Supplement C):4–16. https://doi.org/10.1016/j.energy.2013.01.032
16. Lam HL, Varbanov PS, Klemeš JJ (2011) Regional renewable energy and resource planning. Appl Energy 88(2):545–550. https://doi.org/10.1016/j.apenergy.2010.05.019
17. Klemeš JJ, Varbanov PS, Kravanja Z (2013) Recent developments in process integration. Chem Eng Res Design 91(10):2037–2053. https://doi.org/10.1016/j.cherd.2013.08.019
18. Antonio Bizzo W, Lenço PC, Carvalho DJ, Veiga JPS (2014) The generation of residual biomass during the production of bio-ethanol from sugarcane, its characterization and its use in energy production. Renew Sustain Energy Rev 29 (Supplement C):589–603. https://doi.org/10.1016/j.rser.2013.08.056
19. Lam PSW, Sokhansanj S, Bi X, Lim J, Naimi L, Hoque M, Mani S, Womac AR, Ye XP, Narayan S (2008) Bulk density wet dry wheat straw switchgrass particles. Appl Eng Agri 24. https://doi.org/10.13031/2013.24490
20. Liu Y, Wang X, Xiong Y, Tan H, Niu Y (2014) Study of briquetted biomass co-firing mode in power plants. Appl Therm Eng 63(1):266–271. https://doi.org/10.1016/j.applthermaleng.2013.10.041
21. Shankar Tumuluru J, Wright CT, Boardman RD, Yancey NA, Sokhansanj S (2011) A review on biomass classification and composition, co-firing issues and pretreatment methods. 2011 Louisville, Kentucky, August 7–10, 2011. ASABE Paper No. 1110458. St. Joseph, MI: ASABE. https://doi.org/10.13031/2013.37191
22. Elmay Y, Trouvé G, Jeguirim M, Said R (2013) Energy recovery of date palm residues in a domestic pellet boiler. Fuel Process Technol 112(Supplement C):12–18. https://doi.org/10.1016/j.fuproc.2013.02.015
23. Mani S, Tabil LG, Sokhansanj S (2004a) Grinding performance and physical properties of wheat and barley straws, corn stover and switchgrass. Biomass Bioenergy 27(4):339–352. https://doi.org/10.1016/j.biombioe.2004.03.007
24. Mani S, Tabil L, Sokhansanj S (2004b) Evaluation of compaction equations applied to four biomass species. Can Biosyst Eng 46
25. Chevanan N, Womac AR, Bitra VSP, Igathinathane C, Yang YT, Miu PI, Sokhansanj S (2010) Bulk density and compaction behavior of knife mill chopped switchgrass, wheat straw, and corn stover. Bioresour Technol 101(1):207–214. https://doi.org/10.1016/j.biortech.2009.07.083
26. Tumuluru JS, Wright CT, Richard Hess J, Kenney KL (2011) A review of biomass densification systems to develop uniform feedstock commodities for bioenergy application. Biofuels, Bioprod Bioref 5(6):683–707. Wiley. https://doi.org/10.1002/bbb.324
27. Kaliyan N, Morey RV (2010) Densification characteristics of corn cobs. Fuel Process Technol 91(5):559–565. https://doi.org/10.1016/j.fuproc.2010.01.001
28. Jaworek A, Czech T, Sobczyk AT, Krupa A (2013) Properties of biomass vs. coal fly ashes deposited in electrostatic precipitator. J Electrostat 71(2):165–175. https://doi.org/10.1016/j.elstat.2013.01.009
29. Zamorano M, Popov V, Rodríguez ML, García-Maraver A (2011) A comparative study of quality properties of pelletized agricultural and forestry lopping residues. Renewable Energy 36:3133–3140.

30. Theerarattananoon K, Xu F, Wilson J, Ballard R, Mckinney L, Staggenborg S, Vadlani P, Pei ZJ, Wang D (2011) Physical properties of pellets made from sorghum stalk, corn stover, wheat straw, and big bluestem. Ind Crops Prod 33(2):325–332. https://doi.org/10.1016/j.indcrop.2010.11.014
31. Samuelsson R, Thyrel M, Sjöström M, Lestander TA (2009) Effect of biomaterial characteristics on pelletizing properties and biofuel pellet quality. Fuel Process Technol 90(9):1129–1134. https://doi.org/10.1016/j.fuproc.2009.05.007
32. Fasina OO (2008) Physical properties of peanut hull pellets. Bioresour Technol 99(5):1259–1266. https://doi.org/10.1016/j.biortech.2007.02.041
33. Abdullah N, Sulaiman F, Gerhauser H (2011) Characterisation of oil palm empty fruit bunches for fuel application. J Phys Sci 22(1):1–24
34. Cardoso CR, Oliveira TJP, Santana JA Jr, Ataíde CH (2013) Physical characterization of sweet sorghum bagasse, tobacco residue, soy hull and fiber sorghum bagasse particles: density, particle size and shape distributions. Powder Technol 245(Supplement C):105–114. https://doi.org/10.1016/j.powtec.2013.04.029
35. Mani S, Tabil LG, Sokhansanj S (2006) Effects of compressive force, particle size and moisture content on mechanical properties of biomass pellets from grasses. Biomass Bioenergy 30(7):648–654. https://doi.org/10.1016/j.biombioe.2005.01.004
36. Patel B, Gami B, Bhimani H (2011) Improved fuel characteristics of cotton stalk, prosopis and sugarcane bagasse through torrefaction. Energy Sustain Develop 15(4):372–375. https://doi.org/10.1016/j.esd.2011.05.002
37. Sadaka S, Negi S (2009) Improvements of biomass physical and thermochemical characteristics via torrefaction process. Environ Progress Sustain Energy 28(3):427–434. Wiley. https://doi.org/10.1002/ep.10392
38. Sabil KM, Aziz MA, Lal B, Uemura Y (2013) Effects of torrefaction on the physiochemical properties of oil palm empty fruit bunches, mesocarp fiber and kernel shell. Biomass Bioenergy 56(Supplement C):351–360. https://doi.org/10.1016/j.biombioe.2013.05.015
39. Solid Biofuels—Determination of Bulk Density (2009) Management
40. Sims REH (2002) The brilliance of bioenergy: in business and in practice. James & James (Science Publishers). https://books.google.com.my/books?id=UONAkQ6w2qgC
41. Omar R, Idris A, Yunus R, Khalid K, Aida Isma MI (2011) Characterization of empty fruit bunch for microwave-assisted pyrolysis. Fuel 90(4):1536–1544. Elsevier. https://doi.org/10.1016/J.FUEL.2011.01.023
42. Aziz, MKA, Morad NA, Wambeck N, Shah MH (2011) Optimizing palm biomass energy though size reduction. In 2011 fourth international conference on modeling, simulation and applied optimization, pp 1–6. https://doi.org/10.1109/ICMSAO.2011.5775516
43. Phyllis2, Database for Biomass and Waste (n.d.) Energy research centre of the Netherlands. https://www.ecn.nl/phyllis2
44. Serup H, Kofman PD, Falster H (2005) Wood for energy production, Irish Edition. COFORD, Dublin, 72p
45. Ciolkosz D (2010) Characteristics of biomass as a heating fuel, vol 4

A Simple Mathematical Model for Palm Biomass Supply Chain

Dominic C. Y. Foo

Abstract Being the world second largest palm oil producer, Malaysia has a wide range of palm biomass sources generated as by-products from its oil palm industry. These palm biomass resources should be better utilised in order to maximise their potential as high value-added products. This chapter focuses on the synthesis of a *biomass supply chain*. A simple *linear programme* (LP) model is presented for the optimum allocation of palm biomass among its sources and sinks. The LP model is of diverge usage which may be used by different stake holders (industrial players and government department) in order to maximise profit or to minimise cost/CO_2 emission.

Keywords Sink-Source matching · Empty fruit bunch (EFB) · Biomass allocation Superstructural model · Linear programme · Optimisation

1 Introduction

Various palm biomass is generated in the palm oil industry. These include empty fruit bunches (EFBs), palm mesocarp fibres (PMFs), palm kernel shells (PKSs), oil palm fronds (OPFs) and oil palm trunks (OPTs). Loh [12] reported that in 2014, of the 95.38 million t/y of fresh fruit bunches (FFBs) processed in Malaysia, the oil palm biomass generated along its supply chain is estimated as 40.55 million t/y, consisting of 21.03 million t/y pruned OPFs, 7.34 million t/y EFBs, 4.46 million t/y PKSs and 7.72 million t/y of PMFs. These figures were based on the standard extraction rate of biomass to FFBs given in Table 1.

Besides, biomass is also generated from the replanting activity. The amounts of biomass from the oil palm replanted area were estimated as 4.30 million t/y, contributed by 3.60 million t/y OPT and 0.7 million t/y OPF [12]. Hence, a total of

D. C. Y. Foo (✉)
Centre of Excellence for Green Technologies, University of Nottingham Malaysia, Broga Road, 43500 Semenyih, Selangor, Malaysia
e-mail: Dominic.Foo@nottingham.edu.my

D. C. Y. Foo and M. K. Tun Abdul Aziz (eds.), *Green Technologies for the Oil Palm Industry*, Green Energy and Technology, https://doi.org/10.1007/978-981-13-2236-5_6

44.85 million t/y (=40.55 + 4.30 million t/y) of oil palm biomass was generated from replanting, pruning and milling activities for year 2014. These biomass resources have good potential to serve as renewable energy in Malaysia. However, its potential is yet to be fully explored.

In recent years, various research works were reported for the development of *integrated biorefinery*, where palm biomass is served as the main feedstock. An *integrated biorefinery* is a processing facility that integrates a wide range of biomass technologies for the production of value-added products, such as biofuels, bioenergy and bio-chemicals [13]. A recent review by Sadhukhan et al. [15] reported that mature technologies for the integrated biorefinery mainly focused on bioenergy, biogas and biofuels; while developed technologies were reported for platforms or intermediate products, e.g. syngas and bio-oil. In this regards, the palm oil mill owners should maximise their profitability through strategic utilisation of the biomass generated in their plants.

This chapter focuses on the synthesis of a *biomass supplychain*, in order to maximise the potential of biomass as renewable energy resources. A biomass supply chain may be defined as *an integrated value chain with four components, i.e. production and management of biomass, integrated biorefinery, distribution of product and logistics linked through the flow of materials and information with the aims of maximising the sustainability goals* [7]. In recent years, one of the widely accepted techniques for biomass supply chain synthesis is *process integration*; the latter may be defined

Table 1 Oil palm biomass availability based on standard biomass to fresh fruit bunches (FFBs) extraction rate [12]

Type of oil palm biomass	Availability
Empty fruit bunches (EFBs)	Wet basis: 22% of FFB
	Dry weight: 35% of EFB (wet basis)
Palm kernel shell (PKSs)	Wet basis: 5.5% of FFB
	Dry weight: 85% of PS (wet basis)
Palm mesocarp fibres (PMF)	Wet basis: 13.5% of FFB
	Dry weight: 60% of MF (wet basis)
Palm oil mill effluent (POME)	Wet basis: 67% of FFB or 0.65 m^3/t FFB
Oil palm trunks (OPTs)	Dry weight: 74.48 t/ha (replanting), an average of 142 OPT is available from a ha of oil palm, and only 50% can be removed from the plantation
Oil palm fronds (OPFs)	Dry weight: 10.40 t/ha (pruned), 75% of oil palm trees aged 7 years are due for pruning, and only 50% can be removed from the plantation
	OPF (replanting, dry weight): 14.47 t/ha, and only 50% can be removed from the plantation

as a *holistic approach to design operation which emphasises the unity of the process* [2]. Process integration consists of two distinguished families of methodologies, i.e. *pinch analysis* and *mathematical programming* techniques. These techniques are very well established for various process synthesis problems for chemical process plants, e.g. energy recovery [11], mass integration [2], water minimisation [4], etc. In recent years, consideration amount of process integration works have been reported for the synthesis of biomass supply chain. For instance, in the work of Lam et al. [9], a pinch-based graphical technique was proposed to synthesise the biomass supplychain, with the objective to minimise carbon footprint. The authors also proposed the planning of regional biomass supply chain in their later works [10]. Foo et al. [5], on the other hand, made use of mathematical programming techniques for the synthesis of flexible biomass supply chain. An overview of various modelling and optimisation techniques for palm biomass supply chain may be found in Chap. 7 of this book [8].

It is interesting to note that the biomass supply chain synthesis problem is structurally similar to other process integration problems described earlier, where the identified *sources* (output of process units) is to be allocated to the *sinks* (units where resource is needed). For instance, in energy recovery problem, the location of energy sources to the sinks is to be maximised, in order to minimise external energy resources. The same analogy applies to biomass supplychain, where biomass sources are to be allocated to the biomass sinks, in order to maximise profits. Table 2 shows a summary of analogy in various process integration problems.

Table 2 Various sink-source matching problems in process integration

Problems	Purpose	References
Energy recovery	To maximise waste heat recovery from sources to sinks, and to minimise energy resource	Linnhoff et al. [11]
Water minimisation	To maximise water recovery from sources to sinks, and to minimise fresh water resource	Foo [3]
Hydrogen network	To maximise hydrogen recovery from sources to sinks, and to minimise fresh hydrogen resource	Hallale and Liu [6]
Energy planning	To minimise use of renewable energy source	Tan and Foo [16]
Carbon capture and storage	To maximise storage of CO_2 sources to sinks	Ooi et al. [17]

1.1 Palm Biomass Supply Chain for Power Generation

Malaysia was supposed to generate 5% renewable energy of its total power generation mix during its Tenth Malaysia Plan, i.e. by year 2015, however had failed to achieve the target. The next target is to achieve 11% of renewable energy during the 11th Malaysia Plan, i.e. by year 2020 [14]. With this target in mind, the renewable resources in the country, such as biomass resource in the oil palm industry need to be better utilised.

Umar et al. [19] reported that a vast majority of palm oil mills (86%) utilise their excess biomass for self-consumption. In other words, the contribution of renewable energy from biomass source for the overall share in the country's total energy mix is relatively low. This is mainly due to the fact that most mills are located in the remote areas. In their earlier survey, the authors reported that more than one-third of Malaysian palm oil mills are located beyond 10 km from the nearest grid connection point [18], which makes grid extension economically not viable. Hence, it is more wisely if the biomass resource can be channelled to some central facilities for power generation. A case study on the allocation of biomass for power generation in the state of Sabah (northern region in the Borneo Island) was also reported [5]. Apart from generating renewable fuel for the palm oil production process, palm solid biomass and biogas from palm oil mill effluent[1] are sufficient in providing extra electricity for the nearby area [20].

2 Problem Statement

The problem to be addressed is formally stated as follows [5]:

Given a set of biomass sources $i \in I$ to be allocated to a set of biomass sinks $j \in J$. The sinks may make use of the biomass for power generation, or any other value-added activities. The objective of this problem is to determine the optimum allocation of biomass, in order to achieve the objectives set, e.g. minimum cost, carbon footprint, maximum profit, etc. The problem can be represented by the superstructure model in Fig. 1.

3 Mathematical Model for Biomass Sink-Source Allocation

The problem is subject to the following constraints.

The total biomass required by a sink $j(D_j)$ is to be fulfilled through the allocated amount from the various sources ($\Sigma_i F_{i,j}$), given by Eq. (1).

[1] See Chap. 4 for biogas generation from palm oil mill effluent.

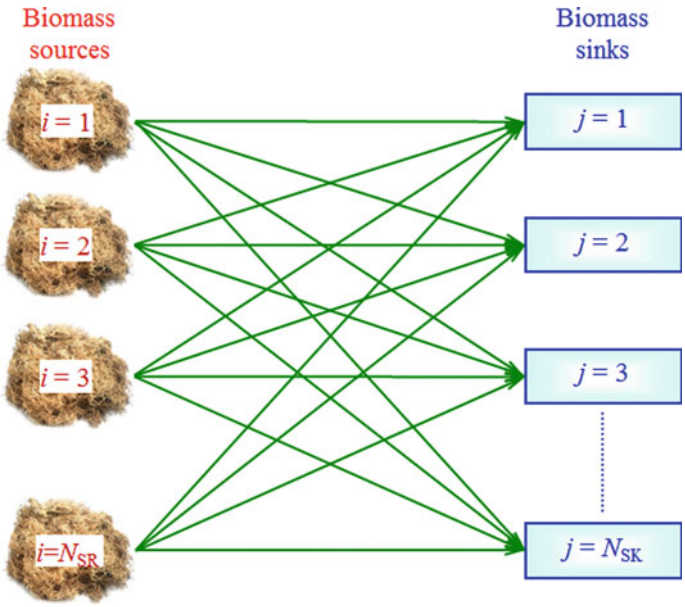

Fig. 1 Superstructural model for biomass sink-source allocation

$$\sum_i F_{i,j} = D_j \quad \forall j \tag{1}$$

Next, Eq. (2) dictates that the total amount of biomass allocated from source i to all sinks ($\Sigma_j F_{i,j}$) should not exceed its availability (S_i).

$$\sum_j F_{i,j} \leq S_i \quad \forall i \tag{2}$$

It is also useful to relate the unutilised biomass with the amount of allocation and the availability, given in Eq. (3).

$$U_i = S_i - \sum_j F_{i,j} \quad \forall i \tag{3}$$

Finally, the allocated biomass amount has to take non-negative values (Eq. 4):

$$F_{i,j} \geq 0 \quad \forall i,\ j \tag{4}$$

Equations (1)–(4) are a LP model for which a global optimum solution is guaranteed when a solution is found. One may make use of any commercial software (e.g. MS Excel, LINGO, GAMS, etc.) to solve the above LP model.

Table 3 Data for EFB consumers and consumers [5]

Suppliers	EFB capacity S_i (kt/y)	Consumers	EFB requirement C_j (kt/y)
S1	90	C1	240
S2	75	C2	200
S3	80	C3	200
S4	85		
S5	82		
S6	86		
S7	92		
S8	78		
S9	80		
S10	88		
S11	84		

The mathematical model has a diverge usage. For POM owners who possess excess biomass in the mill (upon generating steam for mill use), they may make use of the LP model to maximise the profit from their biomass sales. On the other hand, process plant owners who wish to purchase biomass for co-firing can make use of the LP model to minimise the operating cost (transport and/or raw material costs). Local authority or environmentalists who wish to enhance sustainability will find the model useful as they can make the most use of renewable energy (by replacing fossil fuel), and yet minimise CO_2 footprint from the transportation system (in sending biomass). These scenarios will be demonstrated in the case study that follows.

4 Case Study

A case study adopted from Foo et al. [5] is used to illustrate how the superstructural model may be used for the optimum allocation of EFBs among its suppliers (sources) and consumers (sinks). Figure 2 shows the geographical location where these EFB consumers and suppliers are located in the several cities of Sabah (a state of Malaysia located in the northern region of Borneo island). The EFB suppliers are palm oil mills which experience excess energy resources. Hence, these mill may send their EFB to the various EFB consumers in order to maximise their economic potential. These EFB consumers may be process plants (e.g. refineries, oleochemicals) that wish to generate power through combined heat and power scheme, or mills that incorporated biorefinery concept that convert EFB to other value-added products. The capacity and requirement of the EFB suppliers and consumers are given in Table 3, while Table 4 indicates the distances among them.

In order to perform the optimisation study, the superstructural model may be conveniently set up in the widely use commercial spreadsheet software—Microsoft

Fig. 2 Location of EFB supplier and consumers for case study [5]

Table 4 Distance (in km) between EFB suppliers and consumers [5]

$D_{i,j}$	C1	C2	C3
S1	11.9	65.7	164
S2	9.9	69.9	168
S3	12.3	66.5	165
S4	12.3	66.5	165
S5	11.9	65.7	164
S6	8.0	77.8	176
S7	8.0	77.8	176
S8	75.6	0	98
S9	172	96.2	1.9
S10	170	94.5	5.5
S11	168	92.5	7.1

Excel. Figure 3 shows how the superstructural model and its associated constraints are set up in Microsoft Excel, based on the model presented in Sect. 3. Note that some of the constraints (Eq. 3) were embedded as equations in the main Excel spreadsheet interface, while some (Eqs. 1, 2 and 4) are incorporated into the Solver. Three different scenarios are analysed for this case study, and their results are discussed in the following sub-sections.

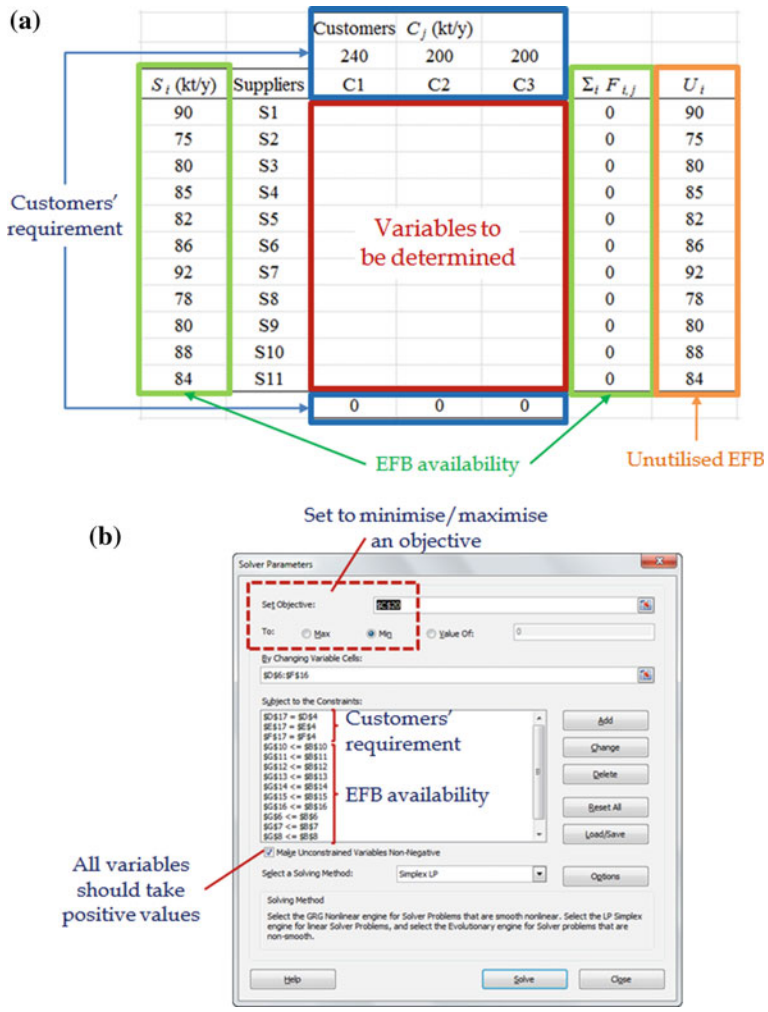

Fig. 3 EFB allocation superstructural model in MS excel spreadsheet: **a** setting for main interface; **b** setting in solver

4.1 Scenario 1—CO_2 Emission Minimisation for Environmental Protection

In Scenario 1, the objective is set to minimise CO_2 emission (E_{CO_2}), given as in Eq. 5. This scenario is meant to be used by the authority in reducing the overall CO_2 emission. The latter is mainly contributed by the transportation of EFB, which is the summation of product of EFB allocation among supplier i and customers j($F_{i,j}$), with the distance among them ($D_{i,j}$), as well as the emission factor of transportation. For

		Customers C_j (kt/y)				
		240	200	200		
S_i (kt/y)	Suppliers	C1	C2	C3	$\Sigma_i F_{i,j}$	U_i
90	S1	0	40	0	40	50
75	S2	62	0	0	62	13
80	S3	0	0	0	0	80
85	S4	0	0	0	0	85
82	S5	0	82	0	82	0
86	S6	86	0	0	86	0
92	S7	92	0	0	92	0
78	S8	0	78	0	78	0
80	S9	0	0	80	80	0
88	S10	0	0	88	88	0
84	S11	0	0	32	32	52
		240	200	200		

	Distance			
$D_{i,j}$ (km)	C1	C2	C3
S1	11.9	65.7	164
S2	9.9	69.9	168
S3	12.3	66.5	165
S4	12.3	66.5	165
S5	11.9	65.7	164
S6	8	77.8	176
S7	8	77.8	176
S8	75.6	0	98
S9	172	96.2	1.9
S10	170	94.5	5.5
S11	168	92.5	7.1

T_{CO2} =	0.092	kg CO_2/km/t
E_{CO2} =	$2\,T_{CO2}\,\Sigma_j\Sigma_i\,F_{ij}D_{ij}$	
	2,008,618	kg/y (same as reported in Foo et al., 2013)

Fig. 4 EFB allocation (kt/y) with minimum carbon footprint (scenario 1)

this scenario, lorry is assumed for use, with the emission factor (T_{CO_2}) of 0.092 kg CO_2/km/t [5]. Note also that CO_2 emission in Eq. 5 is doubled due to the return trip of empty lorries.

$$\text{Minimise} \quad E_{\text{CO}_2} = 2T_{\text{CO}_2} \sum_j \sum_i F_{i,j} D_{i,j} \tag{5}$$

Solving the objective function in Eq. 5 subject to the constraints in Eqs. (1–4) yield the minimum CO_2 emission of 2.0 million kg/y, with the optimum allocation scheme shown in Fig. 4. Note that the minimum CO_2 emission is identical to that reported by Foo et al. [5], however with slightly different allocation scheme. This means that degenerate solutions exist for this case, where different solutions exist for the same objective.

4.2 Scenario 2—Customer's Perspective

In this scenario, the model is assumed to be used by the EFB customer. It is further assumed that the three EFB customers belong to the same company, which possesses their own transportation system (lorries) for EFB collection from the suppliers. Two cases are considered.

In Case 1, it is assumed that the EFBs were sold by the suppliers by the same price (i.e. same company). Hence, the objective is set to minimise the annual operating cost (*AOC*), which is contributed by the transportation cost for the collection of EFB, given in Eq. 6.

		Customers C_j (kt/y)				
		240	200	200		
S_i (kt/y)	Suppliers	C1	C2	C3	$\Sigma_i F_{i,j}$	U_i
90	S1	0	40	0	40	50
75	S2	62	0	0	62	13
80	S3	0	0	0	0	80
85	S4	0	0	0	0	85
82	S5	0	82	0	82	0
86	S6	86	0	0	86	0
92	S7	92	0	0	92	0
78	S8	0	78	0	78	0
80	S9	0	0	80	80	0
88	S10	0	0	88	88	0
84	S11	0	0	32	32	52
		240	200	200		

AOC = $\Sigma_j \Sigma_i F_{i,j} CT_{i,j}$
4,002,680 $/y

Unit cost = transport cost

$CT_{i,j}$ ($)	C1	C2	C3
S1	4.36	24.09	60.13
S2	3.63	25.63	61.60
S3	4.51	24.38	60.50
S4	4.51	24.38	60.50
S5	4.36	24.09	60.13
S6	2.93	28.53	64.53
S7	2.93	28.53	64.53
S8	27.72	0.00	35.93
S9	63.07	35.27	0.70
S10	62.33	34.65	2.02
S11	61.60	33.92	2.60

Fig. 5 EFB allocation (kt/y) with minimum transportation cost (scenario 2—case 1)

$$\text{Minimise} \quad \text{AOC} = \sum_j \sum_i F_{i,j} CT_{i,j}, \tag{6}$$

where $CT_{i,j}$ is the unit cost for transporting the EFB. Similar to earlier scenario, lorries are the main transportation system. The average diesel consumption for lorries is given as 3 km/L (DS), while the unit cost of diesel is 0.55 $/L ($CT_D$). For this case, the distance among EFB customers and suppliers can be conveniently converted into equivalent unit cost ($CT_{i,j}$), given as in Eq. 7. Similar to Scenario 1, the transportation cost in Eq. 7 considers two-ways transportation, i.e. to/fro between the EFB suppliers and customers. For instance, the unit cost for S1 and C1 can be determined as 4.36$ (=2 × 11.9 km/ 3 km/L × 0.55 $/L). Unit cost for other customer-supplier pairs are found in Fig. 5.

$$CT_{i,j} = \frac{2D_{i,j} CT_D}{DS} \tag{7}$$

Solving the objective function in Eq. 6 subject to the constraints in Eqs. 1–4, 7 yield the minimum transportation cost of 4.0 million $/y, with the optimum allocation scheme shown in Fig. 5. One will notice that the allocation for this scenario is the same as that in Scenario 1. The main reason is that, the minimum transportation cost corresponds to the minimum distance travelled by the lorries (in emitting minimum CO_2) as in Scenario 1.

In Case 1, it was assumed that the EFBs were sold at the same unit price, as the suppliers belong to the same company. In Case 2, it is assumed that the EFBs are sold at different price, as the suppliers are owned by different companies. Hence, the unit cost in Eq. 7 is revised as in Eq. 8.

		Customers C_j (kt/y)				
		240	200	200		
S_i (kt/y)	Suppliers	C1	C2	C3	$\Sigma_i F_{i,j}$	U_i
90	S1	0	0	0	0	90
75	S2	17	0	0	17	58
80	S3	0	0	0	0	80
85	S4	45	40	0	85	0
82	S5	0	82	0	82	0
86	S6	86	0	0	86	0
92	S7	92	0	0	92	0
78	S8	0	78	0	78	0
80	S9	0	0	80	80	0
88	S10	0	0	88	88	0
84	S11	0	0	32	32	52
		240	200	200		

Unit cost = transport + raw material cost

$CT_{i,j}$ ($)	C1	C2	C3
S1	14.36	34.09	70.13
S2	13.63	35.63	71.60
S3	14.51	34.38	70.50
S4	12.51	32.38	68.50
S5	12.36	32.09	68.13
S6	10.93	36.53	72.53
S7	10.93	36.53	72.53
S8	35.72	8.00	43.93
S9	71.07	43.27	8.70
S10	74.33	46.65	14.02
S11	73.60	45.92	14.60

AOC = $\Sigma_j \Sigma_i F_{i,j} CT_{i,j}$

9,688,013 $/y

Fig. 6 EFB allocation (kt/y) with minimum operating cost (scenario 2—case 2)

$$CT_{i,j} = \frac{2D_{i,j}CT_D}{DS} + CT_S, \tag{8}$$

where CT_s refers to the unit cost of EFB for supplier i. For this case, the unit costs of EFB are assumed as 10, 8 and 12 $/t for Suppliers 1–3, 4–9 and 10–11, respectively.

Solving the objective function in Eq. (6) subject to the constraints in Eqs. 1–4 and 8 yield the minimum operating cost of 9.7 million $/y, with the optimum allocation scheme shown in Fig. 6. Note that the EFB allocation scheme is no longer the same as compared to those in Figs. 4 and 5. Note also that the CO_2 emission for this scenario is determined as 2,034 t/y (calculation not shown for brevity).

4.3 Scenario 3—Supplier's Perspective

This scenario is meant to be used by EFB suppliers, in order to maximise the profitability in selling their EFBs. It may be assumed that all EFB suppliers belong to the same company. The unit costs of EFB are the same as in Scenario 2—case 2, i.e. 10, 8 and 12 $/t for Suppliers 1–3, 4–9 and 10–11, respectively. Solving the objective function in Eq. (9) subject to the constraints in Eqs. (1–4) yield the maximum profit of 6.3 million $/y, with the optimum allocation scheme shown in Fig. 7. Note that the allocation scheme is different from those in previous scenarios.

$$\text{Maximise PROFIT} = \sum_j \sum_i F_{i,j} CT_{i,j} \tag{9}$$

		Customers C_j (kt/y)				
		240	200	200		
S_i (kt/y)	Suppliers	C1	C2	C3	$\Sigma_i F_{i,j}$	U_i
90	S1	0	0	90	90	0
75	S2	0	49	26	75	0
80	S3	0	80	0	80	0
85	S4	14	71	0	85	0
82	S5	52	0	0	52	30
86	S6	86	0	0	86	0
92	S7	0	0	0	0	92
78	S8	0	0	0	0	78
80	S9	0	0	0	0	80
88	S10	88	0	0	88	0
84	S11	0	0	84	84	0
		240	200	200		

Unit cost = raw material cost

$CT_{i,j}$	C1	C2	C3
S1	10.00	10.00	10.00
S2	10.00	10.00	10.00
S3	10.00	10.00	10.00
S4	8.00	8.00	8.00
S5	8.00	8.00	8.00
S6	8.00	8.00	8.00
S7	8.00	8.00	8.00
S8	8.00	8.00	8.00
S9	8.00	8.00	8.00
S10	12.00	12.00	12.00
S11	12.00	12.00	12.00

$PROFIT = \Sigma_j \Sigma_i F_{i,j} CT_{i,j}$

6,298,000 $/y

Fig. 7 EFB allocation (kt/y) with maximum profit (scenario 3)

Table 5 The payoff table

	$F_1(\mathrm{x}^q)$	$F_2(\mathrm{x}^q)$	…	$F_q(\mathrm{x}^q)$
x^1	$F_1(\mathbf{x}^1)$	$F_2(\mathbf{x}^1)$		$F_Q(\mathbf{x}^1)$
x^2	$F_1(\mathbf{x}^2)$	$F_2(\mathbf{x}^2)$		$F_Q(\mathbf{x}^2)$
…	…	…	…	…
x^Q	$F_1(\mathbf{x}^Q)$	$F_2(\mathbf{x}^Q)$		$F_Q(\mathbf{x}^Q)$

5 Multi-objective Optimisation

For a non-trivial multi-objective optimisation problem, there is no single solution that will achieve all objectives simultaneously. Hence, it is often possible to have infinite number of *Pareto optimal solutions*. For instance, for the EFB case study, it is not possible to achieve minimum CO_2 emission with minimum AOC. One of the method that may be used to solve the multi-objective optimisation problem is the *constrained method*, with the four-step procedure outlined as follows [1].

1. The pay-off table
    a. A number of Q single-objective optimisation problems is to be solved to find the optimal solution for each of the Q objectives. Optimal solution for the qth objective is denoted as $x^q = \left(x_1^q, x_2^q, x_3^q, \ldots, x_I^q\right)$ where x is the decision variables.
    b. Compute the value of each objective at each of the Q optimal solutions: $F_1(\boldsymbol{x}^q)$, $F_2(\boldsymbol{x}^q)$, …, $F_Q(\boldsymbol{x}^q)$, $q = 1, 2, \ldots, Q$. This gives Q values for each of the Q objectives.
    c. A pay-off table (see sample in Table 5) is constructed, with rows corresponding to $\boldsymbol{x}^1, \boldsymbol{x}^2, \ldots, \boldsymbol{x}^Q$ and the columns equal to the number of objectives.

d. The largest and the smallest numbers in the qth row are identified and denoted as M_q and n_q, respectively. This step is repeated for $q = 1, 2, \ldots, Q$.

2. Setting the constraints—Convert the multiple optimisation objectives in Eq. 10 to its corresponding constrained problem (Eq. 11a, 11b).

$$\text{Minimise } F(x) = \left[F_1(x), F_2(x), \ldots . F_Q(x)\right] \tag{10a}$$

subject to,

$$F_q(x) \leq \epsilon_q \quad q = 1, 2, \ldots, Q \tag{10b}$$

$$\text{Minimise } F_h(x) \tag{11a}$$

subject to,

$$F_q(x) \geq \epsilon_q \quad q = 1, 2, \ldots . h-1, h+1 \ldots Q \tag{11b}$$

where hth objective is arbitrarily chosen for minimisation, and all other objective functions of the problem are converted into constraints.

3. Set the right-hand side coefficients—The n_q and M_q represent the lower and upper bounds for the qth objective: $n_q \leq \varepsilon_q \leq M_q$. Choose the number of different values of ε_q and denote it by r.

4. Solving the optimisation problem—To generate a range of non-inferior solutions, solve the constrained problem in Step 2 for every combination of values for ε_q, $q = 1, 2, \ldots, h-1, h+1, \ldots, Q$, where ε_q is given by Eq. 12a, 12b.

$$\varepsilon_q = n_q + \frac{t}{r-1}\left(M_q - n_q\right) \tag{12a}$$

$$t = 0, 1, 2, \ldots, (r-1) \tag{12b}$$

The case study is revisited to demonstrate how the constrained method is used to solve a multi-objective optimisation problem.

6 Case Study (Revisited)

The case study is revisited. It is now assumed that the authority would be working with the mill owners to identify the trade-off between minimum CO_2 emission (Scenario 1) and minimum AOC (Scenario 2, Case 2). Following Step 1 of the constrained method, the payoff table is constructed (Table 6). The column of the payoff table corresponds to the two different objectives, i.e. minimum CO_2 and minimum AOC. For both objectives, their decision variables (CO_2 emission and AOC) are set as rows. For the row of CO_2 emission, the largest (M_1) and smallest (n_1) values are found as 2009 (Scenario 1) and 2034 t CO_2/y (Scenario 2—Case 2). For the row of

Table 6 Payoff table for case study (Step 1)

	Minimum CO_2 (t CO_2/y)	Minimum AOC (×1000 $/y)
CO_2 emission	2009	2034
AOC (x1000 $/y)	9807	9688

Table 7 Results for optimisation (Step 4)

t	AOC (ε_q)	Min CO_2
0	9688	2034
1	9705	2028
2	9722	2021
3	9739	2014
4	9756	2013
5	9773	2011
6	9790	2010
7	9807	2009

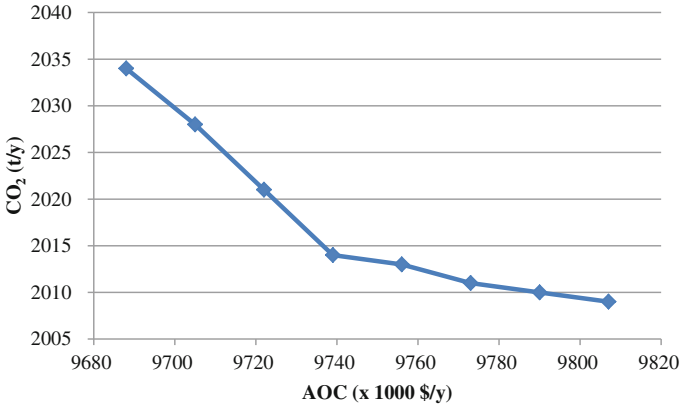

Fig. 8 Pareto front for case study

AOC, largest (M_2) and smallest (n_2) values are found as 9807 (Scenario 1) and 9688 thousand $/y (Scenario 2—Case 2), respectively.

In Step 2 , the multiple-objective problem is converted into single objective problem, by setting the minimum CO_2 emission as the objective, while the objective of AOC is converted into constraint. In Step 3, the lower and upper bounds for the AOC constraints are identified, i.e. 2034 and 9688 million $/y (see Table 6). Note that the value of r is arbitrary taken as 8. In Step 4, a range of ε_q values are first calculated using Eq. (12) (see Table 7). The optimisation is carried out by solving Eq. 5 (i.e. minimum CO_2 emission as in Scenario 1), subject to the constraints in Eqs. (1)–(4), and the ε_q values in Table 7 repeatedly. Results of the optimisation are summarised in Table 7, with the Pareto chart plotted in Fig. 8. As shown in the latter, CO_2 emission may only be reduced at the expense of higher AOC.

7 Conclusions

A simple optimisation model based on linear programming (LP) is presented in this chapter. The model may be used by various stakeholders to determine the optimum allocation of biomass resources in the supply chain, in order to achieve their set objective. Multi-objective optimisation approach is used to identify the trade-off among the stakeholders.

References

1. Azapagic A, Clift R (1999) Life cycle assessment and multiobjective optimisation. J Clean Prod 7(2):135–143
2. El-Halwagi MM (1997) Pollution prevention through process integration: systematic design tools. Academic Press, San Diego
3. Foo DCY (2009) A state-of-the-art review of pinch analysis techniques for water network synthesis. Ind Eng Chem Res 48(11):5125–5159
4. Foo DCY (2012) Process integration for resource conservation. CRC Press, Boca Raton, Florida, US
5. Foo DCY, Tan RR, Lam HL, Kamal M, Klemeš JJ (2013) Robust models for the synthesis of flexible palm oil-based regional bioenergy supply chain. Energy 55:68–73
6. Hallale N, Liu F (2001) Refinery hydrogen management for clean fuels production. Adv Environ Res 6:81–98
7. Hong BH, How BS, Lam HL (2016) Overview of sustainable biomass supply chain: from concept to modelling. Clean Technol Environ Policy 18(7):2173–2194
8. How BS (2018) An overview of palm biomass supply chain modelling. In: Foo DCY, Abdul Aziz MK (eds) Green technologies for the oil palm industry. Springer, Singapore
9. Lam HL, Varbanov PS, Klemeš JJ (2010) Regional renewable energy and resource planning. Appl Energy 88:545–550
10. Lam HL, Varbanov PS, Klemeš JJ (2010) Minimising carbon footprint of regional biomass supply chains. Resour Conserv Recycl 54(5):303–309
11. Linnhoff B, Townsend DW, Boland D, Hewitt GF, Thomas BEA, Guy AR, Marshall RH (1982) A user guide on process integration for the efficient use of energy. Rugby, IChemE
12. Loh SK (2017) The potential of the Malaysian oil palm biomass as a renewable energy source. Energy Convers Manag 141:285–298
13. Ng RTL, Hassim MH, Ng DKS (2013) Process synthesis and optimization of a sustainable integrated biorefinery via fuzzy optimization. AIChE J 59(11):4212–4227
14. Renewables Now (2015) Malaysia eyes 11% renewables contribution by 2020. https://renewablesnow.com. Accessed July 2018
15. Sadhukhan J, Martinez-Hernandez E, Murphy RJ, Ng DKS, Hassim MH, Ng KS, Wan YK, Md Jaye IF, Melissa YLPH, Andiappan V (2018) Role of bioenergy, biorefinery and bioeconomy in sustainable development: strategic pathways for Malaysia. Renew Sustain Energy Rev 81:1966–1987
16. Tan RR, Foo DCY (2007) Pinch analysis approach to carbon-constrained energy sector planning. Energy 32(8):1422–1429
17. Ooi REH, Foo DCY, Ng DKS, Tan RR (2013) Planning of carbon capture and storage with pinch analysis techniques. Chem Eng Res Des 91(12):2721–2731
18. Umar MS, Jennings P, Urmee T (2014) Sustainable electricity generation from oil palm biomass wastes in Malaysia: an industry survey. Energy 67:496–505
19. Umar MS, Urmee T, Jennings P (2018) A policy framework and industry roadmap model for sustainable oil palm biomass electricity generation in Malaysia. Renew Energy 128A:275–284

20. Wu Q, Qiang TQ, Zeng G, Zhang H, Huang Y, Wang Y (2017) Sustainable and renewable energy from biomass wastes in palm oil industry: a case study in Malaysia. Int J Hydrogen Energy 42(37):23871–23877

An Overview of Palm Biomass Supply Chain Modelling

Bing Shen How

Abstract In the Malaysian context, the oil palm industry is one of the key contributors to the country's Gross Domestic Product (GDP) and Comprehensive National Strength (CNS). According to Department of Statistic Malaysia [1], oil palm industries had contributed 3.5% or RM 38.5 billion (approximately 9.6 billion USD) to Malaysia's GDP in 2016. To further enhance the potential of the oil palm industry, valorisation of biomass (waste product generated from the palm oil milling process) has received substantial attention from both academicians and industry players in the past few years. Conceptual design and planning, which involve process modelling, evaluation and optimisation is indeed vital to foster the development of palm biomass industry. Keeping this in mind, this chapter presents an overview of the key concerns of *palm biomass supply chain*, from researchers' perspective. It covers several important topics in supply chain modelling, covering facility location decision (e.g. site selection), transportation decision (e.g. transportation mode selection), evaluation and optimisation methodologies and the latest debottlenecking concepts.

Keywords Biomass supply chain · Sustainability evaluation · Optimisation Decision-making · Modelling

Nomenclature

Abbreviation	Description
ADP	Abiotic depletion potential
AHP	Analytical hierarchy process
AP	Acidification potential
BCR	Benefit–cost ratio
CAPEX	Capital expenditure

B. S. How (✉)
Department of Chemical and Environmental Engineering, University of Nottingham Malaysia Campus, Jalan Broga, 43500 Semenyih, Selangor, Malaysia
e-mail: BingShen.How@gmail.com

D. C. Y. Foo and M. K. Tun Abdul Aziz (eds.), *Green Technologies for the Oil Palm Industry*, Green Energy and Technology, https://doi.org/10.1007/978-981-13-2236-5_7

CF	Carbon footprint
ENF	Energy footprint
GA	Genetic algorithm
GWP	Global warming potential
HTPE	Human toxicity potential by either inhalation or dermal exposure
HTPI	Human toxicity potential by ingestion
ISI	Inherent safety index
LF	Land footprint
MILP	Mixed integer linear programme
NP	Net profit
NPV	Net present value
ODP	Ozone depletion potential
OPEX	Operating expenditure
PC	Principal component
PCA	Principal component analysis
POCP	Photochemical ozone creation potential
PP	Pineapple peel
PS	Paddy straw
RH	Rice husk
ROI	Return on investment
SB	Sugarcane bagasse
SVS	Smart vehicle selection
VLM	Volume-limiting material
VOL	Volume limiting
WEL	Weight limiting
WF	Water footprint
WLM	Weight-limiting material
WPFP	Workplace footprint

Indices	**Description**
d	Index for sustainability dimension (economic, environmental, social)
i	Index for sources
j	Index for processing hubs
k	Index for customers
m	Index for transportation mode

Parameters	**Description**
C_r^{Biomass}	Collection cost of biomass r [USD/t]
$C_t^{\text{CAPEX\_Tech}}$	Capital cost of technology t [USD/t]
$C_{t'}^{\text{CAPEX\_Tech}}$	Capital cost of technology t' [USD/t]
$C^{\text{Construct}}$	Construction cost [USD]
C^{Fuel}	Fuel price [USD/L]
C_r^{General}	Gross profit obtained per t of biomass r [USD/t]
C^{Land}	Land cost [USD]
$C_t^{\text{OPEX\_Tech}}$	Operating cost of technology t [USD/t]

$C_{t'}^{\text{OPEX\_Tech}}$	Operating cost of technology t' [USD/t]
C_m^{Proc}	Procurement cost of vehicle [USD]
C_p^{Prod}	Revenue obtained from final products p [USD/y]
C_m^{Repair}	Estimated repair and maintenance cost of vehicle per km of distance travelled [USD/km]
C^{T}	Linearised transportation cost constant [USD/t biomass.km]
$\text{Cap}_m^{\text{Volume}}$	Volume-capacity limit of vehicle [m^3]
$\text{Cap}_m^{\text{Weight}}$	Load capacity limit of vehicle [t]
CRF	Capital recovery factor
dis	Distance travelled between starting location to the final destination [km]
HW	Hourly wage [USD/h]
LS^{Hub}	Life span of the processing hub [y]
LS_m^{Tr}	Life span of the vehicle [y]
Mag	Magnitude of the sustainable vector
MATD_r	Maximum allowable travel distance [km]
OH	Total operating hour [h/d]
OPD	Estimated total working days per year [d/y]
$\text{rate}_m^{\text{Fuel}}$	Fuel consumption rate of the vehicle [L/km]
rate^{int}	Specified discount rate [%]
w_d	Priority scale assigned to sustainability dimension d
ρ_m	Bulk density of the vehicle capacity [t/m^3]
θ	Angle that reveals the tendency of the system

Variables	**Description**
$C^{\text{Fuel\_Cons}}$	Fuel consumption cost [USD/d]
C^{GP}	Gross profit [USD/y]
$C^{\text{Inv\_Hub}}$	Annualised investment cost [USD/y]
C^{Labour}	Labour cost [USD/d]
C^{Maintc}	Maintenance cost [USD/d]
C^{NP}	Net profit [USD/y]
C^{Proc}	Annualised investment cost for the procurement of vehicles [USD/y]
C^{Tr}	Transportation cost [USD/y]
$F_{l,t',j}$	Flowrate of intermediate l in hub j which is sent to technology t' [t/d]
$F_{p,j}$	Flowrate of product p produced in hub j [t/d]
$F_{r,i}$	Flowrate of biomass r delivered to hub j [t/d]
$F_{r,t,j}$	Flowrate of biomass r in hub j which is sent to technology t [t/d]
F_m^{Volume}	Volume-capacity of materials that are being delivered [m^3/d]
F_m^{Weight}	Weight-capacity of materials that are being delivered [t/d]
F^{Weight}	Amount of materials that are being delivered [t/d]
num^{Hub}	Number of processing hubs
$\text{num}_m^{\text{Trip}}$	Number of trips required
$\text{num}_m^{\text{Vehicle}}$	Number of vehicles
λ	Performance of least satisfied objective

λ_d	Normalised performance in terms of dimension d
λ_{EC}	Normalised performance in terms of economic dimension
λ_{EN}	Normalised performance in terms of environmental dimension

1 Introduction

Being the world second largest producer of palm oil (approximately 5.77 million hectares of planted land and produced 19.9 million tonnes of crude palm oil in 2017 [2]), Malaysia is blessed with tremendous amount of palm oil biomass availability. It is estimated that for each kg of crude palm oil generated, approximately 4 kg of palm biomass are produced; these include empty fruit brunch (EFB), palm kernel shell (PKS), fronds, trunks, etc. [3]. Biomass appears to be a promising substituent of conventional feedstocks for biochemical production [4] and energy generation [5]. This had been the main driving force that attracts the attentions of numerous academicians and investors to venture into this 'green business'.

However, the shift to biomass as a feedstock is yet to be proven feasible and sustainable at industry scale. To achieve this, the development of sustainable biomass supply chain is no doubt vital [6]. The definition of a biomass supply chain differs among scholars. Some of the definitions are shown as follows:

> It comprised of four general system components: (i) biomass harvesting/collection and pre-treatment, (ii) storage, (iii) transport and (iv) energy conversion. Iakovou et al. [7]
>
> The flow of biomass from the land to its end use for producing bioenergy. It includes different types of activities which can be classified into four main categories: harvesting and collecting biomass, storing, transporting and pre-processing. Gold and Seuring [8]
>
> An integrated value chain with four components, i.e. production and management of biomass, integrated biorefinery, distribution of product and logistics linked through the flow of materials and information with the aims of maximising the sustainability goals. Hong et al. [9]

In this chapter, we adopt the concept of Hong et al. [9], where biomass supply chain consists of the following four components:

- biomass harvesting and management
- integrated biorefinery
- product distribution
- logistics management.

The authors claimed that there are no district boundaries among the four components [9]. Fundamentally, they are interdependent and interconnected, resulting in varying degrees of overlapping. A schematic diagram of the conceptual idea of biomass supply chain is shown in Fig. 1, and their issues are next discussed.

The structure of biomass supply chain begins with biomass harvesting and management. In fact, the biomass source of supply is the initial point for the planning and development of the entire supply chain. At this stage, the main issues to be addressed include biomass availability, biomass characteristics (e.g. heating value, nutrition

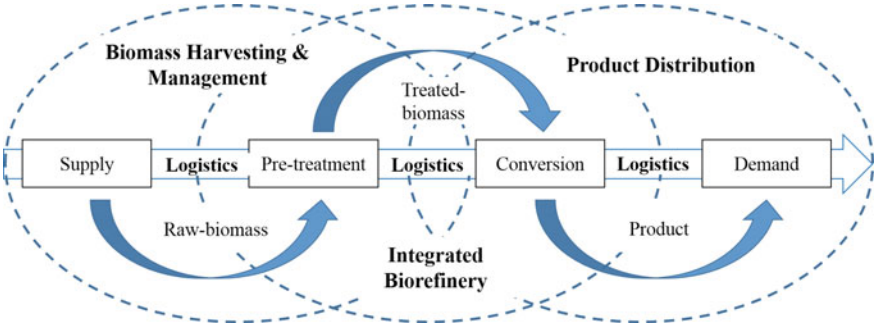

Fig. 1 Conceptual idea of biomass supply chain [9]

content, moisture content, etc.), harvesting planning and scheduling, identification of potential biomass source and implementation of de-centralised pre-treatment activity (the latter may include drying and size reduction to facilitate the storage and transportation of biomass). The followings are some of the key decisions to be made at this level:

- Which biomass to be used?
- Which suppliers should be chosen (e.g. based on location and/or availability)?
- Which agronomy management practices should be conducted to increase biomass yield?
- Do we need to pre-treat the biomass before transporting them? If yes, which treatment facilities should be opted?
- How to ensure constant and continuous supply of biomass feedstock (the seasonality of biomass often results in inconsistent supply in terms of quality and quantity)?

An *integrated biorefinery* is a processing facility that integrates a wide range of biomass technologies to produce various value-added products (e.g. biochemicals, biofuels and bioenergy) [10]. This term is derived from the conventional petroleum refinery since both share a similar functionality. At this stage, raw biomass is first pre-treated in order to improve process efficiency of latter processes. The pre-treated biomass is then converted into value-added products. The key challenges that will be faced at this stage are the determination of facility location and conversion technology [9]. This former decision is usually influenced by various factors, including geographical feasibility, transportation cost (related to the locations of biomass source and potential market) and other basic infrastructures (e.g. roadway, water supply, electricity supply, etc.). The decision on conversion technology, on the other hand, usually made by considering market demands, techno-economic feasibility and other sustainability concerns (usually related to environmental and safety risks). The followings are the summary of the key decisions to be made at this level:

- How many integrated plant(s) is needed in order to meet the product demand?
- Where to locate the integrated plant?

- Which conversion pathway should be selected?
- Do we need to pre-treat the biomass before entering conversion unit? If yes, which treatment facilities should be opted?
- What operating conditions should be opted for the pre-treatment and conversion units?
- How to reduce environmental and safety risks in the integrated biorefinery plant?

Product distribution is defined as the manner in which the products move from the manufacturer to the consumer. Note that the products can also be self-consumed by the integrated plant (e.g. for electricity generation). One of the crucial challenges that will be faced at this stage is the lack of domestic market support. The higher price of bioproducts often appears as a key obstacle that impedes its market penetration [11]. Other decisions to be made at this level are summarised as follows:

- Who are the targeted customers/markets (location, demand)?
- How to deal with the uncertainties in product demand (e.g. customers' behaviour affected by the policy)?
- How to enhance market penetration (marketing strategy and government policy)?

Logistics management (transportation and storage) is the link that connects all components in the supply chain. The logistic network will be greatly affected by product types. Bioenergy in the form of electricity and heat can be transferred to the end user via electricity grid and convection, whereas biofuels and biochemicals can be transported through the existing transportation system (land, water or air) [9]. Given the vehicle capacity (volume and mass limit) and the amount of biomass or products, the required number of vehicle can be determined. To ensure the biomass and bioproducts to arrive at the respective biorefinery and customer on time, while keeping the transportation cost at the minimum, proper scheduling and transportation mode selection play an important role [12]. Besides, choosing a proper storage system is another complex decision-making problem at this stage which considers the uncertainties of biomass and bioproducts quality [13]. The following are the main decisions to be made at this level:

- Materials (biomass and bioproducts) should be stored/delivered in what form?
- Which storage methods/transportation modes should be opted?
- Which transportation routes should be selected?
- How many storage facilities/vehicles are required?

Other key issues during the synthesis of a biomass supply chain are listed as follow:

- How to measure/improve the sustainability performance of the entire supply chain?
- How to improve the computational efficiency especially when dealing with complex problems (e.g. huge model size will increase the solver's burden and thus resulting in high computational time)?
- How to identify/remove the bottlenecks underlying the supply chain effectively?

This chapter represents an overview of the key concerns of palm biomass supply chain, from researchers' perspective. In the following section, the methods to address facilities location decision (i.e. location to set up an integrated biomass processing hubs) are discussed. Next, methods to solve transportation decisions (i.e. transportation mode) are presented. Note that location and transportation decisions are the key concerns in a supply chain synthesis problem [14]. The following section demonstrates the common techniques used in the optimisation of biomass supply chain. The discussion covers conventional single objective to multi-objective optimisation problems, as well as sustainability concerns. Next, two advanced debottlenecking approaches are introduced. A case study is presented to demonstrate how a biomass supply chain problem is addressed.

2 Facilities Location Decision

Placing facilities in the right location is very important so as to minimise the total investment cost (including transportation cost, land price, etc.). The commonly used method for site selection is through 'pre-screening', in which few candidate-locations are selected based on the users' preferences and information gathered. However, due to the inevitable bias and limitation of the users, the optimality of the final decisions is unassured and is often questionable.

To address this issue, How et al. [15] proposed a four-step procedure for the systematic selection of facility location, i.e. area fragmentation, infeasibility elimination, connectivity detachment and economic analysis. The detailed description of each step is discussed in the following subsections. Note that this method is not restricted to the location selection of the biomass processing facilities. Instead, it can be applied to any facility location decision problems.

2.1 Area Fragmentation

Step 1 of the facility location decision procedure involves model size reduction, which will ease the latter selection process. This is achieved by fragmentising the huge area into smaller 'zone' (by horizontal and vertical gridlines). Doing so leads to effective analysis, which significantly reduces computational time due to smaller model size. Each zone is then served as a potential location to set up the biomass processing hub. Figure 2 shows an illustration of this step with a simple example, where the state of Johor (located in the southern part of Peninsular Malaysia; area in white) has been divided into smaller zones. Several works have applied this step before developing their model. For instance, Lam et al. [16] divides the region into several supply and collection zones, while Čuček et al. [17] divides region into smaller zones and classify them as the potential locations for biorefineries. Fundamentally, if smaller zones (i.e. smaller area) are created, the obtained result is more likely to

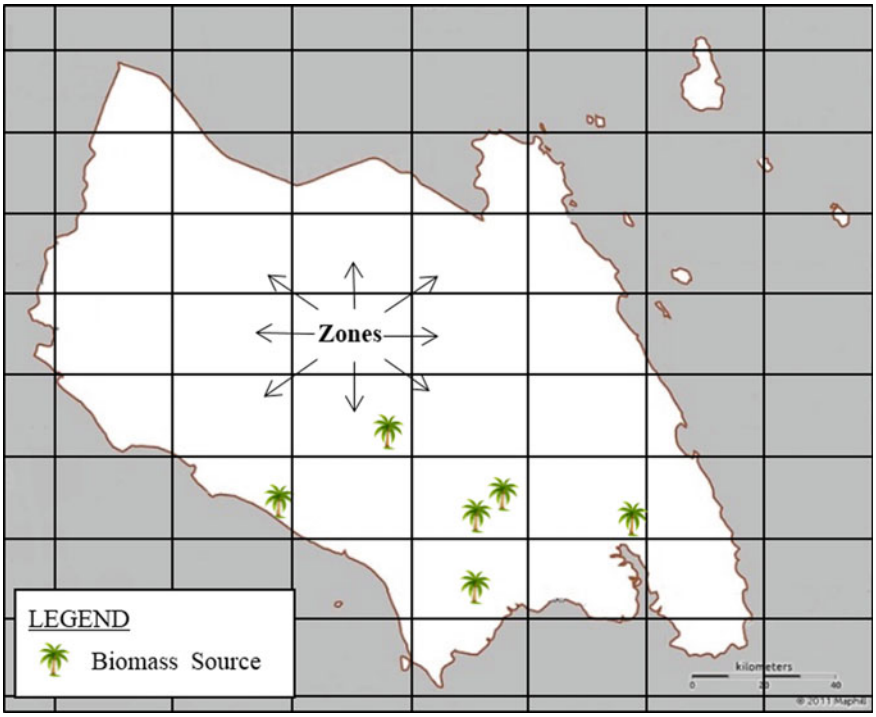

Fig. 2 An illustration example of area fragmentation [19]

achieve the global optimal solution. Therefore, a Pareto analysis may be conducted to investigate the effect of fragmentised area on the objective function; this will be shown in the latter sub-section [18].

2.2 Infeasibility Elimination

Step 2 involves the removal of all 'infeasible' zones (e.g. mountain, residential areas, etc.) which are not suitable or impossible to set up the processing hub(s). Doing this helps to minimise the model size further. In fact, it helps to avoid meaningless results, such as (i) locations which are not suitable to set up hub (normally related to geographical condition, e.g. mountain area, etc.), (ii) locations which are occupied (e.g. residential, commercial areas, etc.) and (iii) locations which are underdeveloped (e.g. lack of water, electricity or worker supply, underdeveloped road system, etc.). Figure 3 is the illustration of this step. For the case of Johor in Fig. 2, the shaded zones are eliminated since they are filled with mountain and protected forest.

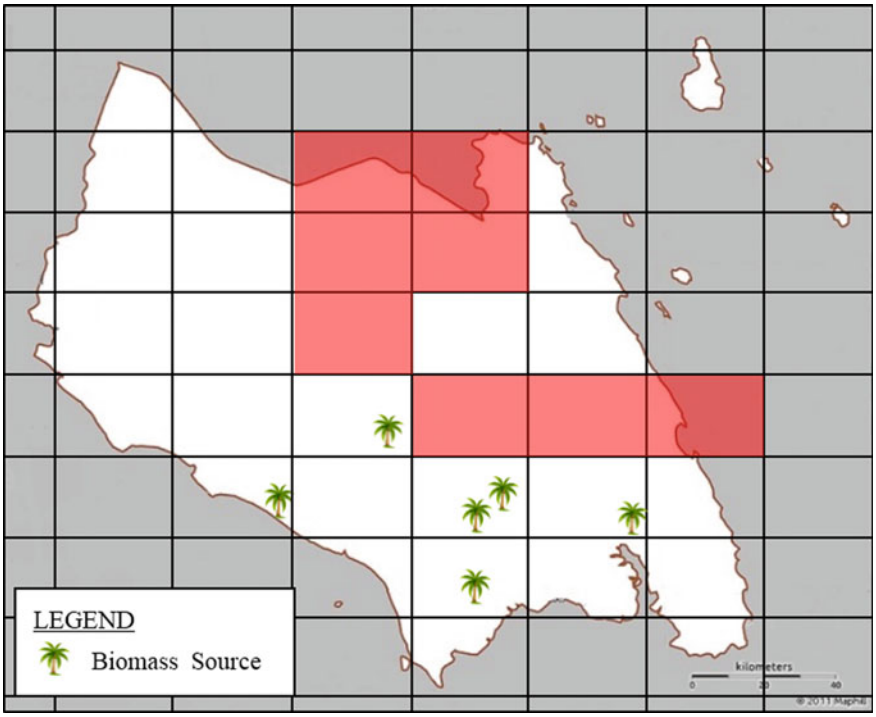

Fig. 3 An illustration example of infeasibility elimination [19]

2.3 Connectivity Detachment

Similar to infeasible elimination, this step also aims to reduce the model size. However, this step removes the infeasible 'connections' instead of 'zones'. Doing this helps to further narrow down the number of candidate-locations. Fundamentally, after step 2, all remaining zones may serve as the potential candidate-locations for all biomass source r. In other words, all entities (biomass sources, integrated biorefineries, demand points) are connected to each other (i.e. source points i to processing hubs j; and processing hubs j to customers k) after step 2. All combinations of connectivity (cross-product multi-dimensional set $I \times J$ and set $J \times K$) create a complex network which will lead to longer computation time. However, in the real scenario, there is an upper bound for the travelling distance, as the profit gained might not be able to compensate the transportation cost of the raw material and product. Therefore, the *maximum allowable travel distance*, MATD_r [in km normally] is introduced to determine the maximum travelling distance for biomass source r which is potentially economic feasible. Generally, MATD_r [km] is directly proportional to the gross profit obtained per ton of biomass, C_r^{General} [USD/t biomass] of the raw material, given as in Eq. (1):

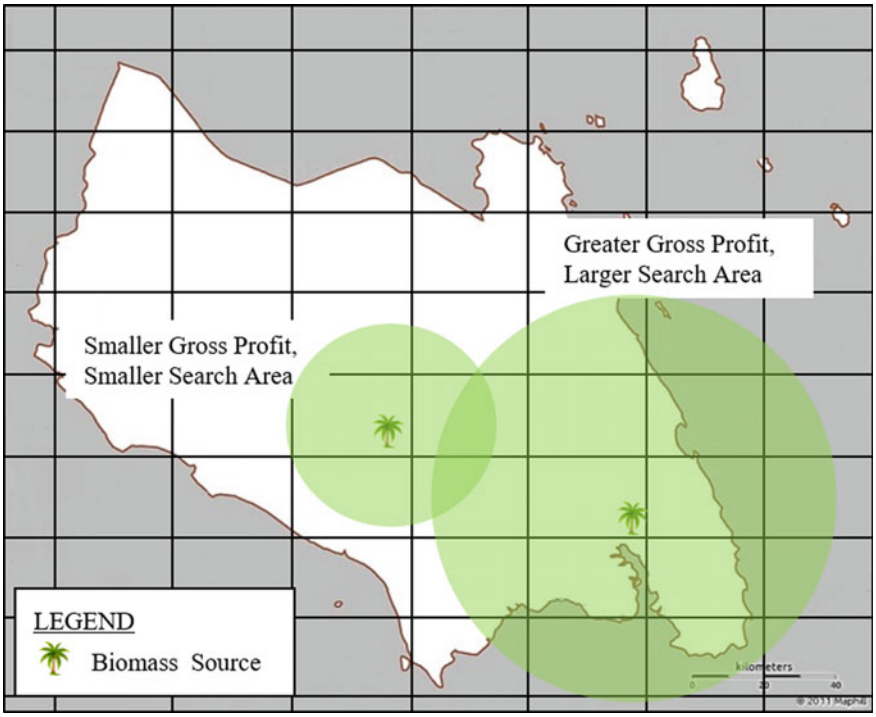

Fig. 4 An illustration example of connectivity detachment [19]

$$\mathrm{MATD}_r = \frac{C_r^{\mathrm{General}}}{C^{\mathrm{T}}} \quad \forall r \in R \tag{1}$$

where C^{T} [USD/t biomass.km] refers to the estimated transportation cost constant, i.e. the linearised transportation cost per unit ton of biomass, per unit km of travelled distance. Figure 4 is the illustration of this step. The figure shows two source points that supply different types of biomass. Each biomass contains different values of C_r^{General}. The one with greater value of C_r^{General} can compensate higher transportation cost, thus it will have a larger search area (i.e. larger MATD_r) compared to the other one. If the biomass is transferred to the zones outside from this search area, the transportation cost will be greater than the maximal gross profit that can be gained in this model. In other words, the zones located outside the search area are no longer cost-feasible and thus, the connectivity between the source point and these zones is unnecessary and should be removed prior to the next step. For the case in Fig. 4, the search areas of the two source points are overlapping with each other. Hence, the overlapping zone will serve as the desired location in setting up the centralised hub.

2.4 Economic Analysis

After the elimination strategies in Steps 1–3, the remaining zones may be served as the candidate-locations to set up the processing hub(s). In order to determine the optimal hub location and optimal biomass allocation pathway, a mathematical model is developed. The model is structured to maximise the net profit, C^{NP}, and is modelled through a *mixed integer linear programme* (MILP), with the objective given in Eq. (2).

$$\max C^{\mathrm{NP}} = C^{\mathrm{GP}} - C^{\mathrm{Inv\_Hub}} - C^{\mathrm{Tr}} \tag{2}$$

Gross profit, C^{GP} [USD/y] in Eq. (2) is determined by the revenue obtained from final products p (C_p^{Product} [USD/t]) subtract the collection cost of biomass r (C_r^{Biomass} [USD/t]), annual operating cost ($C_t^{\mathrm{OPEX\_Tech}}$ [USD/t] and $C_{t'}^{\mathrm{OPEX\_Tech}}$ [USD/t]) and annualised capital cost ($C_t^{\mathrm{CAPEX\_Tech}}$ [USD/t] and $C_{t'}^{\mathrm{CAPEX\_Tech}}$ [USD/t]), given as in Eq. (3).

$$\begin{aligned} C^{\mathrm{GP}} = \Bigg\{ & \sum_p \left(\sum_j F_{p,j} \times C_p^{\mathrm{Prod}} \right) - \sum_r \left(\sum_i F_{r,i} \times C_r^{\mathrm{Biomass}} \right) \\ & \sum_t \left(\sum_r \sum_j F_{r,t,j} \times C_t^{\mathrm{OPEX\_Tech}} \right) \\ & - \sum_{t'} \left(\sum_l \sum_j F_{l,t',j} \times C_{t'}^{\mathrm{OPEX\_Tech}} \right) \\ & - \sum_t \left(\sum_r \sum_j F_{r,t,j} \times C_t^{\mathrm{CAPEX\_Tech}} \right) \\ & - \sum_{t'} \left(\sum_l \sum_j F_{l,t',j} \times C_{t'}^{\mathrm{CAPEX\_Tech}} \right) \Bigg\} \times \mathrm{OPD} \end{aligned} \tag{3}$$

where $F_{p,j}$ [t/y] and $F_{r,i}$ [t/y] refer to the mass flow of product p and biomass r, respectively; $F_{r,t,j}$ [t/y] and $F_{l,t',j}$ [t/y] refer to the biomass r that is consumed in technology t and intermediate l that is consumed in technology t'; while OPD [d/y] refers to the estimated total working days per year. It is worthy to note that $C_t^{\mathrm{OPEX\_Tech}}$ [USD/t] and $C_{t'}^{\mathrm{OPEX\_Tech}}$ [USD/t] cover all operating expenditures, including utility cost, workers' salary, maintenance cost, etc.; while $C_t^{\mathrm{CAPEX\_Tech}}$ [USD/t] and $C_{t'}^{\mathrm{CAPEX\_Tech}}$ [USD/t] cover all the one-time expenses, including machinery cost, legal permit cost, etc.

Annualised investment cost, $C^{\mathrm{Inv\_Hub}}$ [USD/y] in Eq. (2) refers to the fixed cost required to set up a number of processing hubs ($\mathrm{num}^{\mathrm{Hub}}$), which includes land cost (C^{Land} [USD]) and construction expenses ($C^{\mathrm{Construct}}$ [USD]), given as in Eq. (4). It is

annualised by using capital recovery factor (CRF) which converts a present value to a stream of equivalent annual cost over a life span (LS^{Hub} [y]) at a specified discount rate ($rate^{int}$ [%]), given as in Eq. (5).

$$C^{Inv\_Hub} = num^{Hub} \times \left(C^{Land} + C^{Construct}\right) \times CRF \tag{4}$$

$$CRF = \frac{rate^{int}\left(1 + rate^{int}\right)^{LS^{Hub}}}{\left(1 + rate^{int}\right)^{LS^{Hub}} - 1} \tag{5}$$

Annualised transportation cost, C^{Tr} [USD/y] in Eq. (2) can be determined using Eq. (6), where D refers to the distance travelled between starting location to the final destination; while F^{Weight} [t/d] refers to the amount of materials (biomass r or products p) that are being delivered. In this section, the transportation cost is determined based on a linearised transportation cost constant, C^{T} [RM/t/km]. A more accurate transportation cost calculation, which considers physical capacity constraints of the vehicle, delivery lead time, etc., is discussed in the latter section.

$$C^{Tr} = F^{Weight} \times D \times C^{T} \times OPD \tag{6}$$

2.5 Example

In this section, an exploratory case study from How et al. [15] is used to demonstrate how the multi-biomass supply chain can be synthesised. Johor is a state of Malaysia which is located in the southern of Peninsular Malaysia. It is blessed with abundant and diverse biomass. Apart from palm biomass (e.g. EFB, PKS), rice husk (RH), paddy straw (PS), pineapple peel (PP), sugarcane bagasse (SB) are also found. The geographical locations of the biomass sources are presented in the map of Johor in Fig. 5.

Each biomass may be sent to an integrated biorefinery plant for further process. They are converted into various value-added products. For instance, EFB can be used as feedstocks for dry long fibre and syngas production (via fiberizing system and gasification, respectively). PKS can be converted into briquette, and further processed into energy pack in order to maximise its economic value. On the other hand, RH can be fed into pyrolyser which is aimed to produce high-quality biochar and pyrolysis oil. Both fast and slow pyrolysis may be considered in this case study. SB may be used as feedstocks for bioethanol production; however, it must be pre-treated prior to fermentation. There are four different types of treatment considered in this case study, i.e. dilute acid pre-treatment, dilute alkaline pre-treatment, hot water pre-treatment and steam explosion pre-treatment [20]. Furthermore, PP can either be converted into citric acid via solid-state fermentation, or fed to an anaerobic digester (AD) to produce methane gas. Else, PP and PS can also be conditioned into organic

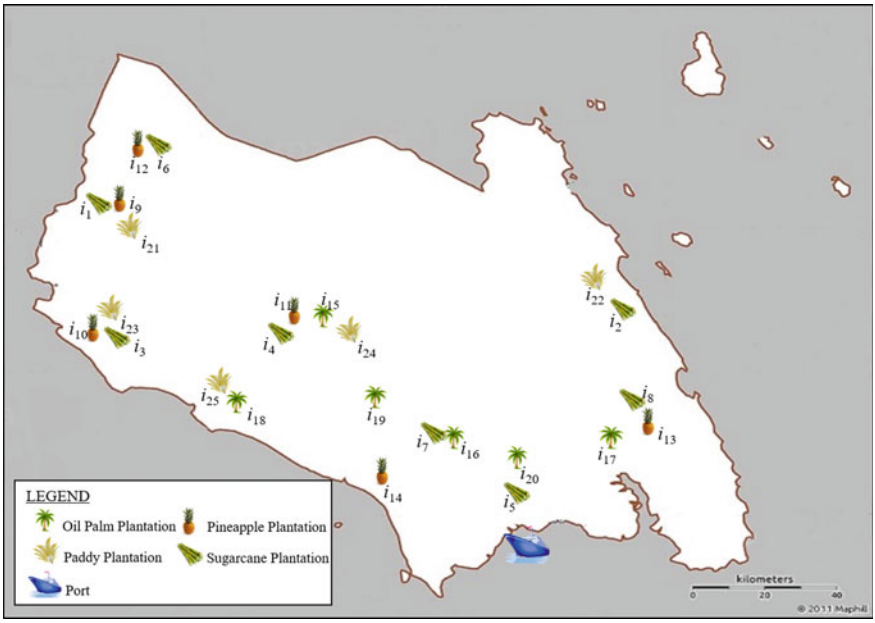

Fig. 5 Biomass sources in Johor [19]

fertiliser. Finally, EFB, PKS, PS and SB can be used as the boiler fuel to generate electricity.

This example aims to identify the optimal conversion pathway for each biomass. Aside from this, the determination of the best location(s) for setting up the integrated biorefinery plant(s) is the other objective of this example.

The optimal conversion pathways can be determined by maximising the Gross profit, C^{GP} which was defined in Eq. (3). The obtained results are illustrated in Fig. 6. In general, EFB and SB are utilised as feedstock for syngas and bioethanol production, respectively, in order to obtain higher revenue. On the other hand, pyrolysis oil and energy pack production are the most cost-effective pathways for RH and PKS, respectively, whereas PP and PS are preferably conditioned into organic fertiliser.

Next, the best location for the integrated biorefinery plant(s) are identified through the four-step procedure described in Sect. 2. In Step 1 (area fragmentation), the area of analysis has been divided into 33 zones, with 600 km^2 per zone (as given in Fig. 2). Similar to the illustration case in Fig. 3, 8 zones which are located in mountain area are removed in Step 2 (feasibility elimination). With Step 3 (connectivity detachment), one of the north-east zones in Johor (see Fig. 7) is removed, as it is located too far from the sources. Now, the superimposed feasible processing hub locations can be visualised in Fig. 7. Figure 8, on the other hand, shows the geographical locations of all 25 remaining plants (i.e., j_1–j_{25}). Finally, in Step 4 (economic analysis), a mathematical model (see Sect. 2.4) is developed to solve this facility location decision

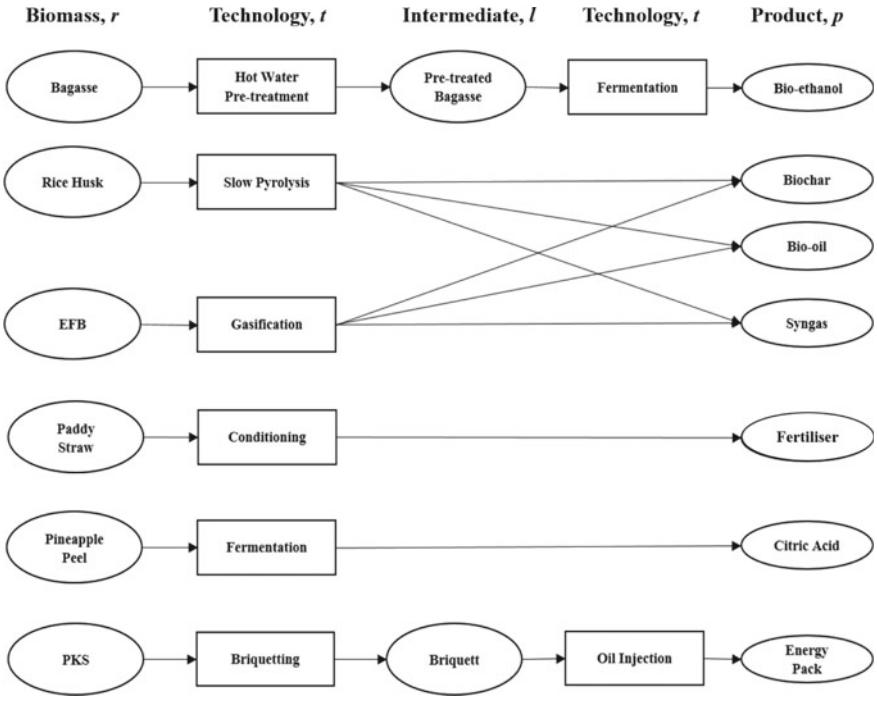

Fig. 6 Optimal conversion pathways [19]

problem. Note that the developed model can be solved using an optimisation software (e.g. Lingo, GAMS).

Table 1 shows the number of variables present in the model and the computational time required in two different scenarios (with and without the elimination strategies). Despite that the marginal reduction in computation time, the results show that the proposed approach is applicable to reduce the model size of the multi-biomass supply chain problems, with the reduction of 67% of the variables. The improvement of computational time is expected to be more significant for larger case study. Aside from this, it is worth noting that the percentage error between the maximum C^{NP} obtained before and after decomposition is negligible (less than 1%) for this case study.

The optimisation results obtained from Step 4 show that the optimal number of processing hubs is five (see Fig. 9). If fewer hubs were built (<5), some of the biomass will be transported to processing hub that is farther away from the source point. Therefore, higher transportation cost is expected. On the other hand, the saving in transportation cost will no longer be sufficient to compensate the hub investment cost, when more hubs (>5) were built [19]. This may lead to lower net profit, C^{NP}.

However, the decision on hub determination is highly influenced by the fragmentation scale used in Step 1 [18]. Theoretically, smaller fragmentised area will lead to

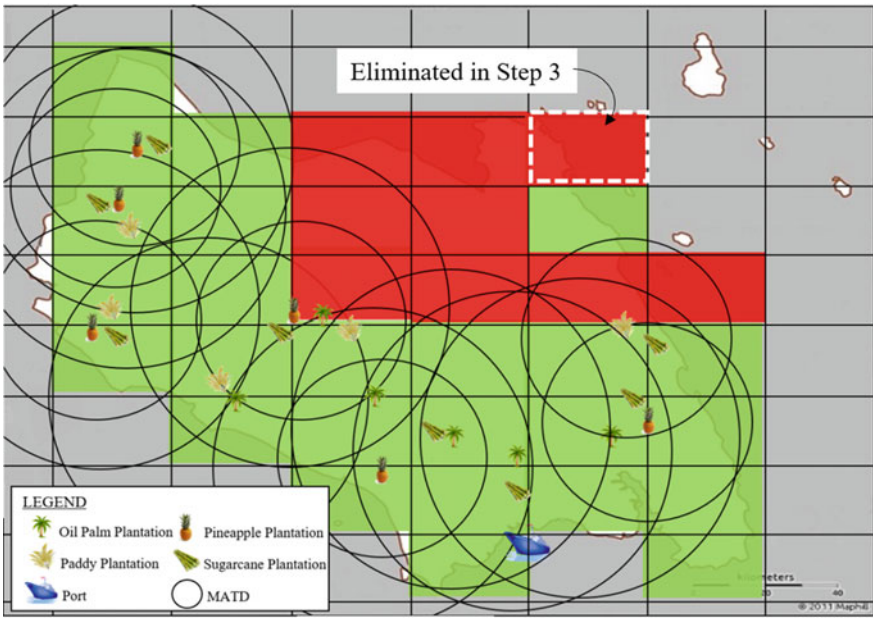

Fig. 7 Superimposed feasible locations [21]

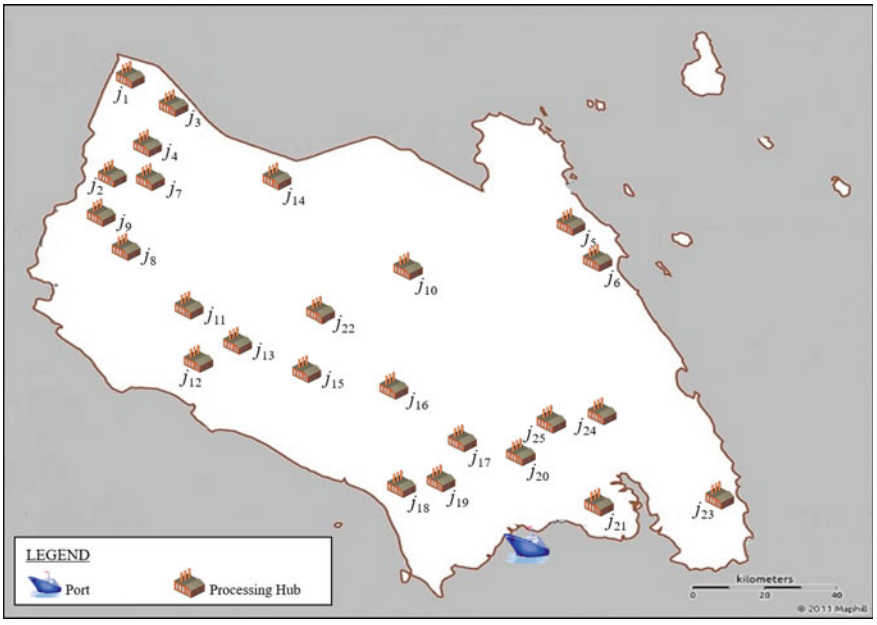

Fig. 8 Geographical location for potential integrated biorefinery plants [19]

Table 1 Computational performance

Case	Non-binary variables	Binary variables	Computational time[a] [s]	C^{NP} [USD/y]
Without four-step procedure	2311	33	0.09	2.00×10^8
With four-step procedure	751	25	0.08	2.00×10^8

[a]Intel Core i7-4720HQ Processor

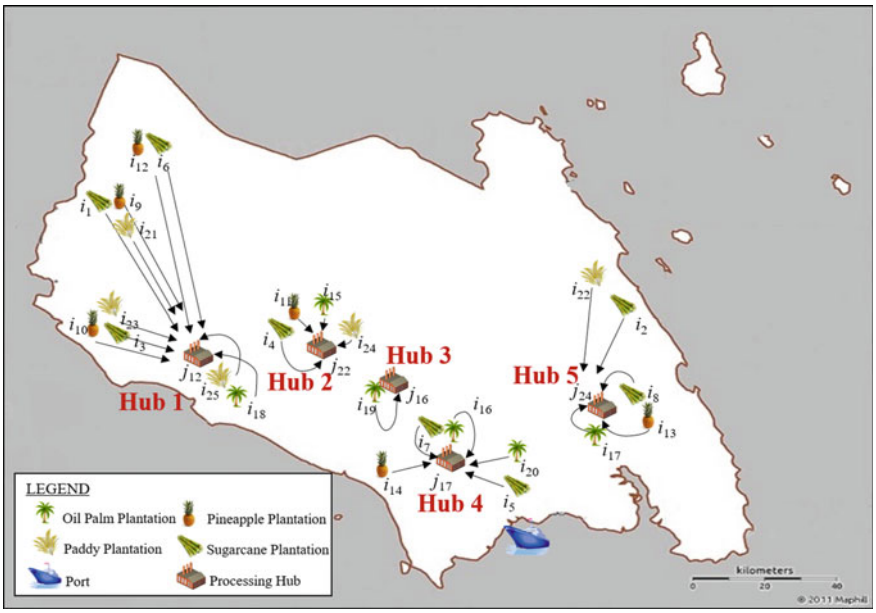

Fig. 9 Optimal biomass allocation design [19]

higher chance of obtaining global optimal in return for greater computational time. A Pareto analysis is conducted to investigate the effect of fragmentised area on annual net profit obtained and the total computational time required. The state of Johor has now been divided into multiple zones via various fragmentised scales (Case A to G) ranging from 100 m^2 (10 m $\times$ 10 m) to 2500 m^2 (50 m $\times$ 50 m) (area of each zone in Fig. 10). As shown in Fig. 11, higher profit is obtained when smaller fragmentised area is used. However, this results in longer computational time. How [18] claimed that 600 km^2 (Case C) is the optimal fragmentised scale for the Johor case. Despite the annual net profit determined under this fragmentised scale is lower as compared to the highest achievable net profit (i.e., USD 2.03×10^8 which is determined from Case A), the error percentage is merely 0.5%. More importantly, the computation time required for Case C is about sixfolds lower compared to Case A. In other words,

Pareto analysis helps decision-makers to determine a compromised solution which ensures the optimality of the result, at the same time, keeping the computational time at minimal.

3 Transportation Decisions

Transportation decision is another key concern in a supply chain problem, as high transportation cost of low-density biomass is a valid hurdle for the biomass industry [22]. However, unnecessary expenses might occur if the transportation cost was determined based on a linearised constant as suggested in Eq. (6). In fact, overestimation of transportation cost (about 15-folds) had occurred for the case study as reported in How et al. [12]. A detailed transportation calculation which considers vehicle capacity constraints in terms of load and volume limits is discussed in this section.

3.1 Vehicle Capacity Constraints Consideration

In detailed calculation, load-capacity limit ($\text{Cap}_m^{\text{Weight}}$) and volume-capacity limit of vehicle m ($\text{Cap}_m^{\text{Volume}}$) are taken into consideration. Due to these constraints, the total amount of materials that can be delivered per vehicle per trip is limited. The required number of trips, $\text{num}_m^{\text{Trip}}$ can be determined using Eqs. (7) and (8) that follow.

$$\text{num}_m^{\text{Trip}} \geq \left\lceil \frac{F_m^{\text{Weight}}}{\text{Cap}_m^{\text{Weight}}} \right\rceil \quad \forall m \in M \tag{7}$$

$$\text{num}_m^{\text{Trip}} \geq \left\lceil \frac{F_m^{\text{Volume}}}{\text{Cap}_m^{\text{Volume}}} \right\rceil \quad \forall m \in M \tag{8}$$

where F_m^{Weight} [t/d] and F_m^{Volume} [m^3/d] refer to the weight-capacity and volume-capacity of materials (biomass r or products p) that are being delivered. Note that $\text{num}_m^{\text{Trip}}$ has to be rounded-up to a positive integer. Decimal number is meaningless as it indicates that the respective vehicle will eventually stop somewhere in between the delivery path, instead of returning to the origin. Note that Eq. (7) is used for weight-limiting materials (WLM) that exceed weight limit (before filling up the available space of vehicle); while Eq. (8) is used for volume-limiting materials (VLM) that exceed the volume limit (before reaching the maximum weight limit).

The detailed estimation of the annualised transportation cost, C^{Tr} [USD/y] is obtained through the summation of operating (OPEX) and capital expenditures (CAPEX) in transportation system [23]. The formulation is given in Eq. (9), where OPEX includes the ongoing operating cost required to deliver the materials to

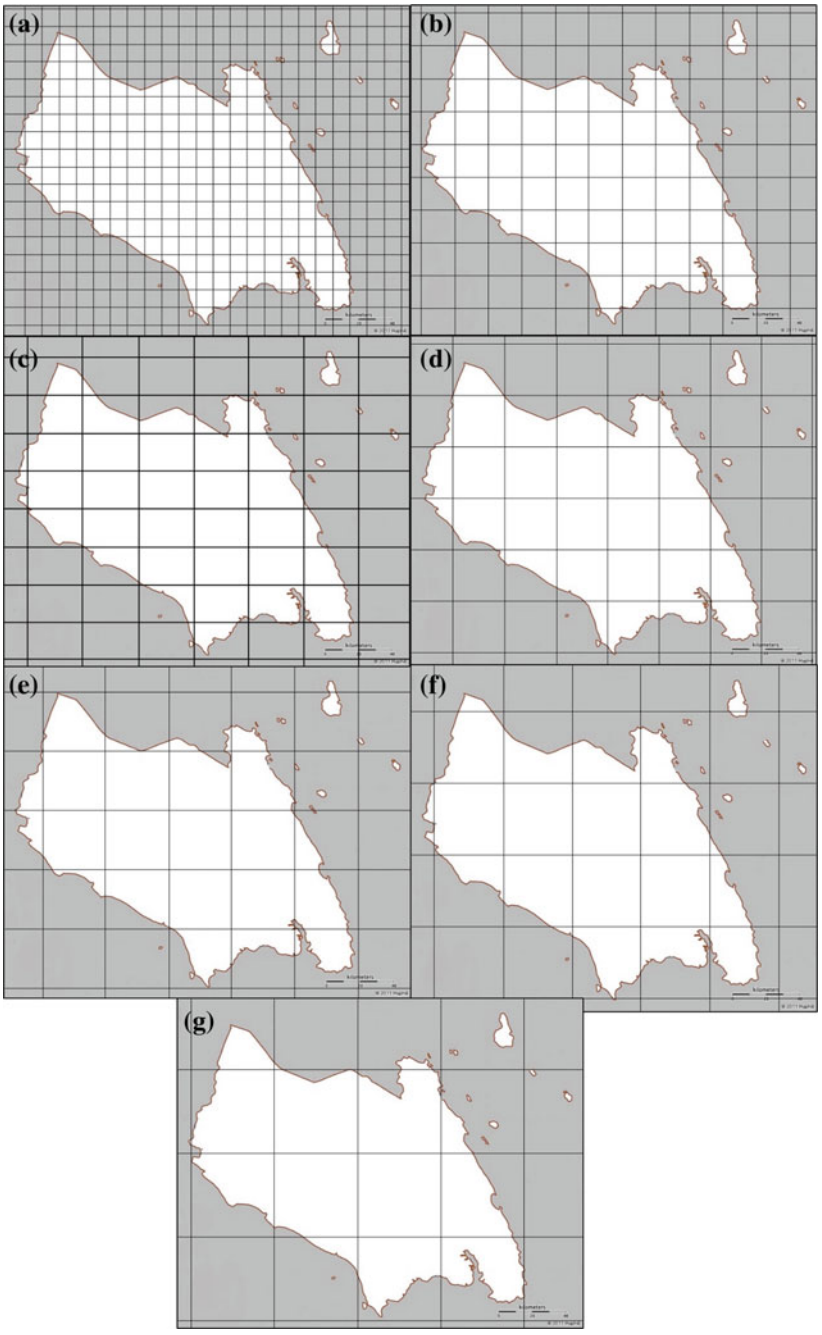

Fig. 10 Area fragmentation: **a** 100 km^2; **b** 300 km^2; **c** 600 km^2; **d** 900 km^2; **e** 1200 km^2: **f** 1600 km^2; **g** 2500 km^2 [18]

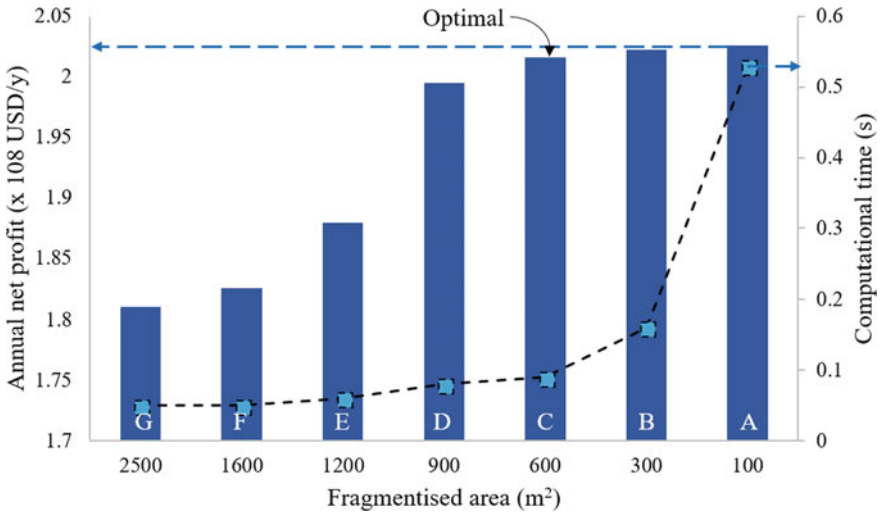

Fig. 11 Pareto analysis for area fragmentation [18]

their destinations, including labour cost (C^{Labour} [USD/d]), fuel consumption cost ($C^{\text{Fuel\_Cons}}$ [USD/d]) and maintenance cost (C^{Maintc} [USD/d]), while CAPEX includes the annualised investment cost for the procurement of vehicles, C^{Proc} [USD/y].

$$C^{\text{Tr}} = (C^{\text{Labour}} + C^{\text{Fuel\_Cons}} + C^{\text{Maintc}}) \times \text{OPD} + C^{\text{Proc}} \tag{9}$$

Note that the three terms in parenthesis on the right side of Eq. (9) correspond to OPEX of the annualised transportation cost. Note also that the labour cost is determined by multiplying the total operating hour, OH [h/d] to the hourly wage, HW [USD/h] of the workers, as given in Eq. (10).

$$C^{\text{Labour}} = \text{HW} \times \text{OH} \times \text{num}_m^{\text{Trip}} \tag{10}$$

Fuel consumption cost, $C^{\text{Fuel\_Cons}}$ in Eq. (9) is determined by multiplying the total distance travelled, D [km] with the fuel consumption rate of the vehicle, $\text{rate}_m^{\text{Fuel}}$ [L/km] and the fuel price, C^{Fuel} [USD/L], as given in Eq. (11):

$$C^{\text{Fuel\_Cons}} = 2C^{\text{Fuel}} \times D \times \text{num}_m^{\text{Trip}} \times \text{rate}_m^{\text{Fuel}} \tag{11}$$

Maintenance cost of the vehicle, C^{Maintc} is estimated using Eq. (12), where C_m^{Repair} [USD/km] refers to the estimated repair and maintenance cost of vehicle per km of the distance travelled.

$$C^{\text{Maintc}} = 2 \times D \times \text{num}_m^{\text{Trip}} \times C_m^{\text{Repair}} \tag{12}$$

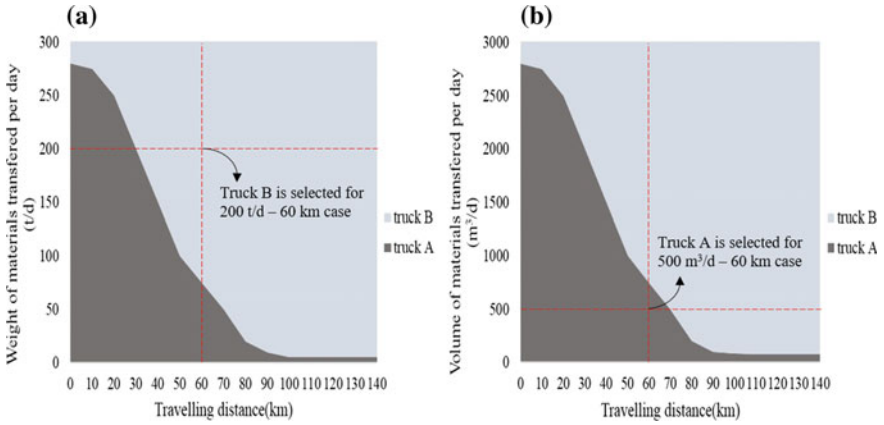

Fig. 12 Example of SVS diagrams: **a** SVS-WEL diagram; **b** SVS-VOL diagram

The procurement cost of vehicles, C^{Proc} is annualised by taking into consideration the estimated life span of the vehicle, LS_m^{Tr} [y]. It can be determined using Eq. (13).

$$C^{\text{Proc}} = \text{num}_m^{\text{Vehicle}} \times \frac{C_m^{\text{Proc}}}{\text{LS}_m^{\text{Tr}}} \tag{13}$$

where $\text{num}_m^{\text{Vehicle}}$ refers to the total number of vehicle required to deliver all the materials; while C_m^{Proc} [USD] refers to the procurement cost of vehicle.

3.2 Graphical Decision-Making Tools

User-friendly decision-making tools are important for decision-makers to put research output into practise. A graphical decision-making tool, called *smart vehicle selection (SVS) diagram* has been proposed in a recent work [12]. The SVS diagram is constructed based on the travelling distance and capacity of materials. Since weight and volume limits of the vehicle are the main concerns for transportation selection, two versions of SVS diagram were developed, i.e. SVS-weight-limiting (SVS-WEL) diagram and SVS-volume-limiting (SVS-VOL) diagram (see Fig. 12).

The SVS diagrams in Fig. 12 share the same x-axis, which refers to the travelling distance between source (start point) and sink (end point). However, y-axis of the SVS-WEL diagram represents the weight-capacity of the material to be transported per day (Fig. 12a); while that of the SVS-VOL diagram refers to the volume-capacity of the material (Fig. 12b). Each (x, y) point in the diagram defines a sub-problem. As shown in Fig. 12, these sub-problems are shaded with different colour. Each colour indicates the optimal transportation mode to be used in that particular sub-problem. The diagrams are constructed based on the optimised results obtained from the mathe-

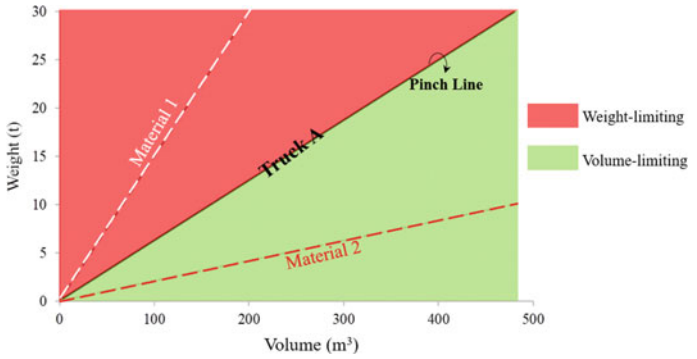

Fig. 13 Weight–volume graph for vehicles and materials

matical model presented in the Sect. 3.1. For instance, in considering weight-capacity, truck B is the best transportation mode to deliver 200 t/d of WLM to customer which is located 60 km from the hub (see Fig. 12a). On the other hand, truck A is more cost-effective to deliver 500 m^3/d of VLM to customer which is 60 km away from the hub, for a volume-limiting case (see Fig. 12b). With the aid of these diagrams, together with the required information (i.e., transportation distance and the total amount of material flow), users can determine the optimal transportation mode directly without re-running the mathematical model.

WLM refers to materials that exceed the weight limit before filling up all the available space of the vehicle. Likewise, VLM refers to materials which exceed the volume limit before the maximum load limit is reached. Hence, SVS-WEL and SVS-VOL diagrams should be used for WLM and VLM, respectively. In order to identify which category that the materials belong to, the weight–volume graph in Fig. 13 may be used. It shows the weight–volume line for the vehicle (solid line) and the transported materials (dotted line). The gradient indicates its bulk density (ρ_m [t/m^3]), which is defined by Eq. (14):

$$\rho_m = \frac{\text{Cap}_m^{\text{Weight}}}{\text{Cap}_m^{\text{Volume}}} \quad \forall m \in M \tag{14}$$

If the material has larger bulk density as compared to the bulk density of vehicle (gradient $\geq \rho_m$), it is considered as WLM (e.g. material 1 in Fig. 13). Otherwise, it is considered as VLM (e.g. material 2 in Fig. 13). In other words, the bulk density of vehicle capacity is noted as the pinch line. If the weight–volume line for the transported material is to the left of the pinch line, it is a weight-limiting problem; otherwise it is a volume-limiting problem. In some cases, the same transported material can be WLM and VLM for two different vehicles respectively, as its bulk density is greater than the bulk density of one vehicle and lower than the other. These cases are considered as dual limiting problems. In order to address this issue, special adjustment has to be made. For instance, material 1 is WLM for truck A, but as VLM

for truck B. Thus, in this model, Eq. (7) is used to determine C^{Tr} [t/y] for truck A, while Eq. (8) is used to determine C^{Tr} [t/y] for truck B.

3.3 Example (Revisited)

This section aims to conduct a comparative study on transportation cost estimation via two different methods, i.e. linearised cost and detailed calculation. The same example shown in Sect. 2.5 is used for demonstration. In previous example (Sect. 2.5), Eq. (6) is used to estimate the annual transportation cost required in the biomass supply chain. As reported in Lam et al. [24], the linearised cost constant, C^{T} can be assumed as 0.2 [USD/t/km] in Malaysian context. In this section, the transportation cost is re-calculated using the thorough mathematical model in Sect. 3.1. The results are illustrated in Fig. 14, in which the transportation cost for different number of processing hubs is presented. Fundamentally, it shows that the transportation cost determined using linearised cost is much higher than that determined through detailed calculation. This is not surprising as C^{T} is not capable in representing the realistic of case study. For instance, in real life, it costs about the same to deliver 0.5 or 5 t of WLM to the same location with the same transportation mode. However, if linearised cost constant were used, the cost required to deliver 5 t of WLM will become ten times higher than that required to deliver 0.5 t of WLM [12]. With inaccurate cost estimation, the optimality of the solution is no longer guaranteed.

Figure 15 shows the annual net profit that can be obtained with different number of hubs. The results obtained from both methods show a similar convex curve pattern. In other words, the net profit will increase with the number of hubs initially, but will decrease after it reached a maximum point. Note that at this maximum point, the corresponding x-axis indicates the optimal number of processing hubs. From Fig. 15, it is shown that the optimal number of hubs for both methods (i.e. linearised cost and detailed calculation methods) is clearly different (five and three processing hubs, respectively). This indicates that the linearised cost method has failed to provide accurate results. In fact, with all these inaccurate results, decision-makers could be misled, and thus making wrong decisions which further lead to unnecessary financial loss.

Apart from the comparative study, this section also aims to highlight the development of SVS diagrams. To date, the application of the SVS diagrams had been reported in a Malaysian case study [12]. Four common trucks in Malaysia had been considered in their work [12]. Table 2 summarised the dimension of each truck, while the developed SVS diagrams are presented as Figs. 16 and 17.

Furthermore, the SVS diagram can be upgraded to a *cost-profile diagram* by adding a third axis (i.e. transportation cost; see Figs. 18 and 19) [18]. Similar to the SVS diagrams, Figs. 18 and 19 are also derived from the optimised results determined from the mathematical model (see Sect. 3.1). These diagrams present the transportation cost required for a given set of information (defined by amount of material to be delivered and the travelling distance). The relationship between the

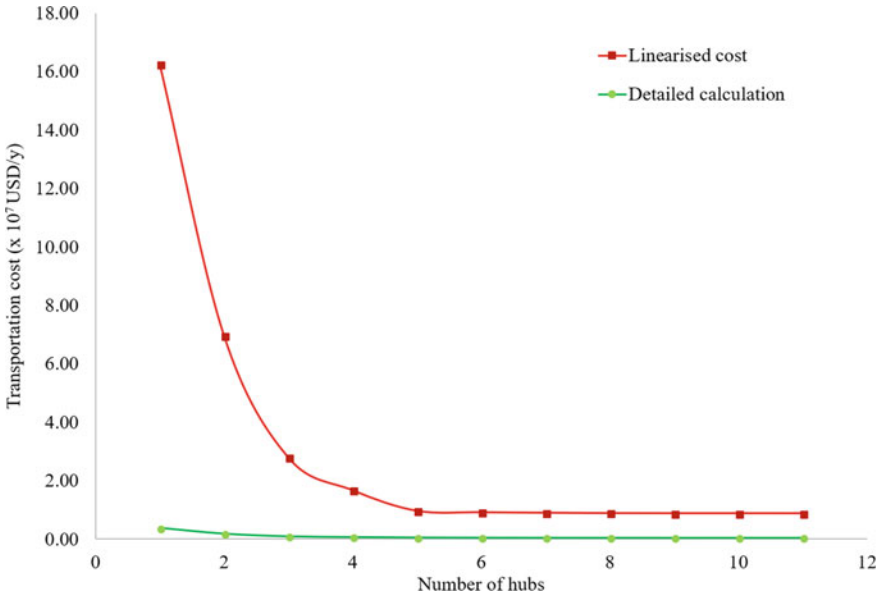

Fig. 14 Estimated transportation cost of case study [12]

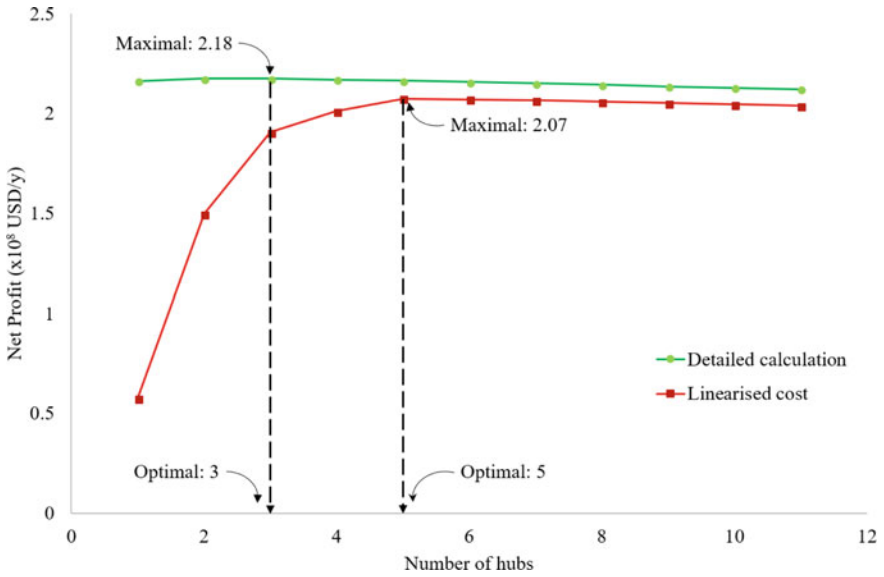

Fig. 15 Estimated net profit of case study [12]

transportation cost, travelling distance, and delivered amount is visualised in these diagrams. With the aid of these diagrams, decision-makers from different stages can

Table 2 Dimension of each transportation mode and its weight limit [12]

Mode	Length (m)	Width (m)	Height (m)	Weight limit (t)
m_1	5.02	2.13	2.13	5.00
m_2	6.00	2.40	2.13	10.00
m_3	12.00	2.40	1.50	20.00
m_4	13.62	2.48	2.70	32.00

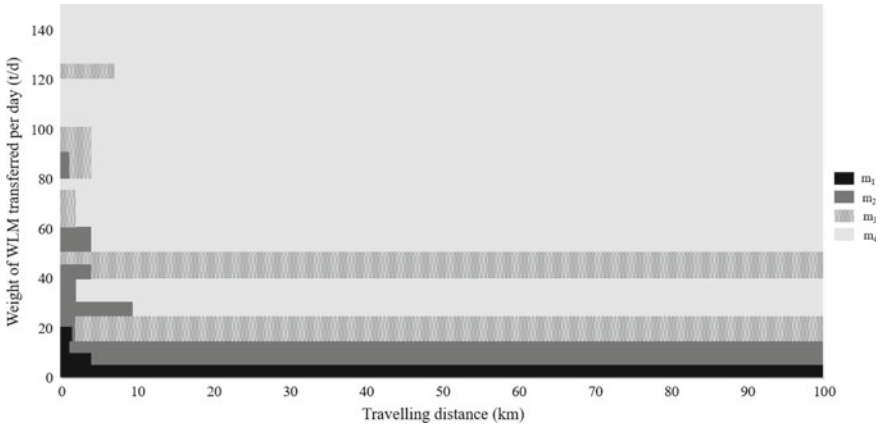

Fig. 16 SVS-WEL diagram developed from How et al. [12]

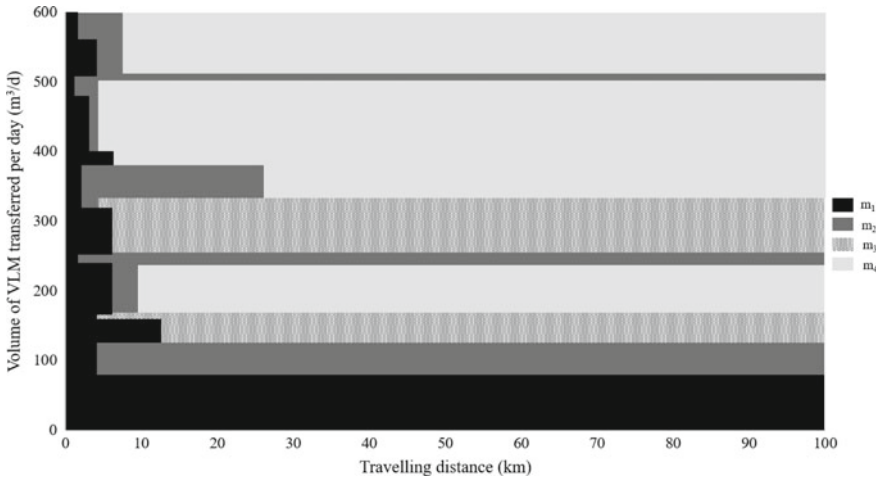

Fig. 17 SVS-VOL diagram developed from How et al. [12]

analyse the economic viability of the transportation problem easily. For instance, these diagrams can help decision-makers to select the most suitable logistics company (minimal and reasonable logistics cost) for their specific cases. To illustrate,

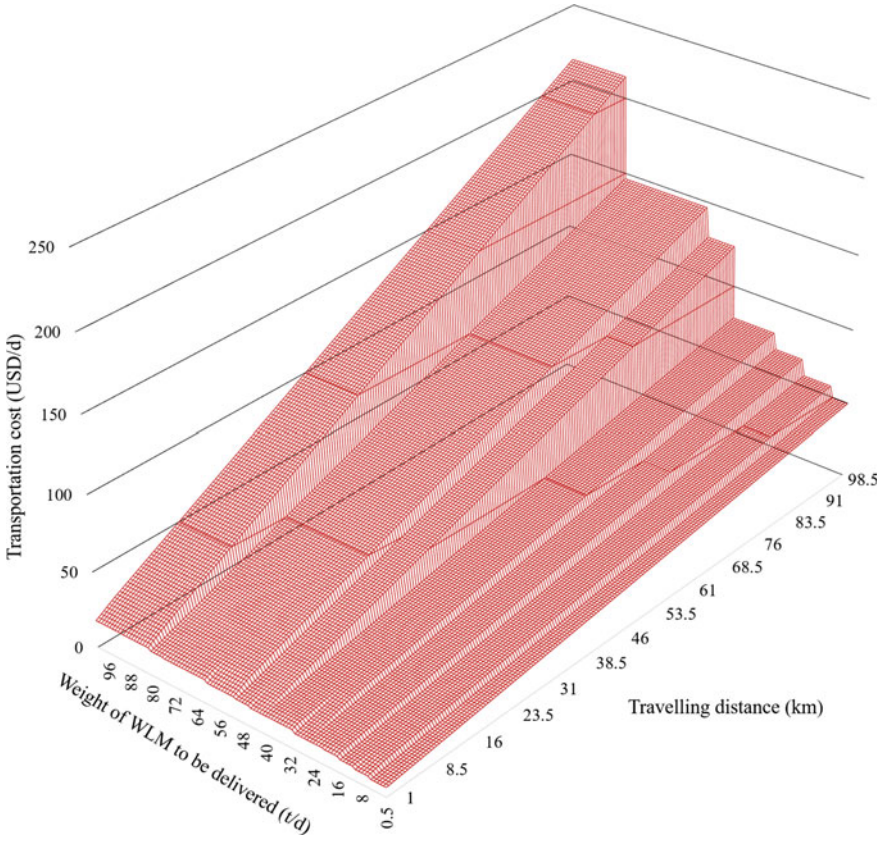

Fig. 18 Cost-profile for SVS-WEL diagram

assuming 100 m^3 of VLM should be delivered to a location which is located 20 km apart. By using Fig. 19, it is found that the estimated logistics cost is around USD 50.00/d. Thus, decision-makers can now evaluate whether the quotation given by the logistic companies are reasonable. All the developed graphical tools are no doubt useful for decision-makers, especially for those who do not acquire strong modelling and mathematics background.

4 Sustainability Evaluation and Optimisation

Biomass supply chain optimisation is essential to determine the best biomass conversion pathway that achieves the goals set by the decision-makers. This section shows an overview of the various optimisation approaches used in supply chain modelling. In addition, a graphical representation method, called *sustainability vector* is intro-

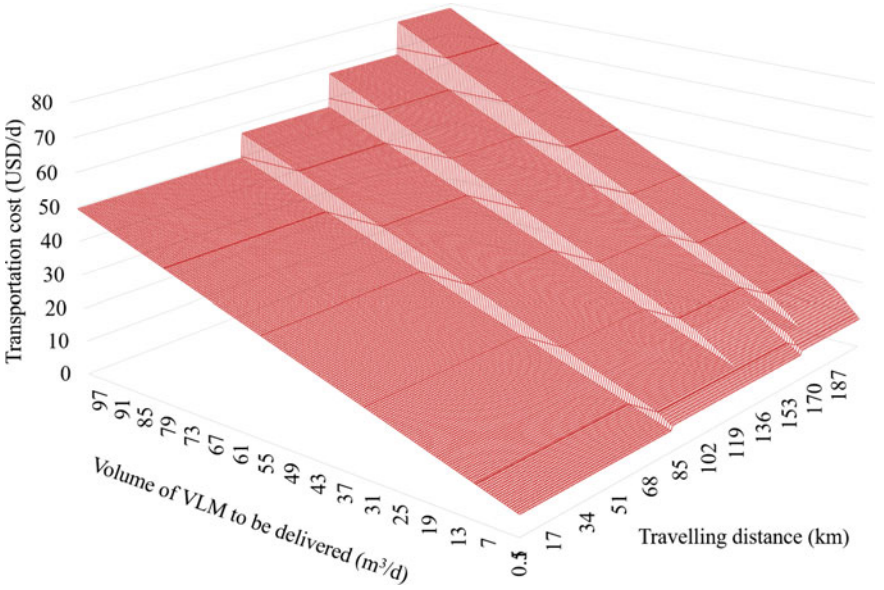

Fig. 19 Cost-profile for SVS-VOL diagram

duced in this section. This method helps decision-makers to visualise, study, and understand the tendency of the system toward each of the sustainability dimension [25].

4.1 Optimisation Consideration

Traditionally, the design of biomass supply chain focuses on single-objective optimisation, i.e. maximising the revenue. However, several industries (e.g. power sectors [26], manufacturing industry [27], etc.) have shifted their conventional business model to become more sustainable in terms of economic, environmental and social dimensions. This is mainly driven by the raising concerns on sustainability development as well as the snowballing global pressure to reduce carbon emission [28]. Therefore, to date, leading researchers have put significant effort in incorporating sustainability indexes into the optimisation model for palm biomass supply chain (see Fig. 20). Table 3 shows a list of indexes given in Fig. 20, which can be used to evaluate the respective sustainability dimension of a palm biomass supply chain.

Table 3 List of key indexes that can be used to evaluate the sustainability performance of a biomass supply chain

Economic dimension	
Indicator/Index	Description
Gross profit	Gross profit refers to the profit made after deducting the costs associated with making and selling its products. It is widely used to reflect the core profitability of a company and illustrate the financial successfulness of a given product or service
Net present value (NPV)	NPV reflects the present value of cash inflow and cash outflow, which considers the monetary inflation rate over the operational lifespan [24]
Benefit–cost ratio (BCR)	BCR identifies the relationship between cost and benefits of a proposed project. It can be determined by dividing the present value of benefit by the present value of cost. The proposed project should be rejected if BCR is less than 1 [29]
Payback period	Payback period refers to the time required to recover the total investment cost, or to reach the break-even point. It can be determined by dividing the annualised capital expenditure (CAPEX) by the gross profit [30]
Return on investment (ROI)	ROI evaluates the efficiency and effectiveness of an investment [31]. It is measured by dividing the net outcome of an investment (can be negative) by the investment cost. The result is expressed as a percentage
Environmental Dimension	
Environmental footprints	
Carbon footprint (CF)	CF represents the land area for plantation required to absorb the CO_2 (or other greenhouse gases) emitted which will lead to climate change and global warming in the life cycle of product or process [32]
Water footprint (WF)	WF measures the total volume of fresh water used and/or polluted water generation per unit of time of the process [33]
Energy footprint (ENF)	ENF concerns on the area of forestation required to compensate the total amount of CO_2 emission originating from energy consumption [34]
Land footprint (LF)	LF concerns on the land demand, i.e. the total land area that are directly and indirectly required to satisfy the consumption [35]
Potential environmental impact	

(continued)

Table 3 (continued)

Global warming potential (GWP)	GWP represents the potential change in climate due to the increased concentration of greenhouse gases (GHG), such as CO_2, CH_4, etc. [36]
Ozone depletion potential (ODP)	ODP measures the potential damage in the protective ozone layer, which is caused by the ozone depleting substances [36]
Photochemical ozone creation potential (POCP)	POCP represents the potential in forming ground-level ozone or photochemical smog due to the increased concentration of volatile organic compounds (VOCs) and nitrogen oxides (NO_x) [37]
Acidification potential (AP)	AP measures the acidifying potential of some chemicals (e.g. NO_x, SO_x, etc.), i.e., forming acidifying hydrogen ion (H^+) [38]
Nutrification potential (NP)	NP represents the potentials of eutrophicating substances (i.e. N, NO_x, NH_4^+, PO_4^+, P) and chemical oxygen demand (COD) in causing over-fertilisation of water and soil which can result in increased growth of biomass
Abiotic depletion potential (ADP)	ADP represents the depletion of abiotic raw material (non-renewable resources) [39]
Toxicity potential (Aquatic/Terrestrial)	These indexes show the maximum tolerance of concentration/amount of toxic substances in water by aquatic organisms and in soil by terrestrial plants [40]
Social dimension	
Human toxicity potential	Human toxicity potential by ingestion (HTPI) and human toxicity potential by either inhalation or dermal exposure (HTPE) are used to evaluate health performance of a given supply chain [36]
Inherent safety index (ISI)	ISI describes both chemical aspects of inherent safety (e.g. flammability, explosiveness, etc.) and other process related aspects (e.g. pressure, temperature, etc.) [41]
Workplace footprint (WPFP)	WPFP measures the work-related casualties in a given supply chain (i.e. statistical fatality rate per unit of activity) [42]
Philanthropic responsibility	Involving in philanthropic activities (e.g. charity, renovation of school, etc.) might be beneficial to the company [28]

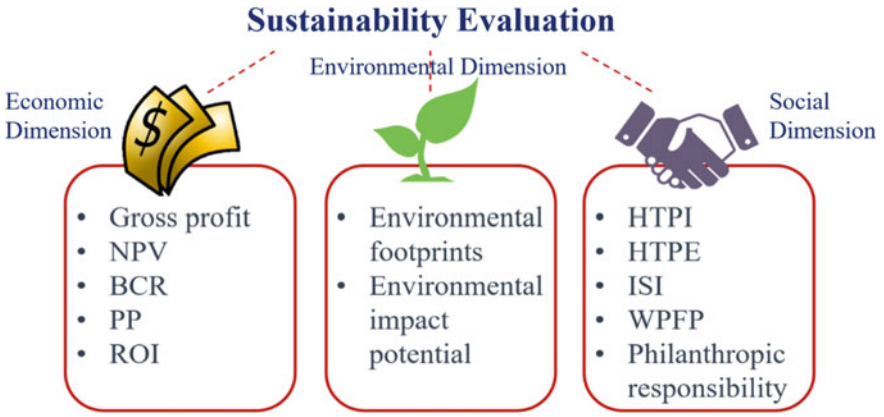

Fig. 20 Key indexes and indicators for sustainability evaluation [18]

4.2 Multi-objective Optimisation Techniques

It is a rarely existing single solution that simultaneously satisfied all objectives. Therefore, achieving optimum for one objective requires compromise of other objectives. In order to determine a compromise solution for this multiple-goal decision in supply chain design, various optimisation techniques have to be implemented. In this subsection, three optimisation approaches, i.e. *genetic algorithm*, *weighted-sum approach*, *max-min aggregation approach* that are widely being used nowadays are introduced.

Genetic algorithm (GA) is a heuristic algorithm that is designed to solve optimisation problems based on the inspiration of natural biology selection (selection of fittest individuals from a population) [43]. As shown in Fig. 21, there are five phases incorporated in a GA model (including 'Initial Population', 'Fitness function', 'Selection', 'Crossover' and 'Mutation'). The algorithm will terminate when the population has converged (i.e. does not produce new solution which are significantly different from the previous solutions). Then, it is said that the GA has provided a set of solutions to our problem. Although GA shows its capability in solving complex operational management problems, this technique does not guarantee a global optimum solution [44].

Weighted-sum approach is one of the simplest techniques to solve multi-objective optimisation problems. It allows the transformation of a set of objectives into a single-objective problem by assigning a preferred priority scale (i.e. weightage) to each objective. These values can be determined using *analytical hierarchy process* (AHP), a powerful multi-criteria decision-making method developed by Saaty [45]. Generally, the objective function is set to maximise the sustainability performance, SP of the synthesised supply chain, as given in Eq. (15).

$$\max \mathrm{SP} = \sum_{d} (w_d \times \lambda_d) \tag{15}$$

```
START
Generate the initial population
Compute fitness
REPEAT
    Selection
    Crossover
    Mutation
    Compute fitness
UNTIL population has converged
STOP
```

Fig. 21 Pseudocode of GA

where d denotes the sustainability dimension (i.e. economic, environmental or social); w_d indicates the priority scale assigned to d dimension; while λ_d refers to the normalised performance in terms of dimension d. Note that the solution obtained from this method is highly dependent on the priority scale given.

Max-min aggregation approach (also named as fuzzy optimisation) is another abundantly used optimisation method. This approach ensures that none of the objectives is over-improved while omitting the importance of another objective [46]. By using this approach, the performance of the least satisfied objective, λ is being maximised (see Eq. 16), while keeping it lower than the normalised performance index, λ_d. Note that by using this optimisation method, all sustainability goals are treated equally important.

$$\max \lambda \tag{16}$$

$$\lambda \leq \lambda_d \tag{17}$$

4.3 Graphical Representation

In a recent work, How and Lam [25] developed a graphical representation method, named as *sustainability vector* that can be understood easily by decision-makers from different background. The sustainability vector is defined as Vector (λ_{EC}, λ_{EN}) (EC refers to economic while EN refers to environmental dimension). Any positive attributes (e.g. profit gained, negative carbon footprint) will lead to a positive value in the vector; contrarily, negative value in the vector represents negative attributes (e.g. profit loss, carbon emission). It can be plotted in a quadrant diagram (see Fig. 22).

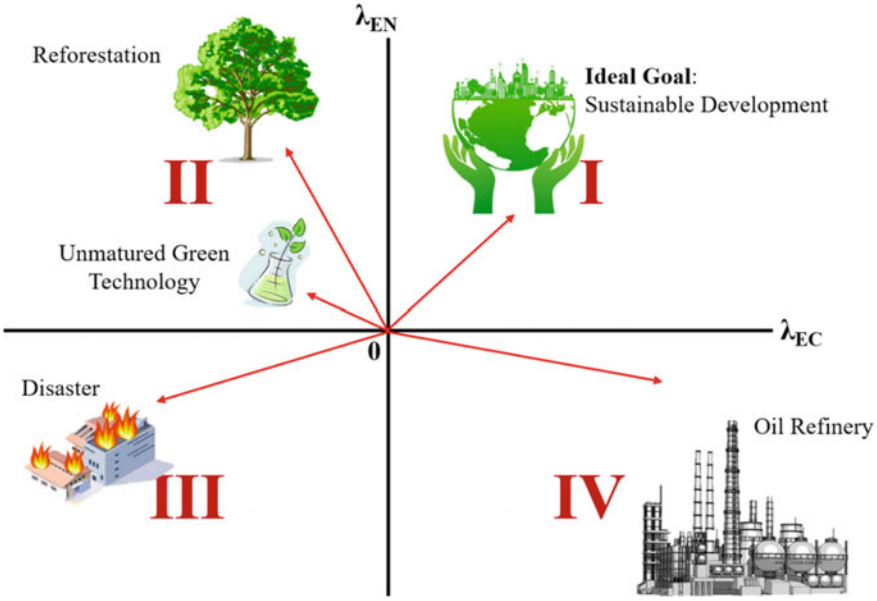

Fig. 22 Quadrant diagram for sustainability vector

As shown in Fig. 22, the conventional practices that are often relied on fossil-based energy are normally plotted on the forth quadrant (positive attribute on economic but negative attribute to environment). On the other hand, the activities that fall in second quadrant are related to some of the noneconomically profitable 'green policies' (e.g. reforestation) that raised by the environmentalists. In addition, the unmatured green technologies which are yet to be economically feasible and other treatment facilities (e.g. wastewater treatment) also fall in this quadrant. The activities that falls on the third quadrant should be avoided since these activities will lead to a negative impact on both economic and environmental objectives. Disasters, such as plant fire and explosion will fall in this quadrant as well. Finally, the ideal goal is to emerge the green technologies into the first quadrant (provide positive attribute to both objectives), in order to enhance the sustainable development.

Sustainability vector can also be expressed in polar form (i.e. Vector(θ, Mag)), where θ is the angle that reveals the tendency of the system toward economic or environmental dimension; while Mag refers to the magnitude of the sustainable vector (determined through Eqs. 18 and 19). They can be used to evaluate the sustainability of each process. In the first quadrant, the process with a smaller θ, indicates that this process has a higher tendency toward economic sustainability. Therefore, decision-makers can select the process path which meets their personal preference in each sustainability dimension based on this θ value. For processes with same or near-range of θ ($\pm 5°$), Mag is used as selection reference as the process with larger Mag indicates that the degree of satisfaction on both economic and environmental

dimensions of this process is relatively higher. Note that for the second quadrant ($90° < \theta < 180°$), smaller θ indicates better performance in environmental dimension (but in tandem with negative economic performance). Similar trend can be found in the third quadrant ($180° < \theta < 270°$), where smaller θ indicates that this process has a higher tendency toward environmental sustainability. On the other hand, the larger θ in the fourth quadrant ($270° < \theta < 360°$) indicates better performance in economic sustainability (but with negative environmental sustainability).

$$\Theta = \tan^{-1} \frac{\lambda_{EN}}{\lambda_{EC}} \tag{18}$$

$$\text{Mag} = \sqrt{\lambda_{EC}^2 + \lambda_{EN}^2} \tag{19}$$

The sustainability vector is easy to read and analyse, since the tendency of the system towards each sustainability dimension is visualised in the quadrant diagram. Keeping this in mind, the sustainability vector can now be used as an effective comparison tool to analyse the sustainability performance of various technologies (including green technologies and conventional technologies). This work can be further extended to consider the social dimension in the sustainability vector development. To achieve this, one additional quadrant diagram (e.g. economic dimension versus social dimension; or environmental dimension versus economic) has to be constructed in order to visualise the tendency of the process towards all three sustainability dimensions.

4.4 Example (Revisited)

The examples demonstrated in the previous sections are merely focusing on economic goal (see Sects. 2.5 and 3.3). Hence, in this section, the developed mathematical model is revised to consider the environmental sustainability of each biomass conversion pathway. In this example, the various indicators (i.e., GWP, ODP, POCP, AP, NP, ADP, toxicity potential, WF and LF) are used to account the environmental risk in biomass supply chain. With all the data collected from How and Lam [47], the optimal pathway for each biomass can be determined through weighted-sum approach (see Eq. 15). Note that the obtained solutions will vary with the priority scale assigned to each sustainability goal [18]. The impact of the priority scale on technology selection is presented in Fig. 23. In Fig. 23, x-axis refers to the priority scale assigned to the economic goal. Take EFB for example, when high w_{EC} is assigned, gasification is the most cost-effective pathway. This is in agreement with the results obtained from Sect. 2.5. If w_{Ec} drops below 20%, biomass combustion which generates electricity has become the better option. The use of bioenergy helps to reduce the reliance on fossil-based energy. With Fig. 23, decision-makers can make decisions based on their own preference.

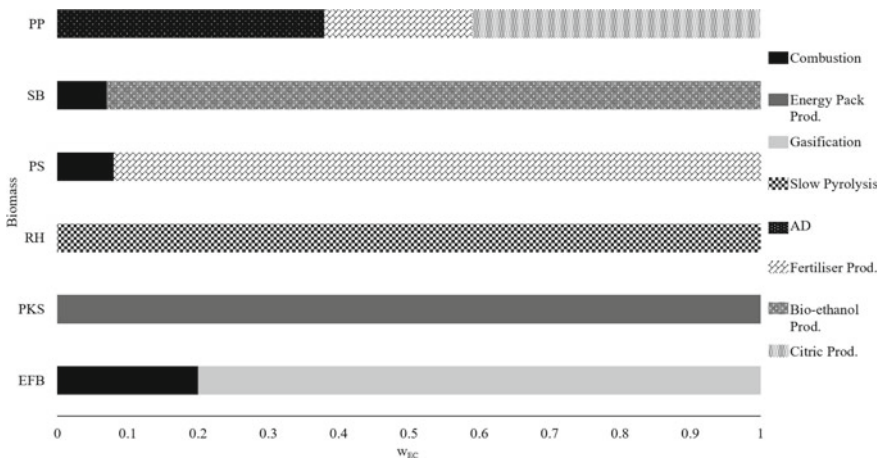

Fig. 23 Technology selection for different priority scales

Aside from this, the sustainability performance of these biomass conversion pathways can be represented in the form of sustainability vector. Recently, How and Lam [25] had reported the sustainability vector of various palm biomass conversion technologies, including combustion, gasification, dry long fibre and energy pack production (see Fig. 24). The results show that energy pack production that falls in the first quadrant is the most preferred processing pathway. Apart from its decent economic value [48], the use of energy pack as an alternative energy fuel will gradually reduce the environment impact [49]. Contrarily, combustion pathway that generates electricity poses a different situation. It falls in the second quadrant which indicates the presence of negative profit. This is mainly due to the unattractive feed-in-tariff rate, unsupportive incentive policy and low boiler efficiency [50].

5 Debottlenecking

The problem of identifying bottlenecks in biomass supply chain and subsequently debottlenecking them is another significant topic of research. This section presents the fundamental concept of *bottleneck* and debottlenecking. Besides, two advanced debottlenecking approaches are introduced in this section.

5.1 Concept

The term 'bottleneck' is defined differently at different phases of supply chain development (see Fig. 25). Most works on debottlenecking focus on the operational-phase

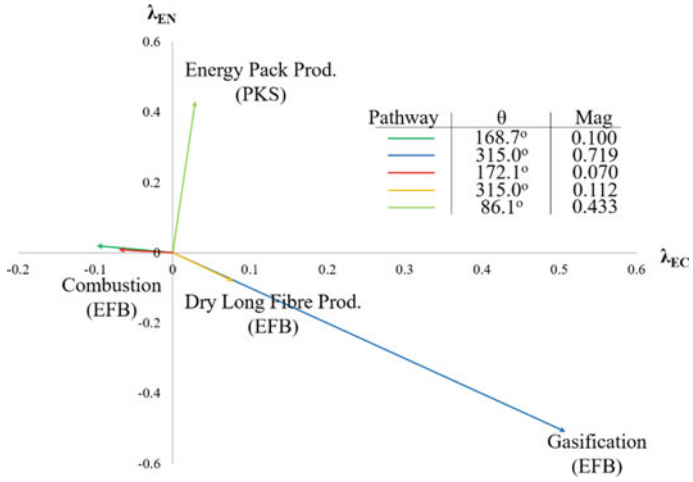

Fig. 24 Sustainability vector of each conversion pathway for palm biomass [25]

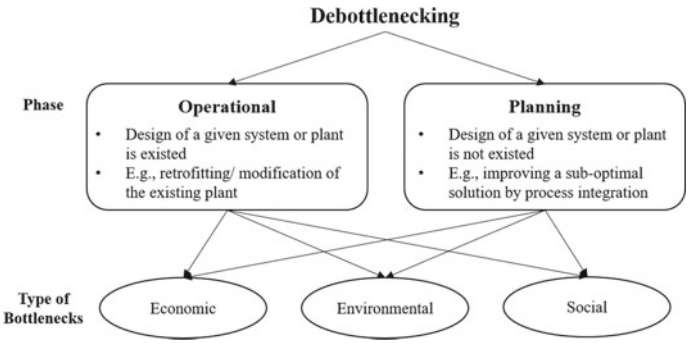

Fig. 25 Debottlenecking classification [52]

of an existing system/plant. Debottlenecking at this phase is defined as a strategy of achieving desired performance of a system/plant (e.g. higher yield, purity or productivity), which is currently incapable of in the current design [51].

On the other hand, How et al. [21] had considered the debottlenecking at planning phase, whose configuration of a system or a plant is yet to be designed. At this phase, debottlenecking refers to the process of revealing root causes that leads to an unpreferable solution, and subsequently revamping it to improve its overall preferability. Debottlenecking at this preliminary stage of design is vital for the better understanding of the potentials embedded in each solution (technology selection, logistics management, operation strategy, etc.), which enables accurate decision-making in selecting appropriate technologies or designs to ensure business sustainability [53]. In addition, the term 'bottleneck' should not merely limit to economic-related barriers (e.g. throughput, makespan, process efficiency), but may be linked

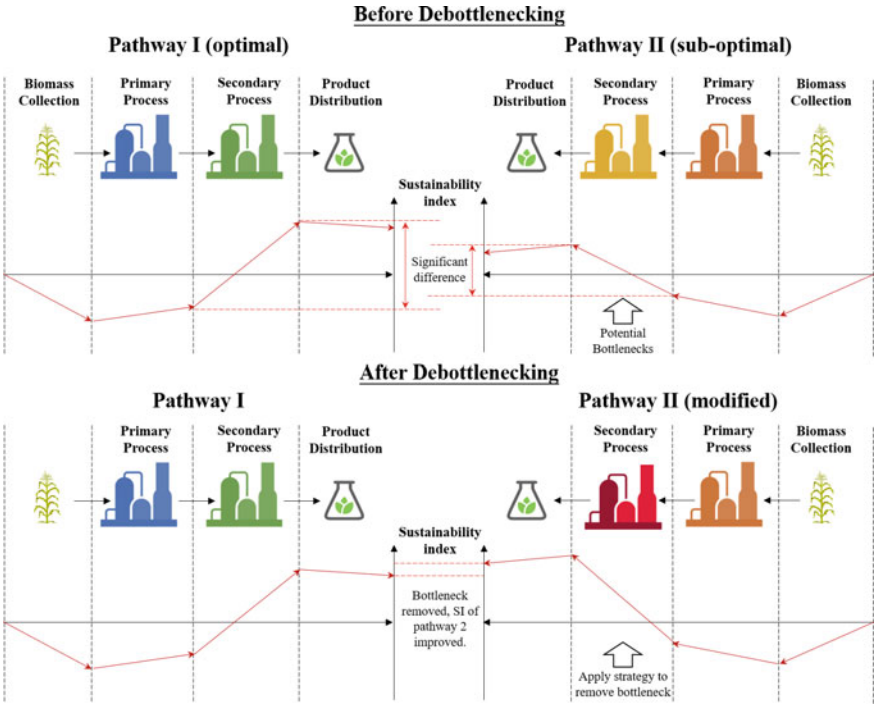

Fig. 26 Conceptual illustration of debottlenecking at planning phase [52]

to other environmental-related (concern on environmental risks, e.g. extensive land requirement, gigantic fuel consumption, etc.) and social-related barriers (restriction on social factors, e.g. exposure to various social risks, lack of domestic support, etc.). Figure 26 shows the conceptual illustration of debottlenecking at planning phase. As shown, there are two available pathways (I and II) which convert a given biomass into a given bio-product. Pathway II is less preferable due to its low sustainability performance for the secondary process. However, the optimality of the suboptimal solution can be improved by removing bottlenecks via implementation of appropriate strategies (e.g. process integration, emission abatement planning, regulatory policy amendment, etc.).

5.2 Debottlenecking Approaches

Two advanced approaches based on *principle component analysis (PCA)* and *Process-graph* (*P-graph)* may be used for biomass supply chain debottlenecking. Their core concepts are briefly described next.

- *PCA-aided approach* [52]

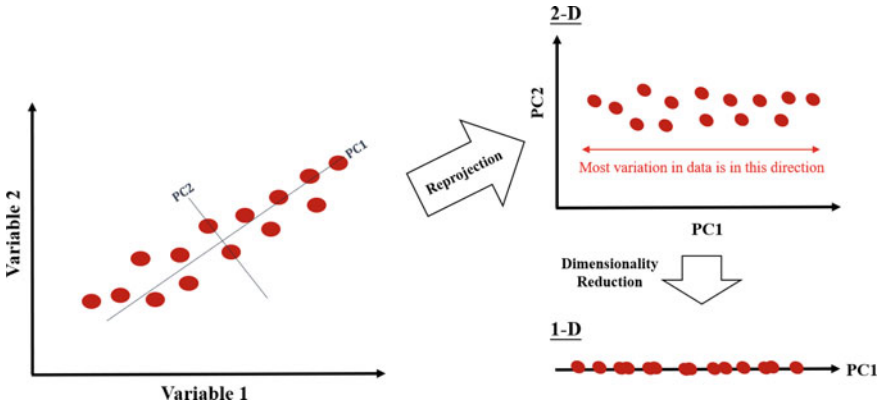

Fig. 27 Dimensionality reduction using PCA [52]

PCA is a multivariate statistical technique that is widely used to reduce the dimensionality of data, by converting a series of correlated variables into a set of uncorrelated variables known as *principal components* (PCs), without losing too much information [54]. Figure 27 illustrates the dimensionality reduction via PCA method [52]. In principle, the original data series (on the right side of Fig. 27) will be re-projected onto two new axes (*PC*1 and *PC*2). From Fig. 27, it is clearly seen that most variations in data are described in the x-axis after reprojection. In other words, the data can still be adequately defined by using only PC1 [55]. The utility of has been burgeoned into diverse scientific fields, including colour industry [56], cybersecurity [57], facial recognition [58], biomass supply chain [52], etc. How and Lam [52] claimed that PCA is an ideal tool in analysing the sustainability performance of biomass supply chain which normally involves numerous variables or parameters. In a recent work, How and Lam [52] proposed a PCA-aided debottlenecking approach for biomass supply chain. Note that in this approach, the generated PCs scores serve as reference indicators for the identification of bottlenecks. The PC that has the largest difference is notified as *critical PC*, while the variables that contribute a substantial portion to the responding critical PC is notified as *critical variables*. Critical variable that contributes the most will be the first variable to be improved. The remaining critical variables will be improved accordingly, based on their contribution rate (from highest to lowest), until the results are satisfied.

- *P-graph-aided approach* [21]
  P-graph is a powerful graph-theoretic and combinatorial algorithm-based framework, which was introduced by Friedler et al. [59]. This framework has several advantageous features, such as (i) capability of providing multiple feasible solutions (optimal and suboptimal) simultaneously [60], (ii) more efficient search of solution space [61] and (iii) visual interface that is easy to understand, learn and apply [62]. To date, P-graph has matured sufficiently for inclusion in modern

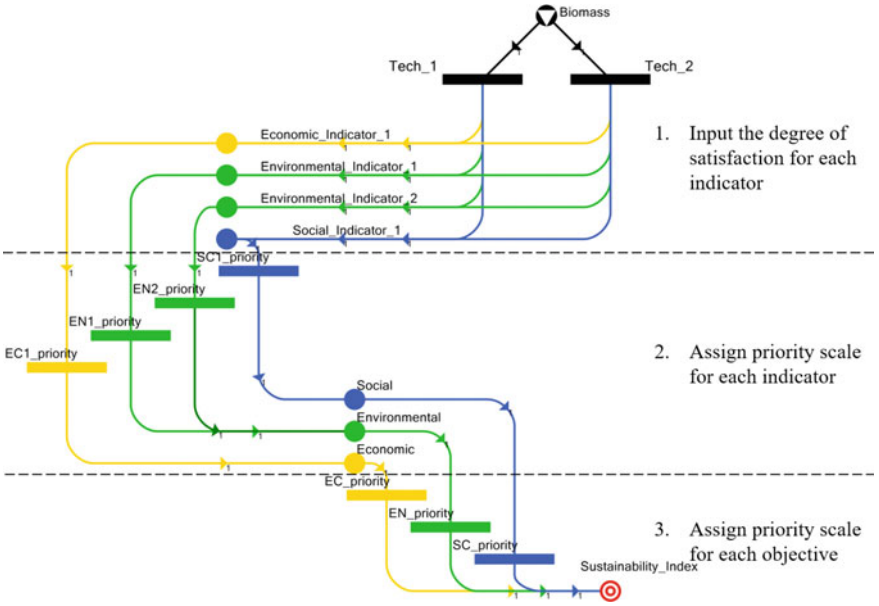

Fig. 28 P-graph model for debottlenecking [52]

textbooks [63], reference books [64] and chemical engineering curriculums [62]. Furthermore, this framework has been applied extensively in various forms of research, e.g. biomass supply chain synthesis [19], carbon management network [65], combined heat and power system [66]. Recently, P-graph is further extended to debottlenecking application [21] (see Fig. 28). The construction of P-graph model can be divided into three subsequent steps, i.e. (i) input of data, (ii) assign priority scale to each indicator in a given sustainability dimension and (iii) assign priority scale to each sustainability goal. As mentioned in Sect. 4.2, all these priority scales can be determined through AHP [21]. In this approach, the bottleneck(s) of the suboptimal solution can be identified by comparing its sustainability performance with the best solution. The sustainability dimension that has the largest difference is notified as the potential bottleneck. Next, the least satisfied indicator under this sustainability should be the first targeted indicator to be improved. The remaining indicators will be improved accordingly (from lowest to highest score), until the suboptimal solution is successfully debottlenecked. It is worth noting that the visual interface of P-graph enables users to structure their case study easily and efficiently without the need of strong mathematical programming background.

Table 4 Sustainability performance before debottlenecking [52]

Pathway	λ_{EC}	λ_{EN}	SP	Rank
Syngas production (gasification)	1.00	0.37	0.68	1
Dry long fibre production	0.46	0.62	0.54	2
Electricity generation (combustion)	0.00	0.68	0.32	3

5.3 Example (Revisited)

The example in Sect. 4.4 is extended to show how the underlying bottlenecks are identified and removed, following the proposed procedure. In order to provide a clear elucidation of this step, this section will only focus on the EFB conversion pathways. As mentioned in Sect. 2.5, there are three conversion pathways which are considered in the examples, i.e. electricity generation, syngas and dry long fibre production. The sustainability performance of each possible pathway is tabulated in Table 4. Similar to the previous example in Sect. 3.3, two sustainability goals (i.e. maximising revenue and minimising environmental impacts) are considered in this section. Assuming that both goals are equally important (i.e., $w_{EC} = 50\%$; $w_{EN} = 50\%$), the ranking of each pathway can be determined using Eq. (15) (i.e. weighted-sum approach). The results show that syngas production is the optimal pathway (highest sustainability performance, SP), followed by dry long fibre production.

Using combustion as an example, by comparing its SP to the optimal pathway, it can be clearly seen that economic dimension is the least satisfied dimension (see Table 4). Literature shows that this economic unfavorability of biomass combustion is often due to the massive and continuous governmental support for the conventional energy source [67]. Therefore, regulatory amendments should be carried out in order to advocate the development of biomass industry. The proposed debottlenecking strategy is listed in Table 5. Policy restructuration such as reduction or elimination of government subsidies for fossil fuels is required so that the bioenergy can become price competitive [50]. Note that the sustainability performance and ranking of each technology after debottlenecking is tabulated in Table 6. It shows that EFB combustion is successfully debottlenecked (from third-ranked to first-ranked). It is worth mentioning that the selection of technology for debottlenecking study is solely based on decision-makers interest. For instance, it can be merely based on research purpose or even based on companies' agenda [52].

Table 5 Debottlenecking strategy [52]

Criteria	Current	Strategy
Feed-in-tariff rate	<10 MW: USD 0.078/kWh 10–20 MW: USD 0.073/kWh 20–30 MW: USD 0.068/kWh	Increase 50%
Government support for fossil energy	Subsidies, incentives and tax reduction	Eliminated

Table 6 Sustainability performance after debottlenecking [52]

Pathway	λ_{EC}	λ_{EN}	SI	Rank
Syngas production (gasification)	0.92	0.37	0.65	2
Dry long fibre production	0.00	0.62	0.31	3
Electricity generation (combustion)	1.00	0.68	0.84	1

6 Conclusion

Biomass supply chain is deemed as a waste-to-wealth business. It connects all entities along the supply chain, starting from upstream biomass sources to the downstream product distribution. Within the chain, integrated biorefinery(s) serves as a crucial node that converts biomass into valuable bioproducts, including biofuels, bioenergy and biochemicals. The economic value of biomass utilisation has been frequently cited in literatures. Nevertheless, the shift to biomass as a feedstock is yet to be proven feasible and sustainable at industry scale. To achieve this, sufficient knowledge and in-depth understanding on biomass supply chain modelling are essentially needed.

This chapter, therefore, provides an overview of the key concerns of biomass supply chain modelling. It serves as a general guide to industry practitioners, academicians and researchers who have interest in learning fundamentals of biomass supply chain modelling and (or) developing sustainable biomass supply chain. Illustrative examples are used to demonstrate how the biomass supply chain problem can be modelled and addressed. On top of that, various state-of-the-art approaches, methodologies and frameworks for biomass supply chain modelling are also introduced in this chapter. All these contents will help readers to understand biomass supply chain modelling from a broader perspective before they decided to venture into this waste-to-wealth business.

Acknowledgements The author would like to acknowledge the financial support from the Ministry of Education (MOE), Malaysia, via LRGS Grant (Program code: LRGS/2013/UKM/PT) and the University of Nottingham Malaysia Campus via Dean Scholarship.

References

1. Department of Statistic Malaysia (2017) Selected agricultural indicators. Department of Statistic Malaysia Official Portal, Malaysia [Online]. Available at: www.dosm.gov.my. Accessed 06 June 2018
2. Bernama (2017) Oil palm acreage reaches 5.77 million hectares—MPOB. Bernama, Kuala Lumpur, Malaysia [Online]. Available at: www.bernama.com. Accessed 21 June 2018
3. Abdullah N, Sulaiman F (2013) The oil palm wastes in Malaysia. In: Modrag DM (ed) Biomass now—sustainable growth and use. InTech, Rijeka, Croatia, pp 75–100
4. Ibeto CN, Ofoefule AU, Agbo KE (2011) A global overview of biomass potentials for bioethanol production: a renewable alternative fuel. Trends Appl Sci Res 6(5):410–425
5. Collard F, Blin J (2014) A review on pyrolysis of biomass constituents: mechanisms and composition of the products obtained from the conversion of cellulose, hemicelluloses and lignin. Renew Sustain Energy Rev 38:594–608
6. Lam HL, How BS, Hong BH (2015) Green supply chain toward sustainable industry development. In: Klemeš JJ (ed) Assessing and measuring environmental impact and sustainability. Elsevier, Oxford, U.K., pp 409–443
7. Iakovou E, Karagiannidis A, Vlachos D, Toka A, Malamakis A (2010) Waste biomass-to-energy supply chain management: a critical synthesis. Waste Manage 30(10):1860–1870
8. Gold S, Seuring S (2011) Supply chain and logistics issues of bio-energy production. J Clean Prod 19(1):32–42
9. Hong BH, How BS, Lam HL (2016) Overview of sustainable biomass supply chain: from concept to modelling. Clean Technol Environ Policy 18(7):2173–2194
10. Ng RTL, Hassim MH, Ng DKS (2013) Process synthesis and optimization of a sustainable integrated biorefinery via fuzzy optimization. AIChE J 59(11):4212–4227
11. Mondal MAH, Kamp LM, Pachova NI (2010) Drivers, barriers, and strategies for implementation of renewable energy technologies in rural areas in Bangladesh—an innovation system analysis. Energy Policy 38:4626–4634
12. How BS, Hong BH, Lam HL, Friedler F (2016) Synthesis of multiple biomass corridor via decomposition approach: a P-graph application. J Clean Prod 130:45–57
13. Kudakasseril Kurian J, Raveendran Nair G, Hussain A, Vijaya Raghavan GS (2013) Feedstocks, logistics and pre-treatment processes for sustainable lignocellulosic biorefineries: a comprehensive review. Renew Sustain Energy Rev 25:205–219
14. Kaviani M (2009) Location-inventory problem. In: Zanjirani FR, Hekmatfar M (eds) Facility location: concepts, models, algorithms and case studies. Physica-Verlag, Heidelberg, Germany
15. How BS, Hong BH, Lam HL, Friedler F (2015) Synthesis of multiple biomass corridor via decomposition approach: a P-graph application. Chem Eng Trans 45:1363–1368
16. Lam HL, Klemeš JJ, Kravanja Z (2011) Model-size reduction techniques for large-scale biomass production and supply networks. Energy 36(8):4599–4608
17. Čuček L, Martin M, Grossmann IE, Kravanja Z (2013) Multi-period synthesis of a biorefinery's supply networks. Comput Aided Chem Eng 32:73–78
18. How BS (2018) Novel sustainable evaluation approach for multi-biomass supply chain. Ph.D. thesis, University of Nottingham, Semenyih, Malaysia
19. How BS, Tan KY, Lam HL (2016) Transportation decision tool for optimisation of integrated biomass flow with vehicle capacity constraints. J Cleaner Prod 136(Part B):197–223
20. Kumar D, Murthy G (2011) Impact of pretreatment and downstream processing technologies on economics and energy in cellulosic ethanol production. Biofuels 4(1):1–19
21. How BS, Yeoh TT, Tan TK, Chong KH, Ganga D, Lam HL (2018) Debottlenecking of sustainability performance for integrated biomass supply chain: P-graph approach. J Clean Prod 193:720–733
22. MiGHT (Malaysia Industry-Government Group for High Technology) (2013) Malaysian biomass industry action plan 2020: driving SMEs towards sustainable future. Selangor, Malaysia

23. Gasol CM, Martínez S, Rigola M, Rieradevall J (2009) Feasibility assessment of popular bioenergy systems in the Southern Europe. Renew Sustain Energy Rev 13(4):801–812
24. Lam HL, Ng WPQ, Ng RTL, Ng EH (2013) Green strategy for sustainable waste-to-energy supply chain. Energy 57:4–16
25. How BS, Lam HL (2017) Integrated palm biomass supply chain toward sustainable management. Chem Prod Process Model 12(4). ISSN (Online) 1934-2659
26. Bhattacharyya SC (2007) Sustainability of power sector reform in India: what does recent experience suggest? J Clean Prod 15(2):235–246
27. Rajala R, Westerlund M, Lampikoski T (2016) Environmental sustainability in industrial manufacturing: re-examining the greening of interface's business model. J Clean Prod 115:52–61
28. Mani V, Gunasekaran A, Papadopoulos T, Hazen B, Dubey R (2016) Supply chain social sustainability for developing nations: evidence from India. Resour Conserv Recycl 111:42–52
29. Kasivisvanathan H, Tan RR, Ng DKS, Abdul Aziz MK, Foo DCY (2014) Heuristic framework for the debottlenecking of a palm oil-based integrated biorefinery. Chem Eng Res Des 92:2071–2082
30. Teo KY, Ng TY, Wau CM, Liew JTS, Andiappan V, Ng DKS (2017) Hybrid optimisation model for the synthesis of centralised utility system in eco-industrial park. Process Integr Optim Sustain 1(1):33–57
31. Deng Y, Parajuli PB (2016) Return of investment and profitability analysis of bio-fuels production using a modeling approach. Inf Process Agric 3(2):92–98
32. De Benedetto L, Klemeš JJ (2009) The environmental performance strategy map: an integrated LCA approach to support the decision making process. J Clean Prod 17:900–906
33. Galli A, Wiedmann T, Ercin E, Knoblauch D, Ewing B, Giljum S (2012) Integrating ecological, carbon and water footprint into a "Footprint Family" of indicators: definition and role in tracking human pressure on the planet. Ecol Ind 16:100–112
34. Palmer AR (1998) Evaluating ecological footprints. Electron Green J 1(9):1–8
35. Giljum S, Lutter S, Bruckner M, Aparcana S (2013) State-of-play of national consumption based indicators: a review and evaluation of available methods and data to calculate footprint-type (consumption based) indicator for materials, water, land and carbon. Sustainable Europe Research Institute, Vienna, Austria
36. Young DM, Cabezas H (1999) Designing sustainable processes with simulation: the waste reduction (WAR) algorithm. Comput Chem Eng 23:1477–1491
37. Altenstedt J, Pleijel K (2000) An alternative approach to photochemical ozone creation potentials applied under European conditions. J Air Waste Manage Assoc 50(6):1023–1036
38. Čuček L, Klemeš JJ, Kravanja Z (2015) Overview of environmental footprints. In: Klemeš JJ (ed) Assessing and measuring environmental impact and sustainability. Elsevier Inc., Oxford, UK, pp 131–193
39. Heijungs R, Guinee JB, Huppes G, Lankreijer RM, Udo de Haes HA, Sleeswijk W (1992) Environmental life cycle assessment of product guide. Centre of Environmental Science, Leiden, Netherland
40. Fan LT, Zhang T (2012) Life cycle assessment. In: Foo DCY, El-Halwagi MM, Tan RR (eds) Advances in process system engineering-vol. 3: recent advances in sustainable process design and optimization. World Scientific Publishing Co. Pte. Ltd., Toh Tuck Link, Singapore, pp 65–78
41. Hurme M, Heikkilä AM (1998) Synthesis of inherently safe chemical processes by using genetic optimisation and case-based reasoning. In: Koikkalainen P, Puuronen S (eds) Human and artificial information processing. Finnish Artificial Intelligence Society, Espoo, Finland, pp 134–143
42. Wan YK, Ng RTL, Ng DKS, Aviso KB, Tan RR (2016) Fuzzy multi-footprint optimisation (FMFO) for synthesis of a sustainable value chain: Malaysian sago industry. J Clean Prod 128:62–76
43. Akanle OM, Zhang D (2008) Agent-based model for optimising supply-chain configurations. Int J Prod Econ 115(2):444–460

44. Moncayo-Martinez L, Zhang D (2011) Multi-objective ant colony optimization: a meta-heuristic approach to supply chain design. J Prod Econ 131(1):407–420
45. Saaty TL (2008) Decision making with the analytic hierarchy process. Int J Serv Sci 1(1):83–98
46. Ng LY, Chemmangattuvalappil NG, Dev VA, Eden MR (2016) Mathematical principles of chemical product design and strategies. In: Martin M, Eden MR, Chemmangattuvalappil NG (eds) Tools for chemical product design. Elsevier, Amsterdam, Netherlands, pp 3–37
47. How BS, Lam HL (2018) Sustainability evaluation for biomass supply chain synthesis: novel principal component analysis (PCA) aided optimisation approach. J Clean Prod 189:941–961
48. Ng WPQ, Lam HL, Yusup S (2014) Waste-to-wealth: energy pack as an integrated biofuel. Chem Eng Trans 39:925–930
49. Čuček L, Varbanov PS, Klemeš JJ, Kravanja Z (2012) Total footprints-based multi-criteria optimisation of regional biomass energy supply chains. Energy 44(1):135–145
50. Ahmad S, Ab Kadir MZA, Shafie Ahmad S (2011) Current perspective of the renewable energy development in Malaysia. Renew Sustain Energy Rev 15(2):897–904
51. Schneider EF (1997) Debottlenecking options and optimisation. Stratus Engineering Inc, Houston, Texas
52. How BS, Lam HL (2018) PCA method for debottlenecking of sustainability performance in integrated biomass supply chain. Process Integr Optim Sustain. https://doi.org/10.1007/s41660-018-0036-3
53. Foo DCY (2017) Extended graphical technique for the evaluation of carbon dioxide emission reduction projects. Process Integr Optim Sustain 1(4):269–274
54. Aitchison J (1983) Principal component analysis of compositional data. Biometrika 70(1):57–65
55. Flury B (1988) Common principal components and related models. Wiley, New York
56. Tzeng DY, Berns RS (2005) A review of principal component analysis and its applications to color technology. Color Res Appl 30(2):84–98
57. Morita T, Yogo S, Koike M, Hamaguchi T, Jung S, Koshijima I, Hashimoto Y (2013) Detection of cyber-attacks with zone dividing and PCA. Procedia Comput Sci 22:727–736
58. Zhou C, Wang L, Zhang Q, Wei X (2014) Face recognition based on PCA and logistic regression analysis. Optik Int J Light Electron Opt 125(20):5916–5919
59. Friedler F, Tarjan K, Huang YW, Fan LT (1992) Graph-theoretic approach to process synthesis: axioms and theorem. Chem Eng Sci 47:1973–1988
60. Friedler F, Tarjan K, Huang YW, Fan LT (1992) Combinatorial algorithms for process synthesis. Comput Chem Eng 16:313–320
61. Friedler F, Tarjan K, Huang YW, Fan LT (1992) Graph-theoretic approach to process synthesis: polynomial algorithm for maximal structure generation. Comput Chem Eng 17:929–942
62. Lam HL, Tan RR, Aviso KB (2016) Implementation of P-graph modules in undergraduate chemical engineering degree programs: experiences in Malaysia and the Philippines. J Cleaner Prod 136 (Part B):254–265
63. Peters MS, Timmerhaus K, West RE (2003) Plant design and economics for chemical engineers, 5th edn. McGraw-Hill, New York, U.S
64. Klemeš JJ, Friedler F, Bulatov I, Varbanov PS (2011) Sustainability in the process industry: integration and optimization. McGraw-Hill Inc, New York, U.S
65. Tan RR, Aviso KB, Foo DCY (2017) P-graph and monte carlo simulation approach to planning carbon management networks. Comput Chem Eng 106:872–882
66. Ong BHY, Walmsley TG, Atkins MJ, Walmsley MRW (2017) Total site mass, heat and power integration using process integration and process graph. J Clean Prod 167:32–43
67. Foo KY (2015) A vision on the opportunities, policies and coping strategies for the energy development in Malaysia. Renew Sustain Energy Rev 51:1477–1498

Cooperative Game Theory Analysis for Implementing Green Technologies in Palm Oil Milling Processes

Viknesh Andiappan, Denny K. S. Ng and Raymond R. Tan

Abstract Recent developments in the palm oil industry have encouraged mill operators to expand downstream operations. In this regard, mill operators have considered implementing green technology systems such as *biorefineries*. Green technology systems significantly alter the way that an industry operates in order to improve economic performance and sustainability of the plant and can expand the firm's business portfolio. However, there is a challenge in convincing stakeholders to invest in such systems, especially when the technology is still unproven and/or is uncommon. In this chapter, an integrated approach is presented to determine the allocation of incremental profits for green technology systems such as a palm-based biorefinery (PBB) in a palm-based eco-industrial park (PEIP). The integrated approach presented in this chapter consists of cooperative game theory and stability analysis. The results suggest that the optimal allocation of incremental profits is 14% (US$800,000) for the PBB. Subsequent stability analysis determines that the green technology system with the PBB is economically stable for as long as additional investment costs are within the range of 10–30% of the PBB's raw material costs.

Keywords Incremental profits allocation · Eco-industrial park
Green technology systems · Cooperative game theory · Stability analysis

V. Andiappan (✉)
School of Engineering and Physical Sciences, Heriot-Watt University Malaysia, Wilayah Persekutuan Putrajaya, 62200 Putrajaya, Malaysia
e-mail: v.murugappan@hw.ac.uk

D. K. S. Ng
Department of Chemical and Environmental Engineering/Centre of Sustainable Palm Oil Research (CESPOR), The University of Nottingham, Malaysia Campus, Broga Road, 43500 Semenyih, Malaysia

R. R. Tan
Chemical Engineering Department, De La Salle University, 2401 Taft Avenue, 0922 Manila, Philippines

D. C. Y. Foo and M. K. Tun Abdul Aziz (eds.), *Green Technologies for the Oil Palm Industry*, Green Energy and Technology, https://doi.org/10.1007/978-981-13-2236-5_8

Nomenclature

Indices

u Index for technology systems
z Index for coalitions
w Index for coalitions with technology u

Variables

$GP^{OVERALL}$	Total gross profit of all technology systems u in USD/yr
GP_u	Gross profit of technology system u in USD/yr
IP_u	Incremental profits of technology system u in USD/yr
IP_z	Incremental profits of a technology coalition in USD/yr
IP_w	Incremental profits of a coalition without technology u in USD/yr
C_u^{EIP}	Cost of material in technology u from EIP in USD/yr
C_u^{Ext}	Cost of material technology u from external facilities in USD/yr
PA_u	Allocation of incremental profits to technology system u in USD/yr
AI_u	Additional investment cost of technology u in USD
cf_u	Fraction of raw material costs in technology u
DC_u	Distribution coefficient of each technology u
ADC_u	Asymmetric distribution coefficient of each technology u

Parameters

AOT	Annual operating time in h/yr
ADC_u^{max}	Maximum limit for asymmetric distribution coefficient of each technology u
ADC_u^{min}	Minimum limit for asymmetric distribution coefficient of each technology u
PR_u	Product revenue for technology u
RMC_u	Raw material cost for technology u

1 Introduction

The palm oil industry contributes to Malaysia's economy significantly, providing both employment and income from exports. This sector accounts for about 8.7% of Malaysia's gross domestic product [5]. Therefore, palm oil is an important product

that has helped to shape Malaysia's agriculture and economy. Despite its positive contributions, the palm oil industry also contributes to environmental degradation. This is evident as palm oil milling processes generate large quantities of waste, including solid (which are potential by-products), liquid effluent (palm oil mill effluent, POME) and air-borne emission. The solid residues consist of empty fruit bunches (EFBs), palm mesocarp fibers (PMFs) and palm kernel shells (PKSs). The liquid effluents are mainly generated from decanter where wastewater is separated from extracted oil. This direct liquid effluent, combined with the wastes from cooling water and sterilizer, form the POME, which is typically treated in conventional wastewater treatment system (anaerobic, aerobic treatment systems) prior to environmental discharge. During anaerobic digestion, POME is converted into biogas. The latter mainly consists of methane gas and a small quantity of carbon dioxide; which are both greenhouse gases (GHGs). At present practise, biogas is not captured and utilized in many palm oil mills, but is just released into the atmosphere via open ponds which contributes to climate change. Nevertheless, EFB, PMF, PKS and POME contain useful amount of energy which can be utilized to meet energy demands in the mill, or exported to the grid in case of energy surplus. In addition, they can be used to produce renewable biofuels and other valuable bio-products through *biorefineries* [1]. Clearly, these residual palm-based biomasses are currently underutilized. Thus, maximizing energy and material recovery from these biomass residues is desirable for both economic and environmental reasons.

Recent developments suggests that mill operators are open to investments that lead to new products generation in the downstream operations, including biorefineries [2, 12]. Biorefineries may be considered as *green technology* systems that can significantly alter the way that businesses operate and create new business portfolios [2] in the palm oil mill. A green technology system is a technical system, equipment or process that minimizes degradation of the environment and promote the use of renewable resources [9]. In this respect, biorefineries offer alternatives to the mainstream palm oil business within the industry. Green technology systems of this kind are particularly important because they also provide positive implications on palm oil sustainability [20]. Based on such positive implications, several works have assessed the possibility of including biorefineries within a *palm-based eco-industrial park* (PEIP). For instance, Kasivisvanathan et al. [8] proposed an approach to retrofit a palm oil mill into a sustainable biorefinery which fulfils the conflicting objectives of economic performance and environmental impact. Kasivisvanathan et al. [7] then developed a mixed-integer linear programming (MILP) model to determine the optimal process adjustments to address partial inoperability in the biorefinery reported in their earlier work [8]. The MILP model determines the optimal reallocation of process streams and operating levels of the process units in order to maximize profits from the product portfolio. Meanwhile, Ng et al. [14] applied fuzzy optimization to synthesize a sustainable integrated palm oil biorefinery which considers economic, environmental, inherent safety, and inherent occupational health performances. Ng et al. [16] extended the work by presenting a fuzzy programming design approach based on the individual targets of multiple owners in a *palm oil processing complex* (POPC); the latter consists of a cogeneration system, palm oil mill, biorefinery, and

palm oil refinery. This approach was then extended to disjunctive fuzzy programming to determine the optimal pathways based on each plant owner's targets and option to withdraw from the coalition, if any economic target is not satisfied [17]. Andiappan et al. [3] proposed an approach to design a cogeneration system with cooling applications for a palm oil mill operation. In Andiappan et al. [3], a multi-period optimization approach was applied to consider variations in palm-based biomass supply and energy demand. Similarly, Teo et al. [19] presented a hybrid model that combines multi-period optimization and automated targeting to synthesize a centralized utility system for a POPC.

Despite the usefulness of considering green technology systems in palm oil mill, the challenge remains of how to convince stakeholders to invest in them. Stakeholders are often hesitant due to concerns such as low or volatile returns in investment, as well as highly variable investment costs for unproven or immature technologies. As such, this chapter analyzes the potential incremental profits each participating technology systems can obtain when forming a coalition in a PEIP and subsequently evaluate their respective economic stability. In the context of PEIPs, stability refers to the ability of a PEIP to absorb changes in additional investment costs [6, 10, 13]. In a PEIP, each system is prone to deviations in additional investment costs. Additional investment cost is the cost that each system requires to engage in material and energy exchange with other systems in a PEIP. Additional investment costs may include expenditures on transportation, piping, and instrumentation, shipment, labor, conveyor systems, etc. Thus, this chapter adapts the integrated approach developed by Andiappan et al. [4] to rationally allocate incremental profits among participating technology owners in a PEIP, based on their respective contributions [11]. A *stability analysis* method developed by Wang et al. [21] is used to determine the economic stability of systems in a PEIP. Unlike the work presented in Ng et al. [15], this chapter extends the stability analysis method to determine the stability threshold of a PEIP coalition. The stability threshold measures the robustness (i.e., resistance to withdrawal of dissatisfied partners) of the coalition to deviations in key assumptions pertaining to additional investment costs. By determining the optimal allocation of incremental profits and the corresponding stability, the economic viability can be determined.

The rest of the chapter is organized as follows. Section 2 presents a formal problem statement. Section 3 describes the approach adapted and the corresponding mathematical formulation. A PEIP case study is then solved in Sect. 4, followed by its discussion in Sect. 5, before the final conclusions are drawn.

2 Problem Statement

The problem addressed in this chapter is stated as follows: A given set of technologies, each with a respective owners ($u = 1, 2, \ldots, U$) interested in forming a coalition within a PEIP. However, as each technology contributes uniquely to the PEIP, it is not clear as to how much the owner of a given technology is entitled to receive from the

collective incremental profits obtained by the PEIP. As such, the objective of this work is to determine the fair allocation of incremental profits among participating technology systems owners based on their respective contributions toward the PEIP. Following this, the second objective is to investigate the stability threshold of the PEIP coalition in order for the invested green technology systems to remain economically viable.

3 Mathematical Model

The following sub-sections present mathematical formulations on the economic correlations, incremental profits allocation and stability analysis of each technology u in a PEIP.

3.1 Incremental Profit Allocation

In this section, the incremental profits allocation approach is divided into two sequential steps. The first step consists of the determination of the optimal configuration and the corresponding incremental profits for all possible system coalitions in a PEIP. Note that these incremental profits are required as an input for the second step and is obtained from repeated optimizations for each possible coalition. The optimization for a given coalition is performed by maximizing the summation of gross profits for technology owner u, as shown in Eq. 1.

$$\text{Maximise GP}^{\text{OVERALL}} = \sum_{u=1}^{U} \text{GP}_u, \tag{1}$$

where,

$$\text{GP}_u = \text{AOT} \times (\text{PR}_u - \text{RMC}_u) \quad \forall u, \tag{2}$$

where AOT is the annual operating time. Note that GP_u in Eqs. 1 and 2 is determined from the differences between product revenue (PR_u) and raw material cost (RMC_u) of each technology owner u, based on the scenario considered. For instance, if the scenario considers a coalition between two out of three parties, economic transactions between coalition parties are waived or subsidized. This means that RMC_u would be zero, given that the raw material was obtained from the other party within the coalition. Meanwhile, the remaining party that is not part of the coalition would have to pay for resources, given that the resources are obtained from the coalition.

The corresponding incremental profits is calculated based on the amount of savings gained by technology owner u in a PEIP as compared to a stand-alone operating

system that imports material and utilities from external suppliers. As shown in Eq. 3, the incremental profits for technology u (IP_u) is calculated based on the difference in cost of a certain material used by technology owner u from the EIP $\left(C_u^{\mathrm{EIP}}\right)$, compared to cost of importing the same material externally $\left(C_u^{\mathrm{Ext}}\right)$.

$$\mathrm{IP}_u = \mathrm{AOT} \times \left(C_u^{\mathrm{EIP}} - C_u^{\mathrm{Ext}}\right) \quad \forall u \tag{3}$$

The corresponding incremental profits for all possible coalitions are then compiled and used as input data for the second step. The second step uses a *cooperative game theory* model [11] to fairly allocate incremental profits among the cooperative systems of the PEIP, based on their respective contributions. This model is a mathematical programming-based approach proposed as an alternative to well-established concepts such as the Shapley value [18]. In Maali's cooperative game theory model, z is a set of possible coalitions that can be formed among owners u (e.g., $z = 1, 2; 1, 3; 1, U$). Equation 4 is included in the optimization model to determine the weightage (C_u) of incremental profits allocation (PA_u) for technology owner u.

$$\frac{1}{C_u}\mathrm{PA}_u \geq \lambda \quad \forall u \tag{4}$$

The weights are determined based on the incremental contribution of technology owner u in a coalition. As shown in Eq. 5, IP_z represents the incremental profits for a coalition, while IP_{z-u} is the incremental profits of a coalition without technology owner u. Note that IP_z and IP_{z-u} are obtained from the first step described in Eqs. 1–3.

$$C_u = \sum_z \left[\mathrm{IP}_z - \mathrm{IP}_{z-u}\right] \Bigg/ \sum_{u=1}^{U} \mathrm{IP}_u \quad \forall u \tag{5}$$

Equation 6 is included in the model to determine PA_u for each technology owner u. In Eq. 6, PA_u for each technology owner u must be greater than the incremental profits attained individually by each technology owner u (IP_u).

$$\mathrm{PA}_u \geq \mathrm{IP}_u \quad \forall u \tag{6}$$

Equation 7 is included to ensure that the summation of all PA_u is equal to that of IP_u.

$$\sum_{u=1}^{U} \mathrm{PA}_u = \sum_{u=1}^{U} \mathrm{IP}_u \tag{7}$$

The objective function for this model is shown in Eq. 8, where λ is maximized to give the optimum allocation of incremental profits in Eq. 4.

$$\text{Maximize } \lambda \tag{8}$$

Once the optimum allocation is obtained, the stability analysis, which is to be discussed in the next section, is performed to analyze the stability threshold of the PEIP coalition.

3.2 Stability Analysis

The stability analysis is conducted by measuring *incremental investment return* (IIR) to indicate if the incremental profit from the PEIP is sufficient to offset the additional investment cost required. The total additional investment cost ($AI^{OVERALL}$) is determined by the summation of the additional investment cost of participating technology owner u (AI_u) in the PEIP (as shown in Eq. 9).

$$AI^{OVERALL} = \sum_{u=1}^{U} AI_u \tag{9}$$

The total incremental profit ($IP^{OVERALL}$) is then determined by the summation of IP_u of the participating technology owners in the PEIP as shown below.

$$IP^{OVERALL} = \sum_{u=1}^{U} IP_u \tag{10}$$

Following this, the overall distribution coefficient ($DC^{OVERALL}$), which is defined as the ratio of total incremental profits ($IP^{OVERALL}$) to the total additional investment cost ($AI^{OVERALL}$) can be determined, given as in Eq. 11;

$$DC^{OVERALL} = \frac{IP^{OVERALL}}{AI^{OVERALL}} \tag{11}$$

The $DC^{OVERALL}$ functions are used as a basis for symmetrical distribution of incremental profits among technology owners in a PEIP. Ideally, each technology owner u would aim to achieve distributions equal to $DC^{OVERALL}$. This would mean that distribution of incremental profits is in symmetry, whereby each technology owner u can obtain the same allocation, making this an ideally equitable status for technology owner u to strive for. However, in reality, the distributions of incremental profits and additional investment cost of each technology owner u may deviate from $DC^{OVERALL}$. The deviation from ideal status is measured via the *asymmetric distribution coefficient* of each technology owner u (ADC_u) [21], given as in Eq. 12

$$ADC_u = \frac{DC_u}{DC^{OVERALL}} - 1 \quad \forall u, \tag{12}$$

where,

$$DC_u = \frac{PA_u}{AI_u} \quad \forall u, \tag{13}$$

where PA_u is the incremental profit allocated to technology owner u in Maali's cooperative game model. Note that the ADC_u coefficient can be positive, negative, or zero and is highly dependent on the incremental profits associated with the additional investment cost required for the implementation of the PEIP. Based on Eq. 13, a higher ADC_u indicates that higher incremental profit can be obtained, and thus results in higher DC_u for technology owner u, and vice versa. In the event where ADC_u is equal to 0, technology owner u experiences no deviation of the distribution coefficient from the ideal status (when DC_u is equal to $DC^{OVERALL}$). In cases where ADC_u is negative, the incremental profits of technology owner u gained from PEIP is below the ideal status. For cases where $ADC_u = -1$ and $DCu = 0$, technology owner u does not gain any incremental profits from being in the PEIP. In this respect, it would be desirable for ADC_u value to be greater than 1 in order to encourage technology cooperation in the PEIP [21].

To ensure a stable PEIP coalition, ADC_u is bounded within maximum $\left(ADC_u^{max}\right)$ and minimum $\left(ADC_u^{min}\right)$ limits that are predefined by the participating technologies, whereby $ADC_u \in \left(ADC_u^{min}, ADC_u^{max}\right)$. As such, the coalition is considered stable if their respective ADC_u of each technology u is located within the predefined limits. On the other hand, if ADC_u falls out of the given range, the stability of the PEIP will be compromised due to unreasonable distribution of the incremental profits [21]. As mentioned by Wang et al. [21], ADC_u^{min} and ADC_u^{max} might not be the same for all technology owners u, and the limits can be altered based on technologies' requirements or policies.

4 Case Study

The PEIP considered in this case study consists of three technology systems, i.e., palm oil mill (POM), a biomass-based cogeneration system (BCS) [3] and a palm-based biorefinery (PBB). Note that each of these systems has its respective owner, and their AOT are taken as 5000 h/yr. In the proposed PEIP, the POM is taken as an existing facility, while the BCS and PBB are facilities that are to be newly installed in the PEIP. Figure 1 illustrates the possible interactions among these technologies.

As shown in Fig. 1, the POM is fed with fresh fruit bunches (FBBs, from the oil palm plantations) as raw material. POM requires utilities such as low pressure steam (LPS), cooling water, chilled water, and power. These utilities can be purchased from the BCS within the PEIP, or from an external facility; with the associated prices listed in Table 1. Note that POM operation produces crude palm oil (CPO) as the main product and EFB, PMF and PKS as biomass waste. The latter may be sold as feedstock to the BCS and PBB, with selling prices given in Table 2. Note that the BCS and PBB can purchase these biomass residues from external facilities (with

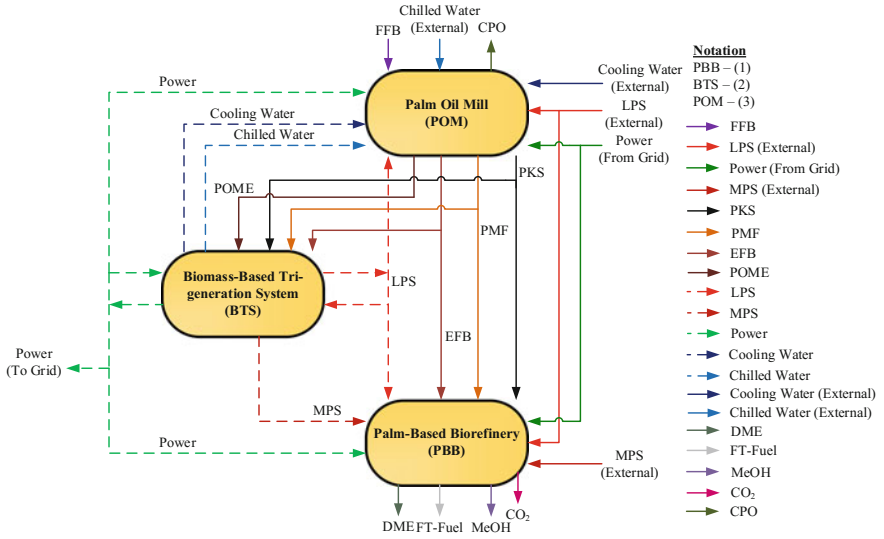

Fig. 1 Initial PEIP configuration for case study

Table 1 Utility prices from BCS and external facility

Utility	BCS (US$)	External (US$)
Low pressure steam (LPS)	0.0184/kg	0.0207/kg
Medium pressure steam (MPS)	0.0460/kg	0.0483/kg
Cooling water	0.000069/kg	0.000092/kg
Chilled water	0.00046/kg	0.00069/kg
Power	0.0667/kWh	0.0897/kWh

prices listed in Table 2). POME produced by the POM can be treated by the POM internally, at cost of 4.48 US$/kg; or outsourced to the BCS (with no charge) to produce biogas for power generation. If EFBs are not utilized by the BCS or PBB, it would be disposed of at the cost of 0.0023 US$/kg. Apart from that, PBB would require utilities such as medium pressure steam (MPS) and power for its operation. These utilities can be purchased from the BCS, or from an external facility at higher prices (see Table 1). The potential end products of PBB are biofuels such as methanol (MeOH), dimethyl-ester (DME), biodiesel and biogasoline. These fuels may be sold to external customer at the given prices (see Table 3).

Table 2 Material prices from POM and external facility

Material	POM (US$/kg)	External (US$/kg)
Crude palm oil (CPO)	0.69	–
Empty fruit bunches (EFBs)	0.0046	0.0069
Palm mesocarp fiber (PMF)	0.0161	0.0184
Palm kernel shell (PKS)	0.0373	0.0414

Table 3 Material prices from PBB

Material	Selling price (US$/kg)
Dimethyl-Ester (DME)	0.474
Biodiesel	0.122
Biogasoline	0.242
Methanol (MeOH)	0.805

Table 4 Different scenarios studied in case study

Scenario	Description of Scenario
1	No coalition within PEIP
2	Coalition between BCS and POM
3	Coalition between PBB and POM
4	Coalition between BCS and PBB
5	Coalition between all three systems

4.1 Incremental Profits Allocation

Following to the proposed approach, the incremental profits of all possible coalitions in the PEIP are computed. These incremental profits are obtained by considering five different scenarios, as shown in Table 4. In Scenario 1, no coalition is to be formed among the three parties in the PEIP. For this scenario, $GP^{OVERALL}$ is maximized and its value is determined as US$43,800,000. The corresponding incremental profits for BCS, PBB and POM are determined as US$400,000, US$200,000 and US$900,000, respectively.

For Scenarios 2–4, coalition is assumed to be formed among technology owners in the PEIP. In Scenario 2, coalition between BCS and POM is first analyzed. For this case, economic transactions between BCS and POM are assumed to be waived by both technology owners. For instance, energy produced by BCS can be supplied to POM at no cost, since both owners of these technologies are in coalition. Similarly, palm-based biomass from the POM can be supplied to the BCS at no fee. As shown in Table 5, $GP^{OVERALL}$ of Scenario 2 is determined as US$43,800,000; while the total incremental profits of the POM and BCS coalition is US$4,100,000. In Scenario 3, coalition is formed between owners of PBB and POM, i.e., economic transactions between these technology owners are subsidized. The $GP^{OVERALL}$ for Scenario 3 is determined as US$43,800,000, while the total incremental profits of the PBB and

Table 5 Distribution of available palm-based biomasses in PEIP

Palm-based biomass	Available from POM (kg/h)	Utilized by BCS (kg/h)	Utilized by PBB (kg/h)
EFB	12375.0	12375.0	0.0
PMF	6875.0	6875.0	0.0
PKS	3437.5	619.8	2817.7
POME	40700.0	40700.0	0.0

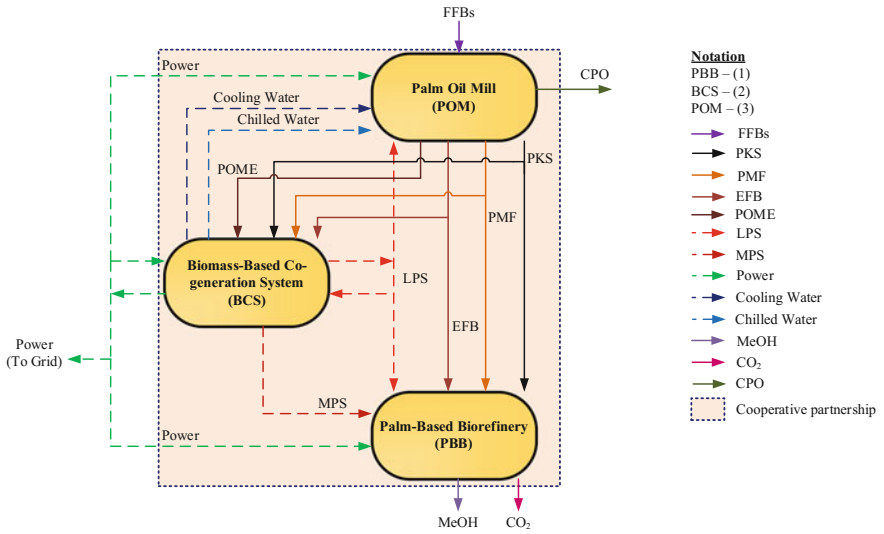

Fig. 2 Optimized PEIP configuration

POM coalition are US$1,600,000. Similar with the previous scenarios, Scenario 4 assumes economic transactions for the BCS and PBB coalition are subsidized. The $GP^{OVERALL}$ of this scenario is determined as US$43,800,000, with the total incremental profit of the BCS and PBB coalition as US$1,200,000. Lastly, Scenario 5 considers a coalition between all three technology owners. In this case, the costs for these three parties are subsidized as they are operating under a single coalition. $GP^{OVERALL}$ is determined as US$43,800,000 and the total incremental profits for all three parties is US$5,400,000. The optimal PEIP configuration (Fig. 2) in Scenario 5 is taken as the final configuration as this is the coalition desired for further analysis.

Table 5 shows the distribution of the available palm-based biomass within the PEIP in Fig. 2. As shown, all EFB, PMF and POME are utilized by the BCS in order to meet the energy demands of the POM and the PBB. Specifically, the EFB and PMF biomasses are sent to the water tube boiler in the BCS to produce steam and generate power via steam turbines (Fig. 3). Besides, POME is processed in an anaerobic digester to yield biogas which is then purified and sent to a gas turbine for power generation. The resulting waste heat from the gas turbine is then recovered

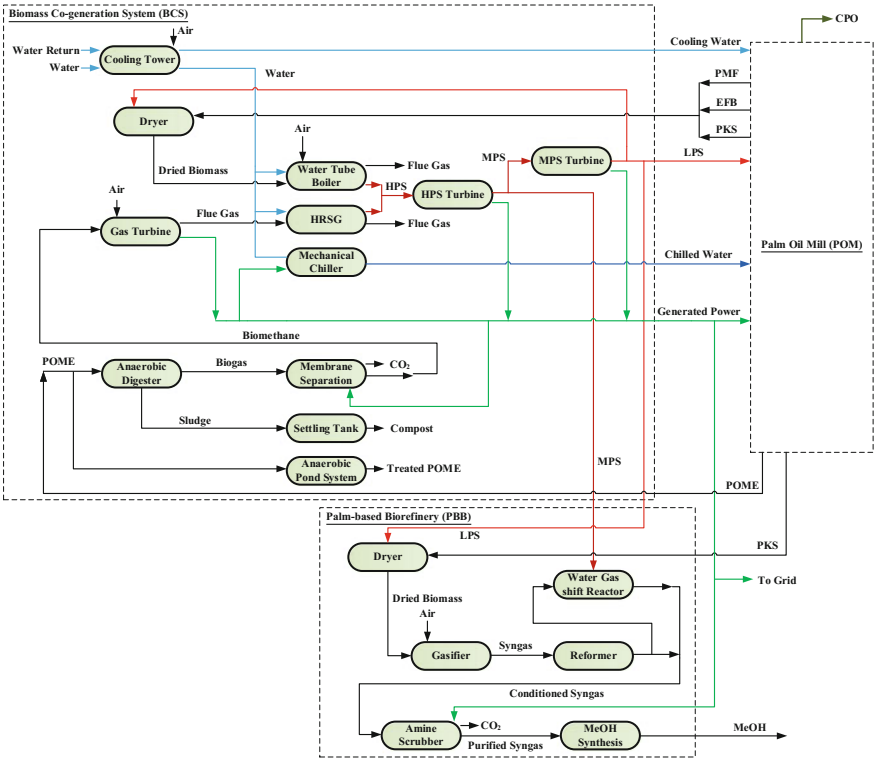

Fig. 3 Detailed configuration of synthesized PEIP

via a heat recovery steam generator (HRSG) to produce additional amount of steam (Fig. 3). A total of 82% of the PKS biomass is distributed to the PBB to produce methanol fuel while the remaining 18% is sent to the BCS for generating steam and power (Table 5).

Following this, the cooperative game model is formulated as shown in Eqs. 14–23. Note that Eqs. 14–16 are formulated based on the generic representation in Eq. 4. Meanwhile, Eqs. 17–19 and 20–22 are formulated according to Eqs. 5 and 6 respectively. Lastly, Eq. 23 is formulated in accordance to Eq. 7. Also, in this case study, the index u of 1, 2, and 3 refer to the owners of BCS, PBB and POM, respectively.

$$\left(1/C_1\right)\mathrm{PA}_1 \geq \lambda \tag{14}$$

$$\left(1/C_2\right)\mathrm{PA}_2 \geq \lambda \tag{15}$$

$$\left(1/C_3\right)\mathrm{PA}_3 \geq \lambda \tag{16}$$

$$C_1 = \left(\mathrm{IP}_{123} - \mathrm{IP}_{23} + \mathrm{IP}_{12} - \mathrm{IP}_2 + \mathrm{IP}_{13} - \mathrm{IP}_3 + \mathrm{IP}_1\right)/\mathrm{IP}_{123} \tag{17}$$

$$C_2 = \left(\mathrm{IP}_{123} - \mathrm{IP}_{13} + \mathrm{IP}_{12} - \mathrm{IP}_1 + \mathrm{IP}_{23} - \mathrm{IP}_3 + \mathrm{IP}_2\right)/\mathrm{IP}_{123} \tag{18}$$

Table 6 Input for Maali's cooperative game model in PEIP case study

IP_z	(10^6 US$/yr)
IP_1	0.40
IP_2	0.20
IP_3	0.90
IP_{13}	4.10
IP_{23}	1.60
IP_{12}	1.20
IP_{123}	5.40

$$C_3 = (IP_{123} - IP_{12} + IP_{13} - IP_1 + IP_{23} - IP_2 + IP_3) \big/ IP_{123} \tag{19}$$

$$PA_1 \geq IP_1 \tag{20}$$

$$PA_2 \geq IP_2 \tag{21}$$

$$PA_3 \geq IP_3 \tag{22}$$

$$PA_1 + PA_2 + PA_3 = IP_{123} \tag{23}$$

In order to solve the formulated model, input values of IP_1, IP_2, IP_3, IP_{13}, IP_{23}, IP_{12}, and IP_{123} must be obtained. These input data are obtained from Scenarios 1–5 considered earlier. As shown in Table 6, the corresponding incremental profits for BCS, PBB, and POM in Scenario 1 are taken as IP_1, IP_2, and IP_3 respectively. The incremental profits in Scenarios 2–5 are taken as IP_{13}, IP_{23}, IP_{12}, and IP_{123} respectively. With these values, the allocation problem is solved by maximizing Eq. 8.

Solving Eq. 8 determines the total incremental profit for the PEIP coalition as US$5,500,000 (Table 7). Of this total incremental profit, the BCS, PBB and POM owners would receive US$2,100,000, US$800,000 and US$2,600,000 respectively. In other words, BCS, PBB, and POM owners have been allocated 38, 14, and 48% of the total incremental profits based on their respective contributions in the PEIP coalition. Based on these allocations, Table 7 indicates that the incremental profits of BCS, PBB and POM have increased by US$1,700,000, US$600,000, and US$1,700,000, respectively. Such increase shows that incremental profit allocated to PBB within the coalition is significantly higher as compared to when they operated in isolation (Scenario 1). This also suggests that the PBB is economically viable to be installed along with BCS and POM.

Besides, the allocations for the BCS in Table 7 shows that investing in power generation systems yields relatively higher incremental profits as compared to the PBB. The latter has the least profit share, due to its limited contribution to the PEIP. Apart from utilizing the biomass produced by the POM, the PBB can increase its incremental profits if a portion of its product portfolio is contributed to the POM and/or BCS. For instance, if some of the methanol produced by PBB is used as a fuel in the BCS, it would mean that the PBB is contributing much more to the coalition than it previously did. Consequently, the PBB would receive much higher

Table 7 Incremental profits comparison of PEIP

	Incremental profits without coalition (10^6 US$/yr)	Incremental profits with coalition (10^6 US$/yr)	Allocation from total (%)	Increase/decrease ($\pm 10^6$ US$/yr)
BCS (1)	0.40	2.10	38	+1.70
PBB (2)	0.20	0.80	14	+0.60
POM (3)	0.90	2.60	48	+1.70
Total	1.50	5.50	100	+4.00

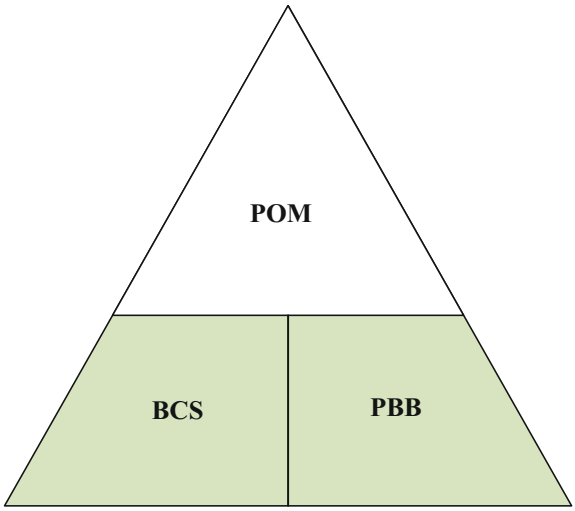

Fig. 4 Decision hierarchy of PEIP case study

incremental profits since it is not only utilizing the biomass from the coalition, but also contributing methanol to the coalition.

In the next section, the allocations shown in Table 7 are then utilized to analyze the stability threshold of the coalition.

4.2 Stability Analysis

For stability analysis, this case study assumes that the additional investment cost of a technology owner u (AI_u) is given as a fraction (cf_u) of the owner's raw material costs (shown in Eq. 24). As such, the stability threshold is determined by investigating the range in which values of cf_u would provide a stable PEIP. Moreover, it is assumed that all technology owners agree that the PEIP is considered stable only when ADC_u of each party is within the range of -0.5 to 0.5. Following this, the stability analysis

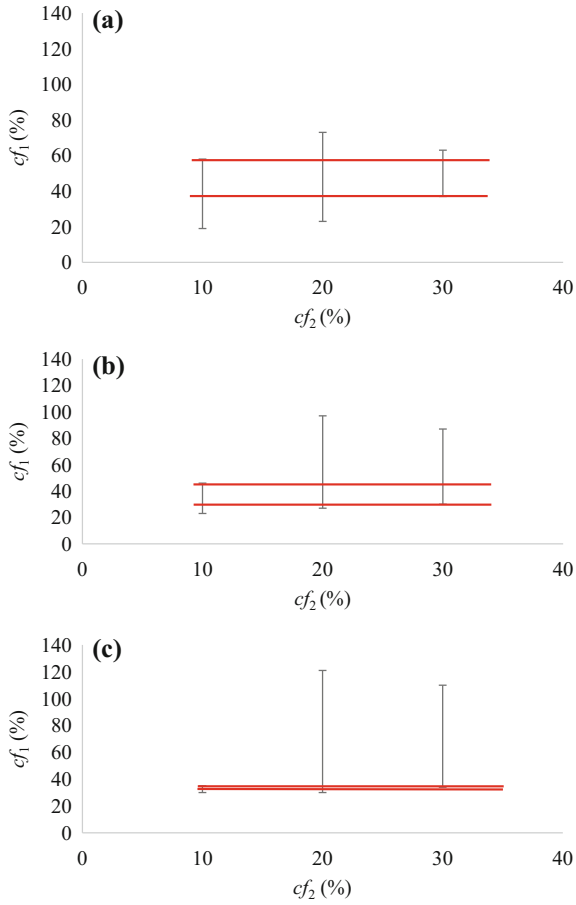

Fig. 5 **a** Range of cf_1 based on cf_2 with respect to cf_3=20%, **b** with respect to cf_3=25%, **c** with respect to cf_3=30%

is formulated in Eqs. 25–33. Equations 25–33 are formulated based on the generic representation presented in Eqs. 9–13.

$$\mathrm{AI}_u = cf_u \times \mathrm{RMC}_u \quad \forall u \tag{24}$$

$$\mathrm{AI}^{\mathrm{OVERALL}} = \mathrm{AI}_1 + \mathrm{AI}_2 + \mathrm{AI}_3 \tag{25}$$

$$\mathrm{IP}^{\mathrm{OVERALL}} = \mathrm{IP}_1 + \mathrm{IP}_2 + \mathrm{IP}_3 \tag{26}$$

$$\mathrm{DC}^{\mathrm{OVERALL}} = \frac{\mathrm{IP}^{\mathrm{OVERALL}}}{\mathrm{AI}^{\mathrm{OVERALL}}} \tag{27}$$

$$\mathrm{ADC}_1 = \frac{\mathrm{DC}_1}{\mathrm{DC}^{\mathrm{OVERALL}}} - 1 \tag{28}$$

$$\mathrm{ADC}_2 = \frac{\mathrm{DC}_2}{\mathrm{DC}^{\mathrm{OVERALL}}} - 1 \tag{29}$$

$$\mathrm{ADC}_3 = \frac{\mathrm{DC}_3}{\mathrm{DC}^{\mathrm{OVERALL}}} - 1 \tag{30}$$

$$\mathrm{DC}_1 = \frac{\mathrm{PA}_1}{\mathrm{AI}_1} \tag{31}$$

$$\mathrm{DC}_2 = \frac{\mathrm{PA}_2}{\mathrm{AI}_2} \tag{32}$$

$$\mathrm{DC}_3 = \frac{\mathrm{PA}_3}{\mathrm{AI}_3} \tag{33}$$

Prior to determining the stability threshold, a decision hierarchy is first defined for the PEIP. The decision hierarchy describes which system in the PEIP has a higher influence on its operational decisions. Since the POM is the sole provider of raw materials in the PEIP in Fig. 2, operational decisions in the POM would outweigh the decisions in the BCS and PBB. If any variations or disturbances are experienced in the POM, it would cause a "ripple" effect toward BCS and PBB operations and subsequently destabilizing the PEIP economically. In that respect, the POM is placed on the top of the decision hierarchy as shown in Fig. 4. Based on Fig. 4, the stability threshold is determined by investigating the behavior of cf_1 (BCS) and cf_2 (PBB) values with respect to cf_3 (POM), with results shown in Fig. 5. As shown in Fig. 5a, the range of stability for fractions cf_1 and cf_2 is investigated empirically when $cf_3 = 20\%$. The verticals lines shown in the plot represent the range in which cf_1 values give a stable PEIP when cf_2 is gradually increased. Meanwhile, the horizontal lines indicate the common region of stability of cf_1 for different values of cf_2. Similarly, results for $cf_3 = 25\%$ and $cf_3 = 30\%$ are shown in Fig. 5b, c respectively. The common region of stability for the stability threshold of the PEIP is given as follows;

$$37\% \leq cf_1 \leq 46\%$$
$$10\% \leq cf_2 \leq 30\%$$
$$20\% \leq cf_3 \leq 25\%$$

If additional investment cost of one (or more) system falls outside the above-mentioned stability threshold, the stability of the PEIP is compromised and further action must be taken.

Based on these thresholds, it can be seen that the POM has a smaller range as compared to BCS and POB. This suggests that the PBB is able to absorb a wide range of deviations in their respective additional investment costs in order to maintain an acceptable economic stability within the coalition.

5 Conclusion

In this chapter, an integrated approach was presented to determine the allocation of incremental profits for in a coalition that implements a green technology system.

The approach is applied to the specific case of a palm-based biorefinery (PBB) in a palm-based eco-industrial park (PEIP). The results suggest that the optimal allocation of incremental profits is 14% (US$800,000) for the PBB. This allocation indicates that incremental profits allocated to PBB within the PEIP coalition are significantly higher compared to when the PBB operates without coalition. Based on this allocation, further stability analysis determined that the PBB is economically stable for as long as its additional investment costs are within 10–30% of its raw material costs.

Acknowledgements The financial support from the Ministry of Higher Education, Malaysia through the LRGS Grant (Project Codes: LRGS UPM Vot 5526100 and LRGS/2013/UKM-UNMC/PT/05) are gratefully acknowledged.

References

1. Abdullah N, Sulaiman F (2013) The oil palm wastes in Malaysia. In: Biomass now—sustainable growth and use. InTech
2. Ali AAM, Othman MR, Shirai Y, Hassan MA (2015) Sustainable and integrated palm oil biorefinery concept with value-addition of biomass and zero emission system. J Clean Prod 91:96–99
3. Andiappan V, Ng DKS, Bandyopadhyay S (2014) Synthesis of biomass-based trigeneration systems with uncertainties. Ind Eng Chem Res 53:18016–18028
4. Andiappan V, Tan RR, Ng DKS (2016) An optimization-based negotiation framework for energy systems in an eco-industrial park. J Clean Prod 129. https://doi.org/10.1016/j.jclepro.2016.04.023
5. Department of Statistics Malaysia (2017) Gross domestic product third quarter 2017
6. Holling C (1996) Engineering within ecological constraints. National Academies Press, Washington, DC
7. Kasivisvanathan H, Barilea IDU, Ng DKS, Tan RR (2013) Optimal operational adjustment in multi-functional energy systems in response to process inoperability. Appl Energy 102:492–500
8. Kasivisvanathan H, Ng RTL, Tay DHS, Ng DKS (2012) Fuzzy optimisation for retrofitting a palm oil mill into a sustainable palm oil-based integrated biorefinery. Chem Eng J 200–202:694–709
9. KeTTHA (2010) Definition of green technology (WWW document). http://www.gpnm.org/e/articles/Definition-of-Green-Technology-by-KETTHA-Ministry-of-Energy-Green-Technology-and-Water-a5.html. Accessed 31 Jan 2018
10. Kronenberg J (2007) Ecological economics and industrial ecology: a case study of the integrated product policy of the European union. Routledge, New York
11. Maali Y (2009) A multiobjective approach for solving cooperative n-person games. Int J Electr Power Energy Syst 31:608–610
12. Malaysian Innovation Agency (2011) National biomass strategy 2020 : New Wealth Creation for Malaysia's Palm Oil Industry
13. Mayer AL (2008) Ecologically-based approaches to evaluate the sustainability of industrial systems. Int J Sustain Soc 1:117–133
14. Ng RTL, Hashim MH, Ng DKS (2013) Process synthesis and optimization of a sustainable integrated biorefinery via fuzzy optimization. AIChE J 59:4212–4227
15. Ng RTL, Ng DKS, Tan RR (2015) Optimal planning, design and synthesis of symbiotic bioenergy parks. J Clean Prod 87:291–302
16. Ng RTL, Ng DKS, Tan RR (2013) Systematic approach for synthesis of integrated palm oil processing complex. Part 2: multiple owners. Ind Eng Chem Res 52:10221–10235

17. Ng RTL, Ng DKS, Tan RR, El-Halwagi MM (2014) Disjunctive fuzzy optimisation for planning and synthesis of bioenergy-based industrial symbiosis system. J Environ Chem Eng 2:652–664
18. Shapley LS (1953) A value for n-person games. In: Contributions to the theory of games. Annals of mathematical studies. Princeton University Press, Princeton, pp. 307–317
19. Teo KY, Ng TY, Wau CM, Liew JTS, Andiappan V, Ng DKS (2017) Hybrid optimisation model for the synthesis of a central utility system in eco-industrial park. Process Integr Optim Sustain
20. Waage S (2013) Disruptive innovation is key for a sustainable economy (WWW document). Guard. https://www.theguardian.com/sustainable-business/disruptive-innovation-sustainable-economy
21. Wang G, Feng X, Chu KH (2013) A novel approach for stability analysis of industrial symbiosis systems. J Clean Prod 39:9–16

Index

D. C. Y. Foo and M. K. Tun Abdul Aziz (eds.), *Green Technologies for the Oil Palm Industry*, Green Energy and Technology, https://doi.org/10.1007/978-981-13-2236-5